ISSN 0021-9673

VOL. 648 NO. 2 OCTOBER 8, 1993

THIS ISSUE COMPLETES VOL. 648

JOURNAL OF CHROMATOGRAPHY

INCLUDING ELECTROPHORESIS AND OTHER SEPARATION METHODS

ELSEVIER

JOURNAL OF CHROMATOGRAPHY

INCLUDING ELECTROPHORESIS AND OTHER SEPARATION METHODS

Scope. The *Journal of Chromatography* publishes papers on all aspects of **chromatography, electrophoresis** and related methods. Contributions consist mainly of research papers dealing with chromatographic theory, instrumental developments and their applications. The section *Biomedical Applications*, which is under separate editorship, deals with the following aspects: developments in and applications of chromatographic and electrophoretic techniques related to clinical diagnosis or alterations during medical treatment; screening and profiling of body fluids or tissues related to the analysis of active substances and to metabolic disorders; drug level monitoring and pharmacokinetic studies; clinical toxicology; forensic medicine; veterinary medicine; occupational medicine; results from basic medical research with direct consequences in clinical practice. In *Symposium volumes*, which are under separate editorship, proceedings of symposia on chromatography, electrophoresis and related methods are published.

Submission of Papers. The preferred medium of submission is on disk with accompanying manuscript (see *Electronic manuscripts* in the Instructions to Authors, which can be obtained from the publisher, Elsevier Science Publishers B.V., P.O. Box 330, 1000 AH Amsterdam, Netherlands). Manuscripts (in English; *four* copies are required) should be submitted to: Editorial Office of *Journal of Chromatography*, P.O. Box 681, 1000 AR Amsterdam, Netherlands, Telefax (+31-20) 5862 304, or to: The Editor of *Journal of Chromatography, Biomedical Applications*, P.O. Box 681, 1000 AR Amsterdam, Netherlands. Review articles are invited or proposed in writing to the Editors who welcome suggestions for subjects. An outline of the proposed review should first be forwarded to the Editors for preliminary discussion prior to preparation. Submission of an article is understood to imply that the article is original and unpublished and is not being considered for publication elsewhere. For copyright regulations, see below.

Publication. The *Journal of Chromatography* (incl. *Biomedical Applications*) has 40 volumes in 1993. The subscription prices for 1993 are:

J. Chromatogr. (incl. *Cum. Indexes*, *Vols. 601–650*) + *Biomed. Appl.* (Vols. 612–651):
Dfl. 8520.00 plus Dfl. 1320.00 (p.p.h.) (total *ca.* US$ 5466.75)

J. Chromatogr. (incl. *Cum Indexes*, *Vols. 601–650*) only (Vols. 623–651):
Dfl. 7047.00 plus Dfl. 957.00 (p.p.h.) (total *ca.* US$ 4446.75)

Biomed. Appl. only (Vols. 612–622):
Dfl. 2783.00 plus Dfl. 363.00 (p.p.h.) (total *ca.* US$ 1747.75).

Subscription Orders. The Dutch guilder price is definitive. The US$ price is subject to exchange-rate fluctuations and is given as a guide. Subscriptions are accepted on a prepaid basis only, unless different terms have been previously agreed upon. Subscriptions orders can be entered only by calender year (Jan.–Dec.) and should be sent to Elsevier Science Publishers, Journal Department, P.O. Box 211, 1000 AE Amsterdam, Netherlands, Tel. (+31-20) 5803 642, Telefax (+31-20) 5803 598, or to your usual subscription agent. Postage and handling charges include surface delivery except to the following countries where air delivery via SAL (Surface Air Lift) mail is ensured: Argentina, Australia, Brazil, Canada, China, Hong Kong, India, Israel, Japan*, Malaysia, Mexico, New Zealand, Pakistan, Singapore, South Africa, South Korea, Taiwan, Thailand, USA. *For Japan air delivery (SAL) requires 25% additional charge of the normal postage and handling charge. For all other countries airmail rates are available upon request. Claims for missing issues must be made within six months of our publication (mailing) date, otherwise such claims cannot be honoured free of charge. Back volumes of the *Journal of Chromatography* (Vols. 1–611) are available at Dfl. 230.00 (plus postage). Customers in the USA and Canada wishing information on this and other Elsevier journals, please contact Journal Information Center, Elsevier Science Publishing Co. Inc., 655 Avenue of the Americas, New York, NY 10010, USA, Tel. (+1-212) 633 3750, Telefax (+1-212) 633 3764.

Abstracts/Contents Lists published in Analytical Abstracts, Biochemical Abstracts, Biological Abstracts, Chemical Abstracts, Chemical Titles, Chromatography Abstracts, Current Awareness in Biological Sciences (CABS), Current Contents/Life Sciences, Current Contents/Physical, Chemical & Earth Sciences, Deep-Sea Research/Part B: Oceanographic Literature Review, Excerpta Medica, Index Medicus, Mass Spectrometry Bulletin, PASCAL-CNRS, Referativnyi Zhurnal, Research Alert and Science Citation Index.

US Mailing Notice. *Journal of Chromatography* (ISSN 0021-9673) is published weekly (total 52 issues) by Elsevier Science Publishers (Sara Burgerhartstraat 25, P.O. Box 211, 1000 AE Amsterdam, Netherlands). Annual subscription price in the USA US$ 4446.75 (subject to change), including air speed delivery. Second class postage paid at Jamaica, NY 11431. **USA POSTMASTERS**: Send address changes to *Journal of Chromatography*, Publications Expediting, Inc., 200 Meacham Avenue, Elmont, NY 11003. Airfreight and mailing in the USA by Publications Expediting.

See inside back cover for Publication Schedule, Information for Authors and information on Advertisements.

0021-9673/93/$06.00

Printed in the Netherlands

CONTENTS

(Abstracts/Contents Lists published in Analytical Abstracts, Biochemical Abstracts, Biological Abstracts, Chemical Abstracts, Chemical Titles, Chromatography Abstracts, Current Awareness in Biological Sciences (CABS), Current Contents/Life Sciences, Current Contents/Physical, Chemical & Earth Sciences, Deep-Sea Research/Part B: Oceanographic Literature Review, Excerpta Medica, Index Medicus, Mass Spectrometry Bulletin, PASCAL-CNRS, Referativnyi Zhurnal, Research Alert and Science Citation Index)

REGULAR PAPERS

Column Liquid Chromatography

Gas Chromatography

(Continued overleaf)

Contents (continued)

SHORT COMMUNICATIONS

Column Liquid Chromatography

Gas Chromatography

Journal of Chromatography, 648 (1993) 307–314
Elsevier Science Publishers B.V., Amsterdam

CHROM. 25 357

Correlation analysis in liquid chromatography of metal chelates

III. Multi-dimensional models in reversed-phase liquid chromatography

A.R. Timerbaev* and O.P. Semenova

Department of Analytical Chemistry, Johannes Kepler University, Altenbergstrasse 69, A-4040 Linz (Austria)

I.G. Tsoi and O.M. Petrukhin

Department of Analytical Chemistry, Mendeleev University of Chemical Technology, Moscow 125190 (Russian Federation)

(First received May 4th, 1993; revised manuscript received June 7th, 1993)

ABSTRACT

A number of multiparametric retention models for metal chelates in reversed-phase high-performance liquid chromatography (RP-HPLC) were developed and compared. The most significant structural descriptors of the chelates and mobile phase parameters were selected with the help of one-dimensional correlation analysis performed in this and previously published papers of this series. Log k' values for metal di-*n*-alkyldithiophosphates used as test solutes were determined using a C_{18} column and dioxane as organic modifier and subjected to multiple regression analysis. The predictive ability of the resulting multiparametric regression equations was evaluated in terms of their statistical significance. The most meaningful retention model is described by the linear regression equation $\log k' = 0.716 + (0.236 \pm 0.010)n_C - (0.040 \pm 0.018)E_n - (0.048 \pm 0.003)c + (0.029 \pm 0.010)Z$ ($R = 0.976$; S.D. = 0.111), where n_C is the carbon number, E_n is the orbital electronegativity of the metal atom, c is the volume concentration of the organic modifier and Z is the parameter of proton-donating ability of the mobile phase. The results confirm the modern representations of the separation mechanism for metal chelates of moderate polarity in RP-HPLC, present rather valuable sets of solute structural descriptors and eluent parameters to approximate the experimental retention values and open new possibilities in the application of multivariate statistical methods to interpret a large number of chromatographic data.

INTRODUCTION

Reversed-phase high-performance liquid chromatography (RP-HPLC), in spite of growing competition from other chromatographic methods, can be still considered the preferred mode for metal chelate separation by HPLC. In this respect, the problems of forecasting the chromatographic behaviour of chelates (including an *a priori* prediction of retention parameters), understanding the mechanism of chromatographic retention at a molecular level and optimizing the ligand selectivity are of considerable interest. Our previous investigations [1–5] showed that these problems can be solved by using one-dimensional correlation models of the retention–structure and retention–mobile phase composi-

* Corresponding author. On leave from Mendeleev University of Chemical Technology, Moscow 125190, Russian Federation.

0021-9673/93/$06.00

tion type. Using this approach, we have developed a mathematical model for a metal chelate in a given chromatographic system. This is just one of the ultimate goals of multiparametric equations derived and evaluated in this paper.

EXPERIMENTAL

Preparation of chelates

Metal dialkyldithiophosphates were prepared directly by mixing aqueous solutions of metal nitrate (cadmium, copper, mercury, nickel, lead or zinc) and the potassium salt of the corresponding reagent (dimethyl-, diethyl-, di-*n*-propyl, di-*n*-butyl-, di-*n*-hexyl-, di-*n*-octyl-, di-*n*-decyldithiophosphate).

Apparatus and chromatographic conditions

We used a Waters (Milford, MA, USA) high-performance liquid chromatograph consisting of a Waters 600E programmable multisolvent delivery system, a Waters 991 computer-controlled photodiode-array detector monitoring at 254 nm and a Waters 5200 printer–plotter. An ODS-Hypersil column (250 × 4 mm) (particle size 5 μm) was purchased from Österreichisches Forschungszentrum, Seibersdorf, Austria. 1,4-Dioxane of analytical reagent grade (Merck, Darmstadt, Germany) and double-distilled water were used as the solvent system providing the optimal resolution of metal dithiophosphates [3,4].

Solute and eluent parameters

The structural parameters calculated according to ref. 3 or taken from the literature are listed in Tables I–III. Parameters for the dioxane–water mixtures which were considered (see Table V) were taken from refs. 4 and 6–11.

Deriving multiparametric retention models

Retention values (logarithms of capacity factors) were related to solute and eluent parameters by means of multiparametric regression analysis processed with the program SigmaPlot (Jandel Scientific, USA) on a personal computer. The equations derived were tested according to the requirements of a meaningful correlation

TABLE I

PARAMETERS FOR METAL ATOMS

Metal	Electronegativity (E_n) [6]	Hydrophobic increment (Δ_M)
Cd	−1.15	0.105
Cu	−1.60	0.300
Hg	−4.40	0.756
Ni	−0.70	0.010
Pb	−1.25	0.210
Zn	−0.60	−0.010

TABLE II

PARAMETERS OF DIALKYLDITHIOPHOSPHATE LIGANDS

Ligand	Carbon number	Hydrophobic constant (f)	Molar volume (ml/mol)
Methyl	1	2.808	139.56
Ethyl	2	4.916	180.48
Propyl	3	7.024	262.32
Butyl	4	9.132	303.24
Hexyl	6	13.348	385.08
Octyl	8	17.564	466.92
Decyl	10	21.780	548.76

TABLE III

MOLECULAR PARAMETERS OF METAL DIALKYLDITHIOPHOSPHATES

Ligand	Metal atom					
	Cd	Cu	Hg	Ni	Pb	Zn
Molecular connectivity index						
Methyl	21.24	18.68	24.34	18.68	24.15	18.98
Ethyl	23.59	21.03	26.69	21.03	26.50	21.33
Propyl	25.59	23.03	28.69	23.03	28.50	23.33
Butyl	27.59	25.03	30.69	25.03	30.50	25.33
Hexyl	31.59	29.03	34.69	29.03	34.50	29.33
Octyl	35.59	33.03	38.69	33.03	38.50	33.33
Decyl	39.59	37.03	42.69	37.03	42.50	37.33
Stability constant (log β_n)						
Butyl	8.5	15.1	29.6	5.9	12.3	7.9
Distribution constant (log K_D)						
Ethyl	0.170	0.369	1.217	0.148	0.285	0.011

analysis, taking into account the correlation coefficient, standard deviation, significance level of the whole equation, t-test value and number of data points used to derive the equation.

RESULTS AND DISCUSSION

General conclusions from single-parametric correlation analysis

In earlier papers of this series [3,4], we have confirmed that one-dimensional retention models can be widely applied in RP-HPLC of neutral chelates. Non-polar sulphur-containing metal chelates such as dialkyldithiocarbamates and dialkyldithiophosphates were used as test solutes. The results of these studies can be briefly summarized as follows.

Retention–structure dependences observed for metal chelates (at least for those that are sufficiently stable in a chromatographic process) can be well described at the quantitative level in terms of linear free-energy relationships [3]. However, the polyfunctional structure of these solutes means that three types of structure-dependent parameters have to be taken into account as variables of the corresponding models. All the structural descriptors already studied and subdivided into three groups are collected in Table IV. Obviously, the structural complexity of chelates makes the task of correlation analysis more complicated than that for organic substances; in addition, the selection of the parameters is more critical (see below) and requires a knowledge of some special aspects of coordination chemistry.

The most recent application of correlation analysis to RP-HPLC of metal chelates was the correlation of chelate retention with the mobile phase composition and physico-chemical characteristics of solvents [4]. We found that the effect of the mobile phase can be evaluated by a variety of macroscopic and microscopic (molecular) parameters of binary water–organic mixtures listed in Table V, the former providing more reliable predictions of retention data. An analysis of linear retention models derived allowed us to conclude that, according to the solvophobic theory of RP-HPLC, the retention of metal chelates is governed mainly by the solvophobic effect or, in other words, by the hydrophobic, bulk-dependent nature of a molecule, whereas specific intermolecular interactions in the mobile phase (mostly hydrogen bonds involving solute

TABLE IV

STRUCTURAL PARAMETERS OF METAL CHELATES APPLICABLE TO DESCRIPTION OF THE RETENTION BEHAVIOUR IN RP-HPLC

Parameter	Refs.
(A) Molecular parameters	
Distribution constant (log K_D)	2, 3
Stability constant (log β_n)	1, 3
Molecular connectivity index (χ)	3, 5
Molar volume (V_m)	3
Solubility in the mobile phase	12
(B) Parameters of metal atom	
Effective charge, ρ_M	3
Electronegativity	3
Ratio of electronegativity to ionic radius	3, 13
Orbital electronegativity (E_n)	1, 3
Distribution coefficient	14, 15
Metal increment in the distribution constant (Δ_M)	2, 3
(C) Ligand parameters	
Carbon number of alkyl homologies (n_C)	3, 15
Induction constant (σ^*)	3
Steric constant (E_S)	3
Hydrophobic constants, π and f	3
Molecular connectivity index of the ligand	3, 5
Molar volume of the ligand	3

TABLE V

PARAMETERS OF BINARY WATER–ORGANIC MOBILE PHASES USED IN RP-HPLC OF METAL CHELATES [4]

(A) Macroscopic parameters
Volume concentration of an organic modifier (c)
Molar concentration of an organic modifier (log C)
Hydrophobicity (log P_S)
Methylene selectivity (log α_{CH_2})
Surface tension (γ)
Viscosity (η)
Dielectric constant (ε)
(B) Molecular parameters
Solvent dipolarity/polarizability by Kamlet–Taft (π^*)
Acceptor strength by Dimroth–Reichardt (E_T)
Proton-donating ability by Kosower (Z)
Solvent strength by Brounstein (S)

molecules and proton-donor eluent molecules) are responsible for the differences in the retention and hence the separation.

However, the predictive value of the aforementioned one-dimensional relationships is restricted because of the limited nature of the approach itself, which takes advantage of only one of the possible parameters. In practice, the retention behaviour of a metal chelate quantified by log k' depends on *all* possible parameters characterizing its structure, the mobile phase nature and the chromatographic system as a whole. Therefore, only a multiparametric approach for the correlation analysis of retention dependence on both structure and chromatographic experimental conditions can provide a sufficiently complete answer. This approach necessarily includes choosing the most informative sets of chelate structural parameters and parameters of the chromatographic system (or of a mobile phase at a given stationary phase), taking into account the most likely retention mechanism, and the search for a number of multiparametric models based on various parameter sets and providing the most adequate description of experimental data. Statistically most significant models will characterize the retention behaviour of a given class of chelates and, thereby, represent a certain mathematical pattern of the solutes in RP-HPLC.

Selection of parameters

In this paper, we shall first discuss the choice of the most significant parameters to be used as variables for the multiple linear regression analysis. The first selection principle utilized is to reject some less important parameters based on results obtained earlier in our one-dimensional correlations. Then, to facilitate the development of multivariate models, the set of the parameters is further reduced using one-dimensional correlation analysis for particular chelates and the separation system studied in this work. Finally, the rest of the most valuable parameters will be grouped as "solvophobic" and "hydrogen bonding" terms.

Of the molecular structural descriptors listed in Table IV, we do not consider here molar volume, which shows a poor correlation with log k' values owing to inaccuracy in the evaluation of the metal increment, and solubility, which requires special experiments to be performed. The retention values of metal dithiophosphates (as the chelates of the *S,S*-type) in RP-HPLC did not correlate with the effective charge or electronegativity of a metal atom, or with the ratio of electronegativity to metal ion radius. This is because specific electrostatic interactions in the chromatographic system do not significantly influence the retention behaviour of these chelates. Data on distribution coefficients are not available, and their experimental evaluation is out with the scope of this work. The application of electronic and steric constants of alkyl substituents, characterizing the hydrogen bonding capability of donor atoms, is limited by the comparatively small number of carbon atoms in a ligand (not more than four atoms). Both types of hydrophobic constants well describe the hydrophobic nature of a chelate molecule in RP-HPLC. However, since the Rekker constants (f) can more accurately evaluate the hydrophobicity, we give preference to this parameter.

The majority of mobile phase parameters presented in Table V can be used to describe the chelate retention in terms of one-dimensional linear models. Therefore, we have omitted only two of them at the stage of the initial choice. Although viscosity should reflect intermolecular solute–eluent interactions, non-linear dependences for log k' values of metal dithiophosphates were observed (for more details see ref. 4). Solvent polarity parameter E_T is sensitive only to the proton-donating properties of the mobile phase and, consequently, is linearly correlated with log k' values only for water–alcoholic eluents.

Table VI shows the statistical criteria of one-dimensional regression equations calculated from experimental retention data. Molar volumes show a slightly lower correlation with log k' values than carbon numbers and hydrophobic constants, while the last two parameters possess identical predictive value owing to the high intercorrelation between them. Therefore, we limited the ligand descriptors to the number of carbon atoms in alkyl substituents. Of the parameters reflecting the ability of the mobile

TABLE VI

AVERAGE CORRELATION COEFFICIENTS AND STANDARD DEVIATIONS FOR ONE-DIMENSIONAL CORRELATIONS

Statistical criteria calculated and averaged from six sets of retention data consisting of 28 and 21 data points for structural and eluent parameters, respectively.

Parameter	R	S.D.	Parameter	R	S.D.
n_C	0.9859	0.071	c	0.9890	0.080
f	0.9859	0.071	log C	0.9874	0.096
V_m	0.9829	0.076	log P_S	0.9801	0.121
π	0.9890	0.080	γ	0.9880	0.086
Z	0.9820	0.119	ε	0.9871	0.089
S	0.9724	0.142	α_{CH_2}	0.9868	0.099

phase to participate in intermolecular interactions of different types, π^* and Z will be considered below as those that are characterized by higher correlation factors. The list of eluent macroscopic parameters has been reduced to the volume concentration of the organic modifier and surface tension of the mobile phase based on the same principle.

Deriving and estimation of multiparametric retention models

Following the separation mechanism described above, we subdivided selected solute and eluent parameters into "solvophobic" and "hydrogen bonding" terms and then composed a number of multiparametric retention models given by the following equation:

$$\log k' = a_0 + a_1x_1 + a_2x_2 + a_3x_3 + a_4x_4$$

In this equation, the parameters x_1 and x_2 characterize the hydrophobicity and hydrogen bond accepting ability of the chelates, respectively; x_3 and x_4 are the corresponding terms of the mobile phase (the eluent property complementary to solute hydrogen bond accepting ability is hydrogen bond donating ability). Independent variables of the retention models subjected to multiple linear regression analysis are collected in Table VII. For convenient comparison, the characteristics of statistical significance for derived correlation equations are assembled in Table VIII together with intercepts and coefficients of the independent variables (only one, the "best", equation for each retention model is included).

TABLE VII

VARIABLES OF MULTIPARAMETRIC CORRELATION MODELS

Eqn.	x_1	x_2	x_3	x_4	Eqn.	x_1	x_2	x_3	x_4
1a	log K_D	–	c	π^*	1c	log K_D	–	γ	π^*
1b	log K_D	–	c	Z	1d	log K_D	–	γ	Z
2a	log K_D	E_n	c	π^*	2c	log K_D	E_n	γ	π^*
2b	log K_D	E_n	c	Z	2d	log K_D	E_n	γ	Z
3a	χ	E_n	c	π^*	3c	χ	E_n	γ	π^*
3b	χ	E_n	c	Z	3d	χ	E_n	γ	Z
4a	χ	log β_n	c	π^*	4c	χ	log β_n	γ	π^*
4b	χ	log β_n	c	Z	4d	χ	log β_n	γ	Z
5a	n_C	E_n	c	π^*	5c	n_C	E_n	γ	π^*
5b	n_C	E_n	c	Z	5d	n_C	E_n	γ	Z
6a	n_C, Δ_M	E_n	c	π^*	6c	n_C, Δ_M	E_n	γ	π^*
6b	n_C, Δ_M	E_n	c	Z	6c	n_C, Δ_M	E_n	γ	Z
7a	Δ_M	log β_n	c	π^*	7c	Δ_M	log β_n	γ	π^*
7b	Δ_M	log β_n	c	Z	7d	Δ_M	log β_n	γ	Z

TABLE VIII

PARAMETERS OF MULTIPARAMETRIC CORRELATION MODELS DERIVED FROM EQN. 1

Eqn.	a_0	a_1	a_2	a_3	a_4	n	R	S.D.
1c	9.09	0.528	–	−0.665	21.94	12	0.8878	0.158
2d	−7.10	3.22	0.837	−0.075	0.121	12	0.9136	0.127
3c	−0.718	0.061	0.033	−0.339	17.45	43	0.8716	0.200
4d	−12.98	−0.038	0.020	−0.163	0.247	14	0.8533	0.272
5b	0.716	0.236	−0.040	−0.048	0.029	43	0.9760	0.111
6c	−4.08	0.237; 0.275	0.008	−0.199	15.91	43	0.9736	0.117
7c	7.80	3.31	−0.094	−0.752	30.60	14	0.9143	0.193

It is seen that retention models based on *n*-octanol–water distribution constants, which correspond to eqns. 1 and 2 of Table VII, as well as on stability constants (eqns. 4 and 7), are of less importance than might be expected, mainly because of a small number of retention data used to derive regressions (only log K_D and log β_n values for the chelates of one ligand were available for calculations). This emphasizes the limiting nature of experimentally determined molecular descriptors as variables in a regression equation. On the other hand, the lack of reliable distribution and stability constant data (owing to the complexity of their experimental determination) makes worthwhile the solution of the reverse problem, *i.e.* evaluation of these parameters from chromatographic data.

The statistical goodness of eqn. 1, including only one solute parameter, log K_D, increases if the hydrogen bonding parameter, E_n, is introduced, as in eqn. 2 (see Figs. 1 and 2), but this increase is not very large. We attributed this to the fact that the distribution constant partly accounts for the input of specific electrostatic interactions to the RP-HPLC retention.

If molecular connectivity indices are considered instead of log K_D values, eqn. 3 results. We must admit that on the grounds of our earlier correlations we had expected better fitting of χ values to the retention models. This is probably because of some uncertainties resulting from a comparatively short set of test chelates of different metal atom nature considered here (the predictive potency of this molecular parameter for metal chelates with different alkyl substituents is beyond doubt [3]). When eqns. 4 and 7 are compared, it is quite evident that the contribution of the metal atom to molecular size (or hydrophobicity) is less well expressed by χ than by Δ_M. However, χ parameters are more easily determined irrespective of the molecular complexity.

The most meaningful models describing log k' are shown in regression eqns. 5 and 6. In these

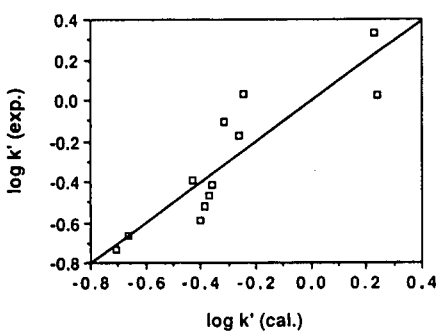

Fig. 1. Relationship between the retention parameters of metal di-*n*-alkyldithiophosphates determined experimentally and calculated using eqn. 1d.

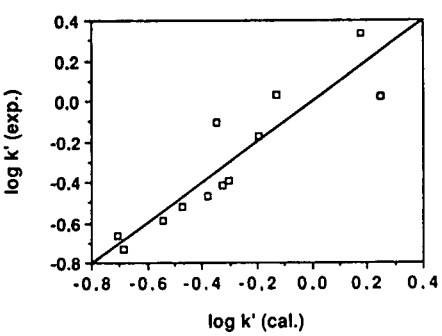

Fig. 2. Relationship between the retention parameters of metal di-*n*-alkyldithiophosphates determined experimentally and calculated using eqn. 2d.

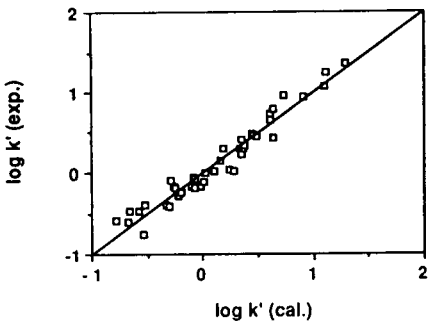

Fig. 3. Relationship between the retention parameters of metal di-*n*-alkyldithiophosphates determined experimentally and calculated using eqn. 5b.

equations we incorporated a combination of ligand and metal atom hydrophobic descriptors as a measure of the hydrophobicity of the whole molecule, thus yielding five-parametric models. Interestingly, the correlations obtained with eqn. 6 are not higher than those with eqn. 5, which includes only the ligand hydrophobic term. As a parameter of metal complex-forming ability [16], E_n reflects indirectly the ability of chelates to take part in hydrogen bonding interactions [1]. The predictive quality of both sets of retention models is illustrated in Figs. 3 and 4. It can be seen that fitted log k' values agree quite well with experimental data (the average difference between observed and predicted log k' values is 0.097 and 0.096 log units, respectively).

The quite good agreement between the four combinations of mobile phase parameters in Table VII indicates that we have achieved a rather precise algorithm for selection of the most valuable parameters. Note that the differences in correlation coefficients observed in eqns. 1, 2, 4 and 7 are not surprising in the light of the fact that only small subsets of log k' data could be used for these correlations. Thus, one can widely recommend volume concentration of the organic solvent, which provides predictions of log k' that are less dependent on organic modifier nature, as a measure of mobile phase solvophobic effect in relation to metal chelates. Both π^* and Z parameters are less universal since they are limited to mobile phases modified by aprotic solvents [4].

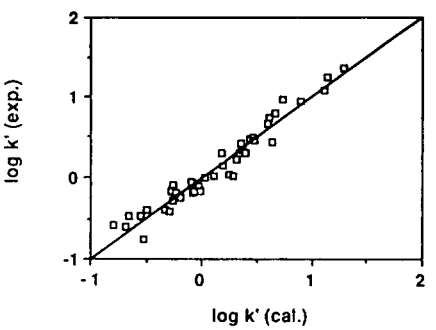

Fig. 4. Relationship between the retention parameters of metal di-*n*-alkyldithiophosphates determined experimentally and calculated using eqn. 6c.

CONCLUSIONS

As demonstrated above, the multiparametric approach for analysing the dependence of chromatographic retention of metal chelates on structure and on the composition of the mobile phase provides an adequate description and rational interpretation of RP-HPLC data. Owing to sufficiently high statistical significance, correlation models derived here can be widely applied for forecasting the chromatographic behaviour, including prediction of retention data, and searching for optimal separation systems (including optimization of the chelating ligand). Evidently, further progress in coordination chemistry and accessibility of molecular modelling methods for metal chelates will result in more informative molecular descriptors, the shortage of which might hinder the practical application of retention models. Another promising approach in this direction consists in determinations of structural parameters from back-calculations of HPLC data. Also, taking into account the parameters of stationary phase materials is worthy of further investigations.

At the same time, meaningful retention models involving certain sets of structural and eluent parameters generally support the observed separation mechanism and confirm the dominant factors defining the intermolecular interactions of metal chelates of moderate polarity in RP-HPLC. Hence, the usefulness of multivariate correlation analysis in chromatography is

based on its ability to select the solute and chromatographic characteristics that significantly influence the retention and to analyse the retention mechanism. Thus, it can be considered an important prospective tool for investigating the chromatographic behaviour of metal complexes in other HPLC modes and related separation techniques (*e.g.*, micellar electrokinetic chromatography or capillary zone electrophoresis).

ACKNOWLEDGEMENTS

This work was supported in part by Grant No. 45.213/2-27b/91 from the Austrian Ministry of Science and Research, Vienna. The authors are grateful to F. Eibensteiner, Johannes Kepler University, for his kind assistance with the calculations.

REFERENCES

1 A.R. Timerbaev and O.M. Petrukhin, *Zh. Anal. Khim.*, 44 (1989) 1424.
2 A.R. Timerbaev, I.G. Tsoi and O.M. Petrukhin, *Zh. Anal. Khim.*, 44 (1989) 1846.
3 A.R. Timerbaev, I.G. Tsoi and O.M. Petrukhin, *J. Chromatogr.*, 498 (1990) 337.
4 A.R. Timerbaev, I.G. Tsoi and O.M. Petrukhin, *J. Chromatogr.*, 555 (1991) 163.
5 A.R. Timerbaev, I.G. Tsoi and O.M. Petrukhin, *Zh. Anal. Khim.*, 47 (1992) 858.
6 H.B. Patel and T.M. Jefferies, *J. Chromatogr.*, 389 (1987) 21.
7 K.A. Connors and J.L. Wright, *Anal. Chem.*, 61 (1989) 194.
8 J. Timmermans, *The Physico-Chemical Constants of Binary Systems in Concentrated Solutions*, Vol. 4, Interscience, New York, 1960.
9 M.J. Kamlet, J.-L.M. Abboud, M.H. Abraham and R.W. Taft, *J. Org. Chem.*, 48 (1983) 2877.
10 E.M. Kosower, *J. Am. Chem. Soc.*, 80 (1958) 3253.
11 K. Burger, *Solvation, Ionic and Complex Formation Reactions in Non-aqueous Solvent*, Akademiai Kiado, Budapest, 1983.
12 L. Saitoh, *Bunseki Kagaku*, 35 (1986) 895.
13 M. Kobayashi, K. Saitoh and N. Suzuki, *Chromatographia*, 20 (1985) 49.
14 F. Vlačil and V. Hamplova, *Coll. Czechosl. Chem. Commun.*, 50 (1985) 2221.
15 W. Schunk and G. Schwedt, *Chromatographia*, 17 (1983) 37.
16 O.M. Petrukhin and N.A. Borsch, *Koord. Khim.*, 8 (1982) 255.

Journal of Chromatography, 648 (1993) 315–324
Elsevier Science Publishers B.V., Amsterdam

CHROM. 25 349

Effects on analyte peak performance by separated system peaks in ion-pair adsorption chromatography

Torgny Fornstedt and Douglas Westerlund*

Department of Analytical Pharmaceutical Chemistry, Biomedical Centre, Uppsala University, P.O. Box 574, S-751 23 Uppsala (Sweden)

(First received January 22nd, 1993; revised manuscript received May 28th, 1993)

ABSTRACT

Organic ionic components added to the eluent in ion-pair chromatography often have retention volumes similar to the analytes. The performance of analyte peaks may be influenced by the system peaks derived from such mobile phase components. Earlier work has mainly dealt with situations in which the retention times of analyte and system peaks are close. However, distortions of analyte peaks (peak deformation and peak compression) can be caused by large system peaks even when the two different kinds of peaks are separated. In this work, systematic investigations of this situation were performed. It was found that the analyte peaks were more easily deformed by counter-ion system peaks than by co-ion system peaks. In addition, guidelines are given for the design of general ion-pair chromatographic systems which do not suffer from peak distortion effects.

INTRODUCTION

When a solution with a composition different from the bulk eluent is injected into a chromatographic system, the equilibria at the top of the column will be disturbed. As a result, concentration changes of the eluent components (system zones) will be generated, which will migrate along the column with a speed that is characteristic for the system peak components [1–5]. When the zones containing an excess of shortage of the eluent components are detected at the column outlet, they appear as either positive or negative system peaks.

System peaks will always be induced when samples are introduced in systems containing more than one eluent component, if the sample components interact with one or several of the mobile phase components. If a sample is injected into an equilibrated system, this will give rise to as many migrating system zones as there are interacting components in the eluent, except the main solvent [4]. However, only the retarded eluent components will be discriminated from the front disturbances. In most systems such components do not have UV or fluorescence properties, and an universal detector principle, such as refractive index (RI), may be necessary to visualize the system zone.

A broad spectrum of different kinds of analyte peak shapes may result upon combined elution with system zones. In most cases the analyte peaks will be deformed, but under certain conditions extremely narrow and well-shaped peaks are obtained. The common detectors used are often only selective for the analytes, whereas the presence of system peaks is often indicated only by the distorted analyte peaks. Peak deformation and compression effects due to interferences with large system peaks were first reported in ion-pair adsorption chromatography of metal ions in 1984 [6], and of substituted benzamides 1 year later [7]. Since then, several studies have outlined the parameters of importance for obtaining optimum peak compression effects [8–

* Corresponding author.

0021-9673/93/$06.00

12], as well as those responsible for peak deformations in order to prevent the appearance of such peaks [10–14]. A model system based on alkyl-modified silica and an acidic eluent containing an organic UV-absorbing amine, protriptyline, has been used for the basic investigations [5,10–12]. Since the analytes were cationic amines, the analyte retention volumes were strongly dependent on the concentration of the eluent amine (co-ion). A photodiode array UV detector was used for those studies, which made it possible to obtain independent signals from both eluent and analyte components.

Deformations, which certainly are undesired, will occur more easily than compressions. The risk of deformation increases when the system peaks are large. This is especially true for coupled column systems, in which a large fraction of the mobile phase from a preceding column is introduced into the separation column [14,15]. However, serious deformations may also appear when only a single column is used in the analysis of biological fluids (bioanalysis), because of the complex samples injected [13].

Effects on analyte peaks by separated system peaks have only been mentioned occasionally in the literature [14]. The present study is a systematic investigation of the effects of system peaks that analyte peaks may be subjected to, even when they are separated from the large system peak at the column outlet. More particularly, a comparison has been made of distortions of anionic and cationic analytes in systems containing an organic amine in the eluent.

Parameters of importance in the design of chromatographic ion-pair systems in order to prevent distortions by system peaks will also be discussed.

EXPERIMENTAL

Chemicals

Acetonitrile (LiChrosolv), phosphoric acid (99% crystalline) and 1 *M* sodium hydroxide solution (Titrisol) were obtained from Merck (Darmstadt, Germany). N,N-Dimethyloctylamine (DMOA) was obtained from Janssen Chimica (Beerse, Belgium), and N,N-dimethylnonylamine (DMNA) and N,N-dimethyldecylamine (DMDA) from Ames Labs. (Millford, CT, USA). The amines were distilled before use. Protriptyline (PT) was obtained from Merck, Sharp and Dohme (Haarlem, Netherlands).

The substituted benzamides used as cationic analytes are denoted FLA in combination with a number [5]. They were synthesized at CNS Research and Development, Astra Arcus (Södertälje, Sweden).

Alprenolol, atenolol, metoprolol and propranolol hydrochloride also used as cationic analytes were obtained from Astra Hässle (Mölndal, Sweden) and pronethalol hydrochloride from Imperial Chemical Industries (Macclesfield, UK). Sodium naphthalene-2-sulphonate was obtained from Eastman-Kodak (Rochester, NY, USA) and sodium anthraquinone-2-sulphonate was obtained from Fluka (Buchs, Switzerland), and they were both used as anionic analytes.

Chromatographic system

Detection was performed by UV photometry (HP 1040A photodiode array or Linear 206 PHD) and by RI (Beckman 156 refractive index detector) coupled in series. The volume between the UV detector and the RI detector was chromatographically determined to be 0.07 ml. An LKB 2150 HPLC pump was used and the sample injector was a Rheodyne 7125, with a 50- or 100-μl loop. A Kipp & Zonen dual-channel recorder (Model BD 112) was used.

Conventionally sized columns with an inner diameter of 4.6 mm and lengths of 100 mm and 150 mm were used. They were either obtained ready-packed from the supplier (Spherisorb S5ODS-1 and Kromasil 100-5-C_{18}) or packed by a slurry technique (Nucleosil 100-5 C_{18}). The status of the packed columns was frequently tested with phenolic analytes and water–methanol as eluent. The performance of the columns remained unchanged during this work. The system (column and eluent reservoir) was carefully thermostated in a water bath (25.00 ± 0.01°C).

The eluents were mixtures of acetonitrile and phosphate buffers, with or without the addition of the organic amines DMOA, DMDA or PT. The preparation of the PT eluent was made as

described previously [5]. When the eluent contained PT, UV wavelengths were chosen such that the analytes and the PT system peak could be detected independently. The non-UV-absorbing amines were detected with RI detection. The flow-rate was 0.80 ml/min in all experiments. No recirculation of the eluent was used.

Retention volume, asymmetry factor (*asf*) and peak width (w_b), were determined as described previously [10].

When the analyte peak is affected by the system peak, its performance is compared with the corresponding injection when the system peaks are made as small as possible. This so-called "isocratic situation" is achieved by using the eluent as injection solvent; however, even in this case the analyte peak may be distorted by the system peak.

RESULTS AND DISCUSSION

Retention behaviour

Retention equations for these kinds of systems, based on the stoichiometric ion-pair adsorption model, were described earlier [5,16,17]. The adsorption of the eluent amine as ion pair with the anionic buffer component increases at higher eluent amine concentrations, resulting in greater competition for the adsorption sites. Thus the retention of the amine analyte decreases with increasing concentration of the eluent amine, which then acts as a co-ion. On the other hand, the retention of the anionic analyte increases with higher eluent amine concentrations. The anionic analyte is adsorbed to the surface as ion pair with the eluent amine, which in this case acts as a counter-ion.

Equations similar to those for the analytes are valid also for small system peaks [4,5]. The eluent amine often has a high concentration in the eluent, indicating that the capacity factor for its system peak is governed by the position in the non-linear part of the adsorption isotherm at the actual bulk concentration in the eluent. However, when the equilibrium disturbances are very small, the deviation from this position is infinitesimal; therefore, very small system peaks can be treated as linear concentration pulses [1–5,18]. On the other hand, the large excess system zone has a higher velocity than the large deficiency system zone, which results in a lower capacity factor for the positive system peak as compared with the negative one. This is also the reason why the large positive system peak shows tailing (the front is steeper than the rear), and why the large negative one shows fronting (the rear is steeper than the front) [10] (see Fig. 1).

Effects of system peaks on co-eluting analytes

The front and rear parts of the large system zones consist of either increasing or decreasing concentration gradients of mobile phase components. In ion-pair adsorption chromatography, the effect on the analyte zone (compression or

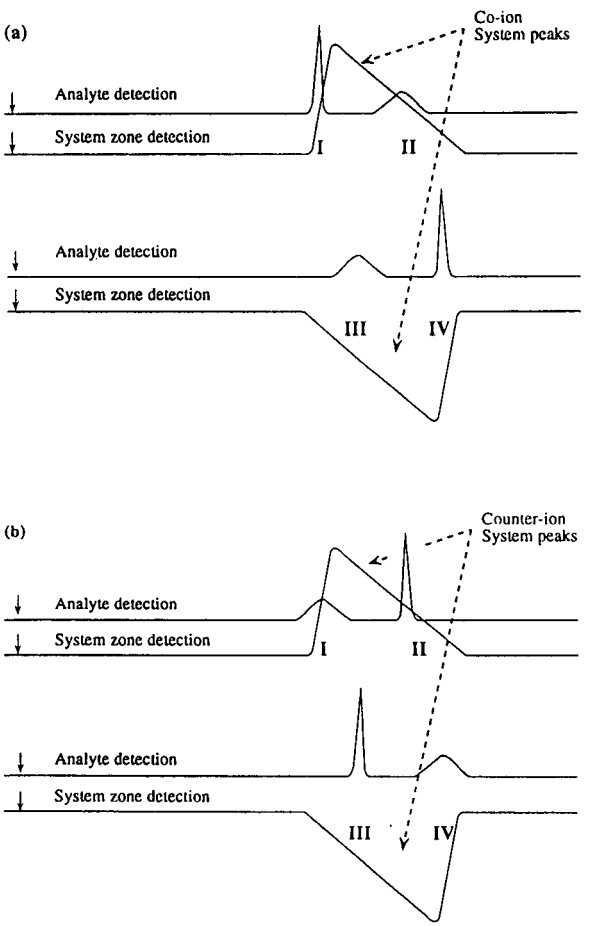

Fig. 1. Schematic illustration of the effects on analyte peaks of elution with different parts of a large positive or negative system peak. (a) The system peak component acts as a *co-ion*. (b) The system peak component acts as a *counter-ion*.

broadening) depends on the position of the analyte peak in the positive or negative system peak, and whether the system peak component is a co-ion or a counter-ion of the analyte. The different situations are schematically depicted in Fig. 1a and b. The effects represented in Fig. 1a result from the interactions with a system peak component acting as a co-ion towards the analytes; the situation in Fig. 1b refers to a system peak component acting as a counter-ion. In this work system peak effects by an organic amine in the eluent were studied. Fig. 1a describes in this case effects on cationic analytes and Fig. 1b effects on anionic analytes.

The analyte zone will be narrower than if eluted isocratically if it migrates in a gradient causing a continuously increasing migration rate; the rear part of the analyte zone will then experience a more accelerated velocity than the front part. These conditions prevail in a gradient of either increasing co-ion concentration or of decreasing counter-ion concentration. The cationic analyte peak is therefore compressed at the front part of the large positive co-ion system peak [9] or at the rear part of the negative one [7,10–12] (Fig. 1a, positions I and IV). On the other hand, the anionic analyte peak is narrower at the rear part of the positive counter-ion system peak [10,13,19] or at the front part of the negative one (Fig. 1b, positions II and III). The mechanisms behind the effects are different. In the increasing co-ion gradient, the cationic analyte experiences increasing competition for adsorption sites, whereas in the decreasing counter-ion gradient the analyte experiences a weaker ion-pair adsorption effect.

Gradients giving a continuously decreasing migration rate for the analyte zone result in broader analyte peaks than if eluted isocratically; the front part of the analyte zone moves under conditions which speed up the migration rate as compared with the rear part. Analyte elution at the rear part of the positive co-ion system peak or at the front part of the negative one [10] will therefore lead to broadening (Fig. 1a, positions II and III), as well as analyte elution at the front part of the positive counter-ion system peak or at the rear part of the negative one (Fig. 1b, positions I and IV).

If the analyte is eluted only partly in a co-ion or counter-ion gradient, peak deformation or splitting occurs [14]. Splitting also occurs at high analyte concentrations in a gradient normally giving a compressed analyte peak [10].

Even if the analyte zone is separated from the system zone at the column outlet, they have been eluted together at an earlier stage of their migration along the column. The distortions may therefore also occur, albeit with less pronounced effects, if the analyte is eluted before or after the actual system peak concentration gradient appearing at the column outlet.

To investigate the effects of system peaks on analyte peaks eluting earlier or later than the system peak, the analytes were injected either in pure buffer (lacking protriptyline), yielding positive system peaks, or in buffer–acetonitrile (*i.e.* eluent lacking protriptyline), giving negative system peaks. The two situations were experimentally evaluated in a system with 0.91 m*M* protriptyline in buffer–acetonitrile as eluent. UV detection was performed at 337 nm, giving selective information about protriptyline; for this purpose the non-selective and non-sensitive RI detection could not be used. The initial conditions for the two situations are schematically shown (at the moment after the equilibria disturbance) in Fig. 2a and b. In both cases protriptyline diffuses into the injection zone from the bulk eluent and from the mobile phase ahead of the injection zone. In the case of buffer injection there will be an increased adsorption of protriptyline to the stationary phase as the protriptyline molecules reach the buffer zone (Fig. 2a). The mobile phase shortage of protriptyline in the injection zone is eluted with the non-retained buffer, while the stationary phase excess of protriptyline in the injection zone is eluted as a positive system zone. The zones appear as a negative front peak and a positive system peak on the chromatogram, respectively (Fig. 3a). An increased level of the baseline was observed; this started at the rear part of the negative front peak and continued until the positive system peak (Fig. 3a). This phenomenon could not be explained; it may be connected to the large disturbance of the acetonitrile equilibrium.

The analytes are adsorbed more strongly in

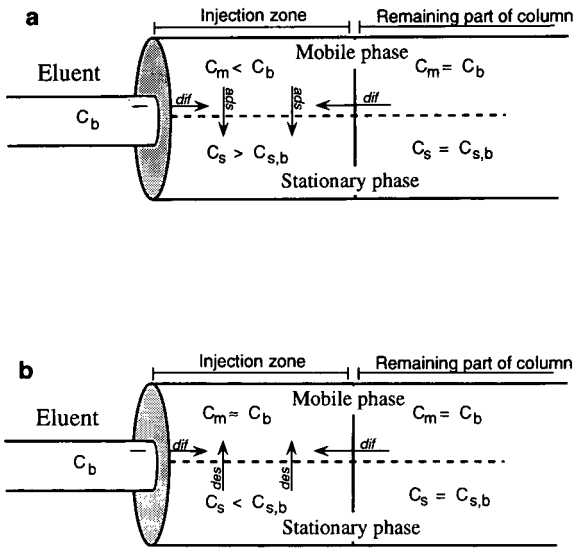

Fig. 2. Schematic illustration of the conditions in the injection zone after injection of (a) buffer and (b) buffer–acetonitrile into a system equilibrated with protriptyline in buffer–acetonitrile. C_m and C_s are the actual mobile phase and stationary phase concentrations of protriptyline, respectively. C_b is the bulk concentration of protriptyline and $C_{s,b}$ the stationary phase concentration at equilibrium with the bulk. The arrows indicate the diffusion (dif), adsorption (ads) and desorption (des) processes.

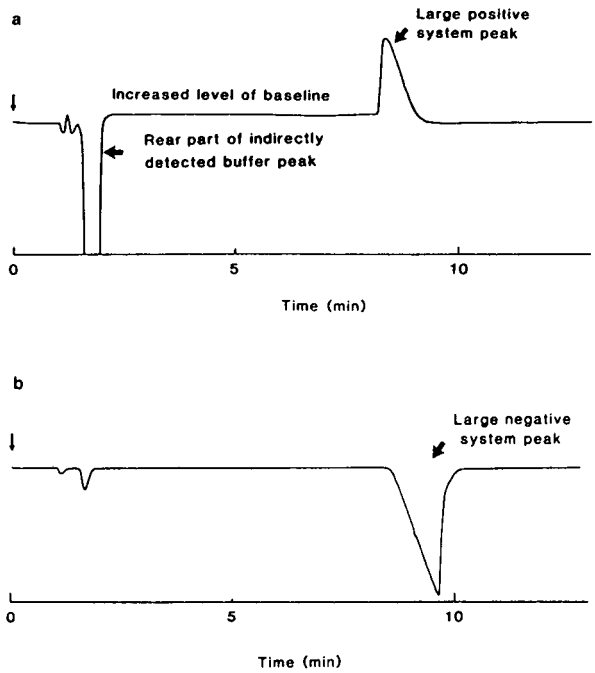

Fig. 3. Injection of (a) buffer or (b) buffer–acetonitrile into a chromatographic system equilibrated with protriptyline. Sample: 100 μl of (a) buffer or (b) eluent without protriptyline. Eluent: 0.91 mM protriptyline in phosphate buffer (pH 1.9, ionic strength = 0.05)–acetonitrile (3:1). Column: Nucleosil C_{18} (100 × 4.6 mm). UV detection was performed at 337 nm.

the buffer zone than in the other regions in the column; this causes enhanced enrichment of the incoming analyte solution, but also a gradient effect caused by the rear part of the buffer zone on the analyte zone before resolving. In Fig. 3a, the buffer zone is indirectly detected as a negative protriptyline peak in the front. The rear part of the buffer zone will consist of a steeply increasing organic amine gradient as well as a steeply decreasing buffer gradient; both gradients would have narrowing effects on co-eluting cationic analytes, but for anionic analytes the opposite effect would be caused by the amine (counter-ion) gradient. However, the closer the anionic analytes were eluted to the buffer zone, the narrower the analyte peak was compared with the injection in eluent. This indicates that the decreasing buffer gradient, causing a narrower analyte zone, dominates in effect over the increasing counter-ion gradient in this case.

When eluent lacking protriptyline was injected, some of the protriptyline molecules adsorbed to the stationary phase will desorb and diffuse to the mobile phase in the injection zone (Fig. 2b). This leaves a shortage of protriptyline in the stationary phase in the injection zone to elute as a negative system peak, which can be seen on the chromatogram in Fig. 3b.

Effects of counter-ion system peaks

Anionic analytes were dissolved in buffer and injected into a chromatographic system containing 1.4 mM DMOA (counter-ion) in the eluent (Fig. 4a). The positive DMOA system peak was detected by RI detection. The first anion peak had a smaller retention volume than the system peak and was deformed owing to its initial elution with the increasing counter-ion concentration in the front part of the system peak (Fig. 1b, position I). When the eluent was used as injection solvent, the positive system peak was much smaller and the first anion peak became well shaped (Fig. 4b). The second anion peak

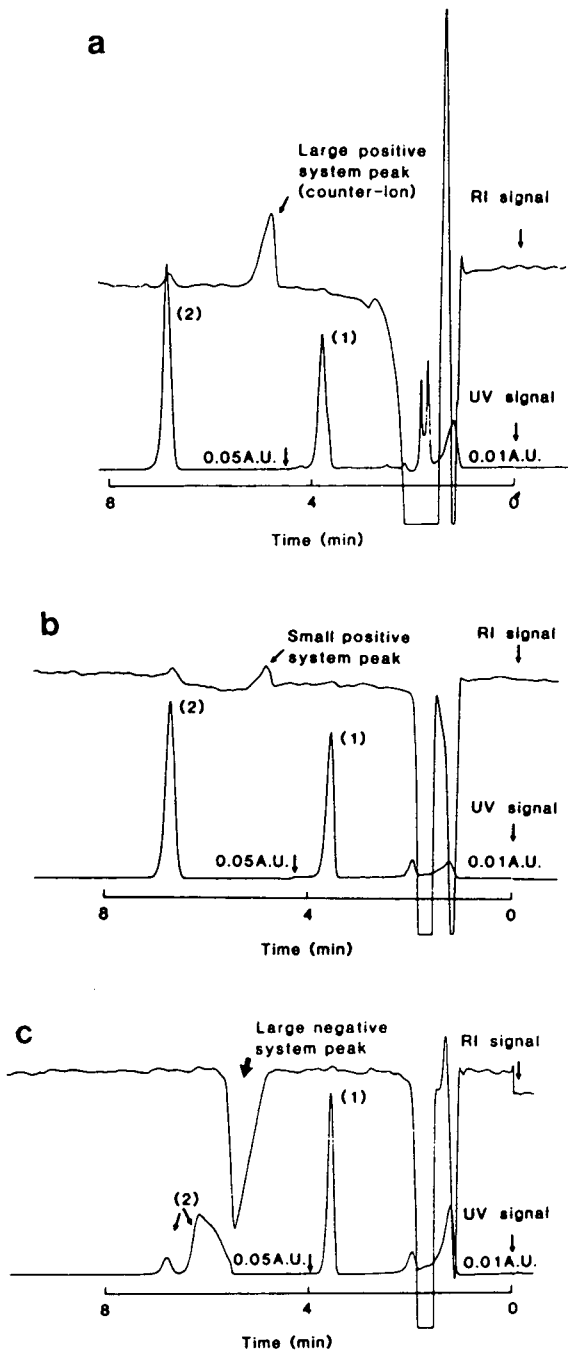

Fig. 4. Effects on anionic analyte peaks at elution before or after a counter-ion system peak. Sample: 100 μl of 10 μM (1) sodium naphthalene-2-sulphonate and (2) sodium anthraquinone-2-sulphonate in (a) buffer, (b) eluent, (c) eluent without N,N-dimethyloctylamine (DMOA). Eluent: 1.4 mM DMOA in phosphate buffer (pH 2.6, ionic strength = 0.1)–acetonitrile (3:1). Column: Spherisorb ODS-1 (100 × 4.6 mm).

had a longer retention time than the system peak, thus the anion had initially eluted at the decreasing counter-ion concentration in the rear part of the system zone (Fig. 1b, position II). The anion peak width was narrower when the buffer was used as injection solvent (Fig. 4a) as compared with the isocratic conditions (Fig. 4b). However, the reduction in peak width was not stronger than that expected, because of the initial enrichment effect on the column top caused by the buffer.

The anions were also dissolved in eluent lacking DMOA prior to injection, which resulted in a negative DMOA system peak (Fig. 4c). Now, the first anion peak is compressed compared with the eluent as injection solvent (Fig. 4b). In this case the anion is not adsorbed more strongly in the injection zone than in the other regions in the column. The reduction in peak width was only due to the initial elution of the anion with the decreasing counter-ion concentration in the front part of the negative system zone (Fig. 1b, position III).

The more retained anion was eluted partly with the increasing counter-ion concentration gradient in the rear part of the negative system zone and partly after the system zone and the anion peak was severely deformed and even split (Figs. 4c and 1b, position IV).

Effects of positive co-ion system peaks

Cationic analytes, which were eluted before or after the positive co-ion system peak (created by injecting the analytes dissolved in buffer), were affected only if they were eluted very close to the system peak. When the analytes were eluted before the system peak, the increased adsorption in the buffer zone also resulted in narrower analyte peaks compared with the injection in the eluent and it was not possible to discriminate between the two effects. Therefore, another approach, resulting in basically the same situation, was used to investigate the effects.

With Kromasil C_{18} as the stationary phase the amine analytes showed peak tailing to a lesser degree than with Nucleosil C_{18} and Spherisorb ODS-1. It was possible to separate the analytes with good peak symmetries without adding an organic amine to the eluent (Fig. 5a). When 2.0

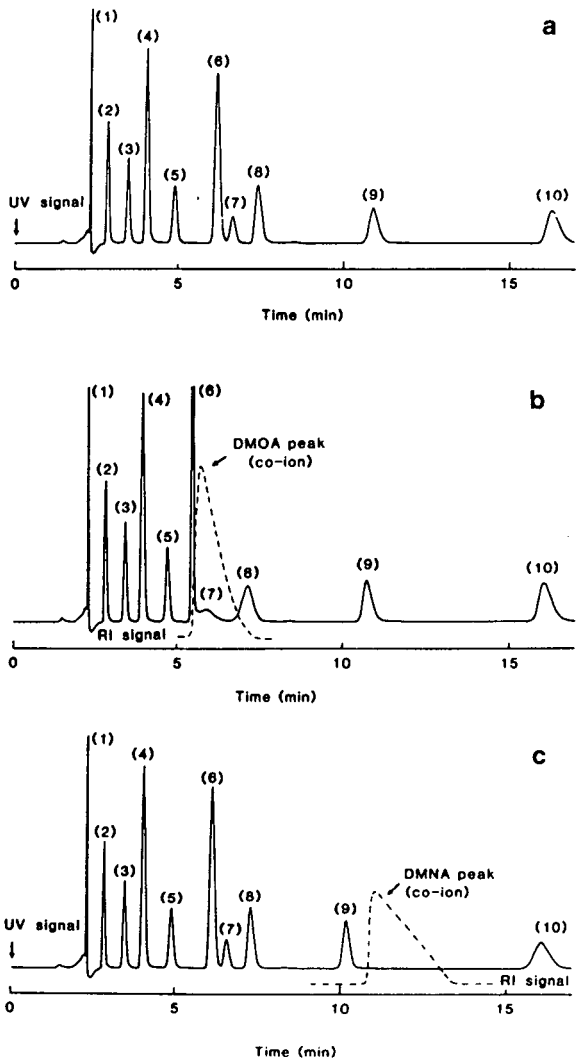

Fig. 5. Effects on cationic analyte peaks upon elution with a large amount of a hydrophobic co-ion added to the sample. Sample: 100 μl of 10 μM analytes in (a) buffer (reference rune), (b) buffer with 2.0 mM N,N-dimethyloctylamine (DMOA), (c) buffer with 2.0 mM N,N-dimethylnonylamine (DMNA). Analytes; 1 = atenolol; 2 = metoprolol; 3 = FLA 731; 4 = pronethalol; 5 = FLA 913; 6 = propranolol; 7 = alprenolol; 8 = FLA 797; 9 = FLA 870; 10 = FLA 659. Eluent: phosphate buffer (pH 2.9, ionic strength = 0.05)–acetonitrile (7:3). Column: Kromasil C_{18} (150 × 4.6 mm). The RI signal is slightly delayed compared with the UV signal because of the dead volume between the two detectors.

mM DMOA was added to the injection solution, propranolol was eluted with the steeply increasing co-ion concentration in the DMOA front; hence the propranolol was compressed (Fig. 5b). Even if the injection conditions differ from the situation with a positive system peak, the conditions for propranolol were basically the same as shown in Fig. 1a, position I. This situation has been described for two-component mixtures by Katti and Guiochon [20] and the effects have been utilized to increase the production rate of especially the first-eluting component in preparative chromatography.

The large DMOA peak was detected by RI detection; its signal was incorporated from the RI trace as a dotted line alongside the UV signal. Alprenolol was eluted directly after propranolol, together with the steeply decreasing co-ion concentration in the initial rear part of the large DMOA peak, and its peak was largely deformed. FLA 797 was eluted with the last rear part of the DMOA peak; and this peak was also broadened but to a smaller extent (*cf.* Fig. 5a). The cationic analytes which were eluted after the DMOA peak were not affected. Of the cationic analytes that were eluted before the large DMOA peak, only the two peaks closest to the DMOA front were affected, *i.e.* pronethalol and FLA 913. They were slightly narrower and higher than in the run without addition of DMOA in the injection solution (Fig. 5a).

The more hydrophobic DMNA (2 mM) was added to the injection solution and its large peak had a position between FLA 870 and FLA 659 (Fig. 5c). The FLA 870 peak was narrower and the FLA 659 peak was broader and both their retention volumes were decreased in comparison with the experiment without addition of DMNA in the injection solvent (Fig. 5a). The cationic analytes eluting earlier than FLA 870 were not significantly affected. In this case FLA 659 was closer to the rear part of the large amine peak than FLA 870 was in the earlier example (Fig. 5b), when no effects on its peak shape were observed.

Effects of negative co-ion system peaks

Cationic analytes are deformed at the front part of the negative co-ion system peak and compressed at the steeply increasing co-ion concentration in the rear part (Fig. 1a, positions III and IV). In a system containing 0.91 mM protriptyline in the eluent and Nucleosil C_{18} as

stationary phase, 100 μl of 10 μM FLA 797 were injected dissolved in eluent lacking protriptyline. FLA 797 was eluted before the negative system peak and was broader than in the experiment in which it was dissolved in eluent (containing protriptyline), despite a rather large separation factor of 1.7. The peak width increased from 0.32 to 0.39 ml.

When a cationic analyte was eluted after the negative system peaks (created in this way), it was only affected if it was eluted very soon after the negative system peak. In systems containing about 1 mM protriptyline or DMOA the separation factor between the analyte peak and the system peak had to be 1.3 or less, in order to give reductions in analyte peak widths.

An example of how confusing these effects on the analyte peaks can be, when only the analytes are detected, is shown in the chromatogram in Fig. 6a; the second peak is broader than the third peak. Four different cations (substituted benzamides) at a concentration of 10 μM were injected dissolved in eluent lacking PT in a system with 0.94 mM PT in the eluent. The reason for the anomalous peak-width behaviour is revealed when the position of the negative system peak is made visible by the detector (Fig. 6b).

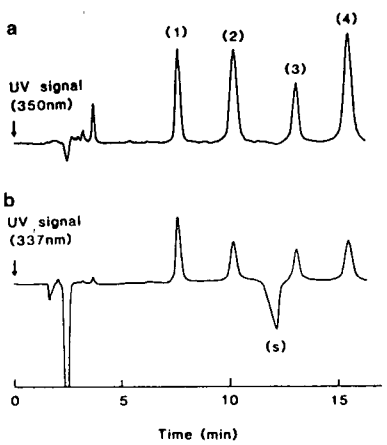

Fig. 6. Weak peak-broadening and peak-narrowing effects on cationic analytes due to elution slightly before and slightly after the negative protriptyline (co-ion) system peak, respectively. (a) The UV signal detected only the analytes (350 nm). (b) The system zone (s) was also visualized (337 nm). Sample: 100 μl of 10 μM (1) FLA 797, (2) FLA 870, (3) FLA 965 and (4) FLA 659 in eluent lacking protriptyline. Eluent: as in Fig. 3 (but 0.94 mM PT). Column: Nucleosil C_{18} (150 × 4.6 mm).

Comparison between the effects of co-ion and counter-ion system peaks

In the chromatographic systems described above, the magnitudes of the analyte peak-broadening and -deforming effects were generally larger than the analyte peak-width reductions. In addition, the deformations were much larger in situations when the analytes were affected by a counter-ion gradient compared with a co-ion gradient. The initial adsorption of the analytes was stronger when injected in buffer than when eluent lacking the amine was used as injection solvent (compare Figs. 2 and 3). This fact, in combination with the larger sizes of the negative system peaks compared with the positive ones, is probably the explanation for the stronger effects when analytes were eluted close to the negative system peaks. This is valid for analytes with similar separation coefficients to the different system peaks in the chromatographic systems.

Parameters determining the degree of the distortions

The distortions of analyte peaks which are resolved from large system peaks are especially serious at short separation distances, at large injection volumes and analyte loads and at high bulk concentrations of the organic ion in the eluent. The effects on the analyte peaks from the initial migration together with the large system peak decreased generally with increasing separation at the column outlet. This tendency is evident from the chromatograms in Fig. 5b and c.

In case of a larger injection volume containing either buffer or eluent without the organic amine (or any other equilibrium disturbance agent), an increased amount of the mobile phase components will be redistributed in the injection zone. The system zone of the organic amine will contain a larger deviation from the eluent and its interaction with the analyte zones will consequently be increased.

The effects of increasing the amount of analyte injected were also important. A 100-μl aliquot of 0.01 mM anionic analyte dissolve in buffer was

injected into a system with 0.9 m*M* DMDA in the eluent. The anion peak seemed to be well shaped and had a much smaller retention volume than the positive system peak of the counter-ion (Fig. 7a). When a ten-fold higher analyte concentration was injected, again with the analyte dissolved in the buffer, the analyte peak was broad and deformed (Fig. 7b). The interactions between the analyte and the counter-ion system peak increased because not only the system peak but also the analyte peak involved a large concentration deviation from the eluent. The same tendency was observed when a hydrophobic counter-ion was injected together with the analytes instead of having the counter-ion incorporated in the eluent [12].

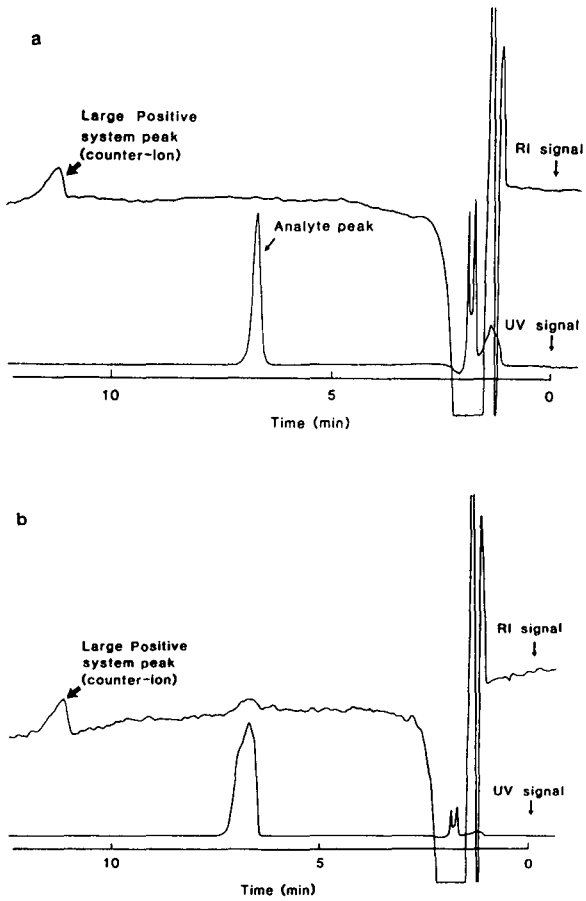

Fig. 7. Effects on an anionic analyte peak at elution well separated in front of a positive counter-ion system peak (DMDA) at (a) low and (b) high analyte concentration. Sample: 100 μl of sodium naphthalene-2-sulphonate in buffer: (a) $C_{analyte} = 10\ \mu M$; (b) $C_{analyte} = 0.1$ m*M*. Eluent and column: as in Fig. 4 but 0.9 m*M* N,N-dimethyldecylamine (DMDA) was added to the eluent.

Larger positive or negative system peaks are obtained with increasing bulk concentration of the actual eluent component when the same concentration of an equilibrium disturbance agent is injected [1,2,5,11]. This is because of the comparatively larger amounts of adsorbed and/or desorbed eluent component in the injection zone. Anionic analyte peaks were therefore more affected by the system peak of the counter-ion at higher bulk concentrations of the counter-ion. As an example, distortion of the anionic analyte peaks demonstrated in Fig. 4 was found at a concentration of the counter-ion (DMOA) in the eluent of 1.4 m*M*. At a three times lower counter-ion concentration in the eluent, no analyte peak distortions could be observed at otherwise similar conditions.

Design of systems avoiding peak deformations

System peaks will develop at all times when a sample deviating from the eluent is injected. Large deviations result in large system peaks, which means that the introduction of complex matrices, such as biological fluids or extracts thereof, may cause disturbances of analyte peak shapes due to interfering system peaks. It is therefore essential to be aware of such risks, and the use of RI detectors is recommended in order to reveal the existence of such peaks during the development of assay methods for complex matrices [13].

Parameters determining the selectivity between the analyte and the system peak have been outlined earlier; essential factors are the pH and the ionic strength of the buffer [8,13,21]. The concentration and character of the organic ion are very important parameters, especially in its role as a counter-ion towards the analytes, but may also be important when it acts as a co-ion [11]. Large effects on the selectivity due to batch variations of the solid phase have also been observed [9,13].

For the more common positive system peaks, the conditions chosen should be such that the system peak is eluted before the analytes, since the effects on analyte elutions after the positive

system peaks are rather weak. The injection volume should be as small as possible and the analytes should be dissolved in the eluent whenever possible. In quantitative determinations, peak-area measurements are to be preferred to peak-height measurements to avoid errors due to slight changes in the widths of the analytes or of the internal standard [13].

Peak deformation of a cationic analyte using an organic amine as co-ion in the eluent can often be easily eliminated by changing to a more hydrophilic co-ion. The retention of the system peak will decrease and the retention of the analytes will increase. Then the co-ion concentration can be tuned until suitable analyte retentions are obtained.

When analytes are separated using an organic ion as counter-ion, it is often necessary to have a hydrophobic counter-ion that may elute rather close to the analytes. Serious disturbances due to the risk of more severe deformations in such systems may arise even when the analytes are separated from the system peak in the column outlet. If peak deformation occurs, a change in the concentration of the counter-ion should be made to improve the analyte separation from the system peak. A positive system peak should preferably be regulated to elute before the analyte, whereas a negative system peak should elute after the analyte. The retention of the analyte will increase at an increasing counter-ion concentration and the retention of the system peak is decreased, giving a higher separation factor between the anion and the system peak.

ACKNOWLEDGEMENTS

We thank Dr. Anders Sokolowski for fruitful discussions. This project was financially supported by The Swedish Natural Science Research Council (NFR).

REFERENCES

1 S. Levin and E. Grushka, *Anal. Chem.*, 58 (1986) 1602.
2 S. Levin and E. Grushka, *Anal. Chem.*, 59 (1987) 1157.
3 S. Golshan-Shirazi and G. Guiochon, *Anal. Chem.*, 62 (1990) 923.
4 G. Schill and E. Arvidsson, *J. Chromatogr.*, 492 (1989) 299.
5 A. Sokolowski, T. Fornstedt and D. Westerlund, *J. Liq. Chromatogr.*, 10 (1987) 1629.
6 R.M. Cassidy and M. Fraser, *Chromatographia*, 18 (1984) 369.
7 L.B. Nilsson and D. Westerlund, *Anal. Chem.*, 57 (1985) 1835.
8 L.B. Nilsson, *J. Chromatogr.*, 506 (1990) 253.
9 L.B. Nilsson, *J. Chromatogr.*, 591 (1992) 207.
10 T. Fornstedt, D. Westerlund and A. Sokolowski, *J. Liq. Chromatogr.*, 11 (1988) 2645.
11 T. Fornstedt, D. Westerlund and A. Sokolowski, *J. Chromatogr.*, 506 (1990) 61.
12 T. Fornstedt, D. Westerlund and A. Sokolowski, *J. Chromatogr.*, 535 (1990) 93.
13 T. Fornstedt, *J. Chromatogr.*, 612 (1993) 137.
14 T. Arvidsson, *J. Chromatogr.*, 407 (1987) 49.
15 M. Johansson and D. Westerlund, *J. Chromatogr.*, 452 (1988) 241.
16 A. Tilly-Melin, Y. Askemark, K.-G. Wahlund and G. Schill, *Anal. Chem.*, 51 (1979) 976.
17 A. Tilly-Melin, M. Ljungcrantz and G. Schill, *J. Chromatogr.*, 185 (1979) 225.
18 S. Levin and S. Abu-Lafi, *J. Chromatogr.*, 556 (1991) 277.
19 K. Slais, M. Krejcí and D. Kourilová, *J. Chromatogr.*, 352 (1986) 179.
20 A. Katti and G. Guiochon, *Adv. Chromatogr.*, 31 (1992) 1–118.
21 B.A. Bidlingmeyer and F.W. Warren, *Anal. Chem.*, 54 (1982) 2351.

Journal of Chromatography, 648 (1993) 325–331
Elsevier Science Publishers B.V., Amsterdam

CHROM. 25 337

Hummel–Dreyer method in high-performance liquid chromatography for the determination of drug–protein binding parameters

S.F. Sun* and C.L. Hsiao

Department of Chemistry, St. John's University, Jamaica, NY 11439 (USA)

(First received March 9th, 1993; revised manuscript received May 25th, 1993)

ABSTRACT

Two types of Hummel–Dreyer elution pattern were developed, one with a positive peak followed by a negative peak and the other with two positive peaks. The evaluation of the area of the second peak, whether positive or negative, makes it possible to determine the value of L_b (the number of moles of the ligand bound to macromolecule) or $[L]_b$ (the concentration of the ligand bound to macromolecule). Three techniques were employed for the evaluation of the area: planimeter, geometry and integrator. Planimeter and geometry can be used for both types of elution profiles and for both external calibration and internal calibration. The integrator can only be used for the second type of elution profile, namely two positive peaks and hence, can only be used in conjunction with internal calibration. The results in terms of the two binding parameters, n (the number of binding sites) and k (the affinity constant) in binding equilibrium for L-tryptophan–bovine serum albumin system were compared. Realizing that uncertainty involved is large for the binding studies in any experimental method for the binding studies, we believe that any of the five combinations (among external calibration, internal calibration, planimeter reading, geometry reading and integrator reading) would lead to a reasonably accurate result.

INTRODUCTION

The Hummel–Dreyer method [1] in high-performance liquid chromatography (HPLC) has been demonstrated as a useful tool for the determination of drug–protein binding parameters [2,3]. The chromatogram shows a positive peak, which represents the drug–protein complex, followed by a negative peak, which represents the elution volume (or time) of the drug. It is the negative peak that provides the information about the amount of the drug bound to the protein. The evaluation of the area of the negative peak makes it possible to calculate $[L]_b$ or L_b, where $[L]_b$ is the concentration of bound drug in M and L_b is the absolute quantity of bound drug in mol. Experimentally, $[L]_b$ is obtained with external calibration technique and L_b is obtained with an internal calibration technique [4,5].

However, a Hummel–Dreyer pattern of elution profile does not have to be in the form of a positive peak followed by a negative peak. Instead, we can have two positive peaks [6–8]. This is done by adjusting the concentration of drug in the protein sample solution in a reasonable excess over that in the eluent.

Thus, there are two different patterns to run a Hummel–Dreyer experiment. In either pattern, the evaluation of the area of the second peak is a time-consuming process. So far there is no way to tell which pattern is superior over the other. It all depends on which pattern is easy to be dealt

* Corresponding author.

0021-9673/93/$06.00

with in the evaluation of the area of the second peak. In this paper we compare three different techniques for the evaluation of the area of the second peak: planimeter, integrator and geometry. The first two techniques are not new, whereas the third one perhaps is the first time to be described in detail in HPLC. Since the evaluation of the area of a curve is a common problem in many fields such as diffusion and sedimentation, we believe the techniques we learn in HPLC could be extended to the other experimental fields and *vice versa*. As a test system, we choose L-tryptophan–bovine serum albumin (BSA) binding for study. Not only the subject is of great interest in biochemistry and pharmacology [9–11], but also data obtained from different experimental methods, *e.g.* equilibrium dialysis, is abundant in literature. Hence, it is relatively easy to asses the validity of a new method to be introduced.

EXPERIMENTAL

Materials

L-Tryptophan (lot No. 6766) was obtained from Mann Research Lab. (New York, NY, USA) and BSA (lot No. 29F9315) was a product of Sigma. Sodium hydrogenphosphate and sodium dihydrogenphosphate were reagent grade of J.T. Baker. All the chemicals were used as received. Glass-distilled water was used in all experiments.

Preparation of solutions

The procedure for the preparation of solutions was similar to the one described in previous publications [4,5]. Table I describes the preparation of the mobile phase of L-tryptophan solutions and Table II describes the preparation of protein–tryptophan samples to be injected onto the column. In the preparation of mobile phase, we diluted the stock solution (77.2 μM) into five different concentrations. Those mobile phases selected in Table I are best for the internal calibration measurement. Samples A, B, C, D, E in Table II were prepared for the internal calibration technique and F and G were prepared for the external calibration technique.

TABLE I

PREPARATION OF MOBILE PHASE

Stock solution: L-tryptophan, 77.2 μM; phosphate buffer 0.05 M, pH 7.4.

Mobile phase	L-Trp (ml)	Buffer (ml)	Dilution factor	$[L]_f$ (μM)
1	200	1300	0.14	10.3
2	400	1100	0.28	20.6
3	500	1000	0.35	25.7
4	600	900	0.42	30.9
5	800	700	0.56	41.2

Chromatography

The size-exclusion chromatography was carried out at room temperature (near 25°C) with one Waters Assoc. pump A-6000, an injector UK-2, an UV variable-wavelength detector, a recorder and a Hewlett-Packard integrator 3965. The column used was Waters I-125 (30 cm × 7.8 mm I.D., particle size 37–53 μm). This column is not an ideal one, but it is easily accessible.

Evaluation of the peak area

As mentioned before, we used three entirely different methods for the estimation of the second peak in the chromatogram.

Planimeter. Planimetry is the oldest and classi-

TABLE II

PREPARATION OF PROTEIN–TRYPTOPHAN SAMPLES

Stock solutions: L-tryptophan, 77.2 μM; BSA, 495 μM; phosphate buffer 0.05 M, pH 7.4.

Sample	BSA solution (ml)	L-Trp solution (ml)	Buffer (ml)
A	2.0	9.0	4.0
B	2.0	10.0	3.0
C	2.0	11.0	2.0
D	2.0	12.0	1.0
E	2.0	13.0	0
F	2.0	0	13.0
G	0	0	15.0

cal technique. It is reasonably reliable and it can be applied to any shape of the graph. But it is tedious and it requires the techniques of the user. In previous publications [4,5] this technique was used exclusively for the evaluation of area.

The integrator. The integrator available to us such as Hewlett-Packard 3395 cannot be used for the evaluation of the area of a negative peak. For this reason it cannot be used for the external calibration method to determine the binding parameters. It can only be used for the internal calibration method with a two-positive-peak elution profile. However, since the data of the area are automatically printed out, the integrator is the best tool to save time in reading the area.

Affine geometry. We believe this is the first time affine geometry is introduced to estimate the area of a peak in scientific research. For this reason, we shall describe the geometry briefly. According to affine geometry, for any triangle ABC with the coordinates of three vertices known, namely, $A(x_1,y_1)$, $B(x_2,y_2)$ and $C(x_3,y_3)$, the area can be accurately calculated in terms of the following determinant:

$$A = 1/2 \begin{vmatrix} x_1 & y_2 & 1 \\ x_2 & y_2 & 1 \\ x_3 & y_3 & 1 \end{vmatrix}$$

This theorem has been rigorously proved [12]. In a HPLC chromatogram, the peak or trough is often shown almost as a triangle. This is particularly so when the column is new or the number of theoretical plates is high. If the units of x and y coordinates are cm, then the area is in cm^2; if in inch (1 in. = 2.54 cm), then $in.^2$. We can even choose any arbitrary units as is the case with integrator, since the final scale is the concentration of the ligand.

RESULTS AND DISCUSSION

Fig. 1 shows a representative elution profile of L-tryptophan–BSA binding. This is a regular Hummel–Dreyer pattern with one positive peak followed by a negative peak. Here we used the external calibration method. The left part profile has one peak only, (the negative peak), which is

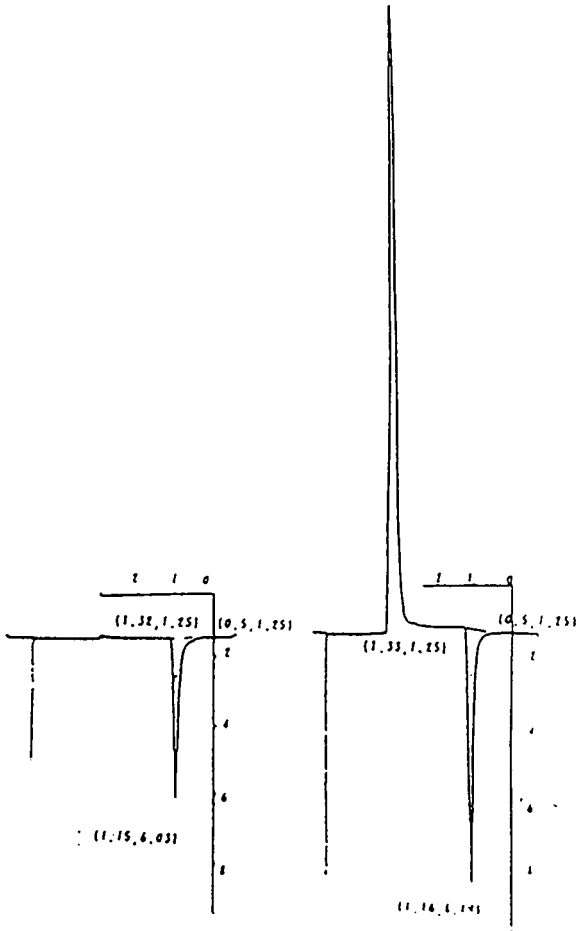

Fig. 1. Elution profile of the binding of L-tryptophan to BSA. Column: Protein Pack I-125 (Waters Assoc.), Detector: UV at 280 nm, 0.4 AUFS. Flow-rate: 1.0 ml/min. Mobile phase: 10.29 μM (see Table I). Sample: 100 μl of G and F (see Table II).

used for the correlation of the peak area with the concentration of the L-tryptophan. Such a correlation is expressed in Fig. 2. Since our integrator was not used for the external calibration method, we do not have integrator data for the correlation. Fig. 2 presents the results of only two techniques. The standard deviation for each value of the area is not shown in order to maintain the clarity of the graph. The uncertainty is within 2%. For example, the numerical values for the first pair in Fig. 2 are 0.74 ± 0.01 (planimeter); 0.82 ± 0.02 (geometry), both in the unit of cm^2.

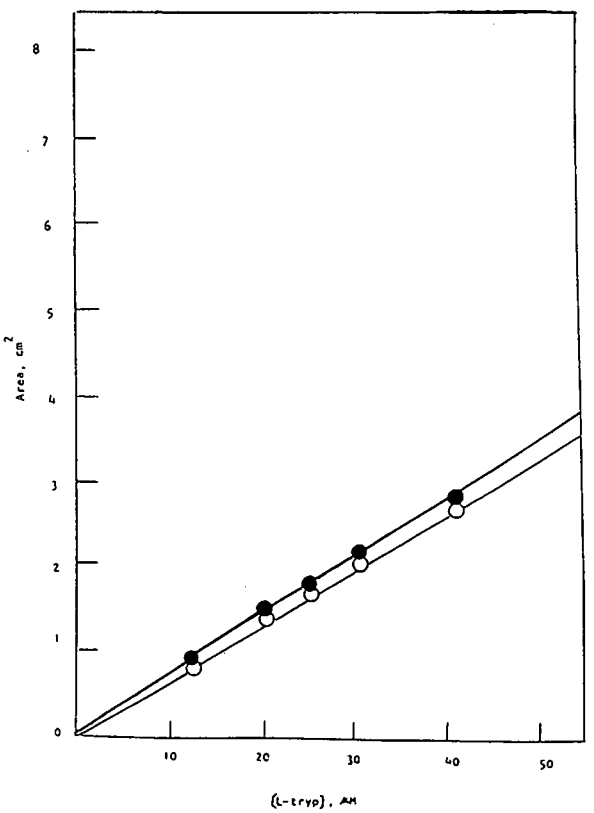

Fig. 2. Correlation of the area of the negative peak with the concentration of L-tryptophan for the external calibration method using planimeter and geometric calculation methods. ● = Geometric calculation; ○ = planimeter.

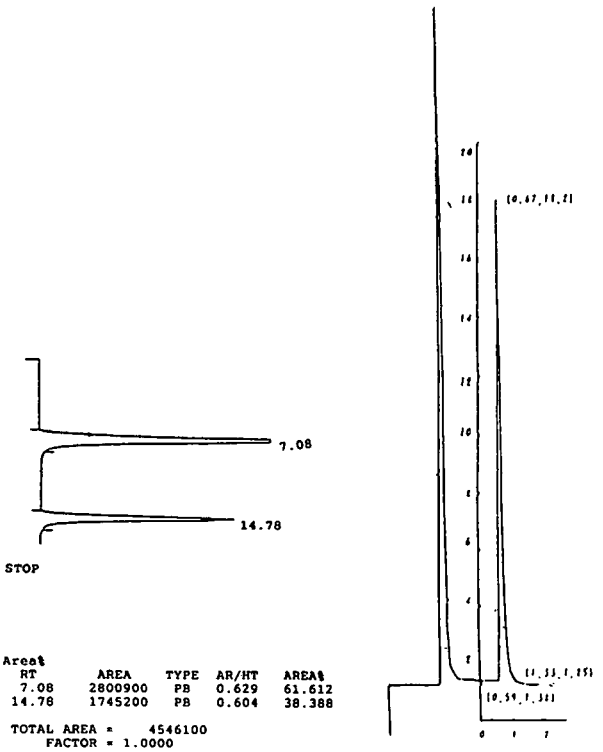

Fig. 3. Elution profile of the binding of L-tryptophan to BSA. Column: Protein Pack I-125 (Waters Assoc.), Detector: UV at 280 nm, 0.4 AUFS. Flow-rate: 100 μl of B (see Table II). Area measured by integrator and geometric calculation methods. RT = Retention time in min; AR = area; HT = height; PB = peak separation code.

The negative peak area of the right profile in Fig. 1 is converted to $[L]_b$ by reading the calibration curve (a straight line) in Fig. 2. The coordinates of the triangular vertices are indicated in both negative peaks, (one for the correlation and the other for the determination of $[L]_b$). These are used for geometric calculations. To use planimetry for the estimation of the area, no such coordinates are necessary. Although there is some discrepancy between geometry and planimeter readings as shown in the calibration curve (Fig. 2), such a discrepancy is rather negligible in view of the certain uncertainty involved in the experiment.

Fig. 3 shows a representative profile of L-tryptophan–BSA binding, using the internal calibration method. In order to emphasize the use of the integrator, we choose the two-positive-peak pattern as representative. For a two-positive-peak profile, we can use all the three techniques (planimeter, integrator and geometry) to evaluate the area of the second peak, and we did use all the three techniques. The left part in Fig. 3 was printed by the integrator with elution time and areas on the same paper; this is for illustration only. The right part pattern was obtained simultaneously with the left part pattern by the regular recorder which we used for planimeter and geometry readings. The coordinates are given to indicate the use of geometrical calculation. In the internal calibration method we do not need a correlation graph between the area and the concentration of L-tryptophan as in the external calibration. Instead we plot the area *versus* the amount of L-tryptophan in mol in five different mobile phases, each of which was

injected with five samples of different L-tryptophan concentrations, respectively. The extrapolation to zero abscissa gives the quantity L_b, the absolute amount of tryptophan bound to the protein. Such plots are shown in Figs. 4, 5, 6. They represent three different methods for the evaluation of areas: planimeter, integrator and geometry. Again, the uncertainty in each experiment point with respect to area is within 2%. The scatter is somewhat greater with the integrator than with the other two techniques.

In Tables III and IV we list the calculations of binding quantities $\bar{r}$ and $\bar{r}/[L]_f$, where $[L]_f$ is the concentration of free L-tryptophan. Table III is based on external calibrations while Table IV is based on internal calibrations. We use the concentration of L-tryptophan in the mobile phase as the concentration of free L-tryptophan in the dynamic equilibrium. The Scatchard plot is shown in Fig. 7. The five straight lines represent the results of five different techniques. They do not superimpose into a single line, but the experimental points cluster reasonably together, indicating the feasibility in using any of them to study drug–protein binding phenomena. The integrator reading seems to show a relatively larger discrepancy from the other techniques. It is, however, the simplest, fastest and least labourious technique.

The binding parameters n and k are given in Table V. We see that the numerical values of

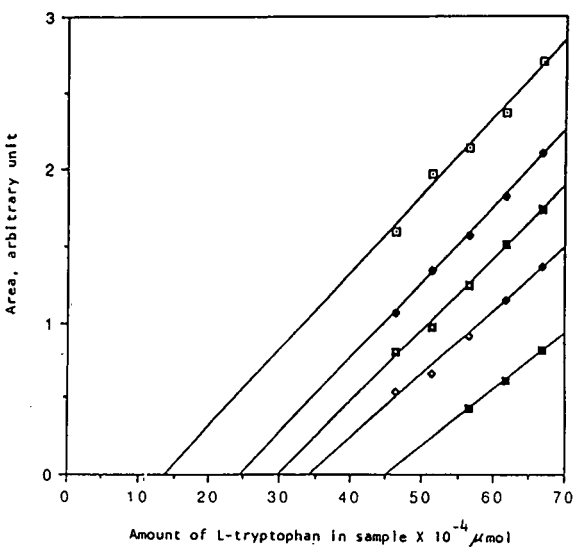

Fig. 4. Internal calibration for the determination of the amount of L-tryptophan that binds to BSA using the integrator method. Lines connect equal concentrations of L-tryptophan. From left to right: 10.29 μM, 20.58 μM, 25.73 μM, 30.87 μM, 41.16 μM.

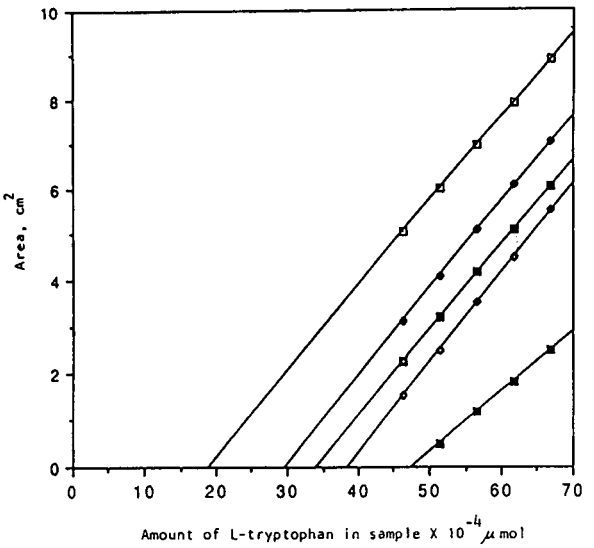

Fig. 5. Internal calibration for the determination of the amount of L-tryptophan that binds to BSA using the geometric calculation method. Concentrations of L-tryptophan as in Fig. 4.

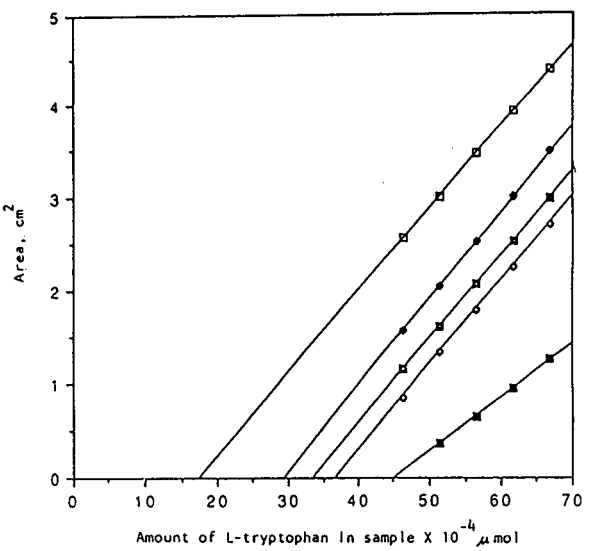

Fig. 6. Internal calibration for the determination of the amount of L-tryptophan that binds to BSA using the planimeter method. Concentrations of L-tryptophan as in Fig. 4.

TABLE III

L-TRYPTOPHAN–BSA BINDING BY EXTERNAL CALIBRATION ([p] = 66.09 μM; p = protein)

$[L]_f$ (μM)	$[L]_b$ (μM)	$\bar{r} = [L]_b/[p]$	$\bar{r}/[L]_f \times 10^4$
Planimeter			
10.3	17.5	0.265	2.60
20.6	28.9	0.437	2.10
25.7	33.0	0.499	1.90
30.9	38.1	0.576	1.90
41.2	45.4	0.687	1.70
Geometric calculation			
10.3	18.0	0.272	2.60
20.6	28.4	0.430	2.10
25.7	34.7	0.524	2.00
30.9	37.8	0.572	1.90
41.2	45.9	0.695	1.79

these two parameters are reasonably in agreement to each other. The n values are higher than those reported in the previous publication [5]. This is due to the fact that in ref. 5 the plot was not started from the origin. We believe that the

TABLE IV

L-TRYPTOPHAN–BSA BINDING BY INTERNAL CALIBRATION ($p = 66.09 \cdot 10^{-4}$ μmol; p = amount of protein)

Mobile phase $[L]_f$ (μM)	Intercept L_b ($\times 10^{-4}$ μmol)	$\bar{r} = L_b/p$	$\bar{r}/[L]_f \times 10^4$
Integrator			
10.3	14.0	0.212	2.06
20.6	24.0	0.363	1.76
25.7	28.0	0.424	1.65
30.9	32.0	0.484	1.60
41.1	38.0	0.575	1.40
Geometric calculation			
10.3	19.1	0.289	2.81
20.6	29.8	0.451	2.19
25.7	34.2	0.517	2.01
30.9	38.2	0.583	1.89
41.2	46.1	0.698	1.69
Planimeter			
10.3	17.4	0.263	2.55
20.6	29.4	0.445	2.16
25.7	33.6	0.509	1.98
30.9	37.0	0.559	1.81
41.2	45.2	0.683	1.66

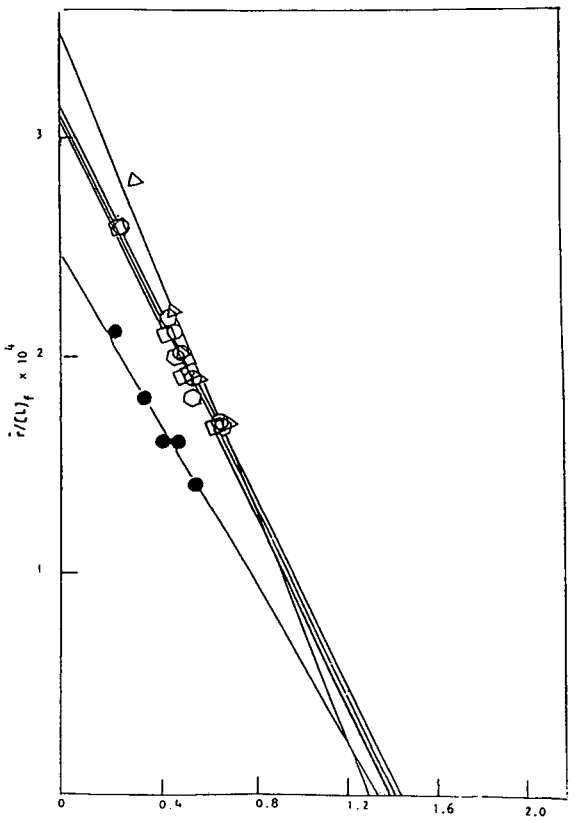

Fig. 7. Scatchard plot for the binding of L-tryptophan by BSA. ● = Internal by integrator; △ = internal by geometric calculation; ⬡ = internal by planimeter; □ = external by planimeter; ○ = external by geometric calculation.

results reported in this paper are more reliable than all those previously published including those classical ones [9–11]. The reason is that we reached the conclusions with two different methods (*i.e.* external calibration and internal cali-

TABLE V

BINDING PARAMETERS OF L-TRYPTOPHAN–BSA SYSTEM

Area evaluation method	Internal (I) or external (E)	n	$k \times 10^4$
Planimeter	I	1.41	2.22
	E	1.44	2.22
Geometric	I	1.29	2.72
calculation	E	1.43	2.21
Integrator	I	1.35	1.80

bration) and three different techniques (planimeter, integrator and geometry). The numerical values as listed in Table V, while not identical, are in good agreement within the experimental error.

CONCLUSIONS

On the basis of our experience in the study of binding of L-tryptophan to serum albumin using the Hummel–Dreyer method, we conclude that any of the following techniques would reach almost the same conclusion: external calibration/planimeter reading, external calibration/geometric reading, internal calibration/planimeter reading, internal calibration/geometric reading and internal calibration/integrator reading.

The choice of any method depends on experimental conditions including laboratory facilities available. We were reminded by a referee that nowadays integrators are available that can handle negative peaks . If that is the case, we shall be able to use an integrator to evaluate the areas of the peaks obtained with external calibration method as well as internal calibration method of the Hummel–Dreyer elution pattern. This would further facilitate the study of drug–protein bindings.

REFERENCES

1 J.P. Hummel and W.J. Dreyer, *Biochim. Biophys. Acta*, 63 (1962) 530.
2 B. Sebille, N. Thuaud and J.P. Tillement, *J. Chromatogr.*, 167 (1978) 159.
3 B. Sebille, R. Zini, C.V. Madjar, N. Thuaud and J.P. Tillement, *J. Chromatogr.*, 531 (1990) 51.
4 S.F. Sun, S.W. Kuo and R.A. Nash, *J. Chromatogr.*, 288 (1984) 377.
5 S.F. Sun and F. Wong, *Chromatographia*, 20 (1985) 495.
6 N. Yoza, *J. Chem. Educ.*, 54 (1977) 284.
7 N. Yoza, K. Kouchiyama, T. Miyajima and S. Ohashi, *Anal. Lett.*, 8 (1975) 641.
8 K. Kouchiyama, N.Yoza and S. Ohashi, *J. Chromatogr.*, 147 (1978) 271.
9 G.F. Fairclough and J.S. Fruton, *Biochemistry*, 5 (1966) 673.
10 R.H. McMenamy and J.L. Oncley, *J. Biol. Chem.*, 233 (1958) 1436.
11 C.J. Bowmer and W.E. Lindup, *Biochim. Biophys. Acta*, 624 (1980) 260.
12 H.S.M. Coxeter, *Introduction to Geometry*, Wiley, New York, 1961.

Journal of Chromatography, 648 (1993) 333–347
Elsevier Science Publishers B.V., Amsterdam

CHROM. 25 276

Chiral stationary phases based on intact and fragmented cellobiohydrolase I immobilized on silica☆

Ingrid Marle*, Stefan Jönsson, Roland Isaksson and Curt Pettersson

Department of Pharmaceutical Chemistry, Analytical Pharmaceutical Chemistry, Uppsala University, Biomedical Center, P.O. Box 574, S-751 23 Uppsala (Sweden)

Göran Pettersson

Department of Biochemistry, Uppsala University, Biomedical Center, P.O. Box 576, S-751 23 Uppsala (Sweden)

(First received January 21st, 1993; revised manuscript received May 3rd, 1993)

ABSTRACT

Cellobiohydrolase I (CBH I) was enzymatically degraded into two fragments which were immobilized on silica. Each fragment was shown to contain at least one enantioselective site for propranolol. The dominating enantioselective site of propranolol and other solutes is located on the main part of the enzyme —the core (C).

CBH I was immobilized via its carboxylic groups onto aminopropyl silica and via its amino groups to aldehyde silica. The CBH I–aminopropyl silica separates enantiomers with higher enantioselectivity than does the CBH I–aldehyde silica, whereas the latter phase promotes high retention. Slow adsorption–desorption kinetics dominates the band broadening process of solutes on CBH I–silicas. Addition of dimethyloctylamine to the mobile phase resulted in a significant improvement of the peak efficiency of β-blocking agents.

INTRODUCTION

Chiral stationary phases (CSPs) based on proteins are frequently and successfully used for separations of enantiomers of various kinds. Proteins commonly utilized as chiral selectors on these CSPs are macromolecules with molecular masses ranging from 25 000 to 70 000 and possessing complicated three-dimensional structures, thus displaying a multitude of possible interaction sites, stereospecific as well as non-stereospecific. The sites are frequently ligand specific and have different locations in the macromolecule [1–3]. The presence of such sites is indicated by the structurally great variety of chiral compounds separated on some of the protein-based materials [4]. Some such sites have been localized by means of enzymatic fragmentation of the proteins [5,6] and also by crystallographic methods [3]. One of the bovine serum albumin (BSA) fragments tested as chiral selector had lost enantioselectivity for some analytes and retained it for others as compared to the intact protein [5]. The poor loadability combined with the relatively low column efficiency limit the possibility to use these kinds of CSPs for tracing chiral substances, for instance, in biomatrices.

There are several ways to covalently immobilize proteins to a support, as they contain many functionalities. One can expect that chromato-

* Corresponding author. Present address: Pharmaceutical and Analytical R&D, Astra Pain Control AB, S-151 85 Södertälje, Sweden.

☆ Presented in part at *15th International Symposium on Column Liquid Chromatography, Basel, June 3–7, 1991.*

0021-9673/93/$06.00

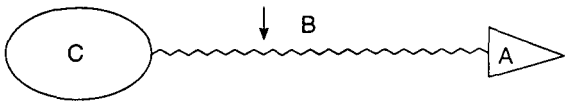

Fig. 1. Structural organisation of CBH I. C = Core, consisting of 425 amino acid residues; B = connecting region, consisting of 35 amino acid residues; A = cellulose-binding domain, consisting of 35 amino acid residues. Papain cleaves at the arrow.

graphic performance depends on the amount of protein as well as on the method used to immobilize it on the support [7]. A BSA–silica CSP obtained by adsorption of BSA on the silica was unable to differentiate between enantiomers of some sulphoxides [8] which were separable on the CSP with covalently immobilized BSA [9,10].

Compared to that for the intact protein, the column efficiency of chiral solutes on a CSP based on a fragment should be improved if the fragmentation strips off non-specific binding sites with high affinity and/or multiple stereospecific sites of the analyte. However, if the dominant stereospecific site shows slow adsorption and desorption kinetics for the analyte, *i.e.*, is rate determining, no significant improvement of the efficiency should be expected. As a consequence of the lower molecular mass of the fragment compared to the intact protein it should be possible to covalently bind a higher molar amount of fragment sites to the support and thus improve the loadability of analytes.

The cellulase, cellobiohydrolase I (CBH I), can easily be cleaved enzymatically into two fragments, as indicated by the arrow in Fig. 1, both of which can be purified by conventional methods. The purpose of this study was to immobilize these fragments on silica, to evaluate the chromatographic performance of the obtained CSPs and to locate stereospecific site(s).

EXPERIMENTAL

Apparatus

The pumps used were a 114 M solvent delivery module in the micro mode (Beckman Instruments, Fullerton, CA, USA) and a Model 2150 dual-piston high-performance liquid chromatographic pump (Pharmacia LKB Biotechnology, Uppsala, Sweden). The injectors were a Model 7520 with a 0.5- or 1-μl loop and a Model 7125 with a 20-μl loop (Rheodyne, Cotati, CA, USA). The variable-wavelength detectors SpectroMonitor 3100, fluid cell volume 1 μl (3 mm path length) and SpectroMonitor D, fluid cell volume 14 μl (10 mm path length) (LDC Analytical, Riviera Beach, FL, USA), were connected to a recorder Model BD 40 (Kipp & Zonen, Delft, Netherlands).The columns were made of stainless steel (Skandinaviska GeneTec, Kungsbacka, Sweden) with PTFE-coated (Svefluor, Uppsala, Sweden) inner surface.

A water bath type 02 PT 923 (Heto, Birkerød, Denmark) was used to thermostat the mobile phase reservoir and the columns at 20.0 ± 0.1°C.

The pH meter was a Model E 623 equipped with a combined pH glass electrode (Metrohm, Herisau, Switzerland).

The spectrophotometer was a Model UV-160 A (Shimadzu Europa, Duisburg, Germany).

Chemicals

Concentrated culture filtrate from the fungus *Trichoderma reesei* chain QM9414 was a kind gift from VTT, the Technical Research Centre of Finland (Espoo, Finland). Papain was supplied by Boehringer Mannheim Scandinavia (Bromma, Sweden). Spherical diol-silica (300 Å, 10 μm, 60 m^2/g, 5 $\mu mol/m^2$ of diol) was obtained from Perstorp Biolytica (Lund, Sweden). Spherical aminopropyl modified silica, Nucleosil 100–10NH_2 (100 Å, 10 μm, 350 m^2/g of the unmodified silica, 5 $\mu mol/m^2$ of NH_2) and Nucleosil 300–7NH_2 (300 Å, 7 μm, 100 m^2/g of the unmodified silica, 5 $\mu mol/m^2$ of NH_2), was obtained from Macherey–Nagel (Düren, Germany). N-Hydroxymaleimide, triethylamine (TEA), tetrabutylammonium hydrogensulphate (TBA) and 1-hexanesulphonic acid sodium salt monohydrate (HS) were from Fluka (Buchs, Switzerland). 1-Ethyl-3-(3-dimethylaminopropyl)carbodiimide hydrochloride (EDC), *p*-nitrophenyl β-D-lactopyranoside, (*R*)-, (*S*)- and *rac*-propranolol hydrochloride, *rac*-warfarin,

(D)- and (L)-N-*tert.*-butoxycarbonyl-phenylalanine (N-t-Boc-phenylalanine), and (*R*)- and (*S*)-1-phenylethanol were from Sigma (St. Louis, MO, USA). N,N-Dimethylethylamine (DMEA), N,N-dimethyloctylamine (DMOA), 1-dodecanesulphonic acid sodium salt (DS), 1-octanesulphonic acid sodium salt monohydrate (OS) and (+)-norephedrin hydrochloride were from Janssen Chimica (Beerse, Belgium). *rac*-Omeprazole, *rac*-oxprenolol hydrochloride, (*R*)- and (*S*)-alprenolol tartrate monohydrate, *rac*-alprenolol hydrochloride, (*R*)- and (*S*)-metoprolol hydrochloride, *rac*-metoprolol and *rac*-H 125/72 hydrochloride were kindly supplied by Astra Hässle (Mölndal, Sweden). (*RR*,*SS*)-Labetalol hydrochloride was supplied by Glaxo Group Research (Greenford, UK). (*R*)- and (*S*)-warfarin were kindly supplied by Dr. Istvan Szinai, Central Research Institute for Chemistry of the Hungarian Academy of Sciences (Budapest, Hungary). (*R*)-, (*S*)- and *rac*-prilocaine hydrochloride were kindly supplied by Astra Pain Control (Södertälje, Sweden). The organic solvents as well as the acids and salts used for the preparation of buffers were of analytical grade.

N-Hydroxysulfosuccinimide sodium salt (HSSI) was prepared from N-hydroxymaleimide according to a previously reported method [11].

The solute structures are shown in Fig. 2.

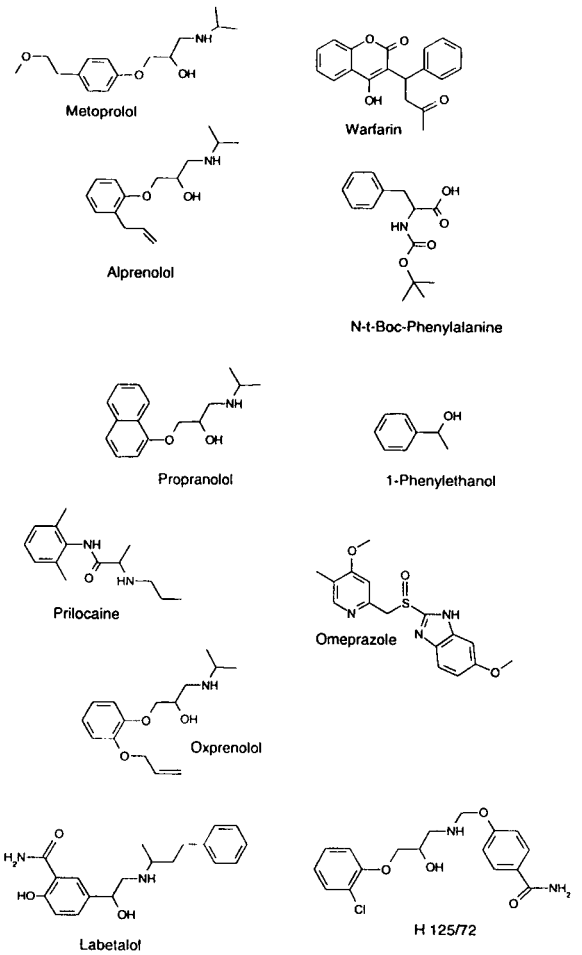

Fig. 2. Solute structures.

Preparation and isolation of intact and fragmented CBH I

CBH I was isolated from the crude concentrated culture filtrate of *T. reesei* by chromatographic techniques as described previously [12]. Limited proteolysis of CBH I (M_r 65 000) by papain yielded the enzymatically active core protein (M_r 56 000) and a C-terminal protein (M_r 9000) [13] consisting of a part of the connecting region, B, plus the cellulose-binding domain, A [14]. The two fragments, core and BA, were baseline separated and purified by gel filtration according to ref. 13. The purity of the BA fragment was controlled by amino acid analysis [14] and by reversed-phase chromatography on a C_{18} column.

Different batches of crude culture filtrates were used for the preparation of intact CBH I and its fragments.

Preparation of protein solid phases

Immobilization on aldehyde silica. The oxidation of diol-silica to aldehyde silica and the subsequent immobilization of CBH I via the amino groups of the protein have been described previously [12]. In this study 150 mg, 75 mg and 38 mg CBH I were allowed to react per gram of aldehyde silica in order to obtain CBH I silicas with different amounts of protein. The core silica was prepared as done with the CBH I–silica [12] and 150 mg of core fragment were added to the

reaction mixture. Prior to the immobilization reaction, both intact CBH I and the core fragment were stored in an ammonium acetate buffer, pH 5.0.

Carbon and nitrogen elemental analysis of dried CBH I–and core–silica were done by Mikro Kemi (Uppsala, Sweden). The results from the carbon analysis indicated a higher amount of CBH I immobilized to silica than did the nitrogen analysis. This discrepancy was ascribed to the carbohydrate content of the protein. Therefore, the amount of protein immobilized on the silica was calculated from the nitrogen content alone. The amounts of immobilized CBH I were 40.4, 35.8 and 22.1 mg/g silica. The amount of immobilized core fragment was 36.3 mg/g silica.

The CSPs were packed into steel columns as described previously [12].

Immobilization on aminopropyl silica. Intact and fragmented CBH I were immobilized on aminopropyl silica via the carboxylic groups of the proteins [15]. Lyophilized protein was added to aminopropyl silica suspended in 0.1 *M* phosphate buffer (pH 7) and the suspension was treated with an ultrasonic bath for 0.5 min. The resulting slurry was agitated on a rocker table for 24 h, after which EDC and HSSI dissolved in 0.1 *M* phosphate buffer were added and the reaction mixture was rocked again for 24 h. The resulting protein–silica was washed with 0.1 *M* phosphate buffer.

A 155-mg amount of CBH I and 41 mg BA fragment were added separately to 1-g samples of 100 Å aminopropyl silica, each suspended in 5 ml buffer. A 0.2-g amount of EDC and 0.1 g HSSI dissolved in 0.5 ml buffer were added to effect the coupling reactions.

Two samples of CBH I, 29 and 62 mg, were added to separate 0.5 g 300 Å aminopropyl silica, each suspended in 2.5 ml phosphate buffer. A 2.5-mg amount of EDC and 2.5 mg HSSI dissolved in 0.25 ml buffer were added to the slurry containing 29 mg CBH I. A 5.0-mg amount of EDC and 5.0 mg HSSI dissolved in 0.25 ml buffer were added to the slurry containing 62 mg CBH I.

Elemental analysis of the dried solid phases showed that 122 mg CBH I/g silica and 35.7 mg BA fragment/g silica had become immobilized on the 100 Å silica. The two 300 Å silica samples contained 22.8 and 53.3 mg CBH I/g silica.

Determination of enzymatic activity

The activity of CBH I immobilized on aminopropyl silica was determined by incubating the solid phase with *p*-nitrophenyl β-D-lactopyranoside (pNPL) and comparing the amount of *p*-nitrophenol formed with the amounts formed when CBH I solutions of known concentrations were incubated with the reagent.

A calibration curve was plotted by assaying aliquots of 20 μ*M* CBH I solution with pNPL. To 0-, 5-, 10-, 40- and 100-μl aliquots was added 50 μl 1 *M* acetate buffer pH 5.0 and the volumes were adjusted to 500 μl with Milli-Q purified water. The standards were incubated for 10 min with 0.5 ml 1 mg/ml pNPL. The reaction was stopped by the addition of 1 ml 5 % (w/v) disodium carbonate in Milli-Q purified water. The amount of *p*-nitrophenol formed was measured spectrophotometrically at 410 nm. The calibration curve for the interval 0–2 nmol CBH I was linear with a coefficient of determination, r^2, equal to 0.999.

Two samples, 10 and 100 μl, of a suspension of immobilized CBH I were washed with Milli-Q purified water and centrifuged. The volumes of the samples were adjusted to 450 μl with Milli-Q purified water and 50 μl 1 *M* acetate buffer, pH 5.0, was added to each sample. The assay was performed as above for the standard solutions. The silica content of the CBH I silica suspension was determined by washing the suspension with Milli-Q purified water followed by freeze-drying and weighing. The suspension contained 31 mg silica/ml.

Chromatographic technique

The ionic strength, *I*, was 0.01 unless otherwise stated. The solutes were generally injected in amounts of 1.0–30 pmol dissolved in the mobile phase, corresponding to linear isotherm retention.

Columns with the dimension 100 × 2.1 mm I.D. were used unless stated otherwise. The flow-rate was 0.1 ml/min, equal to a reduced linear flow velocity, ν, of 6. When a column with

the dimension 250 × 5.0 mm I.D. was used the flow-rate was 1 ml/min, corresponding to $\nu = 12$.

The capacity factor (k'), enantioselectivity (α), and resolution of completely resolved peaks (R_s) were calculated as described in ref. 16 and the degree of resolution of partially resolved peaks (f/g) was calculated according to ref. 17. The peak asymmetry at the baseline (asf) was calculated as described previously [12]. V_0 was obtained by injection of 50 pmol (+)-norephedrin when the mobile phase contained acetate buffer or by the inflection point of water when the mobile phase contained phosphate buffer.

RESULTS AND DISCUSSION

Structural organisation of CBH I

CBH I consists of a polypeptide chain made up of 497 amino acid residues, which is stabilized by twelve disulphide bridges and contains about 6% carbohydrate. The CBH I molecule can be divided into three domains (Fig. 1); the core, C, a flexible spacer rich in carbohydrate, B, and a cellulose-binding domain, A [14]. The C-terminal carboxylic group is located in the A domain [18] and the N-terminus of the core domain is a pyroglutamyl group [19]. Furthermore, there are 44 carboxylic groups and 22 amino groups in the side chains of the CBH I molecule. Papain cleaves the protein at a locus shown in Fig. 1 and the BA fragment consists of about 60 amino acid residues. This fragment contains only three charged groups —2 arginines and one histidine, in addition to the N- and C-terminal groups.

Separation of enantiomers on fragments of CBH I immobilized to silica

Perhaps the most interesting result of this study was the successful separation of *rac*-propranolol at pH 6.8 on intact CBH I as well as on both of its fragments (Table I and Fig. 3). It strongly indicates the presence of different stereospecific sites at different locations in the intact protein. At pH 4.7, the resolution of *rac*-propranolol was lost on the BA fragment due to low retention (Fig. 4 and Table I). The BA fragment was immobilized by use of the C-terminus, see below, whereas this part is free in the CBH I–aldehyde silica. As both the amino group

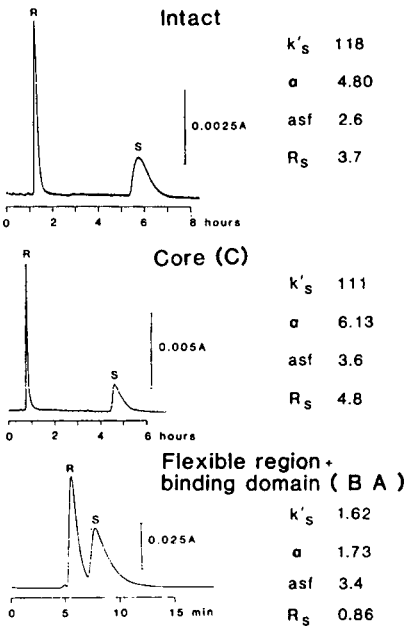

Fig. 3. Separation of the enantiomers of *rac*-propranolol at pH 6.8 on intact and fragmented CBH I immobilized on silica. Mobile phase: 0.065 *M* 2-propanol in phosphate buffer. Sample amount: 1.0 nmol.

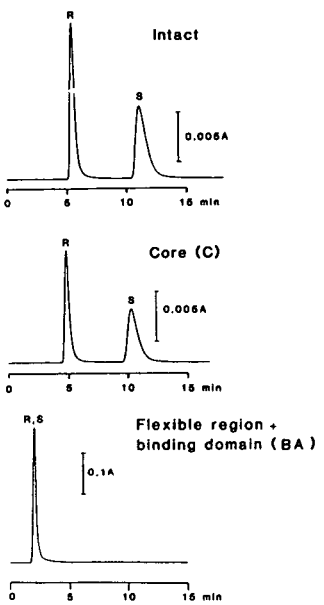

Fig. 4. Separation of the enantiomers of *rac*-propranolol at pH 4.7 on intact and fragmented CBH I immobilized on silica. Mobile phase: 0.065 *M* 2-propanol in acetate buffer. Sample amount: 1.0 nmol.

TABLE I

INTACT AND FRAGMENTED CBH I IMMOBILIZED ON SILICA

Mobile phase: 0.065 *M* 2-propanol in acetate buffer pH 4.7.

Solute	Parameter	Amount of protein (μmol/g)		
		Core[a] 0.64	BA[b] 4.0	CBH I[a] 0.62
Propranolol	k'_S	3.01	0.21	2.84
	α	3.85	1.8	3.31
	asf	1.3	1.4	1.3
	R_s	4.3	[c]	4.1
Warfarin	k'_R	23.9	22.9	22.1
	α	1.09	1.00	1.13
	asf	2.8	2.2	2.3
	f/g	0.34		0.36
Omeprazole	k'_2	3.20	1.68	3.24
	α	1.17	1.0	1.16
	asf		1.7	
	f/g	0.56		0.50
Prilocaine[d]	k'_R	1.01	0.24	2.05
	α	1.77	1.0	1.42
	asf	1.3	2.1	1.9
	f/g	0.99		0.91

[a] Immobilized on aldehyde silica.
[b] Immobilized on 100 Å aminopropyl silica.
[c] No separation of the racemate observed.
[d] Mobile phase: 0.065 *M* 2-propanol in phosphate buffer pH 6.8.

of the analyte and the N-terminus of the BA fragment are protonated at pH 6.8 it seems unlikely that the N-terminus is involved in the chiral recognition mechanism. Neither should the amide linkage between the support and BA fragment be effected by changing pH in this range. The only group of the fragment that changes charge over the interval from pH 4.7 to 6.8 is histidine that should be close to its pK_a at the latter pH. Thus electrostatic repulsion between the positively charged analyte and the BA fragment seems to have a negative effect on the retention. Over the interval from pH 6.7 to 8.7, where the electrostatic repulsion should decrease, the retention of propranolol increased while the enantioselectivity decreased (Table II). This effect was also observed for amines on CBH I–aldehyde silica [12]. It was suggested that conformational changes of the protein at high pH gave rise to the decrease in the enantioselectivity [12]. Since the pK_a of the analyte is 9.5 [20] it cannot be excluded that the binding affinity of

TABLE II

INFLUENCE OF pH ON CHROMATOGRAPHIC PROPERTIES OF THE BA FRAGMENT

Mobile phase: 0.065 *M* 2-propanol in phosphate buffer.

Solute	pH					
	6.7		7.6		8.7	
	k'_S	α	k'_S	α	k'_S	α
Propranolol	2.83	1.81	8.76	1.66	33.2	1.37
Prilocaine	0.57	1.0	1.94	1.01	3.77	1.01
Warfarin	2.66	1.00	0.85	1.0	−0.12	1.0
Omeprazole	1.20	1.0	1.06	1.0	0.66	1.0

the uncharged form is different from its protonated form and that it will bind to a different, achiral site on the protein. Minor changes in the conformations of the BA fragment probably occur upon cleavage from the intact CBH I. Further studies will be made to verify the preliminary findings to make sure that the site on the BA fragment is not induced by cleavage and immobilization.

The BA fragment became immobilized in almost ten-fold higher molar amounts than did the core fragment and the intact CBH I (Table I). Despite these differences, the retention of (*R*)- and (*S*)-propranolol was 4 and 14 times higher, respectively, on the core–silica than on the BA fragment when using a mobile phase pH of 4.7 (Table I) and 30 and 70 times higher, respectively, using pH 6.8 (Fig. 3). The retention and enantioselectivity of propranolol were similar on the CBH I–and core–silica under these conditions. One may thus assume that the dominating enantioselective site for propranolol is located in the core domain and that the binding affinity of propranolol to the BA fragment in the CBH I–silica is almost negligible under linear binding isotherm conditions. However, it should be noted that the observed retention and enantioselectivity of propranolol on the core–silica can be due to several different chiral as well as achiral binding sites.

In Table I are given the chromatographic data for some enantiomeric compounds separated on intact CBH I and fragments. The retention order of enantiomers was the same on fragment–and CBH I–silicas. In Fig. 5 is shown the separation of *rac*-prilocaine using the immobilized core domain of CBH I. The enantiomers of propranolol and warfarin were more retained by the core and the BA fragment than by the intact protein. The pH dependence of solute retention and enantioselectivity on the fragment phases in the range 4.7 to 6.8 followed the same pattern as on solid phases based on intact CBH I [12]. The retention and enantioselectivity of the amines increased with increasing pH, whereas the opposite was found for the acidic compounds. However, only the enantiomers of propranolol were resolved on the BA–silica phase at pH 6.7 to 8.7 (Tables I and II, Figs. 3 and 4).

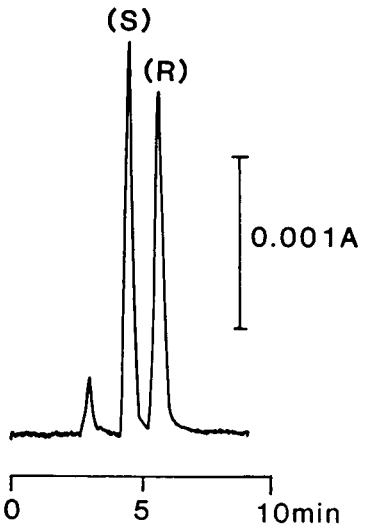

Fig. 5. Separation of the enantiomers of *rac*-prilocaine on CBH I core–silica. Mobile phase: 0.065 *M* 2-propanol in phosphate buffer pH 6.8. Sample amount: 38 pmol.

The loading capacity of the core–silica was investigated at pH 4.7 by injection of (*R*)- and (*S*)-propranolol in amounts ranging from 2.5 pmol to 2.0 nmol. The loading capacity was identical to solid phases prepared from intact CBH I containing the same amount of protein (0.6 μmol/g silica) and immobilized by the same technique, see below. Although the BA fragment was immobilized on silica in almost ten-fold higher molar amount than both the core and intact CBH I, the loading capacity for (*R*)- and (*S*)-propranolol was lower on the BA–silica at pH 6.8. Injection of 5 pmol of each enantiomer on this silica phase resulted in tailing peaks, whereas 0.5 nmol of each was needed to obtain the same overloading on core–or CBH I–silicas.

Covalent immobilization of CBH I and its fragments to silica matrices and chromatographic performance

Immobilization of CBH I via its carboxylic groups to 300 Å amino silica using EDC/HSSI as coupling reagent gave a coupling yield of about 40% (surface density 0.2–0.5 mg/m^2, Table III). Reductive coupling to aldehyde silica via the amino groups of the protein gave a coupling

TABLE III

COUPLING YIELD AND SURFACE DENSITY OF CBH I IMMOBILIZED ON ALDEHYDE AND AMINOPROPYL SILICA

Derivatized silica	Pore diameter (Å)	Ligand density (μmol/g)	Amount of CBH I (mg/g)		Coupling yield (%)	Surface density (mg/m^2)
			In reaction vessel	Immobilized		
Aminopropyl	100	1750	155	122	79	0.35
Aminopropyl	300	500	58	23	39	0.23
Aminopropyl	300	500	124	53	43	0.53
Aldehyde	300	300	38	22	58	0.37
Aldehyde	300	300	75	36	48	0.60
Aldehyde	300	300	150	40	27	0.67

yield that decreased with increasing amount of protein in the reaction vessel. The higher surface area of the amino support, *i.e.*, the higher ligand density, and the higher number of carboxylic groups compared to amino groups on the protein partly explain the more efficient coupling at high protein loading. Differences in pore size distributions between the silica matrices used, in spite of the same mean pore size, might also contribute to the observed differences. The two methods result in different linkages between the protein and the silica spacer; namely amide and amine, respectively. When 100 Å amino silica was used the coupling yield was approximately 80% (surface density 0.4 mg/m^2, Table III).

As expected, the small-sized BA fragment could be bound to amino silica with a high surface area in a higher amount than CBH I. The coupling yield was approximately 90% (surface density 0.1 mg/m^2). This immobilization technique means that the C-terminus of the BA domain is linked to the silica spacer, *i.e.*, the N-terminus is free.

Compared to the activity of the free enzyme in solution, immobilization of 53 mg/g CBH I to 300 Å amino silica led to a 30% decline in enzymatic activity. Similar findings have been reported for chymotrypsin [21]. One simple explanation for the loss of activity might be the very narrow pores of the support. In such pores the enzymatically active site might become hidden by deformation of the protein. It can also be assumed that narrow pores would lead to interactions (collisions) between the macromolecules blocking the enzymatically active site. A high ligand density of the silica allows attachment of a large amount of protein at the expense of specific activities of enzymes [22,23]. The enantioselectivity obtained on the 100 Å CBH I phase was lower than on the 300 Å phase (Table IV). No difference in peak efficiency was observed between the two phases. As expected, the retentions were, in general, higher on the 100 Å phase than on the 300 Å phase, due to the high amount of CBH I immobilized to the former silica.

The effect on the chromatographic performance of increasing the CBH I loading on both amino and aldhyde silica phases was studied (Tables IV and V). Irrespective of the matrix used, the retention of the solutes generally increased with higher CBH I loading. However, on the aldehyde silica the retention of (*R*)-propranolol and (*R*)-alprenolol decreased with increased protein loading. It seems that the (*R*)-enantiomers of the latter compounds have low binding affinity to the protein and are mainly retained by the matrix. Accordingly, inactivation of sites on the matrix should reduce the retention

TABLE IV

IMMOBILIZATION OF CBH I VIA CARBOXYLIC GROUPS ON AMINOPROPYL SILICA

Mobile phase: 0.065 *M* 2-propanol in acetate buffer pH 4.7.

Solute	Parameter	100 Å, 122 mg CBH I/g silica	300 Å, 23 mg CBH I/g silica	300 Å, 53 mg CBH I/g silica
Propranolol	k'_S	1.13	0.68	1.56
	α	2.88	4.65	6.02
	asf	1.5	1.6	1.7
	f/g	0.96	0.97	2.8[a]
Warfarin	k'_R	56.6	6.5	7.24
	α	1.01	1.1	1.17
	asf	2.2		1.7
	f/g		0.07	0.59
Omeprazole	k'_2	1.98	0.85	1.19
	α	1.0	1.0	1.34
	asf	1.2	0.79	1.6
	f/g			0.63
Prilocaine[b]	k'_R	0.36	0.14	0.28
	α	1.2	1.3	1.6
	asf	1.5	2.0	1.6
	f/g	[c]	[c]	0.12

[a] Calculated as R_s.
[b] Mobile phase: 0.065 *M* 2-propanol in phosphate buffer pH 6.8.
[c] No separation of the racemate observed.

(Table V). The retention of (*S*)-propranolol was almost uneffected while the retention of (*S*)-alprenolol increased upon increasing the CBH I loading on aldehyde silica resulting in improved enantioselectivity of propranolol and alprenolol (Table V). A somewhat different chromatographic behaviour of both enantiomers of propranolol was observed at higher protein loadings on 300 Å aminopropyl silica (Table IV). The retention of both enantiomers increased and the enantioselectivity increased at the same time. This may reflect different locations and numbers of attachment points of CBH I to aminopropyl and aldehyde silica as discussed above. The peak symmetry of the solutes on the CBH I–aldehyde silicas was almost uninfluenced by the protein load.

To accurately compare the chromatographic properties of CBH I–aminopropyl and–aldehyde silicas the phases should have contained equal amounts of the protein. Our results show, however, that CBH I–aldehyde silica gives the highest retention, whereas the CBH I–aminopropyl silica gives the highest enantioselectivity (Tables IV and V).

Sample capacity studies on CBH I–aldehyde silicas with different protein loadings using (*R*)- and (*S*)-propranolol as model compounds (Fig. 6a–c) revealed that the enantioselectivity increased with increasing sample amount in the range 1 pmol–0.5 nmol (Table VI). This unusual effect was most pronounced for the stationary phase with the highest CBH I loading. Concentration independent retention and symmetrical peaks (linear isotherm retention) were obtained upon injection of about 1 pmol of each enantiomer on the three phases. Exceeding the pmol range led to reduced retention and increased peak tailing (Fig. 6a–c). The improved enantioselectivity from the pmol to nmol range was due

TABLE V

IMMOBILIZATION OF CBH I VIA AMINO GROUPS ON ALDEHYDE SILICA

Mobile phase: 0.065 *M* 2-propanol in acetate buffer pH 4.7.

Solute	Parameter	mg CBH I/g silica		
		22	36	40
Propranolol	k'_S	2.23	2.84	2.87
	α	1.87	2.58	3.20
	asf	1.4	1.5	1.5
	R_s	2.6	3.3	4.1
Alprenolol	k'_S	1.30	1.92	2.17
	α	3.96	5.89	7.36
	asf	1.3	1.4	1.4
	R_s	2.8	4.0	4.4
Prilocaine[a]	k'_R	1.22	3.33	2.05
	α	1.34	1.18	1.42
	asf	1.8	2.0	1.9
	f/g	0.83	0.85	0.91
Warfarin[b]	k'_R	9.14	14.7	22.0
	α	1.16	1.17	1.12
	asf	1.7	2.4	2.8
	f/g	0.66	0.69	0.34
N-t-Boc-Phenylalanine	k'_L	1.30	2.15	3.96
	α	1.01	1.00	1.00
	asf	1.5	1.8	1.7
Omeprazole	k'_2	2.36	2.62	3.24
	α	1.10	1.19	1.16
	f/g	0.13	0.59	0.50
1-Phenylethanol	k'_S	0.18	0.18	0.24
	α	1.00	1.02	1.01
	asf	1.4	1.4	1.4

[a] Mobile phase: 0.065 *M* 2-propanol in phosphate buffer pH 6.8.

[b] The increased peak asymmetry of warfarin was due to sample overloading. The analyte was highly retarded on the 36 and 40 mg/g CBH I phases and to be able to detect the solute the column had to be overloaded.

to a higher sample capacity for the (*S*)-enantiomer than of the (*R*)-enantiomer. The sample capacity of the binding site for (*S*)-propranolol at sample loadings of more than 0.1 nmol was lower than the capacity of the binding site for the (*R*)-enantiomer on all three phases (Fig. 6a–c, *cf.* Fig. 3 in ref. 12).

Influence of flow-rate on peak efficiency

(*R*)- and (*S*)-propranolol were used to study the effect of flow-rate on the efficiency of CBH I columns containing different amounts of protein. The enantiomers were injected in amounts corresponding to concentration independent retention at $\nu = 6$ (*i.e.*, about 0.1 ml/min). A strong influence of the flow-rate on the efficiency was observed for reduced velocities from 3 to 9 (Fig. 7). This indicates that slow adsorption–desorption kinetics is an important contributor to the

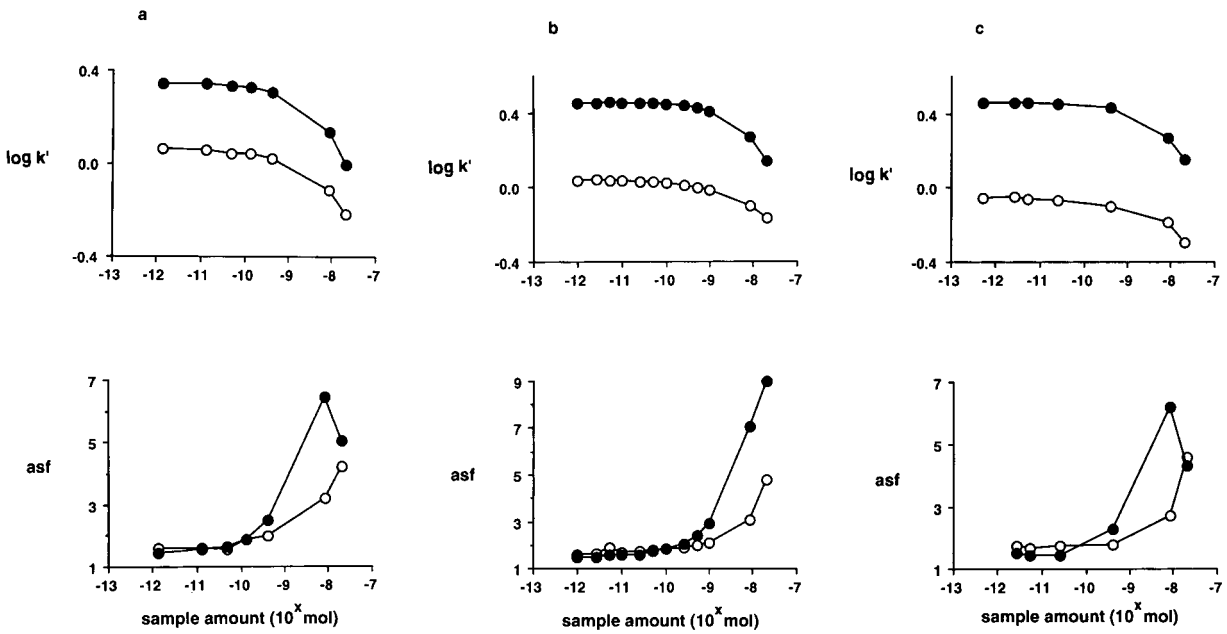

Fig. 6. Loading capacity of CBH I immobilized on aldehyde silica in different amounts. Mobile phase: 0.065 *M* 2-propanol in acetate buffer pH 4.7. Symbols: ○ = (*R*)- and ● = (*S*)-propranolol. (a) 22 mg CBH I/g (0.34 μmol/g); (b) 36 mg CBH I/g (0.55 μmol/g); (c) 40 mg CBH I/g (0.62 μmol/g).

plate height of the CBH I phases. The efficiency of the most retained (*S*)-enantiomer was slightly higher than the (*R*)-enantiomer on all three phases. The efficiency and the flow velocity dependence for the propranolol enantiomers were quite similar on phases containing different amounts of CBH I (Fig. 7).

A notable observation was the peak symmetry decline of (*R*)- and (*S*)-propranolol with decreasing flow-rate (Table VII). At the lowest flow-rates the peaks were high and narrow, but showed strong tailing at the bases. With increasing flow-rate the peaks became low and broad and the peak symmetry improved. Corre-

TABLE VI

SAMPLE LOADING AND ENANTIOSELECTIVITY

Solid phases: CBH I–aldehyde silicas. Mobile phase: 0.065 *M* 2-propanol in acetate buffer pH 4.7. Solute: (*R*)- and (*S*)-propranolol.

Sample amount (mol)	α		
	mg CBH I/g silica		
	22	36	40
$5.0 \cdot 10^{-13}$	1.88	2.60	3.23
$5.0 \cdot 10^{-12}$	1.85	2.61	3.25
$5.0 \cdot 10^{-11}$	1.92	2.64	3.34
$2.5 \cdot 10^{-10}$		2.69	3.37
$5.0 \cdot 10^{-10}$	1.93	2.67	3.42
$8.5 \cdot 10^{-9}$	1.78	2.33	2.94
$2.1 \cdot 10^{-8}$	1.63	2.02	2.58

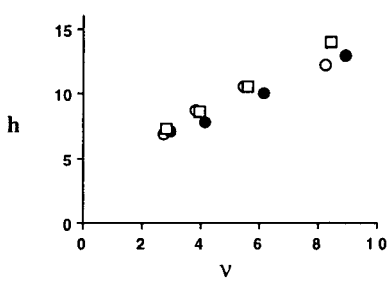

Fig. 7. Influence of flow-rate on efficiency of CBH I immobilized on aldehyde silica in different amounts. Mobile phase as in Fig. 6. Solute: (*S*)-propranolol. Symbols: ● = 22 mg CBH I/g; ○ = 36 mg CBH I/g; □ = 40 mg CBH I/g.

TABLE VII

INFLUENCE OF FLOW-RATE ON PEAK ASYMMETRY

Mobile phase: 0.065 *M* 2-propanol in acetate buffer pH 4.7. Solid phase: 40 mg CBH I/g aldehyde silica. Solute: (*R*)- and (*S*)-propranolol.

Flow-rate (ml/min)	Reduced velocity, ν	*asf*	
		(*R*)	(*S*)
0.010	0.57	1.8	1.7
0.020	1.1	1.7	1.6
0.030	1.8	1.7	1.7
0.049	2.8	1.4	1.4
0.069	3.9	1.5	1.4
0.098	5.6	1.5	1.4
0.147	8.4	1.5	1.4

sponding observations have been reported previously for another kind of chiral system, a chiral counter ion in the mobile phase and porous graphitic carbon as the solid phase [24]. It has been suggested that both kinetic and thermodynamic factors contribute to this kind of peak asymmetry and broadening (Knox and Vasvari [25], Ohkuma and Hara [26]). At low flow velocity the flow-independent, non-linear, partition isotherm is evidenced as a skewed peak [25]. The kinetic effect, which is symmetrical, dominated at high flow velocities [25]. The skewed peak was due to the presence of a small number of secondary tail producing sites characterized by slow adsorption–desorption processes [26]. As the flow-rate increased the retention time was reduced and the number of captured solute molecules at such tail producing sites decreased along with the fractional area of the tail [26]. The peak tailing was suppressed by addition to the mobile phase of an agent which competes with the solute molecules for the tail producing sites [24,26].

Mobile phase additives

As discussed above, protein stationary phases have low adsorption capacities, which means that analyses under non-linear chromatographic conditions sometimes have to be accepted, *e.g.*, sample overloading is often needed when low contents of an enantiomeric impurity have to be determined. The possibility to improve the peak symmetry and efficiency on CBH I–silica by adding charged and uncharged modifiers to the mobile phase was investigated (Tables VIII and IX). To clarify whether the additives would interact differently with the immobilized CBH I at different buffer ion concentrations two ionic strengths ($I = 0.01$ and 0.1) were used. Independently of the ionic strength, addition of the hydrophobic additives, *e.g.*, DMOA, OS and 1-pentanol (PE) decreased the retention of the solutes, but only the charged modifiers (DMOA and OS) improved the peak symmetry (Tables VIII and IX). At elevated buffer concentration the chromatographic performance of the β-blocking agents improved (Table VIII and ref. 12). The influence of DMOA on the peak asymmetry is most pronounced at a low ionic strength. The effect of DMOA on the enantioselectivity was dependent of the solute structure and the total ionic strength. A decrease in the enantioselectivity and resolution was observed for warfarin and omeprazole. The enantioselectivity of the β-blockers in the presence of DMOA increased slightly in mobile phases of low ionic strength, but was almost unaffected at a high ionic strength.

The tertiary structure of proteins is stabilized by numerous electrostatic and hydrophobic interactions. Addition of a charged and hydrophobic agent such as DMOA could disturb such interactions and give rise to conformational changes. Competition of DMOA with the enantiomeric solutes for binding sites (specific and non-specific) on the CBH I molecule as well as for non-specific binding sites on the matrix might also be a plausible explanantion for the observed effects. Similar effects of DMOA on chromatographic properties using the Chiral-AGP phase have been observed [27]. The influence of DMEA and TEA on column efficiency and retention of metoprolol and omeprazole was not as pronounced as was found for the hydrophobic DMOA (Tables VIII and IX). The three cationic modifiers gave no significant difference in enantioselectivity for metoprolol at low ionic strength

TABLE VIII

INFLUENCE OF MOBILE PHASE ADDITIVES ON CHROMATOGRAPHIC PERFORMANCE OF SOLUTES UNDER NON-LINEAR CONDITIONS

Mobile phase: 0 or 5.0 m*M* of the additives 1-octanesulphonate (OS), dimethylethylamine (DMEA), triethylamine (TEA), dimethyloctylamine (DMOA) and 1-pentanol (PE) in acetate buffer pH 5.5 ($I = 0.01$ or 0.1). Solid phase: CBH I–aldehyde silica. Column dimension: 250 mm × 5.0 mm I.D.

Solute		$I = 0.01$						$I = 0.1$			
		–	OS	DMEA	TEA	DMOA	PE	–	OS	DMOA	PE
Metoprolol	k'_S	1.95	1.81	1.54	1.34	0.67	1.62	0.97	0.92	0.46	0.90
	α	1.24	1.25	1.27	1.30	1.27	1.29	1.41	1.45	1.41	1.43
	asf	4.7	4.0	3.5	2.5	1.4	2.9	3.3	2.5	1.4	3.2
	f/g	0.86	0.85	0.89	0.93	0.83	0.90	0.90	0.93	0.88	0.82
Propranolol	k'_S							9.24	8.90	4.90	8.89
	α							2.30	2.37	2.14	2.27
	asf							4.3	3.7	2.0	4.7
	f/g							0.99	3.5[a]	4.6[a]	1.9[a]
Oxprenolol	k'_2	3.13		2.62	2.27						
	α	1.32		1.36	1.39						
	asf	4.7		3.1	2.8						
	f/g	0.92		0.97	0.98						

[a] Calculated as R_s.

TABLE IX

INFLUENCE OF MOBILE PHASE ADDITIVES ON CHROMATOGRAPHIC PERFORMANCE OF SOLUTES UNDER NON-LINEAR CONDITIONS

Conditions as in Table VIII.

Solute		$I = 0.01$						$I = 0.1$			
		–	OS	DMEA	TEA	DMOA	PE	–	OS	DMOA	PE
Warfarin	k'_R	2.77	2.24	3.16	3.19	2.44	2.61	2.85	2.29	2.43	2.69
	α	1.26	1.33	1.20	1.21	1.09	1.28	1.17	1.21	1.09	1.21
	asf	3.6	2.4	3.4	3.5	2.6	2.6	3.5	2.2	2.1	2.6
	f/g	0.85	0.91	0.61	0.63	0.21	0.87	0.68	0.80	0.27	0.72
Omeprazole	k'_2	4.0	3.4	3.91	3.56	2.3	3.6	3.8	3.2	2.4	3.5
	α	1.09	1.10	1.08	1.09	[a]	1.09	1.07	1.10	1.0	1.09
	f/g	0.32	0.25	0.20	0.26		0.16	0.18	0.29		0.10

[a] A tendency to separation of the enantiomers was observed.

of the mobile phase. In contrast to DMOA, DMEA and TEA increased the retention of warfarin (Table IX). Amine modifiers probably have dual function and acts both as ion-pairing reagents and competitors. Depending on the hydrophobicity and character of the additive as

TABLE X

INFLUENCE OF TRIETHYLAMINE (TEA) ON CHROMATOGRAPHIC PERFORMANCE OF AMINO ALCOHOLS

Mobile phase: TEA in acetate buffer pH 5.5 ($I = 0.1$). Solid phase: CBH I–aldehyde silica. The solutes were injected as racemates.

Solute		[TEA] (m*M*)			
		0	1	5	10
Propranolol	k'_S	9.56	9.35	8.61	8.00
	α	3.20	3.15	3.10	3.01
	asf	2.1	1.9	2.2	2.1
	R_s	4.1	4.0	4.1	4.1
Alprenolol	k'_2	7.19	7.12	6.50	6.05
	α	6.44	6.49	6.33	6.32
	asf	1.58	1.56	1.49	1.61
	R_s	5.4	5.6	5.7	5.8
Metoprolol	k'_2	0.89	0.86	0.78	
	α	1.8	1.8	1.8	
	asf	1.3	1.3	1.2	
	R_s	1.6	1.5	1.5	
Oxprenolol	k'_2	1.63	1.50	1.40	1.28
	α	2.17	2.16	2.06	2.06
	asf	1.3	1.3	1.3	1.3
	R_s	2.6	2.4	2.4	2.4

well as of the solute one or the other function will dominate.

The chromatographic data from studies of an increased co-ion (TEA) concentration under almost linear binding isotherm conditions on the separation of enantiomeric amino alcohols are presented in Table X. Only a slight reduction in retention and enantioselectivity without improvement in peak symmetry was registered, even at triethylamine concentrations as high as 10 m*M*.

The possibility to regulate the chiral separation by use of an anionic (alkylsulphonate) or uncharged (PE) modifier was rather limited (Tables VIII, IX and XI). Dodecanesulphonate, a hydrophobic anion, increased the capacity factors for the enantiomeric amino alcohols, probably due to ion-pair retention, but ruined the enantioselectivity (Table XI).

TABLE XI

EFFECT OF SULPHONATES ON CHROMATOGRAPHIC PERFORMANCE OF AMINO ALCOHOLS

Mobile phase: 0.065 *M* 2-propanol and the additives 1-hexanesulphonate (HS), 1-octanesulphonate (OS) and 1-dodecanesulphonate (DS) in acetate buffer pH 4.7. Solid phase: CBH I–aldehyde silica. Column dimension: 250 × 5.0 mm I.D. Flow-rate: 0.5 ml/min. The solutes were injected as racemates.

Solute		Additive (m*M*)			
		–	HS (1.0)	OS (5.0)	DS[a] (1.9)
(*RR*,*SS*)-Labetalol	k'_2	0.40	0.44	0.67	59
	α	2.4	2.2	1.6	1.0
	asf	2.1	2.0	2.6	2.0
H 125/72	k'_2	0.76		0.98	
	α	2.5		1.8	
	asf	1.8		1.4	

[a] The concentration of 1-propanol was 0.13 *M*.

CONCLUSIONS

Stereospecific sites for the enantiomers of propranolol are located in different domains of the CBH I molecule. The dominant enantioselective binding site of the immobilized protein was found in the core (C) domain. The BA domain gave short retention times and separated only the enantiomers of propranolol at high pH.

The immobilization technique is of utmost importance for the retention and enantioselectivity of the CBH I phase. The enantioselectivity of the CBH I–aminopropyl silica was higher than that of the CBH I–aldehyde silica, whereas the retention was lower. However, further studies on different immobilizing reagents and matrices are needed to optimize the immobilization technique for intact as well as fragmented CBH I.

The efficiency of the CBH I columns is strongly influenced by the flow-rate. No significant differences in peak symmetry were observed between the CSPs based on intact CBH I and its fragments. However, additives in the mobile phase may improve the peak symmetry signifi-

cantly and charged additives seems to be more efficient in this respect than are uncharged ones.

ACKNOWLEDGEMENT

Dr. Jerry Ståhlberg is gratefully acknowledged for the experiments on enzymatic activity and Dr. Per Erlandsson for preparing some of the CBH I columns. This work was supported by grants from the Swedish Natural Science Research Council and from the Swedish Natural Board for Industrial and Technical Development. Travel grants from the Swedish Academy of Pharmaceutical Sciences to two of us (I.M., C.P.) are gratefully acknowledged.

REFERENCES

1 I.W. Wainer, T.A.G. Noctor, E. Domenici and P. Jadaud, in S. Ahuja (Editor), *Chiral Separations by Liquid Chromatography*, American Chemical Society, Washington, DC, 1991, Ch. 8.
2 A.-F. Aubry, F. Gimenez, R. Farinotti and I.W. Wainer, *Chirality*, 4 (1992) 30–35.
3 X. Min He and D.C. Carter, *Nature*, 358 (1992) 209–215.
4 I.W. Wainer, in W.J. Lough (Editor), *Chiral Liquid Chromatography*, Blackie, Glasgow, 1989, Ch. 7.
5 P. Erlandsson and S. Nilsson, *J. Chromatogr.*, 482 (1989) 35–51.
6 T.C. Pinkerton and J. Haginaka, presented at the *16th International Symposium on Column Liquid Chromatography, Baltimore, June 14–19, 1992*, poster 287.
7 R.A. Thompson, S. Andersson and S. Allenmark, *J. Chromatogr.*, 465 (1989) 263–270.
8 P. Erlandsson, L. Hansson and R. Isaksson, *J. Chromatogr.*, 370 (1986) 475–483.
9 S. Allenmark, B. Bomgren, H. Boren and P.-O. Lagerström, *Anal. Biochem.*, 136 (1984) 293–297.
10 S. Allenmark and B. Bomgren, *J. Chromatogr.*, 252 (1982) 297–300.
11 J.V. Staros, *Biochemistry*, 21 (1982) 3950–3955.
12 I. Marle, P. Erlandsson, L. Hansson, R. Isaksson, C. Pettersson and G. Pettersson, *J. Chromatogr.*, 586 (1991) 233–248.
13 P. Tomme, H. van Tilbeurgh, G. Pettersson, J. van Damme, J. Vandekerckhove, J. Knowles, T. Teeri and M. Claeyssens, *Eur. J. Biochem.*, 170 (1988) 575–581.
14 G. Johansson, J. Ståhlberg, G. Lindeberg, Å. Engström and G. Pettersson, *FEBS Lett.*, 243 (1989) 389–393.
15 A.L. Klibanov, M.A. Slinkin and V.P. Torchilin, *Appl. Biochem. Biotechnol.*, 22 (1989) 45–58.
16 L.R. Snyder and J.J. Kirkland, *Introduction to Modern Liquid Chromatography*, Wiley, New York, 2nd ed., 1979, Ch. 2.
17 R. Kaiser, *Chromatographie in der Gasphase, I, Gaschromatographie*, Bibliographisches Institut, Mannheim, 1960, p. 35.
18 H. Van Tilbeurgh, P. Tomme, M. Claeyssens, R. Bhikhabhai and G. Pettersson, *FEBS Lett.*, 204 (1986) 223–227.
19 R. Bhikhabhai, G. Johansson and G. Pettersson, *J. Appl. Biochem.*, 6 (1984) 336–345.
20 A.C. Moffat, J.V. Jackson, M.S. Moss and B. Widdop (Editors), *Clarke's Isolation and Identification of Drugs*, The Pharmaceutical Press, London, 2nd ed., 1986.
21 I.W. Wainer, P. Jadaud, G.R. Schombaum, S.V. Kadodkar and M.P. Henry, *Chromatographia*, 25 (1988) 903–907.
22 D. Wu and R.R. Walters, *J. Chromatogr.*, 458 (1988) 169–174.
23 A.-C. Koch-Schmidt and K. Mosbach, *Biochemistry*, 16 (1977) 2105–2109.
24 A. Karlsson, N.H. Huynh and C. Pettersson, in preparation.
25 J.H. Knox and G. Vasvari, *J. Chromatogr.*, 83 (1973) 181–194.
26 T. Ohkuma and S. Hara, *J. Chromatogr.*, 400 (1987) 47–63.
27 J. Hermansson and G. Schill, in M. Zief and L.J. Crane (Editors), *Chromatographic Chiral Separations*, Marcel Dekker, New York, 1988, Ch. 10.

Journal of Chromatography, 648 (1993) 349–356
Elsevier Science Publishers B.V., Amsterdam

CHROM. 25 348

Ion-pair reversed-phase high-performance liquid chromatographic method for the separation of a set of unphosphorylated thiamine-related compounds

A. Kozik* and M. Rapala-Kozik

Department of Biochemistry, Institute of Molecular Biology, Jagiellonian University, Al. Mickiewicza 3, 31-120 Kraków (Poland)

(First received July 10th, 1992; revised manuscript received May 27th, 1993)

ABSTRACT

A set of unphosphorylated thiamine-related compounds including thiamine derivatives [thiamine disulphide, D,L-2-(1-hydroxyethyl)thiamine, O-benzoylthiamine and 2,3,4,5-tetrahydrothiamine], antagonists (oxythiamine, pyrithiamine and amprolium) and thiamine degradation products [4-amino-5-hydroxymethyl-2-methylpyrimidine and 4-methyl-5-(2-hydroxyethyl)thiazole] were successfully separated by ion-pair reversed-phase high-performance liquid chromatography on a standard analytical octadecylsilica column with an aqueous mobile phase containing sodium *n*-octanesulphonate (0.08%) and trifluoroacetic acid (0.08%) in a carefully profiled gradient of tetrahydrofuran. It is suggested that such chromatographic runs may be useful as a homogeneity criterion for synthetic preparations of thiamine-like substances and for following some thiamine reactions in solutions like, *e.g.*, in alkali.

INTRODUCTION

Recent applications of high-performance liquid chromatography (HPLC) in the analytical biochemistry of thiamine (vitamin B_1) were predominantly focused on simultaneous determinations of thiamine and its mono- , di- and triphosphate esters in body fluids [1–4] and various animal tissues [5–9]. Necessary for these purposes, ultrasensitive fluorimetric detection (down to low femtomole levels) is based on either precolumn [1–3,6–13] or postcolumn [4,5,8,14–16] derivatization of thiamine and its esters to the corresponding highly fluorescent thiochromes. Most frequently, the separations of intact thiamine phosphates and thiamine were performed by reverse-phase chromatography including anion pairing by alkyl sulphonates [8,16,17]. Only occasionally have some alternative separation principles been exploited, such as reversed-phase partitioning with cation pairing [17], reversed-phase partitioning with no ion pairing [4], normal-phase partitioning [5] and anion exchange [17].

The ubiquitous natural occurrence and major biological roles of thiamine phosphates has resulted in less attention being paid to analyses for other compounds of structural similarity to thiamine. There are several experimental lines, however, where a biochemist may lack a powerful method suitable for separating unphosphorylated, structural analogues of vitamin B_1 from its major natural forms. Some compounds with vitamin B_1 activity such as thiamine disulphide [18,19] may be present in various extracts of biological origin. Many thiamine antagonists have been used for metabolic studies [20]. The detection and determination of potential thiamine metabolites are also of primary

* Corresponding author.

0021-9673/93/$06.00

importance [21]. An aim of this work corresponds to applications of thiamine-related compounds as chemical probes of binding-site topography in thiamine transport/storage proteins [22] and perhaps also in some thiamine-consuming enzymes such as thiamine pyrophosphokinase [23] or thiaminase [24]. Preparations of such the chemical probes should be ultrapure as any traces of native ligand can lead to false determinations of affinity to a binding protein. HPLC can be given consideration in order to provide necessary, powerful criteria for probe homogeneity.

Organic compounds of structural similarity to unphosphorylated thiamine have only occasionally been the subject of HPLC separations. Two reports were published on the successful separation of oxythiamine from thiamine in some ion-pair reversed-phase systems in which pyrithiamine, another thiamine antagonist, co-eluted with the vitamin, however [17,25]. A third well established vitamin B_1 antagonist, amprolium, was used as an internal standard in thiamine determinations [16] and more recently chloroethylthiamine found a similar application [8].

In this paper we present an ion-pair reversed-phase HPLC method optimized for the separation and simultaneous determination of a range of unphosphorylated thiamine-related compounds including major thiamine antagonists, simple thiamine derivatives and some thiamine degradation products.

EXPERIMENTAL

Thiamine-related compounds

Thiamine hydrochloride (T), amprolium hydrochloride (AMPR), pyrithiamine hydrobromide (PYT), thiamine monophosphate chloride (TP) and thiochrome (TC) were purchased from Sigma (St. Louis, MO, USA), thiamine disulphide trihydrate (TS2) from Aldrich (Milwaukee, WI, USA) and 4-methyl-5-(2-hydroxyethyl)thiazole (TH) from Fluka (Buchs, Switzerland). Other thiamine derivatives were synthesized by published methods: O-benzoylthiamine (BT) by treating T with benzoyl chloride [26], D,L-2-(1-hydroxyethyl)thiamine hydrochloride (HET) by treatment of T with acetaldehyde [26], oxythiamine chloride (OT) from T by refluxing in HCl [26], 4-amino-5-aminomethyl-2-methylpyrimidine dihydrochloride (PYNH2) by acid degradation of TS2 [27], 4-amino-5-aminomethyl-2-methylpyrimidine hydrochloride (PYOH) from PYNH2 by treatment with nitrous acid [28] and 2,3,4,5-tetrahydrothiamine (H4T) by reduction of T with sodium borohydride [29]. The synthesized compounds were identified by their melting points and UV spectra and their purity was routinely checked by thin-layer chromatography on silica gel 60 precoated plates with pyridine–acetic acid–water (10:1:40).

Other chemicals

Sodium 1-pentanesulphonate and 1,4-dioxane of spectrophotometric grade were obtained from Aldrich, trifluoroacetic acid (TFA) (HPLC/Spectro grade) from Pierce (Rockford, IL, USA), aluminium-precoated plates (silica gel 60) for thin-layer chromatography and N,N-dimethylformamide (DMF) for UV-spectrophotometry from Fluka, sodium hexane-1-sulphonate (LiChropur), sodium octane-1-sulphonate (LiChropur), methanol (LiChrosolv, gradient grade), acetonitrile (LiChrosolv, gradient grade), tetrahydrofuran (THF) (LiChrosolv) and other chemicals (ACS grade) from Merck (Darmstadt, Germany). Water was distilled twice from glass and then further purified with a Milli-Q Plus system (Millipore).

Mobile phases

In the procedure finally adopted, an aqueous solution containing TFA (0.16%) and sodium octanesulphonate (0.16%) was diluted twice by volume with either water to give solvent A or with THF to give solvent B. Details on other solvent systems used are given under Results and Discussion. All mobile phases were filtered through 0.45-μm nylon 66 membranes (Supelco, Gland, Switzerland) and then degassed by bubbling helium through for 10 min in a Pharmacia–LKB (Uppsala, Sweden) solvent conditioner.

Samples

Thiamine-related compounds were dissolved in solvent A to a concentration of 1 mg/ml and

were stored refrigerated. Samples were diluted with solvent A as needed and filtered through 0.45-μm disposable filter units (Supelco).

Chromatography

Separations were performed on a Pharmacia–LKB HPLC system consisting of a Model 2249 gradient pump capable of low-pressure mixing of up to three solvents, a Model 2141 dual-channel variable-wavelength UV–Vis monitor, a Rheodyne Model 7125 manual injector equipped with a 50-μl sample loop, a SuperPac cartridge column with a 5-μm Spherisorb ODS-2 cartridge (250 mm × 4 mm I.D.) and a 5-μm Spherisorb ODS-2 guard cartridge (10 mm × 4 mm I.D.). IBM-PC-AT dedicated software HPLC Manager (ver. 2.01) was used for system control and data acquisition and PE Nelson 2600 (ver. 5.0) evaluation software for peak integration. The chromatography was carried out at ambient temperature and a flow-rate of 1 ml/min with simultaneous monitoring of absorbances at 270 and 360 nm.

RESULTS AND DISCUSSION

Optimization of mobile phase composition for isocratic ion-pair reversed-phase HPLC of test thiamine analogues

This work was aimed at the separation of compounds that are either permanently cationic (because of a quaternary nitrogen of a thiazolium ring) or capable of accepting protons in acidic media (amino groups, nitrogen-containing heterocycles). They were expected to interact with an octadecylsilica (ODS) column if paired with suitable anions such as alkyl sulphonates. Because of the marked structural differences between the substances to be separated, solvent systems capable of resolving thiamine from other water-soluble vitamins rather than from thiamine phosphates were chosen as the starting point. Numerous methods have been published on the chromatographic determination of B vitamins in foods and pharmaceuticals [18,30,31, and references therein] on reversed-phase columns (ODS) in mobile phases based on water–methanol mixtures containing acetic acid or an acidic buffer (acetate, citrate, phosphate) and alkyl sulphonates with 5–8 carbon atoms.

In searching for the optimum method for the separation of unphosphorylated thiamine analogues, isocratic elution on a Pharmacia–LKB ODS-2 analytical column was first applied with spectrophotometric detection at 270 nm. The test samples contained thiamine-like compounds of closest structural similarity (T, PYT, HET, OT) and additionally TP (for comparative purposes). To optimize the mobile phase composition, we first followed and then markedly extended its variations reported in the literature. The following factors were tested, as shown schematically in Fig. 1: (i) length of hydrocarbon chain of the ion-pairing reagent; (ii) concentration of alkyl sulphonate in the mobile phase; (iii) nature of organic solvent (methanol, acetonitrile, DMF–methanol, 1,4-dioxane, THF); (iv) organic solvent concentration; and (v) substitution of TFA for acetic acid in the mobile phase.

Finally, the optimum separations of thiamine analogues were obtained with a mobile phase containing a subtle balance of TFA (0.06–0.08%), *n*-octanesulphonate (0.08%) and THF (10–12%). A representative chromatogram is shown in Fig. 2. Using this chromatographic system, PYT and T could be completely separated for the first time by an ion-pair reversed-phase HPLC method.

Recommended gradient elution method for ion-pair reversed-phase HPLC of a series of thiamine-related compounds

When the samples contained some thiamine analogues that interact strongly with the ODS phase (TS2, AMPR, BT), a gradient of organic solvent in the mobile phase had to be applied for their elution. The gradient elution mode had additional positive effects on the overall separations as most peaks were sharpened and any tailing was markedly reduced.

The method finally adopted that meets the aim of work presented here is based on an aqueous mobile phase containing 0.08% of TFA and 0.08% of *n*-octanesulphonate and a biphasic gradient of THF. As shown in Fig. 3, twelve unphosphorylated thiamine-related compounds with very different structures, including thiamine

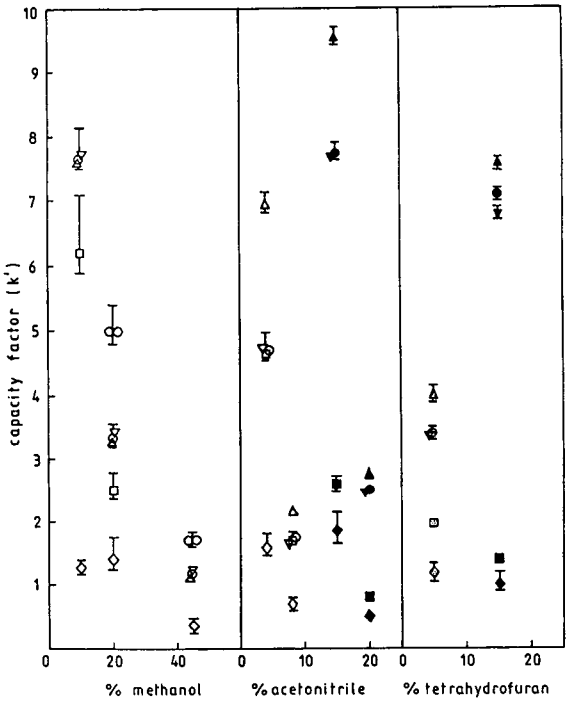

Fig. 1. Schematic representation of the elution behaviour of thiamine derivatives in isocratic ion-pair reversed-phase HPLC on an LKB ODS analytical column. Separations were performed at a flow-rate of 1 ml/min, with an aqueous mobile phase containing (i) an ion-pairing reagent: 0.1% of *n*-pentanesulphonate (white symbols), 0.05% of *n*-hexanesulphonate (shaded symbols) or 0.05% of *n*-octanesulphonate (black symbols) and (ii) an acid: either 1% acetic acid (when methanol was used) or 0.1% TFA. ◇,◆ = TP; □,■ = OT; ▽,▼ = PYT; ○,● = T; △,▲ = HET; ⊙,⬤ = TS2. Capacity factors [$k' = (t_R - t_0)/t_0$, where t_R and t_0 are retention times of an analyte and of an unretained substance, respectively] are plotted together with peak half-widths, represented by bars.

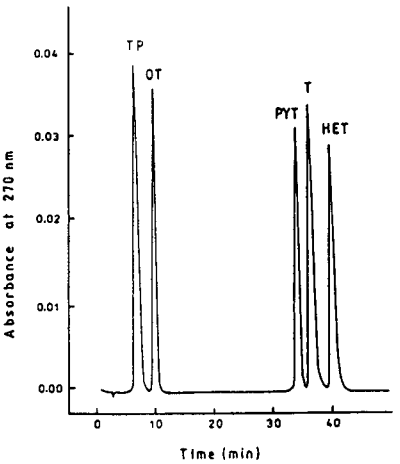

Fig. 2. Representative chromatogram of optimized isocratic ion-pair reversed-phase HPLC of some thiamine derivatives. The separation was performed on the analytical ODS column with an aqueous mobile phase containing 0.08% of *n*-octanesulphonate, 0.08% of TFA and 12% (v/v) of THF at a flow-rate of 1 ml/min, with spectrophotometric detection. About 2 μg of each compound were applied in a total sample volume of 50 μl.

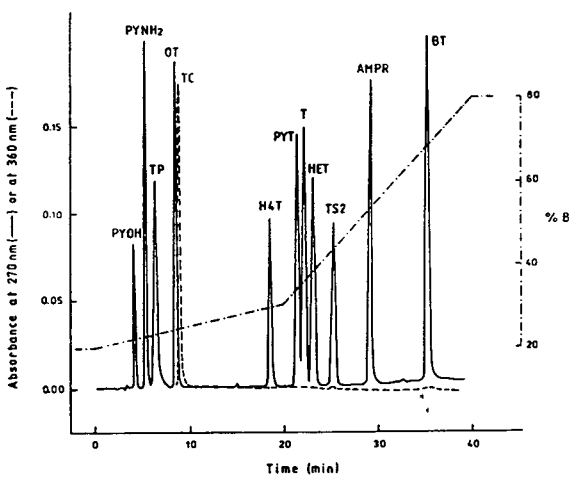

Fig. 3. Separation of a series of thiamine-related compounds by the recommended gradient-elution ion-pair reversed-phase HPLC method. A 50-μl sample containing 2.5 μg of each compound was applied to the analytical ODS column and separated in a binary gradient formed between solvents containing 0.08% of *n*-octanesulphonate and 0.08% of TFA either in water (solvent A) or in 50% (v/v) THF (solvent B). Chromatography was performed at ambient temperature and a flow-rate of 1 ml/min with simultaneous detection at 270 and 360 nm. The gradient profile shown was formed at proportioning valves before entering the pump. The solvent delay between the proportioning valves and the injector was about 1.5 min.

antagonists, derivatives and degradation products, were separated in a single run within 40 min. Additional chromatographic parameters are given in Table I. As can be seen, a reasonable compromise between the chromatographic behaviour of very different compounds was obtained. The peaks are acceptably sharp and usually do not tail, except perhaps for TP (and TH, not listed). For most pairs of closest neighbours on the chromatogram, complete separation is observed. The overlapping of OT and TC does not matter on an analytical scale as the

TABLE I

CHROMATOGRAPHIC PARAMETERS FOR ION-PAIR REVERSED-PHASE HPLC METHOD RECOMMENDED FOR THE SEPARATION OF THIAMINE-RELATED COMPOUNDS

Separation conditions as described in Fig. 3. Each parameter is given as a mean of three independent runs. Capacity factor: $k' = (t_R - t_0)/t_0$, where t_R = retention time and t_0 = retention time for unretained compounds ($t_0 = 2.5$ min). $N_{1/2} = 5.53(t_R/W_{1/2})^2$, $N_{4.4\%} = 25(t_R/W_{4.4\%})^2$, where $W_{1/2}$ and $W_{4.4\%}$ are the peak widths at half or 4.4% of the peak height, respectively. Resolution factor: $R_s = (t_{R_1} - t_{R_2})/[W_{1/2(1)} + W_{1/2(2)}]$.

Compound	k'	$N_{1/2}$ ($\times 10^{-3}$)	$N_{4.4\%}$ ($\times 10^{-3}$)	R_s
PYOH	0.52	4.73	4.95	2.8
PYNH2	0.90	2.74	3.10	1.5
TP	1.21	1.66	1.09	3.5
OT	1.98	5.75	5.06	0.6
TC	2.10	3.59	3.14	16
H4T	6.05	18.3	16.3	4.5
PYT	7.29	17.7	17.2	0.9
T	7.54	22.2	20.4	2.0
HET	8.02	27.5	25.7	3.0
TS2	8.92	17.5	21.2	5.4
AMPR	10.5	63.7	72.0	11
BT	13.3	44.0	39.3	

latter compound is selectively detected (at 360 nm). For better separation of PYT and T, the isocratic mode is suitable, as shown in Fig. 2.

Simultaneous determination of unphosphorylated thiamine-related compounds by ion-pair reversed-phase HPLC

This optimized HPLC method for the separation of unphosphorylated thiamine-related compounds could easily be upgraded to a quantitative procedure. Simultaneous determination of all the compounds tested could be performed on the basis of peak areas. The analytical parameters of the method are given in Table II. Calibration graphs (dose–response) were constructed for each thiamine-related compound separately, in the range 0.01–2.5 μg per injection. Within this range, excellent linearity of the detector response was observed (correlation coefficients always >0.995) and the reproducibility was good (relative standard deviations <6%).

Detection limits were determined by sequential dilution of a standard mixture (Fig. 3) of thiamine-related compounds (2.5 μg each). Slight variation of this parameter was observed, from 1.1 ng for BT to 5.4 ng for PYOH. Obviously, for mixtures of T and PYT, the detection limits are much worse if one compound is in a large excess relative to the other. Such mixtures, however, can easily be analysed by switching to the isocratic mode (Fig. 2).

Application 1: detection and determination of impurities in preparations of synthetic thiamine analogues

The gradient-elution HPLC method introduced here is capable of resolving a number of thiamine-related compounds of very diverse structures. Hence we feel justified in recommending chromatographic runs such as that presented in Fig. 3 to provide a serious homogeneity criterion for synthetic preparations of

TABLE II

ANALYTICAL PARAMETERS OF THE ION-PAIR REVERSED-PHASE HPLC METHOD FOR THE SIMULTANEOUS DETERMINATION OF THIAMINE-RELATED COMPOUNDS

Compound	Calibration graph[a]		Detection limit[b] (ng)	Relative standard deviation[c] (%)
	Slope (10^6 μV s μg^{-1})	Intercept (10^3 μV s)		
PYOH	0.61	3.24	4.9	2.1
PYNH2	1.29	−4.01	2.5	0.9
TP	1.01	−4.95	2.6	4.2
OT	1.19	0.06	2.3	0.8
TC	1.42	14.2	1.8	1.2
H4T	0.93	−12.5	5.0	3.0
PYT	1.18	−6.87	1.9	3.1
T	1.29	−12.4	1.7	0.9
HET	1.10	8.62	2.8	2.5
TS2	0.97	−0.70	2.4	1.0
AMPR	1.77	−11.0	1.4	0.7
BT	2.01	3.71	1.1	1.1

[a] Determined in the range 0.01–2.5 μg of a compound per injection; peak areas (μV s) were plotted *versus* amount of compound injected (μg); calibration graphs fitted by linear regression.
[b] Injection resulting in a peak three times higher than the noise.
[c] Peak area measurements, repeated five times, for 100 ng of a compound per injection.

this class. Impurities can be detected and, if identified, can be directly determined. Taking into account the detection limits in Table II, one can calculate that as little as 0.1% of potential impurities (of "thiamine-related character") can in principle be determined by HPLC of microgram amounts of a tested compound.

Two examples from our own synthetic practice are presented in Fig. 4.

Application 2: monitoring of thiamine degradation in alkaline media

Since early work by Zima [27], processes of thiamine destruction in alkaline solutions have been studied by many workers and have become representative of the chemical properties of vitamin B_1. Various products and in variable yields are formed depending on pH, temperature, nature of alkalinizing compound and the presence of organic solvents and oxidizing reagents *etc.* [32–34]. We performed preliminary studies to test whether the chromatographic method introduced here could be suitable for following this complex model reaction. A relatively sharp gradient of 1,4-dioxane was applied for this purpose, to shorten the separation time and to demonstrate some flexibility of the chromatographic methods introduced here with respect to gradient profile and nature of the organic solvent. Relatively mild degradation media, with no oxidizing agents except dissolved oxygen, were studied. The results are summarized in Fig. 5.

Of potentially expected degradation products [27,32,33], four (PYOH, TH, TS2 and TC) were available as standards. Three of them (PYOH, TH and TS2) were identified in some reaction mixtures in various yields. Two additional compounds were detected although their proper identification was not attempted. That labelled 3 in Fig. 5 absorbed at 360 nm and not at 270 nm and was eluted in a distorted band. The other,

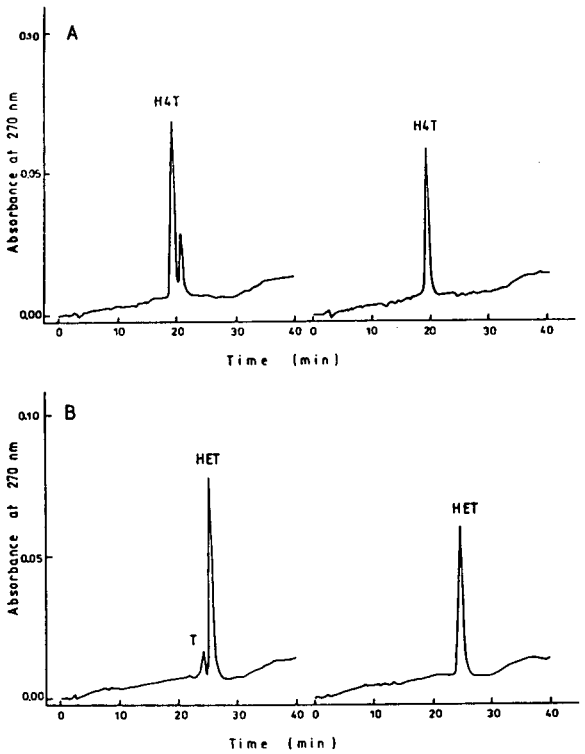

Fig. 4. The recommended gradient-elution ion-pair reversed-phase HPLC method as a homogeneity criterion for selected synthesized preparations of (A) H4T and (B) HET. Left, crude preparations, recrystallized twice; right, preparations after further careful purifications. The impurity in H4T was not identified; that in HET seemed to be T (*ca.* 7%) and could not be easily eliminated.

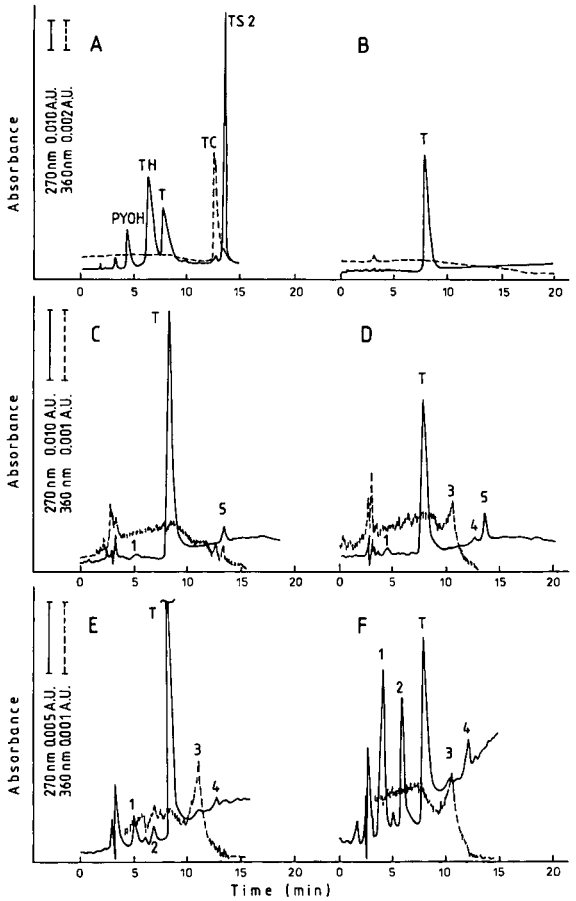

Fig. 5. Degradation of T in mild alkaline media as monitored by ion-pair reversed-phase HPLC. T (0.2 m*M*) was incubated: (B) in 0.1 *M* NaOH at 20°C for 0 min and (C) for 1 h, (D) in 2% Na_2CO_3 at 50°C for 2 h and (E) in 0.1 *M* NaOH at 100°C for 5 min and (F) for 15 min. Samples of 20 μl were applied to the analytical column and separated with an aqueous mobile phase containing 0.08% of *n*-octanesulphonate and 0.08% of TFA in a gradient of 1,4-dioxane (2.5% for 5 min and then to 25% in 10 min) at a flow-rate of 1 ml/min. (A) Some standards were separated under the same conditions.

labelled 4, had a slightly shorter retention time than TC and did not absorb at 360 nm. Whether these unidentified products have any relationship to those originating from the yellow and white thiol intermediates [27,32,34] needs further investigation.

CONCLUSIONS

It is suggested that reversed-phase HPLC on an ODS column with an acid–water mobile phase and with alkyl sulphonates serving as ion-pairing reagents may be of universal suitability for the separation of a wide range of unphosphorylated thiamine-related compounds. *n*-Octanesulphonate (0.08%) for ion-pairing, TFA (0.08%) as the acid component and a carefully profiled gradient of THF content in the mobile phase were found to provide the optimum compromise between different chromatographic properties of the chosen test set of compounds, including well known thiamine analogues, antagonists and degradation products. This and similar separation systems are generally recommended for testing the homogeneity of synthetic preparations of thiamine-related substances. The

suitability of chromatographic monitoring of some chemical (and possibly biochemical) reactions of vitamin B_1 has been opened up as a possibility.

ACKNOWLEDGEMENT

This work was supported in part by grant 6 P203 019 04 from the Polish Research Committee.

REFERENCES

1 L. Bettendorff, C. Grandfils, C. deRycker and E. Schoffeniels, *J. Chromatogr.*, 382 (1986) 297.
2 J.W.I. Brunnekreeft, H. Eidhof and J. Gerrits, *J. Chromatogr.*, 491 (1989) 89.
3 C.M.E. Tallaksen, T. Bohmer, H. Bell and J. Karlsen, *J. Chromatogr.*, 564 (1991) 127.
4 B.L. Lee, H.Y. Ong and C.N. Ong, *J. Chromatogr.*, 567 (1991) 71.
5 K. Ishi, K. Sarai, H. Sanemori and T. Kawasaki, *Anal. Biochem.*, 97 (1979) 191.
6 J. Bontemps, P. Phillipe, L. Bettendorff, J. Lombet, C. Dandrifosse, E. Schoffeniels, F. Nevejans and J. Crommen, *J. Chromatogr.*, 307 (1984) 283.
7 T. Kawasaki, *Methods Enzymol.*, 122 (1986) 15.
8 S. Sander, A. Hahn, J. Stein and G. Rehner, *J. Chromatogr.*, 558 (1991) 115.
9 L. Bettendorff, M. Peeters, C. Jouan, P. Windsand and E. Schoffeniels, *Anal. Biochem.*, 198 (1991) 52.
10 H. Sanemori, H. Ueki and T. Kawasaki, *Anal. Biochem.*, 107 (1980) 451.
11 M. Kimura, B. Panijpan and Y. Itokawa, *J. Chromatogr.*, 245 (1982) 141.
12 L. Warnock, *Anal. Biochem.*, 126 (1982) 112.
13 J. Bontemps, L. Bettendorff, J. Lombet, C. Grandfils, G. Dandrifosse, E. Schoffeniels, F. Nevejans and J. Crommen, *J. Chromatogr.*, 295 (1984) 486.
14 B. Hemming and C. Gubler, *J. Liq. Chromatogr.*, 3 (1980) 1697.
15 M. Kimura, T. Fujita, S. Nishida and Y. Itokawa, *J. Chromatogr.*, 188 (1980) 417.
16 J.T. Vanderslice and M.-H.A. Huang, *J. Micronutr. Anal.*, 2 (1986) 189.
17 C.J. Gubler and B.C. Hemming, *Methods Enzymol.*, 62 (1979) 63.
18 W.C. Ellefson, in J. Augustin, B.P. Klein, D.A. Becker and P.B. Venugopal (Editors), *Methods of Vitamin Assay*, Wiley, New York, 4th ed., 1985, Ch. 13, p. 349.
19 C. Kawasaki, *Vitam. Horm. (N.Y.)*, 21 (1963) 69.
20 E.F. Rogers, *Methods Enzymol.*, 18A (1970) 245.
21 R.A. Neal, *Methods Enzymol.*, 18A (1970) 133.
22 M. Rapala-Kozik and A. Kozik, *Biochim. Biophys. Acta*, 1159 (1992) 209.
23 C.J. Gubler, *Methods Enzymol.*, 18A (1970) 219.
24 J.L. Wittliff and R.L. Airth, *Methods Enzymol.*, 18A (1970) 229.
25 E.C. Nicolas and K.A. Pfender, *J. Assoc. Off. Anal. Chem.*, 73 (1990) 792.
26 T. Matsukawa, H. Hirano and S. Yurugi, *Methods Enzymol.*, 18A (1970) 141.
27 O. Zima, *Chem. Ber.*, 73 (1940) 941.
28 H. Andersag and K. Westphal, *Chem. Ber.*, 70 (1937) 2035.
29 G.E. Bonvicino and D.J. Hennessy, *J. Am. Chem. Soc.*, 79 (1957) 6325.
30 J.W. DeVries, in J. Augustin, B.P. Klein, D.A. Becker and P.B. Venugopal (Editors), *Methods of Vitamin Assay*, Wiley, New York, 4th ed., 1985, Ch. 4, p. 65.
31 T. Kronbach and W. Voelter, in A. Henschen, K.-P. Hupe, F. Lottspeich and W. Voelter (Editors), *High Performance Liquid Chromatography in Biochemistry*, VCH, Weinheim, 1985, Ch. 12, p. 533.
32 G.D. Maier and D.E. Metzler, *J. Am. Chem. Soc.*, 79 (1957) 4386.
33 J.R. Boissier and J.-P. Tillement, *Ann. Pharm. Fr.*, 27 (1969) 595.
34 G. Snatzke and R. Tschesche, in R. Ammon and W. Dirscherl (Editors), *Fermente, Hormone, Vitamine*, Vol. 3/1, Georg Thieme, Stuttgart, 1974, p. 572.

Journal of Chromatography, 648 (1993) 357–365
Elsevier Science Publishers B.V., Amsterdam

CHROM. 25 384

Solid-phase derivatization of amino acids and peptides in high-performance liquid chromatography

F.-X. Zhou and I.S. Krull*

Department of Chemistry, 102 Hurtig Building, Northeastern University, 360 Huntington Avenue, Boston, MA 02115 (USA)

B. Feibush

Supelco Corporation, Supelco Park, Bellefonte, PA 16823-0048 (USA)

(First received April 7th, 1993; revised manuscript received June 23rd, 1993)

ABSTRACT

This paper presents solid-phase derivatization of amino acids and peptides on a hydrophobic polymeric reagent. Using cationic surfactants as a basic pH, the negatively charged amino acids and peptides are ion-paired and derivatized by a 9-fluoreneacetyl tagged polymeric reagent. Using an off-line derivatization approach, the effects of the ion-pair reagent, buffer pH, reaction temperature, etc., on the derivatization are evaluated. Derivatization of peptides of enzymatically digested cytochrome *c* is included to show the feasibility of solid-phase derivatization to peptide mapping.

INTRODUCTION

Amino acids and peptides are important biological compounds. Amino acid analyzers are mostly based on ion-exchange separation and postcolumn derivatization and detection [1]. Reversed-phase liquid chromatography for these species on C_{18}-silica columns is becoming more popular, offering shorter analysis times and higher sensitivity. Such approaches are increasingly replacing the traditional methods. Depending on the HPLC method used, unmodified amino acids and peptides are detected by UV at a short wavelength or derivatized with UV/fluorescence (FL)/electrochemical detectable tags. Direct UV detection is simple and straightforward, but less sensitive and selective. Thus, most of the analytical methods for amino acids and peptides are based on the reaction of amino groups by precolumn or postcolumn FL derivatization, such as with ninhydrin, *o*-phthalaldehyde, flurescamine, 9-fluorenylmethoxycarbonyl chloride (9-FMOC), phenylisothiocyanate, dansyl and dabsyl chloride, as major derivatization reagents for sensitive detection [2,3]. 9-Fluoreneacetyl chloride (9-FA-Cl), was recently introduced as a fluorescent reagent for the derivatization of primary and secondary amines [4]. The 9-FA-Cl reagent has the same reactivity as the 9-FMOC reagent, but it shows improved product stability and less interferences by its hydrolytic byproduct, mainly 9-FA acid.

Hydration of ionic analytes and hydrolysis of reactive derivatization reagents in basic buffer solution are the main obstacles for derivatization in aqueous solutions, particularly at low analyte concentrations. Surfactants have been well known to form an aqueous micellar solution, which has a hydrophobic microenvironment and performs an ion-pair extraction function with ionic compounds [5]. Phase transfer catalysis

* Corresponding author.

0021-9673/93/$06.00

(PTC) was developed on the principle that the hydrophobic ion-pairing reagent transfers ionized analytes from an aqueous phase into an organic phase, where the analytes are derivatized with a fast reaction rate [6]. Using a micellar phase transfer catalysis (MPTC), efficient solution derivatizations have been developed for less nucleophilic ionic analytes, such as carboxylic acids [7–10].

Many solid-phase derivatization reagents have been developed for tagging hydrophobic nucleophiles [11–13]. However, charged amino acids can not easily get into the nonpolar polymeric reagent to be derivatized [14]. Derivatization efficiencies of amino acids were greatly reduced, as the free amino acids and peptides are soluble only in an aqueous phase. Thus, highly reactive solid-phase reagents, such as the polymeric hydroxybenzotriazole with 9-FMOC or 3,5-dinitrobenzoyl tags, were used to enhance the derivatization rate and efficiency for ionic nucleophiles. These solid-phase reagents have a limited stability in aqueous solutions, due to the competing hydrolysis process, especially at elevated temperatures and pH. Actually, reproducible and efficient solid-phase derivatization has never been successful for aqueous amino acids or peptides.

A phase transfer catalysis derivatization is developed in this paper for the efficient, solid-phase reactions of amino acids and peptides (Fig. 1). By incorporation of a cationic surfactant, negatively charged amino acids and peptides form ion-pairs which are extracted into the hydrophobic resin. Such ion-pair formation improves the mass transfer of ionic amino acids and peptides into the porous solid-phase reagent. These ion-paired, neutral complexes with their free amino groups react with the activated derivatization reagents to form an amide derivative bearing the detection tag. Conditions for solid-phase, 9-FA derivatization of amino acids were studied, including reaction time, temperature, buffer composition, and so forth. An example of the overall approach is provided using an enzymatic peptide digest of a cytochrome *c* sample, which was then derivatized and analyzed.

EXPERIMENTAL

Materials

Styrene–divinylbenzene copolymer (12% cross-linked, 60 Å templated, 10–20 μm) was obtained from Supelco (Bellefonte, PA, USA). Amino acids, cytochrome *c* (horse heart), chymotrypsinogen A, trypsin-TPCK and trifluoroacetic acid were all obtained from Sigma (St. Louis, MO, USA). HPLC-grade acetonitrile (ACN) solvent was generously donated by EM Science (Gibbstown, NJ, USA). Cationic surfactants were purchased from Aldrich (Milwaukee, WI, USA).

Instruments

Gradient separations of 9-FA tagged amino acid and peptide derivatives were performed on an automated Gilson HPLC system (Gilson

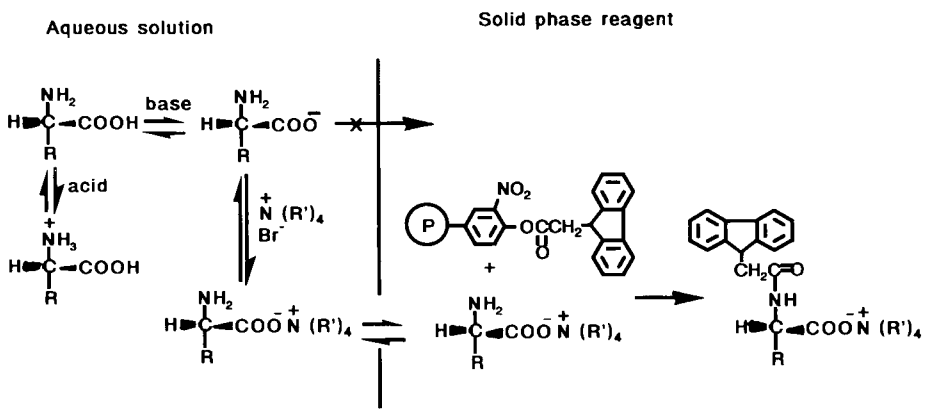

Fig. 1. Mechanism of phase transfer catalysis solid-phase derivatization for amino acids.

Medical Electronics, Middleton, WI, USA). This system consisted of a Gilson 232 auto-sampler, two Gilson 203 HPLC pumps, a Gilson 121 fluorescence detector with excitation at 254 nm and emission from 305–395 nm, a Gilson 811B dynamic mixer (1.5 ml), a Gilson 621 DataMaster, and an AST Premium 286 computer (AST Research, Irvine, CA, USA). The separation column was a YMC AP-303 300 Å ODS column (250 mm × 4.6 mm I.D.) from YMC (Morris Plains, NJ, USA). Chromatographic conditions were: mobile phase A: 0.05% (v/v) TFA in water; mobile phase B: 0.05% (v/v) TFA in ACN. The gradient program was: 0.00 min %B = 30.0; 16.00 min %B = 70.0; 22.00 min %B = 70.0; 22.50 min %B = 30.0.

Preparation of 9-FA tagged solid-phase reagent

The synthesis of the polymeric 9-FA derivatization reagent was performed as described in the literature [13,15]. Loading determinations of tag, by hydrolysis in a basic solution, showed 0.65 ± 0.05 mmol/g ($n = 2$) of tag content [4,11].

Synthesis of 9-FA amino acid standards

The authentic, standard derivatives of four amino acids were prepared by following a modified literature procedure, using 9-fluoreneacetyl chloride [16]. A 7.6 mmol sample of the amino acid was dissolved in 20 ml of 20% sodium carbonate. This solution was cooled to 0°C and 7.6 mmol of 9-fluoreneacetyl chloride (in 10 ml dioxane solution) was added dropwise, under stirring for 30 min. The solution was left at room temperature and stirred for 2 hours. The solution mixture was poured into 100 ml of distilled water. A 37% aqueous HCl solution was added to pH 2. The precipitate was collected and recrystallized from methanol. Mass spectrometric (MS) characterizations of these standards showed the expected structures. For example, the ammonia chemical ionization (Cl) mass spectrum of the 9-FA derivative of phenylalanine showed m/z values: 388.1; 386.1; 342.1; 300.2; 291.1; 170.1; 165.1; 121.1; 106.1; and 41.1 ($M + NH_3 = 388.1$). Other mass spectra of similar 9-FA amino acid derivatives were obtained (not reported).

Acid hydrolysis of proteins

A 1.0-mg sample of lyophilized protein, such as cytochrome *c*, was dissolved in 2 ml of 6 *M* HCl and heated under 90°C for 12 h in a sealed vial. The hydrolysate was dried under vacuum and reconstituted in 2.0 ml distilled water. This hydrolysate solution was directly used in the solid-phase derivatizations.

Trypsin digestion of cytochrome c

A solution of 2 mg/ml cytochrome *c* (from horse heart) was prepared in 100 m*M*, pH 8 ammonium bicarbonate buffer. Trypsin-TPCK was dissolved in the same buffer at a concentration of 0.1 mg/ml. To 0.5 ml of cytochrome *c* solution, 0.5 ml of trypsin solution was added. Digestion was kept at 37°C for 24 h, and then terminated by heating the digested solution at 100°C for 5 min [17]. The digested solution was directly derivatized with a solid-phase reagent.

Off-line derivatization

Off-line derivatizations were performed with 25 μl of analyte solution, 25 μl of sodium borate buffer solution, 25 μl of varying concentrations of a cationic surfactant and 12.5 μl ACN. Derivatization was performed in a water bath in a disposable pipet packed with 10 mg of 9-FA tagged reagent. After derivatization, the solid-phase reagent was washed with 1.0 ml of 70% ACN–water, 20 μl of which was injected into the HPLC.

RESULTS AND DISCUSSION

The cationic surfactants act as phase transfer catalysis agents by ion-pairing with a carboxyl group of the amino acids or peptides. The carboxyl group of amino acids is a weak acid, and needs a quaternary amine surfactant in order to form stable, hydrophobic, ion-pair complexes. Thus, type, size, and concentration of ion-pairing surfactant were important to the final ion-pair formation and to the derivatization efficiency.

Effect of ion-pair surfactant

To investigate the influence of ion-pair surfactant, off-line derivatizations of four amino acids

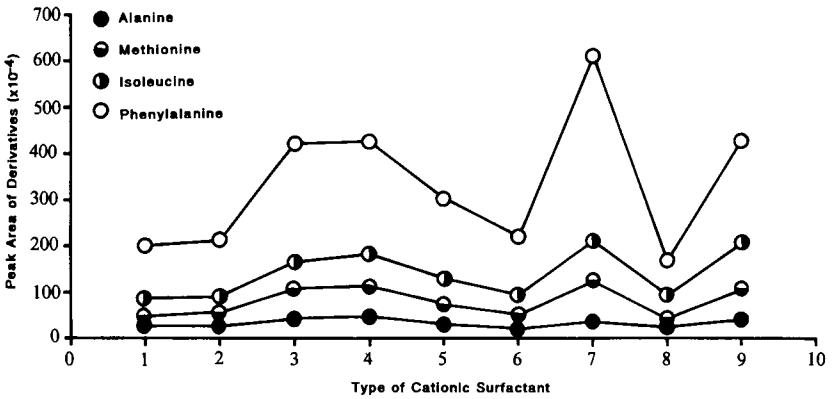

Fig. 2. Effect of surfactant type in solid-phase derivatizations. Off-line derivatization of *ca.* 10 mg 9-FA tagged reagent with 12.5 μl ACN, 25 μl 1.0 m*M* amino acid mixture, 25 μl of 20 m*M* surfactant and 25 μl of $Na_2B_4O_7$ buffer. After 10 min reaction at 75°C, the polymeric reagent was washed with 1.0 ml 70% ACN and 20 μl of the washings was injected. 1 = Tetramethylammonium chloride; 2 = tetraethylammonium hydrogen sulfate; 3 = tetra-*n*-propylammonium hydrogen sulfate; 4 = tetra-*n*-butylammonium bromide; 5 = tetrabutylammonium hydrogen sulfate; 6 = tetrabutylammonium dihydrogen phosphate; 7 = hexadecyl(cetyl)trimethylammonium bromide (CTAB); 8 = trimethylphenylammonium bromide; 9 = benzyltriphenylphosphonium chloride.

with nine cationic surfactants were studied (Fig. 2). These nine surfactants had different ion-pairing tendencies, hydrophobicities, steric hindrances, and thus different phase transfer abilities. Of the nine surfactants tested, hexadecyltrimethylammonium bromide (cetyltrimethylammonium bromide, CTAB) provided the highest derivatization yield. Thus, this ion-pair reagent was chosen as the best surfactant for amino acid and peptide derivations. It is of course possible that for other peptides, different ion-pair reagents may prove more optimal.

The optimum concentration of an ion-pair surfactant is dependent on its ion-pair formation tendency and hydrophobicity in a derivatization buffer. Strong ion-pairing ability and hydrophobicity of the cationic surfactant both enhance the accessibility of amino acids to the immobilized reagent. Solid-phase derivatization efficiencies for amino acids were very low (*ca.* 15% for phenylalanine) without any cationic surfactant catalyst in the derivatization solution. With the CTAB phase transfer surfactant, an 85% derivatization efficiency was obtained for phenylalanine. Investigation of surfactant concentration showed that there was no apparent increase in the derivatization yield when the CTAB concentration was larger than 20 m*M*. Thus, 20 m*M* CTAB was used to perform these solid-phase derivatizations.

Derivatization temperature and time

Temperature optimization was performed by holding the reaction time at 10 min. The derivatization yields of amino acids increased as the reaction temperature increased (Fig. 3).

A temperature of 70°C was selected as the optimum derivatization temperature, although higher derivatization yields were obtained at 85°C. A high derivatization temperature tends to increase hydrolysis of the solid-phase reagent, rendering interference peaks from the hydrolysis by-products. The boiling point of ACN is 82°C, which limits the temperature of the derivatization. Thus, a final temperature of 70°C was a compromise between the desired and undesired effects. The effect of reaction time on the amino acid derivatization was investigated at 70°C (Fig. 4). Although an increase in derivatization yield was possible beyond 10 min, 70°C for 10 min were selected as the derivatization conditions in order to get good reproducibility and a short derivatization procedure.

Buffer pH of derivatization solvent

In order to derivatize amino acids, buffer solutions with a basic pH are needed to provide enough nucleophilicity to the amino group. Fig. 5 shows the pH effect on the derivatization yield of amino acids. At pH 9.1, the amino group is in the free base form and the nucleophilic car-

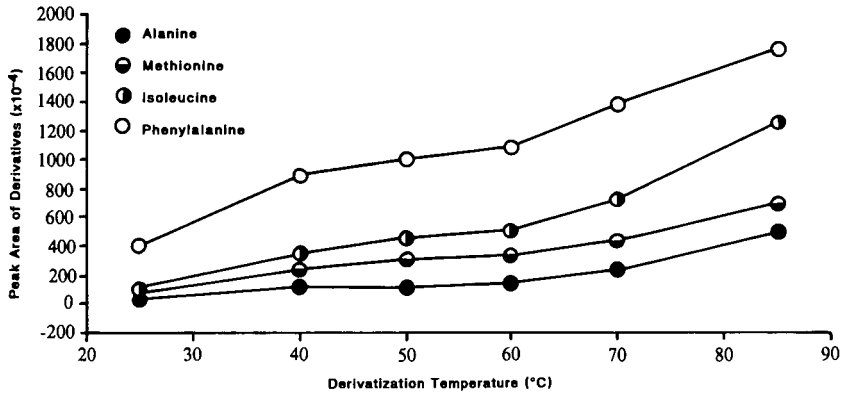

Fig. 3. Effect of temperature on off-line derivatization using CTAB; other conditions as in Fig. 2. Sample: amino acid mixture (1.0 m*M* in water).

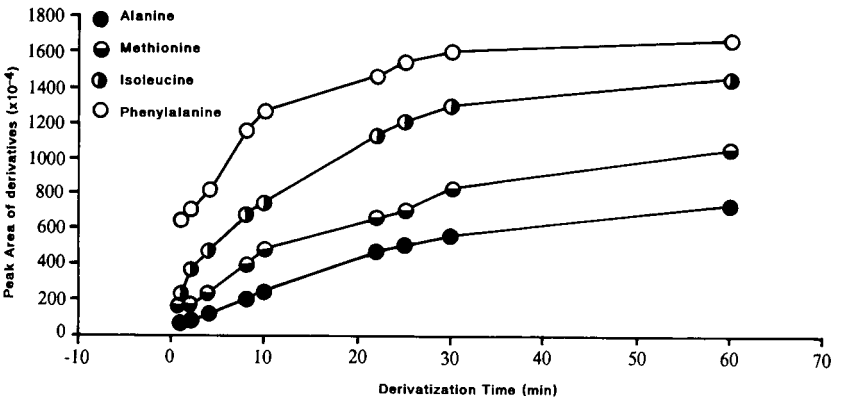

Fig. 4. Effect of time on off-line derivatization. Derivatization temperature 70°C; other conditions as in Fig. 2.

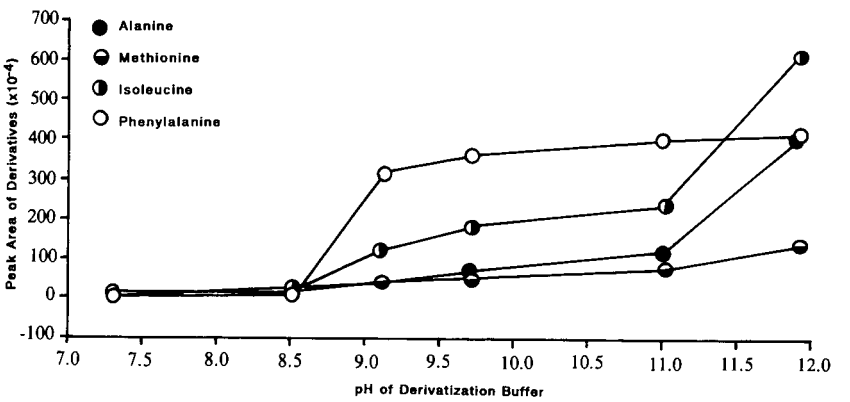

Fig. 5. Effect of pH on the derivatization yield of amino acids. Off-line derivatizations of 1.0 m*M* amino acids prepared in aqueous solution. Conditions as in Fig. 2, derivatization at 70°C for 10.0 min.

boxylate is negatively charged and ion-paired to the quaternary ammonium surfactant. Phase transfer now occurs with ease, and the nucleophilic amino group is derivatized by the hydrophobic polymeric reagent. At pH > 11, decomposition of the activated reagent was fast,

and the 9-FA acid hydrolysis by-product interfered in the chromatographic separation. Thus, pH 9.1 (sodium borate buffer) was selected as a compromise, to get reasonable percent derivatization and minimal reagent hydrolysis.

The ionic strength of the derivatization buffer suppresses the ion-pair dissociation, and affects the percent derivatization of amino acids by increasing the concentration of analyte in the polymeric support. The sodium borate concentration of the derivatization buffer needs to be maintained at levels high enough to ensure its basic buffer capacity and deprotonation of the amines. Derivatization yields of amino acids increased with sodium borate concentration, and a saturated sodium borate solution (0.23 *M* at room temperature) was the best for amino acid derivatizations.

Analyte hydrophobicity

Solid-phase derivatization is directly dependent on the actual concentration of each ion-paired amino acid in the polymeric reagent. This concentration is determined by the formation constant and the partition coefficient of the ion-paired, amino acid–quaternary ammonium complexes. Hydrophobic amino acids have stronger ion-pair formation constants, and with larger partition coefficients, they can be more efficiently extracted by the hydrophobic polymeric reagent. The less hydrophobic amino acids were expected to be less extractable. Consequently, they would be less derivatized by the polymeric reagent, as indeed was observed (Fig. 6).

Percent derivatization efficiencies of alanine, methionine, isoleucine and phenylalanine were 11 (8), 26 (6), 58 (5) and 85 (9), respectively, following their increased hydrophobicity. The numbers in parentheses are relative standard deviations (R.S.D.) of derivatization efficiency ($n = 3$) for each amino acid. Such big differences in derivatization efficiencies make the method somewhat less attractive for quantitative determinations of amino acid mixtures. However, from an applications point of view, this method is still practical, as long as the reaction conditions can ensure reproducibility of the method. The 9-FA tagged amino acid derivatives in the derivatizing buffer solution were stable over a two-week storage at ambient temperature, without any significant changes in peak intensities or retention times. Good stability of the final amino acid derivatives allowed for off-line derivatizations and provided reproducible results.

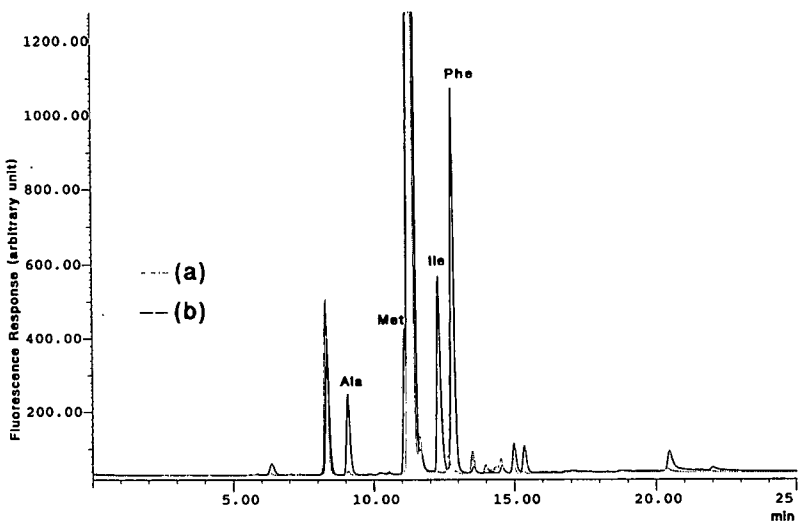

Fig. 6. Chromatogram of solid-phase derivatization of amino acid mixture. Separation column: YMC AP-303 300 Å ODS column, 250 mm × 4.6 mm I.D.; detection: FL, excitation wavelength 254 nm, emission wavelength 305–395 nm, 0.001 relative fluorescence units. Gradient separation in 25 min at flow-rate 1.5 ml/min. Mobile phase A: 0.05% TFA–water, B: 0.05% TFA–ACN in gradient: 0.00 min %B = 30.0; 16.00 min, %B = 70.0; 22.00 min, %B = 70.0; 22.50 min, %B = 30.0. (a) Blank; (b) 1.0 m*M* amino acid mixture.

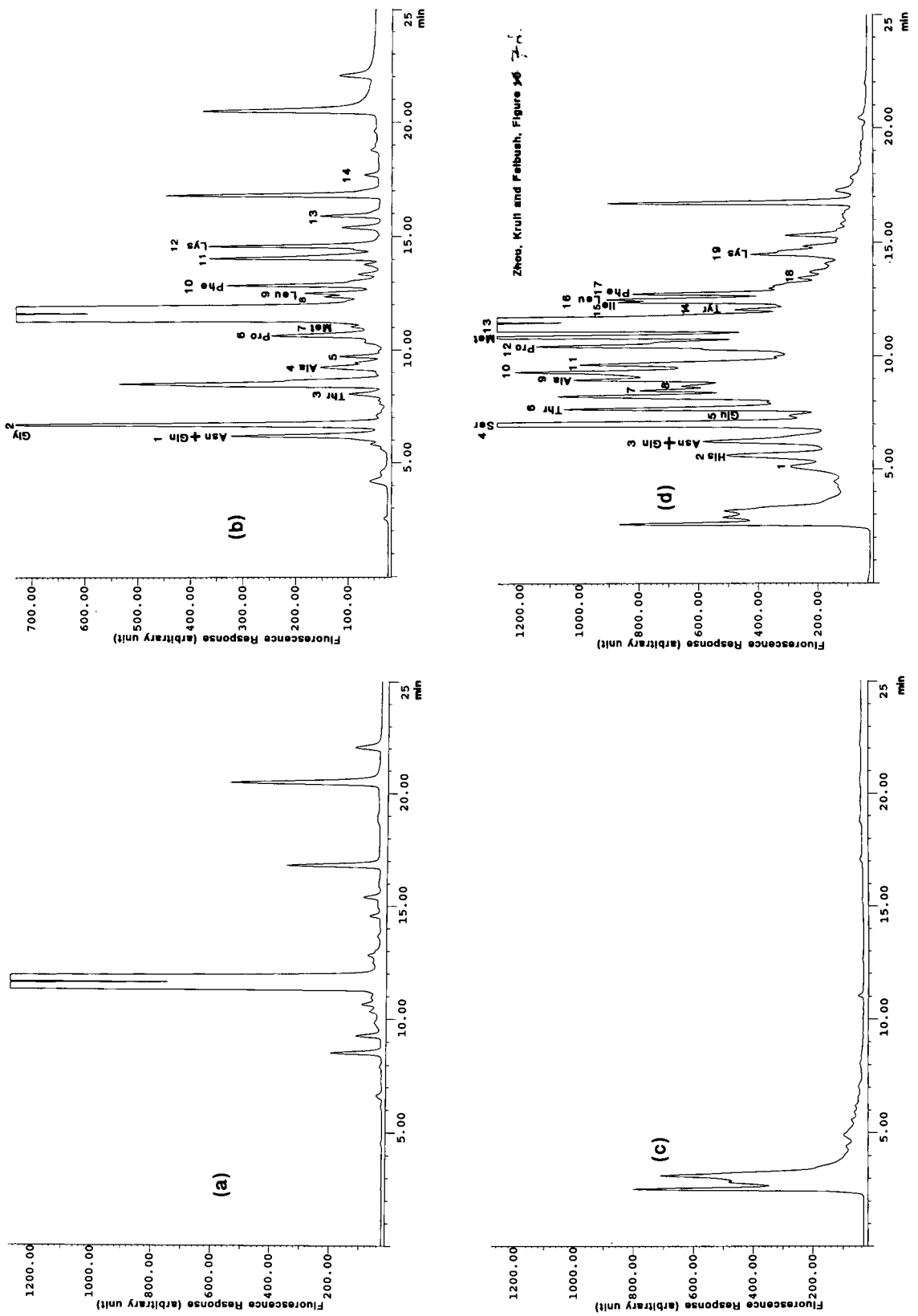

Fig. 7. Solid-phase derivatizations of protein hydrolysate. (a) Blank test of solid-phase reagent with water; (b) solid-phase derivatization of cytochrome *c* hydrolysate; (c) chymotrypsinogen A hydrolysate without derivatization; (d) solid-phase derivatization of chymotrypsinogen A hydrolysate. Separation and derivatization conditions as in Fig. 6.

Derivatization of amino acids from a protein hydrolysate

Fig. 7a is a blank test of the solid-phase reagent by off-line derivatization. The main peak at 11.3 min was confirmed to be 9-fluoreneacetic acid by a retention time comparison with an authentic standard under the same separation conditions. A chromatogram of the cytochrome *c* hydrolysate without derivatization showed no fluorescent response at the detection wavelengths. Fig. 7b shows a gradient separation of the solid-phase derivatized cytochrome *c* hydrolysate. There were 13 major derivative peaks. The resolutions of the 9-FA tagged amino acid derivatives were not fully optimized, some of the derivatives were not fully optimized, and thus some of the derivatives were not fully separated with these specific gradient conditions. However, these qualitative results demonstrated that the amino acids were derivatized by the solid-phase reagent. Because the derivatization percentage of amino acids with this method is analyte dependent, ratios of peak intensity in the chromatogram of the derivatized protein hydrolysate do not represent a quantitative ratio of the amino acid composition. Standard calibration plots would be needed in order to derive such more quantitative data.

Fig. 7c is a chromatogram of the underivatized protein hydrolysate from chymotrypsinogen A. There were few components which had fluorescence responses. Fig. 7d is a chromatogram of the derivatized chymotrypsinogen A hydrolysate. Sixteen major derivatization products were obtained with FL detection. Comparing Fig. 7b and d, obvious differences can be seen in the intensities and positions of derivative peaks. These different chromatograms qualitatively show the differences of the two proteins in their amino acid compositions.

Derivatization of enzymatically digested cytochrome c

An enzymatically digested cytochrome *c* was chosen as a sample of a peptide mixture. There were 14 major peptide peaks separated from digested horse cytochrome *c* with gradient reversed-phase separation and UV detection at 214 nm. Separation of the solid-phase derivatized digestion buffer (trypsin dissolved in ammonium bicarbonate buffer) showed the 9-FA acid from the hydrolysis of the solid-phase reagent and the derivatization product of ammonia, while the digested cytochrome *c* showed no fluorescent response without derivatization. Fig. 8 shows the derivatized peptides from a cytochrome *c* digestion with solid-phase derivatization, which has 15 major derivative peaks.

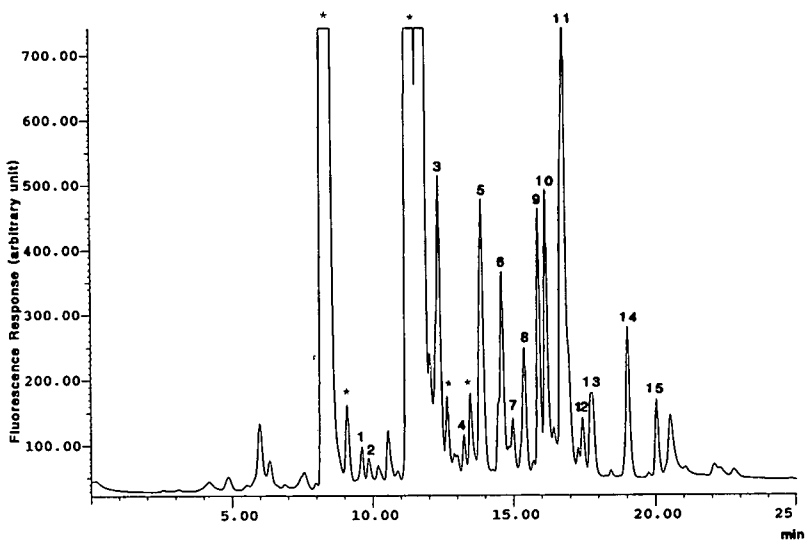

Fig. 8. Solid-phase derivatization of trypsin digested cytochrome *c*. Separation conditions as in Fig. 6. Peaks with * were from the derivatization of blank digestion solution (trypsin with buffer).

CONCLUSIONS

The authors have developed a reaction–detection technique using solid-phase, ion-pairing derivatization of amino acids and peptides. The high sensitivity of fluorescent derivations and the hydrophobic extraction function of polymeric reagents made this approach very promising for ionic nucleophiles. Due to the interference by 9-fluoreneacetic acid produced by hydrolysis of the derivatization reagent, an on-line derivatization of amino acids with this 9-FA tagged solid-phase reagent was unsuccessful. Immobilization of other derivatization tags, which do not introduce detection interference by hydrolysis products, are being investigated in our research group for on-line derivatizations.

ACKNOWLEDGEMENTS

This research was supported by Supelco (Bellefonte, PA, USA). We are very grateful to Gilson Medical Electronics (Middleton, WI, USA) and EM Science (Gibbstown, NJ, USA) for the loan and donations of a Gilson automated system and HPLC solvents, respectively. We also thank Bob Cooley of YMC (Wilmington, NC, USA) for donation of the YMC HPLC columns used in this study. Special thanks are due to Mr. A.J. Bourque, Dr. G. Lai and Ms. J.H. Yu for their experimental help. J.M. Thorne and M.E. Szulc are thanked for helpful discussions in the preparation of the final manuscript.

REFERENCES

1 D.H. Spackman, W.H. Stein and S. Moore, *Anal. Chem.*, 30 (1958) 1190.
2 G. Ogden and P. Foldi, *LC GC*, 5 (1987) 28.
3 C.W. Tabor and H. Tabor, *Anal. Biochem.*, 78 (1977) 543.
4 H.M. Zhang, F.X. Zhou and I.S. Krull, *J. Pharm. Biomed. Anal.*, 10 (1992) 577.
5 R.A. Grohs, F.V. Warren Jr. and B.A. Bildingmeyer, *Anal. Chem.*, 63 (1991) 384.
6 C.M. Starks and C. Liotta, *Phase Transfer Catalysis, Principles and Techniques*, Academic Press, New York, 1978.
7 S. Allenmark, M. Chelminska-Bertilsson and R.A. Thompson, *Anal. Biochem.*, 185 (1990) 279.
8 F.A.L. van der Horst, J.M. Reijn, M.H. Post, A. Bult, J.J.M. Holthuis and U.A.Th. Brinkman, *J. Chromatogr.*, 507 (1990) 351.
9 F.A.L. van der Horst, J. Teeuwsen, J.J.M. Holthuis and U.A.Th. Brinkman, *J. Pharm. Biomed. Anal.*, 8 (1990) 8.
10 F.A.L. van der Horst, *Trends Anal. Chem.*, 8 (1989) 268.
11 A.J. Bourque and I.S. Krull, *J. Chromatogr.*, 537 (1991) 123.
12 Z. Zhang, G. Malikin and S. Lam, *J. Chromatogr.*, 603 (1992) 279.
13 F.X. Zhou, I.S. Krull and B. Feibush, *J. Chromatogr.*, 609 (1992) 103.
14 E.P. Kroeff and D.J. Pietrzyk, *Anal. Chem.*, 50 (1978) 502.
15 B.J. Cohen, H. Karoly-Hafeli and A. Patchornik, *J. Org. Chem.*, 49 (1984) 9922.
16 L.A. Carpino and G.Y. Han, *J. Org. Chem.*, 37 (1972) 3404.
17 P.M. Young and T.E. Wheat, *J. Chromatogr.*, 512 (1990) 273.

Journal of Chromatography, 648 (1993) 367–371
Elsevier Science Publishers B.V., Amsterdam

CHROM. 25 365

Effect of synthetic polymers, poly(N-vinyl pyrrolidone) and poly(N-vinyl caprolactam), on elution of lactate dehydrogenase bound to Blue Sepharose

Igor Yu. Galaev and Bo Mattiasson*

Department of Biotechnology, Chemical Centre, Lund University, P.O. Box 124, S-221 00 Lund (Sweden)

(First received October 19th, 1992; revised manuscript received June 1st, 1993)

ABSTRACT

The synthetic polymers poly(N-vinyl pyrrolidone) and poly(N-vinyl caprolactam) are shown to be more efficient eluting agents of porcine muscle lactate dehydrogenase bound to Blue Sepharose than traditionally used NADH and oxamate or high salt concentration. Preliminary treatment of the Blue Sepharose column with a polymer solution drastically improved the elution effectiveness of the column and the enzyme recovery during "specific elution" with 10 m*M* oxamate and 0.1 m*M* NADH and "unspecific elution" with 1.5 *M* KCl. The effect of the polymers may be attributed to their ability to selectively mask sites on the matrix that are not specific for the nucleotide-binding region of the enzyme, while not seriously impairing interaction with specific sites.

INTRODUCTION

The reactive dye, Cibacron Blue 3 GA, is widely used as a ligand for "dye-affinity", "group-specific affinity" or "pseudoaffinity" chromatography of various proteins, especially dehydrogenases and kinases [1–3]. The success of chromatographic separations on Blue Sepharose (Sepharose to which Cibacron Blue is covalently bound) stems largely from the apparent specific binding between the nucleotide binding sites of these enzymes and the dye ligand [4]. The Cibacron Blue ligand can interact (apart from with nucleotide binding sites) unspecifically with the protein molecule as a result of hydrophobic and ion-exchange interaction. This fact may conceivably reduce the recovery of such a protein by "specific" elution with nucleotide. Unexpectedly low recoveries of nucleotide-dependent proteins in affinity chromatography on Cibacron Blue-containing matrices have been described [5–9].

High salt concentrations reduce protein–dye interactions, and most proteins can be eluted "unspecifically" from dye-containing matrices by 1–1.5 *M* NaCl or KCl [10]. Unspecific elution is often more efficient than specific elution [11].

Previously, we found that the synthetic polymer poly(N-vinyl caprolactam) (PVCL) interacts efficiently with Cibacron Blue and that this interaction is strong enough to prevent "specific" binding of the dye to lactate dehydrogenase (LDH) from porcine muscle [12]. The purpose of this work was to use PVCL and the related polymer, poly(N-vinyl pyrrolidone) (PVP), for the improvement of elution of LDH from Blue Sepharose.

EXPERIMENTAL

Chemicals

Lactate dehydrogenase type XXX-S from porcine muscle, β-NADH grade III and PVP K

* Corresponding author.

0021-9673/93/$06.00

26-35 with an average molecular mass of 40 000 and K 12-18 with an average molecular mass of 10 000 were purchased from Sigma. Oxamic acid was purchased from BDH. PVCL was produced by radical polymerization in isopropanol using azo-bis-isobutyronitrile as initiator [13]. The molecular mass of PVCL, 80 000, was calculated from viscosimetric data [14]. LDH was dialysed before use. Blue Sepharose was synthesized according to ref. 15. The Cibacron Blue content determined according to ref. 16 was 4.9 μmol per ml of swollen gel.

Chromatography

All chromatographic analyses were done at room temperature using a 1.8 × 0.9 cm I.D. column. All solutions introduced to the column were in 20 m*M* Tris–HCl buffer, pH 7.3. LDH (110–140 U) was applied to the column in a volume of 1.6 ml. LDH was eluted at a flow-rate of 0.16 ml/min; fractions were collected every 20 min.

The polymer elution was performed with 0.2 or 1% PVP-40 000 and 1% PVP-10 000 and 1% PVCL. The PVP passivation of the column was performed with 1% PVP-40 000 solution followed by washing with 1.5 *M* KCl, pH 3.4, until no PVP was detected in the eluent and re-equilibration with 20 m*M* Tris–HCl buffer, pH 7.3. The unspecific elution was performed with 1.5 *M* KCl; the specific elution was performed with 10 m*M* oxamate + 0.1 m*M* NADH.

LDH activity was measured in the fractions according to ref. 17. The concentration of PVP or PVCL was measured as absorption of polymer–iodine complex at 480 nm, the complex being produced according to ref. 18.

RESULTS AND DISCUSSION

The efficiency of eluting agents was tested for some different compounds. Fig. 1 shows that 1% PVP-40 000 or PVCL solution is a more efficient unspecific eluting agent than a pulse of 1.5 *M* KCl. In all three cases binding was >99% and recovery was about 75%. Elution of LDH began with the front of polymer in the effluent. Elution with a lower PVP concentration, 0.2%, or with

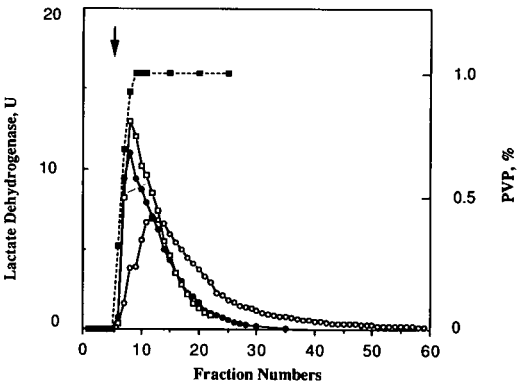

Fig. 1. LDH elution profile from Blue Sepharose with 1.5 *M* KCl (○), 1% PVP (●) and 1% PVCL (□). The arrow indicates when elution was begun. The polymer concentration in fractions eluted with 1% PVP is presented as ■. Experimental conditions: 1.8 × 0.9 cm I.D. column; all solutions introduced to the column were in 20 m*M* Tris–HCl buffer, pH 7.3. Aliquots of 120 U (1.5 *M* KCl and 1% PVP elution) or 135 U (1% PVCL elution) of LDH were applied to the column in a volume of 1.6 ml. LDH was eluted at a flow-rate of 0.16 ml/min. Fractions were collected every 20 min.

PVP of lower molecular mass (10 000) was less efficient (Fig. 2).

Thus, PVP and PVCL, owing to their strong interaction with Cibacron Blue, could displace LDH bound to Blue Sepharose. Neither polymer in 1% concentration had any effect on LDH

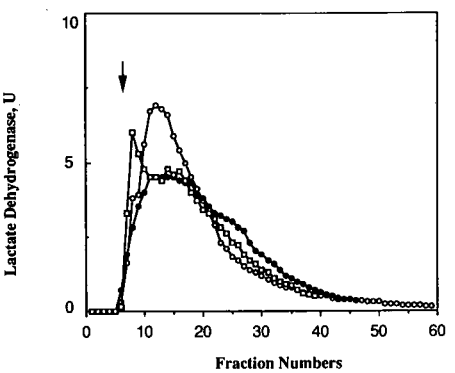

Fig. 2. LDH elution profile from Blue Sepharose with 1.5 *M* KCl (○), 0.2% PVP (molecular mass 40 000) (●) and 1% PVP (molecular mass 10 000) (□). The arrow indicates when elution was begun. Experimental conditions: 1.8 × 0.9 cm I.D. column; all solutions introduced to the column were in 20 m*M* Tris–HCl buffer, pH 7.3. Aliquots of 120 U of LDH were applied to the column in a volume of 1.6 ml. LDH was eluted at a flow-rate of 0.16 ml/min. Fractions were collected every 20 min.

activity. PVP is a commercially available, relatively cheap and biologically compatible polymer, and in some cases PVP elution might be a good alternative to specific elution with nucleotides or unspecific elution with high salt concentrations. PVP is widely used for plasma substitute production because the properties of the polymer solution resemble those of serum albumin [19].

Aqueous solutions of PVCL are characterized by a low critical solution temperature (LCST), and this property can be exploited for polymer recovery from the eluent [12]. On raising the temperature of aqueous solutions of PVCL to a point higher than the lower critical solution temperature (35–40°C), separation into two phases takes place. A polymer-enriched phase and an aqueous phase containing practically no polymer are formed. Both phases can be easily separated by low-speed centrifugation. This phase separation is reversible and PVCL readily dissolves in water on cooling [20,21]. LDH was completely recovered in the aqueous phase during the PVCL thermoprecipitation. The enzyme was stable enough at the temperatures at which phase separation took place [12].

The eluate after PVCL elution of LDH from the Blue Sepharose column was heated up to 45°C, which resulted in the precipitation of PVCL. The pellet was removed by centrifugation at 45°C. The supernatant contained LDH in buffer solution with practically no polymer. The yield of LDH activity during this procedure was 85%. The PVCL pellet was resolubilized at room temperature with polymer recovery of 95–98%. The PVCL solution could be reused for LDH elution.

In Fig. 3 is shown the specific elution of LDH from Blue Sepharose using 10 m*M* oxamate + 0.1 m*M* NADH. After the pulse of specific eluent, a pulse of 1% PVP was added and more LDH was eluted. No LDH could be eluted by 10 m*M* oxamate + 0.1 m*M* NADH after PVP elution. This demonstrated that elution with PVP is efficient.

PVP bound strongly to the Blue Sepharose, and this resulted in a dramatic improvement in the elution effectiveness of the column during subsequent elution, either specific or unspecific

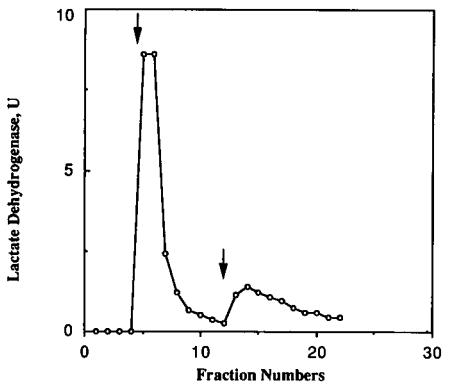

Fig. 3. LDH elution profile from Blue Sepharose with 10 m*M* oxamate and 0.1 m*M* NADH followed by 1% PVP elution. The arrows indicate when elution with 10 m*M* oxamate and 0.1 m*M* NADH and with 1% PVP was begun. Experimental conditions: 1.8 × 0.9 cm I.D. column; all solutions introduced to the column were in 20 m*M* Tris–HCl buffer, pH 7.3. 110 U of LDH were applied to the column in a volume of 1.6 ml. LDH was eluted at a flow-rate of 0.16 ml/min. Fractions were collected every 20 min.

(Fig. 4a and b, respectively). For comparison, LDH elution profiles from a polymer-untreated column under the same conditions are presented

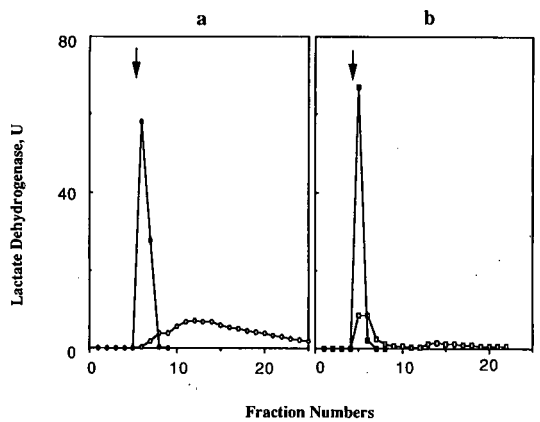

Fig. 4. LDH elution profile from PVP-treated Blue Sepharose with (a) 1.5 *M* KCl (●) and (b) 10 m*M* oxamate and 0.1 m*M* NADH (■). The arrow indicates when elution was begun. For comparison, LDH elution profiles from an untreated column with (a) 1.5 *M* KCl (○) and (b) 10 m*M* oxamate and 0.1 m*M* NADH (□) under the same conditions are presented. Experimental conditions: 1.8 × 0.9 cm I.D. The column was washed with 1% PVP solution and was then washed with 1.5 *M* KCl until no PVP was detected in the eluent. Aliquots of 120 U of LDH were applied to the column in a volume of 1.6 ml. LDH was eluted at a flow-rate of 0.16 ml/min. Fractions were collected every 20 min.

TABLE I

EFFECT OF POLY(N-VINYL PYRROLIDONE) ON AFFINITY CHROMATOGRAPHY OF LACTATE DEHYDROGENASE ON BLUE SEPHAROSE

Experimental conditions are as described in the legend to Fig. 4.

Elution	LDH binding (%)		LDH recovery (%)	
	Untreated column	PVP-treated column	Untreated column	PVP-treated column
Unspecific	>99	>99	76	98
Specific	>99	>99	36	85

in Fig. 4a and b. Polymer treatment of the column improved LDH recovery, especially in the case of specific elution (Table I).

Coating with hydrophilic polymers has previously been used in chromatography of biomolecules either for imparting new properties to the matrix, *e.g.*, formation of anion-exchange phases by cross-linking of polyimines with bifunctional glycidoxy compounds [22], or for decreasing unwanted interactions between protein and the matrix [23,24].

PVP can bind effectively various negatively charged dyes as a result of hydrophobic and ion–dipole interaction [19]. The affinity ligand used in this study, Cibacron Blue 3GA, is a dye of this type. PVP had no effect on LDH elution from unsubstituted Sepharose CL 4B and on peroxidase elution from concanavalin A–Sepharose (data not shown). We propose that the polymer bound tightly to the dye, each polymer molecule interacting with several Cibacron Blue molecules. This interaction was so efficient that PVP could not be completely eluted during re-equilibration of the column. PVP–ligand interaction is stronger than unspecific interaction of LDH with the ligand, but weaker than specific binding to Cibacron Blue ligand at the active site of the enzyme. The bound polymer rather prevented only weak unspecific interactions of LDH with the dye ligands. The realization of only specific interactions between the dye ligand and LDH resulted in an extremely sharp elution profile and improvement of enzyme recovery. After PVP passivation the column retained its high effectiveness of elution, at least in the course of three successive runs. The multisite attachment of PVP to the matrix is assumed to protect the polymer from complete replacement by LDH.

PVP treatment of the Blue Sepharose column thus eliminated many unspecific interactions. It was also noted that the binding capacity of the column was decreased by approximately a factor of two upon polymer treatment. These effects are now being studied in more detail.

There are thus several ways of eluting LDH bound to Blue Sepharose. Traditionally, KCl has been used for unspecific elution and NADH + oxamate for specific elution. To these alternatives can now be added elution by certain polymers. It is still too early to say which method is ideal, since the model studies discussed in this paper all deal with pure enzyme preparations. Work is in progress in our laboratory to evaluate this new elution concept when isolating enzyme from crude homogenates. We hope to be able to report these experiments elsewhere.

A similar improvement in enzyme recovery after pretreatment with bovine serum albumin of a Blue Sepharose column was shown previously [8]. The authors ascribed the effect to the ability of albumin to selectively mask affinity sites on the matrix, which are not specific for the nucleotide-binding region of the enzyme, while not seriously impairing enzyme interaction with specific sites. This explanation seems to be reasonable also for PVP treatment of Blue Sepharose. The use of a synthetic biocompatible

polymer with low or no immunogenicity seems attractive as compared with adding new proteins to a purification system.

ACKNOWLEDGEMENTS

The support of The Swedish Royal Academy of Sciences (KVA), the National Swedish Board for Technical and Industrial Development (NUTEK) and The Swedish Research Council for Engineering Sciences (TFR) is gratefully acknowledged. The authors thank Nora Perotti for the synthesis of Blue Sepharose. The linguistic advice of Dr. Rajni Kaul is gratefully acknowledged.

REFERENCES

1 M.A. Vijayalakshmi, *Trends Biotechnol.*, 7 (1989) 71.
2 F. Qadri, *Trends Biotechnol.*, 3 (1985) 7.
3 C.V. Stead, *Bioseparation*, 2 (1991) 129.
4 E. Stellwagen, R. Cass, S.T. Thompson and M. Woody, *Nature*, 257 (1975) 716.
5 M. Morrill, S.T. Thompson and E. Stellwagen, *J. Biol. Chem.*, 254 (1979) 4371.
6 B. Notton, R. Fido and E. Hewitt, *Plant Sci. Lett.*, 8 (1977) 165.
7 R. Harkins, J. Black and M. Rittenberg, *Biochemistry*, 16 (1977) 3831.
8 C.S. Ramadoss, J. Steczko, J.W. Uhlig and B. Axelrod, *Anal. Biochem.*, 130 (1983) 481.
9 A.J. Anderson, *J. Chem. Educ.*, 65 (1988) 901.
10 R.K. Scopes, in M.A. Vijayalakshmi and O. Bertrand (Editors), *Protein–Dye Interactions: Developments and Applications*, Elsevier, London, 1989, p. 97.
11 A.A. Glemza, B.B. Baskeviciute, V.A. Kadusevicius, J.H.J. Pesliaskas and O.F. Sudziusviene, in M.A. Vijayalakshmi and O. Bertrand (Editors), *Protein–Dye Interactions: Developments and Applications*, Elsevier, London, 1989, p. 107.
12 I.Yu. Galaev and B. Mattiasson, *Biotech. Bioeng.*, 41 (1993) 1101.
13 Yu.E. Kirsh, T.A. Sus, T.M. Karaputadze and V.A. Kabanov, *Vysokomolek. Soed.*, A21 (1979) 2634.
14 Yu.E. Kirsh, I.Yu. Galaev, T.M. Karaputadze, A.L. Margolin and V.K. Svedas, *Biotechnologia*, 2 (1987) 184.
15 W. Heyns and P. DeMoor, *Biochim. Biophys. Acta*, 358 (1974) 1.
16 G.K. Chambers, *Anal. Biochem.*, 83 (1977) 551.
17 *Worthington enzymes and related biochemicals*, Freehold, NJ, 1982, p. 109–110.
18 *European Pharmacopoeia*, Part I, Maisonneuve S.A, Sainte-Ruffine, 2nd ed., 1986, p. 685-2.
19 Yu.E. Kirsh, *Prog. Polymer Sci.*, 11 (1985) 283.
20 A.A. Tager, A.P. Safronov, S.V. Sharina and I.Yu. Galaev, *Vysokomol. Soed.*, A32 (1990) 529.
21 S.F. Sherstyuk, I.Yu. Galaev, A.P. Savitskii, E.Yu. Kirsh and I.V. Berezin, *Biotechnologia.*, 2 (1987) 179.
22 A.J. Alpert and F.E. Regnier, *J. Chromatogr.*, 185 (1980) 375.
23 X. Santarelli, D. Muller and J. Jozefonvicz, *J. Chromatogr.*, 443 (1988) 55.
24 L. Letot, J. Lesec and C. Quivoron, *J. Liq. Chromatogr.*, 4 (1981) 1311.

Journal of Chromatography, 648 (1993) 373–380
Elsevier Science Publishers B.V., Amsterdam

CHROM. 25 376

Simple high-performance liquid chromatographic method for assessing the deterioration of atropine–oxime mixtures employed as antidotes in the treatment of nerve agent poisoning

Brian M. Paddle* and Margaret H. Dowling

Materials Research Laboratory, Defence Science and Technology Organisation, P.O. Box 50, Ascot Vale, Melbourne 3032 (Australia)

(First received March 15th, 1993; revised manuscript received June 25th, 1993)

ABSTRACT

A set of reversed-phase HPLC conditions for determining the degradation of atropine and the oxime (pralidoxime, obidoxime, or HI-6) in autoinjectors designed for use against nerve agent poisoning is described. The assay conditions for atropine do not require its prior separation from the large molar excess of oxime since both the atropine and tropic acid peaks elute well clear of the oxime and its degradation products and the phenolic preservatives. Further dilution of the sample and simple changes to the mobile phase then provide conditions for the oxime and its major degradation products to be quantitated.

INTRODUCTION

A mono-quaternary-pyridinium or bis-quaternary-pyridinium oxime with atropine is the basis of the currently preferred treatment for poisoning by organophosphate compounds [1]. Autoinjectors containing these materials are provided to military personnel for self-aid against nerve agent poisoning.

Despite the many reports of HPLC methods for the analysis of atropine and the above oximes, particularly those that also consider their degradation products [2–11], we have found few if any that can be applied directly to both these components in injection mixtures [12,13]. Typically the autoinjectors contain oxime:atropine millimolar ratios of between 100:1 and 1100:1 and the tailing of the large oxime peak at the solvent front has made the direct assay of atropine and its breakdown products in such mixtures difficult.

Of the oximes, HI-6 is less stable in aqueous solution than either obidoxime or pralidoxime chloride [6,14,15]. Also solutions of HI-6 or pralidoxime chloride are less stable than atropine sulphate [6,13,16]. However, both the atropine and the oxime in injectors could be susceptible to the effects of high ambient temperatures [4,5,10,14,17,18] as might be found under some field conditions.

This paper describes a relatively simple HPLC method for determining the extent of degradation of the oxime and atropine in autoinjectors that does not involve a prior separation of the solution components. The method allows the

* Corresponding author.

detection and assay of one or more of the known breakdown products as well as the assay of the parent compounds.

EXPERIMENTAL

Materials

Atropine sulphate, pralidoxime chloride [2-((hydroxyimino)methyl)-1-methyl pyridinium chloride] (2-PAM-Cl) and pralidoxime methanesulphonate (P2S) were obtained from Sigma (USA). Obidoxime chloride [1,1′-(oxy-bis(methylene)) - bis(4 - (hydroxyimino)methyl) - pyridinium dichloride] (Toxogonin) was obtained from E. Merck (Germany) and HI-6 {1-[((4-(aminocarbonyl)-pyridino)methoxy)methyl]-2[(hydroxyimino)methyl]-pyridinium dichloride} from Drs. P.A. Lockwood and J.G. Clement, Defense Department, Canada. The structures are detailed in Fig. 1.

Other compounds, used as standards, were DL-tropic acid, pyridine-2-aldoxime, pyridine-4-aldoxime, isonicotinic acid (pyridine-4-carboxylic acid), isonicotinamide (pyridine-4-carboxylic acid amide) and methyl paraben (*p*-hydroxybenzoic acid methyl ester) (all from Sigma). Phenol was obtained from International Biochemistry Industries (CT, USA) and α-picolinamide (pyridine-2-carboxylic acid amide) from the Tokyo Chemical Industry Company, Japan.

Tetramethylammonium chloride (TMA) was obtained from Fluka (Germany) and 1-octanesulphonic acid sodium salt (1-OSA) from Sigma.

Other reagents were analytical grade.

Acetonitrile was HPLC grade purchased from Waters Division of Millipore (USA), and distilled water was deionized by a Milli-Q water-purification system (Millipore, USA).

Samples of autoinjectors containing a solution of atropine sulphate and obidoxime chloride (Combopen, Duphar, Amsterdam, Netherlands) or atropine sulphate and HI-6 (Astra Meditec, Mölndal, Sweden) were obtained from the Australian Department of Defence, Canberra, Australia.

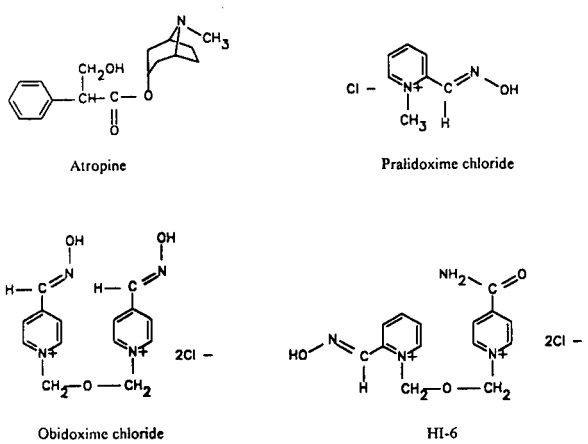

Fig. 1. Structures of atropine and the oximes.

Chromatography

Isocratic, reversed-phase HPLC was carried out using a Waters system comprising a 510 pump, 712 WISP autoinjector, 481 variable-wavelength UV detector and 730 data module. A Zorbax RX-C_{18} column (25 cm × 4.6 mm I.D.) and guard column (1.25 cm × 4.0 mm I.D.) (particle size 5 μm) (Rockland Technologies, USA) was chosen for the analyses. The column temperature was maintained at 25°C.

The limits of composition of the mobile phase, which were optimized for each particular component and its degradation products, were: 50 m*M* sodium dihydrogenorthophosphate, 1–5 m*M* TMA, 0.5–1 m*M* 1-OSA and between 3.0 and 20% (v/v) acetonitrile in Milli-Q water. The pH was adjusted to 3.5 with concentrated orthophosphoric acid. Finally the mobile phase was filtered through a 0.45-μm Millipore filter. During analyses the flow-rate was 1 ml/min. Details of the specific composition of each mobile phase used for estimating the extent of degradation of the different oximes or atropine are given in Table I.

Detection wavelengths (Table II) were selected that would increase the sensitivity of the HPLC analyses to the degradation products of the oximes or better allow the detection of atropine and tropic acid in the presence of up to a 1100-fold excess of oxime. Information in this regard was obtained from absorbtion spectra of 0.1 m*M* solutions of the oximes and atropine and known degradation products in a mobile phase (pH 3.5) containing 50 m*M* sodium dihydrogen-

TABLE I

MOBILE PHASE COMPOSITIONS FOR DEGRADATION STUDIES OF OXIME–ATROPINE MIXTURES

Column: Zorbax RX-C_{18}. Buffer: 50 m*M* NaH_2PO_4, mobile phase pH 3.5.)

Heated mixture (m*M*)	Component assayed	TMA (m*M*)	1-OSA (m*M*)	Acetonitrile (%, v/v)	Mobile phase
2-PAM-Cl–atropine (1740:1.5)	Atropine	1	0.5	20.0	A
Obidoxime–atropine (209:1.4)	Atropine	1	0.5	20.0	A
HI-6–atropine (350:1.5)	Atropine	1	0.5	20.0	A
2-PAM-Cl–atropine (1740:1.5)	2-PAM-Cl	1	1.0	3.0	B
Obidoxime–atropine (209:1.4)	Obidoxime	5	1.0	13.0	C
HI-6–atropine (350:1.5)	HI-6	1	1.0	10.0	D

orthophosphate, 5 m*M* TMA, 1 m*M* 1-OSA and 20% (v/v) acetonitrile. (The instrument used was a Pye-Unicam PU 8800 UV–Vis spectrophotometer). This mobile phase did not account for more than 6% of the absorbance of the oximes or atropine at any of the wavelengths selected and not more than 14% of the absorbance of the degradation standards.

Sample preparation

Concentrated standard solutions of atropine sulphate (0.1 *M*), pyridinium oximes (0.2–1.74 *M*) and certain of their degradation products (see *Materials*) (0.1 *M*) were prepared in Milli-Q water and stored frozen until required. HI-6 was prepared just prior to use.

Aqueous 0.5-ml samples of an oxime and/or

TABLE II

HPLC CONDITIONS FOR DETERMINING THE EXTENT OF DEGRADATION OF THE OXIME AND ATROPINE IN OXIME–ATROPINE MIXTURES

Column and millimolar ratio of oxime–atropine as in Table I. Injection volume 20 μl. Peak heights of the parent compounds were between 50 and 100% of full scale. Temperature 25°C)

Mixture	Component assayed	Detector wavelength (nm)	Dilution factor	Detector gain (AUFS)
2-PAM-Cl–atropine	Atropine	203	10	0.2
Obidoxime–atropine	Atropine	203	10	0.2
HI-6–atropine	Atropine	203	10	0.2
2-PAM-Cl–atropine	2-PAM-Cl	203	10000	0.1
Obidoxime–atropine	Obidoxime	200	1000	0.2
HI-6–atropine	HI-6	208	3500	0.1

atropine (for concentrations see Table I) were sealed in glass ampoules and heated in an oven at 80°C for various time periods between 19 and 120 h (approx. 1–5 days). The heated samples and unheated controls (mixtures or single components) were diluted with Milli-Q water so that the concentration of the material to be assayed (oxime or atropine) was between 0.1 and 0.2 m*M*. The HPLC injection volume was 20 μl.

RESULTS

Measurement of atropine and tropic acid

Controls. In experiments using aqueous pralidoxime chloride–atropine sulphate mixtures in the millimolar ratio of 1740:1.5 (Fig. 2), a complete resolution of the atropine (peak 5) from the broad pralidoxime peak (peak 1) beginning at the solvent front was achieved using mobile phase A (Table I). Tropic acid eluted earlier (peak 4, Fig. 2d) but was also resolved from the oxime peak.

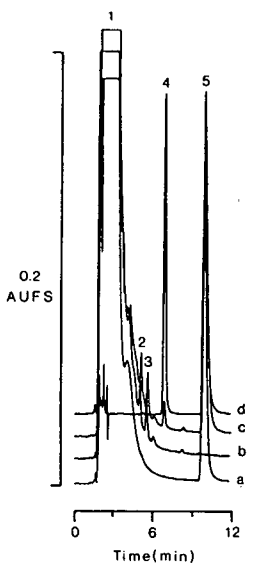

Fig. 2. Chromatograms showing the effect of 5 days at 80°C on an aqueous mixture of 1.5 m*M* atropine sulphate and 1.74 *M* 2-PAM-Cl. HPLC conditions for atropine: see Tables I (mobile phase A) and II. Traces: (a) control (2-PAM-Cl and atropine sulphate), (b) heated 2-PAM-Cl, (c) heated 2-PAM-Cl and atropine sulphate and (d) control (atropine sulphate and tropic acid, each 0.15 m*M*). Peaks: 1 = 2-PAM; 2, 3 = unidentified compounds from the degradation of 2-PAM; 4 = tropic acid; 5 = atropine.

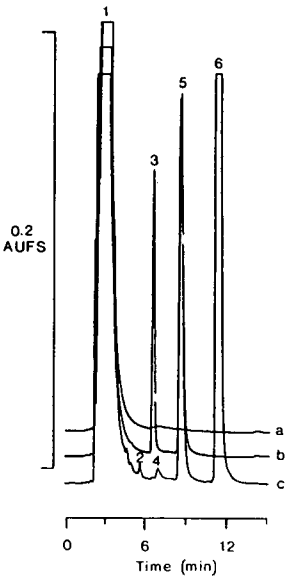

Fig. 3. Chromatograms showing separation of atropine and tropic acid in the presence of excess obidoxime (millimolar ratio of atropine:tropic acid:obidoxime = 1.4:1.0:209). HPLC conditions for atropine: see Tables I (mobile phase A) and II. Traces: (a) obidoxime chloride, (b) obidoxime chloride, atropine sulphate and tropic acid and (c) Combopen contents. Peaks: 1 = obidoxime; 2, 4 = unknowns; 3 = tropic acid; 5 = atropine; 6 = preservative (phenol).

The complete resolution of both atropine and tropic acid (peaks 5 and 3, Fig. 3b) from a 150-fold millimolar excess of obidoxime (peak 1, Fig. 3b) was also obtained using mobile phase A (Table I). The preservative (phenol) (peak 6, Fig. 3c) present in a commercially available solution of obidoxime chloride and atropine sulphate (Combopen) was well separated from atropine and any tropic acid that might form. Traces of unidentified compounds (peaks 2 and 4) occurred in the Combopen sample (Fig. 3c) which were not present in a freshly prepared mixture of obidoxime chloride, atropine sulphate and tropic acid (Fig. 3b).

A similar separation of the components in a mixture of HI-6, atropine sulphate and tropic acid in a millimolar ratio of 350:1.5:1.0 was obtained under the same conditions (peaks 1, 4 and 2, Fig. 4a). The analysis of a freshly constituted injectable solution of HI-6 and atropine

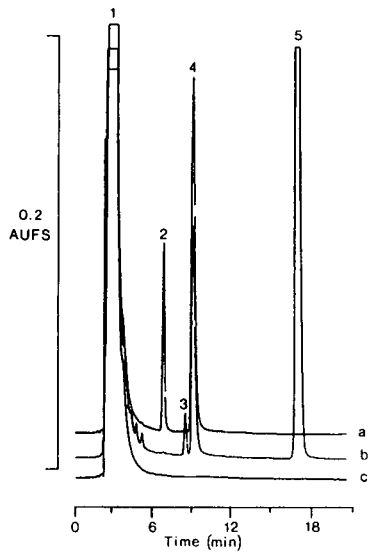

Fig. 4. Separation by HPLC of atropine and tropic acid from HI-6 (millimolar ratio of atropine:tropic acid:HI-6 = 1.5:1.0:350). HPLC conditions for atropine: see Tables I (mobile phase A) and II. Traces: (a) standard mixture, (b) Astra autoinjector contents and (c) HI-6. Peaks: 1 = HI-6; 2 = tropic acid; 3 = unknown; 4 = atropine; 5 = preservative (methyl paraben).

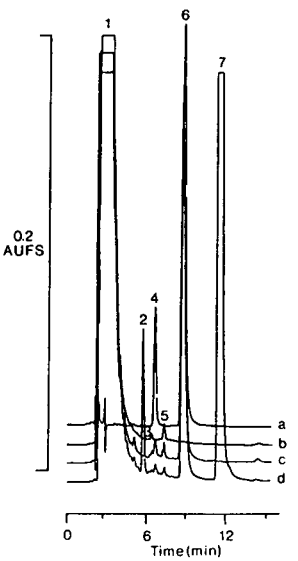

Fig. 5. Chromatograms showing effect of heating an aqueous mixture of 1.4 m*M* atropine sulphate and 209 m*M* obidoxime chloride for 5 days at 80°C. HPLC conditions for atropine: see Tables I (mobile phase A) and II. Traces: (a) heated atropine sulphate, (b) heated obidoxime chloride, (c) heated atropine sulphate and obidoxime chloride and (d) heated Combopen contents. Peaks: 1 = obidoxime; 2 = unknown from Combopen; 3, 5 = unknowns from obidoxime; 4 = tropic acid; 6 = atropine; 7 = preservative (phenol).

sulphate (Astra Meditec) gave an extra peak (peak 5, Fig. 4b), due to the preservative (methyl paraben) [13], as well as several small peaks (*e.g.* peak 3, Fig. 4b) which were not present in our standard mixture (Fig. 4a).

Heat-degraded samples. Atropine sulphate (1.5 m*M*) in unbuffered aqueous solution (pH about 7) was degraded by heating at 80°C over 1–5 days in a sealed ampoule. This is illustrated in Fig. 5a where peak 4 has the same retention time (t_R) (about 6.7 min) as tropic acid in control (unheated) samples (see peak 4, Fig. 2d; peak 3, Fig. 3b and peak 2, Fig. 4a).

However, in the presence of a high concentration of pralidoxime, obidoxime or HI-6 at an initial pH of between 3 and 4, the degradation of atropine sulphate after 4 or 5 days at 80°C appears to be much less. This is illustrated in Figs. 2c and 5c for heat-treated mixtures of atropine sulphate with pralidoxime chloride and obidoxime chloride respectively. In all cases the pH had dropped to between 2 and 3 and only a small amount of material with the retention time of tropic acid was formed.

After heating the contents of a Combopen under the same conditions (Fig. 5d), peak 2, which was a trace component of the injector contents before heating (see peak 2, Fig. 3c), was now increased. This peak was absent from the standard mixture of obidoxime chloride and atropine sulphate heated in the same way (Fig. 5c).

The products of the degradation of pralidoxime chloride (*e.g.* peaks 2 and 3, Fig. 2b) and obidoxime chloride (*e.g.* peaks 3 and 5, Fig. 5b) do not interfere with the measurement of tropic acid or atropine peaks.

The breakdown of HI-6 is much more extensive than that of pralidoxime and especially of obidoxime after 4 days at 80°C. Many rider peaks, which are degradation products of HI-6, appeared on what was now the broader trailing edge of the peaks at the solvent front. Nevertheless it was still possible to distinguish the peaks due to atropine and tropic acid in the heated mixture.

Measurement of oximes

The HPLC separation of each of the three oximes (pralidoxime and the two bis-pyridinium oximes, obidoxime and HI-6) from several of their respective substituted pyridine breakdown products was achieved using mobile phases B, C and D respectively (Table I) and the appropriate sample dilutions (Table II).

Controls. For example, using mobile phase C, isonicotinic acid (t_R 2.4 min), isonicotinamide (t_R 3.1 min) and pyridine-4-aldoxime (t_R 4.2 min) elute well before obidoxime (t_R 10.4 min). Chromatograms of a standard mixture of these four components contained an extra peak (t_R 8.9 min) that was also present in chromatograms of a solution of the original sample of obidoxime and of the contents of a Combopen. NMR data from this laboratory (unpublished results) suggest that this peak is due to the presence of a small amount (*ca.* 4 mol%) of a regioisomer of obidoxime.

Fig. 6a similarly illustrates, using mobile phase D, that isonicotinamide (peak 1, t_R 3.7 min), picolinamide (peak 2, t_R 6.6 min) and pyridine-2-aldoxime (peak 3, t_R 7.3 min) elute well before HI-6 (peak 6, t_R 4.4 min). Peak 4 in this trace is an unknown component of the sample of pyridine-2-aldoxime used in the standard mixture.

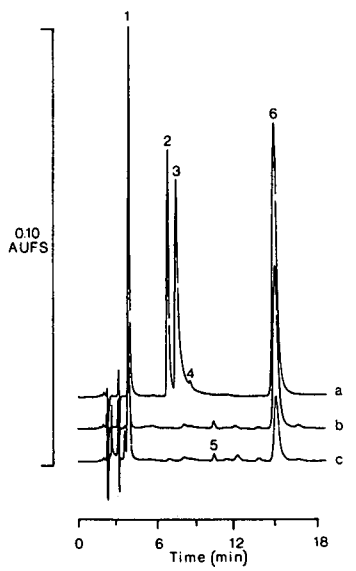

Fig. 6. Degradation of 350 m*M* HI-6 during 4 days at 80°C. HPLC conditions: see Tables I (mobile phase D) and II. Traces: (a) control (unheated) mixture of HI-6, isonicotinamide, picolinamide and pyridine-2-aldoxime, all at 0.1 m*M*, (b) HI-6 heated for 1 day and (c) HI-6 heated for 4 days. Peaks: 1 = isonicotinamide; 2 = picolinamide; 3 = pyridine-2-aldoxime; 4 = unknown from pyridine-2-aldoxime in control mixture; 5 = unknown; 6 = HI-6.

Heat-degraded samples. In chromatograms of heated pralidoxime chloride–atropine sulphate mixtures the breakdown products of the oxime were not specifically identified. However the degradation of 2-PAM-Cl over 5 days at 80°C was clearly demonstrated by the decrease in size of the oxime peak at 12.6 min as well as the progressive growth of four new peaks with retention times of 1.8, 6.2, 7.0 and 9.4 min. Similar results were obtained with P2S.

After 5 days of heating, the breakdown of obidoxime chloride was less extensive than for 2-PAM-Cl. According to the retention times, isonicotinamide (t_R 3.1 min) and pyridine-4-aldoxime (t_R 4.2 min), but not isonicotinic acid (t_R 2.4 min), appear to be the main degradation products. The preservative (phenol) in the Combopen contents elutes at 19.1 min.

The progressive degradation of HI-6 (peak 6, Fig. 6) under similar conditions is greater than that of 2-PAM-Cl and obidoxime chloride. One of the main products again appears to be isonicotinamide (peak 1, t_R 3.7 min, Fig. 6).

DISCUSSION

The major problem in this work was to find a set of HPLC conditions that would allow atropine and tropic acid to be estimated in the presence of a large molar excess of a pyridinium oxime and its breakdown products. We have found few previous references to HPLC methods that could be applied in this way and even these [13,19] lack sufficient detail regarding the extent to which tailing of the oxime peak and the presence of degradation products of the oxime cause any problem for the detection and estimation of the breakdown of atropine.

Atropine salts have long been known to be more stable in acid solution than in neutral or alkaline solution. Their maximum stability has been reported to lie between pH 3 and 4 [2,17,20]. This is presumably due to the higher

susceptibility of atropine to alkaline hydrolysis in comparison with acidic hydrolysis [17,21,22]. At ambient temperatures ($<40°C$) and acidic pH (2.8–6.0) dilute atropine sulphate solutions (3–15 m*M*) have been reported to be stable (*i.e.* $\leq 1\%$ breakdown) for several years [3,16,23]. However, considerable breakdown has been reported when similar solutions of atropine sulphate have been heated at 80–100°C for several days [17] or autoclaved for a few hours [24].

In the current experiments the increased rate of hydrolysis of atropine sulphate in an aqueous unbuffered solution when compared to the rate in a solution containing 0.2–1.7 *M* oxime may be explained by the initial pH. At a pH of around 7.0 atropine is likely to be subject to substantial base-catalysed hydrolysis, whereas at a pH of between 3 and 4 (as in the presence of the oxime) this would be much less [20]. Acid-catalysed hydrolysis at pH 4.0 would also be slow [21].

In acidic solution the major degradation products of the pyridinium oximes detected by HPLC methods are the acid amide and/or carboxylic acid derivatives [4–10,14,25,26]. In the current HPLC measurements a major breakdown product of obidoxime or HI-6 after 4–5 days at 80°C was isonicotinamide. Pyridine-4-aldoxime appeared as a minor breakdown product of obidoxime.

The pK_a values for the three pyridinium oximes lie between 7.28 and 7.80 [27] and their pH in aqueous solution is between 3.5 and 4.0. If one considers the pH–rate profile for the hydrolysis of atropine [20] (see also ref. 21) it might be expected that the decomposition of the oximes and a lowering of the pH to < 3.0 could cause an increased rate of hydrolysis of the atropine sulphate also present. Certainly a small amount of tropic acid was produced after 5 days at 80°C in the presence of degraded oxime. Whether this was due to the direct effect of heat or of a shift in pH on the rate of hydrolysis is unknown.

Under the assay conditions for atropine, the breakdown of the oxime upon heating causes the generation of a broader, composite peak extending from the solvent front. Furthermore, there are small peaks representing traces of oxime degradation products which have retention times in the vicinity of those for atropine and tropic acid. This is also the likely explanation for the trace amounts of unidentified compounds observed in the atropine assay of the contents of the autoinjectors even prior to heat treatment. Nevertheless, neither these factors nor the presence of peaks due to the phenolic preservatives added to the commercial preparations interferes with the analysis of atropine.

Thus the HPLC method outlined in detail in this paper appears to be suitable for estimating the extent of degradation of both atropine and the pyridinium oximes in a binary injection mixture without the need for any prior separation.

REFERENCES

1 P.M. Lundy, A.S. Hansen, B.T. Hand and C.A. Boulet, *Toxicology*, 72 (1992) 99.
2 N.B. Brown and H.K. Sleeman, *J. Chromatogr.*, 150 (1978) 225.
3 U. Lund and S.H. Hansen, *J. Chromatogr.*, 161 (1978) 371.
4 D. Utley, *J. Chromatogr.*, 265 (1983) 311.
5 P. Fyhr, A. Brodin, L. Ernerot and J. Lindquist, *J. Pharm. Sci.*, 75 (1986) 608.
6 A.C. Schroeder, J.H. DiGiovanni, J. von Bredow and M.H. Heiffer, *J. Pharm. Sci.*, 78 (1989) 132.
7 P. Eyer and W. Hell, *Arch. Pharm. (Weinheim)*, 318 (1985) 938.
8 P. Eyer, W. Hell, A. Kawan and H. Klehr, *Arch. Toxicol.*, 59 (1986) 266.
9 N.D. Brown, L. Kazyak, B.P. Doctor and I. Hagedorn, *J. Chromatogr.*, 351 (1986) 599.
10 P. Eyer, I. Hagedorn and B. Ladstetter, *Arch. Toxicol.*, 62 (1988) 224.
11 R.E. Mdachi, W.D. Marshall, D.J. Ecobichon, F.M. Fouad and C.E. Connolley-Mendoza, *Chem. Res. Toxicol.*, 3 (1990) 413.
12 N.D. Brown, L.L. Hall, H.K. Sleeman, B.P. Doctor and G.E. Demaree, *J. Chromatogr.*, 148 (1978) 453.
13 J.W. Schlager, T.W. Dolzine, J.R. Stewart, G.L. Wannarka and M.L. Shih, *Pharm. Res.*, 8 (1991) 1191.
14 I. Christenson, *Acta Pharm. Suec.*, 5 (1968) 249.
15 J.G. Clement, K.J. Simons and C.J. Briggs, *Biopharm. Drug Dispos.*, 9 (1988) 177.
16 E. Linden and G. Schill, *Acta Pharm. Suec.*, 4 (1967) 327.
17 T. Jira and R. Pohloudek-Fabini, *Pharmazie*, 8 (1983) 520.
18 L. Leadbeater, *Technical Note, No.* 171, Chemical Defense Establishment, Porton Down, UK, 1973.

19 T. Okuda, M. Nishida, I. Sameshima, K. Kyoyama, K. Hiramatsu, Y. Takehara and K. Kohriyama, *J. Chromatogr.*, 567 (1991) 141.
20 W. Lund and T. Waaler, *Acta Chem. Scand.*, 22 (1968) 3085.
21 G.M. Loudon, *J. Chem. Educ.*, 12 (1991) 973.
22 E. von Bjerkelund, F. Gram and T. Waaler, *Pharm. Acta Helv.*, 44 (1969) 745.
23 A. Richard and G. Andermann, *Pharmazie*, 39 (1984) 866.
24 S.A.H. Khalil, Y. El-Beltagy and S. El-Masry, *J. Pharm. Pharmacol.*, 23 (1971) 214.
25 J. Lin and D.L. Klayman, *J. Pharm. Sci.*, 75 (1986) 797.
26 I. Christenson, *Acta Pharm. Suec.*, 5 (1968) 23.
27 I. Hagedorn, I. Stark and P. Lorenz, *Angew. Chem., Int. Ed. Engl.*, 11 (1972) 307.

Journal of Chromatography, 648 (1993) 381–388
Elsevier Science Publishers B.V., Amsterdam

CHROM. 25 401

Analytical and preparative resolution of enantiomers of verapamil and norverapamil using a cellulose-based chiral stationary phase in the reversed-phase mode

Larry Miller* and Rosemary Bergeron

Chemical Sciences Department, Searle, 4901 Searle Parkway, Skokie, IL 60077 (USA)

(First received February 23rd, 1993; revised manuscript received June 9th, 1993)

ABSTRACT

Analytical HPLC methods were developed for the chiral resolution of verapamil and norverapamil using a cellulose-based chiral stationary phase (Chiralcel OD) in the reversed-phase mode. The effect of pH, buffer concentration, and temperature on the analytical chiral separation were investigated. It was shown that retention decreased slightly with increasing pH, while α and resolution were unaffected by pH. Increasing buffer concentration from 0.01 to 0.125 *M* resulted in increased retention, while concentrations above 0.125 *M* resulted in decreased retention. Separation was unaffected by buffer concentration, while resolution increased with increasing buffer concentration. Maximum analytical resolution was obtained at subambient temperatures. Separation was unaffected by temperature, while an increase in temperature resulted in decreased retention. In addition, the preparative resolution of the enantiomers of verapamil and norverapamil was investigated. The analytical methods were scaled up to preparative loadings and the chromatographic parameters varied to determine their effect on the preparative separations.

INTRODUCTION

Verapamil (Fig. 1) is a calcium antagonist which is used in the management of hypertension. Norverapamil is the primary metabolite of verapamil. Both verapamil and norverapamil contain a chiral carbon and exist as enantiomers. There are two approaches to obtaining enantiomerically pure chemicals. These are asymmetric synthesis of the desired isomer and resolution of a racemic mixture into individual isomers. Various synthetic methods to produce the individual enantiomers of verapamil have been developed [1]. Methods for the resolution of a racemic mixture include recrystallization of diastereomeric salts, formation of diastereomeric derivatives followed by chromatographic resolution on an achiral stationary phase, and direct chromatographic resolution of enantiomers using a chiral stationary phase or a chiral mobile phase additive. The resolution of verapamil by the re-

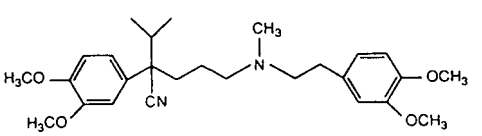

VERAPAMIL

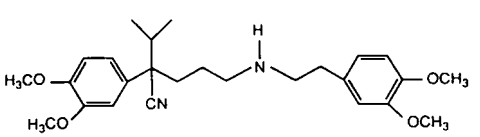

NORVERAPAMIL

Fig. 1. Structure of verapamil and norverapamil.

* Corresponding author.

crystallization of diastereomeric salts has been reported [2]. The enantiomers of verapamil have also been separated by liquid chromatography on various chiral stationary phases [3–6]. Ikeda *et al.* have reported on the analytical chiral separation of verapamil using a cellulose-based phase in the reversed-phase mode [6]. Liquid chromatographic resolution of the enantiomers of norverapamil has also been reported [3]. The preparative separation of the enantiomers of verapamil or norverapamil has not been reported.

This paper reports on the use of liquid chromatography for the direct enantiomeric resolution of verapamil and norverapamil at both analytical and preparative loadings using a cellulose-based chiral stationary phase in the reversed-phase mode. The effect of pH, buffer concentration and temperature on the analytical separation of the enantiomers of verapamil and norverapamil will also be discussed.

EXPERIMENTAL

Materials

The chiral stationary phases used for these studies were obtained from Daicel (Tokyo, Japan) through Regis Chemical (Morton Grove, IL, USA) as prepacked analytical (250 × 4.6 mm I.D.) and preparative columns (500 × 10 mm I.D.). Samples of verapamil were received from Searle Technical Operations. Norverapamil was synthesized in the Chemical Development laboratories of Searle (Skokie, IL, USA). The solvents and other chemicals used were reagent grade or better and were obtained from a variety of sources.

Equipment

The analytical chromatograph consisted of a Spectra-Physics (San Jose, CA, USA) SP8700 pump or a Waters Assoc. (Milford, MA, USA) Model 590 solvent delivery system, a Waters Intelligent Sample Processor Model 712, a Kratos (Ramsey, NJ, USA) Model 757 variable wavelength UV detector, a Kipp and Zonen (Delft, Netherlands) Model BD41 two-channel recorder and a Digital Equipment Corporation (Maynard, MA, USA) VAX 11/785 computer with a Searle chromatography data system. Subambient and elevated temperatures were achieved with a Kariba (Cardiff, South Wales, UK) Research Series advanced air oven.

The preparative chromatograph consisted of two Beckman (Berkeley, CA, USA) Model 101 pumps with preparative heads, a Model 165 variable wavelength detector with a 5 mm semi-preparative flow cell, a Model 450 data system/controller and a Kipp and Zonen Model BD41 two channel recorder. A Rheodyne (Cotati, CA, USA) Model 7125 syringe loading sample injector equipped with a 10 ml loop (Valco, Houston, TX, USA) was used. The column effluent was fractionated using a Gilson (Middleton, WI, USA) Model FC80 or Model FC220 fraction collector.

Recovery of chemical from mobile phase

The purified chemical was recovered from the mobile phase using the following procedure. Fractions containing pure chemical were combined and evaporated under vacuum at 50°C to remove acetonitrile. Sodium chloride (approximately 50 g per 100 ml of mobile phase) was added and the pH adjusted to 11–12 with ammonium hydroxide. The basic aqueous solution was then extracted three times with one equivalent volume of toluene. The toluene phases were combined and the solvent removed using a rotary evaporator. Verapamil and norverapamil were recovered as the free base. The yields for these extractions varied between 60 and 90%.

RESULTS AND DISCUSSION

Analytical HPLC

When developing an analytical chiral HPLC separation that will be scaled up to preparative loadings, it is desirable to achieve maximum resolution of the two enantiomers. It is also desirable to develop the separation on a stationary phase that is available in larger column sizes or as bulk packing and to use a volatile mobile phase, allowing for easy recovery of the separated enantiomers. The separation of the enantiomers of verapamil has been previously reported using an AGP chiral stationary phase (CSP) [3], a cyclodextrin CSP [4], an ovomucoid

CSP [5] and a cellulose-based CSP in the reversed-phase mode [6]. Due to the low loadability of AGP and cyclodextrin and ovomucoid columns, as well as the unavailability of large columns (> 10 mm I.D.), they are not desirable for preparative work. The cellulose-based column used nonvolatile mobile phase additives and was not ideally suited for our work. Pirkle CSP- and cellulose-based phases using normal-phase solvents were investigated and did not separate the enantiomers of verapamil or norverapamil. Since separation was not achieved on any of the other columns attempted or with a mobile phase that contained volatile buffers, the cellulose-based CSP in the reversed-phase mode [6] was chosen for our work.

The reported analytical separation of the enantiomers of verapamil used a Chiralcel OD CSP (See Fig. 2) and a mobile phase of acetonitrile–0.05 *M* sodium perchlorate (pH 3.0 with perchloric acid) (33:67, v/v). While this method only reported on the chiral separation of verapamil, it was shown in our laboratories that the method also separated the enantiomers of norverapamil. The analytical HPLC separations for verapamil and norverapamil using these conditions are shown in Fig. 3. Table I summarizes the capacity factors (k'), separation factor (α), and resolution (R_s) for the enantiomeric separation of these compounds.

Prior to preparative work, further analytical HPLC method development using cellulose-based CSP in the reversed-phase mode was done using verapamil and norverapamil in an attempt to maximize the separation and to determine if buffers were required. The results of this work are summarized in Table II. When a neutral,

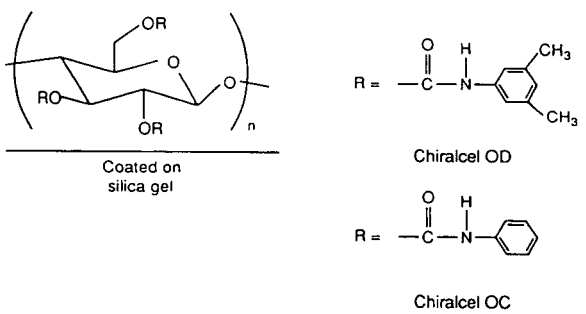

Fig. 2. Structure of Chiralcel OC and OD packings.

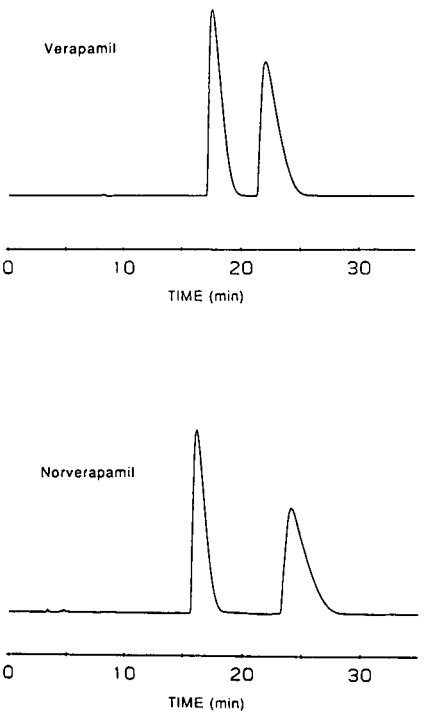

Fig. 3. Analytical HPLC separation of verapamil and norverapamil. Analysis conducted on Chiralcel OD column (250 mm x 4.6 mm I.D.), detection at 205 nm, with a mobile phase of acetonitrile–0.05 *M* $NaClO_4$ (pH 3.0 with $HClO_4$) (33:67) and a flow rate of 1.0 ml/min. 15 μl of a 1 mg/ml solution were injected.

unbuffered mobile phase was attempted, poor peak shape was obtained. Replacing the buffers with volatile acids lead to adequate separations but broad peaks. Further method development using different buffer systems (sodium formate–formic acid, sodium acetate–acetic acid) was attempted. The separations were not as good as

TABLE I

VALUES FOR ANALYTICAL SEPARATION OF ENANTIOMERS OF VERAPAMIL AND NORVERAPAMIL

See Fig. 3 for HPLC conditions.

Compound	k_1' [a]	k_2' [b]	α	R_s
Verapamil	4.92	6.40	1.30	2.12
Norverapamil	4.41	7.06	1.60	3.76

[a] Capacity factor for first eluting enantiomer.
[b] Capacity factor for second eluting enantiomer.

TABLE II

CHROMATOGRAPHIC RESULTS

HPLC conditions: flow rate, 1.0 ml/min; detection, 205 nm.

Mobile phase	Column	Verapamil				Norverapamil			
		k_1' [a]	k_2' [b]	α	R_s	k_1' [a]	k_2' [b]	a	R_s
Acetonitrile–water (40:60)	OD	4.38	4.87	1.11	0.33	1.76	2.33	1.32	0.74
Acetonitrile–aqueous acetic acid (pH 3.0) (15:85)[c]	OD	– [d]	–	–	–	2.91	5.55	1.90	1.79
Acetonitrile–aqueous formic acid (pH 3.0) (15:85)	OD	5.70	9.89	1.74	1.13	8.33	14.74	1.77	2.02
Acetonitrile–0.05 *M* sodium formate (pH 3.6 with formic acid) (20:80)	OD	4.81	6.50	1.35	1.30	4.18	6.86	1.64	2.57
Acetonitrile–0.05 *M* sodium acetate (pH 4.5 with acetic acid) (20:80)[c]	OD	4.41	5.96	1.35	1.40	3.94	6.57	1.67	2.60
Methanol–0.05 *M* sodium perchlorate (pH 3.0 with perchloric acid) (50:50)	OD	8.32	12.09	1.45	0.72	– [e]	–	–	–
Acetonitrile–0.05 *M* sodium perchlorate (pH 3.0 with perchloric acid) (50:50)	OC	5.85	6.40	1.09	0.41	4.29	4.73	1.10	0.39

[a] Capacity factor for first eluting enantiomer.
[b] Capacity factor for second eluting enantiomer.
[c] Detection at 220 nm.
[d] No analysis of verapamil was attempted with these conditions.
[e] No analysis of norverapamil was attempted with these conditions.

that obtained with sodium perchlorate–perchloric acid buffer. Replacing methanol for acetonitrile resulted in reduced separation and broad peaks. We then attempted the separation using a different cellulose-based phase (Chiralcel OC, Fig. 2). Reduced separation was obtained using the Chiralcel OC column. A separation which did not contain non-volatile buffers could not be developed. Therefore, it was decided that the original HPLC conditions reported by Ikeda *et al.* [6] would be used for the preparative work.

Preparative HPLC

To determine the feasibility of isolating the individual enantiomers of verapamil and norverapamil, the analytical methods reported in Fig. 3 were scaled up to preparative loadings. The percent acetonitrile in the preparative mobile phase was increased to 35% to achieve a k' close to that of the analytical column. A 500 × 10 mm I.D. column containing approximately 25 g of stationary phase and a flow rate of 4.2 ml/min was used for preparative method development. The linear velocity for the preparative separation was lower than the analytical separation due to pressure limitations of the preparative column. In order to maximize the throughput of the preparative method, experiments were performed to determine the effect of increasing sample load on the separation. Column loadings of 1, 2 and 4 mg of sample per g of packing were investigated. Preparative loadings greater than 4 mg of sample per g of packing were not investigated due to the small degree of separation seen analytically and the need to keep the isolated yields as high as possible. Loadings less than 1 mg sample per g of packing were not investigated since they would be inefficient to produce the desired quantities of pure enantiomers. Due to greater solubility in the preparative mobile

phase, the hydrochloride salts of verapamil and norverapamil were used for all preparative work. The presence of non-volatile buffers in the mobile phase required an extraction procedure to isolate the enantiomers. This recovery procedure is detailed in the Experimental section.

From these preparative loading experiments it was determined that the first eluting enantiomer could be isolated pure for both verapamil and norverapamil. The results of these experiments are summarized in Table III. These data show that as loading increases, the amount of enantiomer produced per injection increases even though the percentage of enantiomer isolated decreases.

For the preparative separation of verapamil we found that the second eluting enantiomer could not be isolated pure at any of the column loadings attempted; however, the second eluting enantiomer of norverapamil could be isolated at all column loadings attempted. This was expected because of the increased analytical separation seen for the enantiomers of norverapamil compared to verapamil. This also results in greater isolated yields for the first eluting enantiomer of norverapamil.

Effect of pH, buffer concentration and temperature

After completion of the preparative work, further analytical HPLC method optimization was performed. The use of cellulose-based CSP in the reversed-phase mode had not been used previously in our laboratories. In addition, little had been reported in the literature on this subject. The original reference by Ikeda *et al.* [6] only reported on the separation of verapamil; no investigation of the separation parameters of pH, buffer concentration or temperature was reported. Experiments were therefore designed to determine how varying the mobile phase composition affected the separation of the enantiomers of verapamil and norverapamil. The first area investigated was the effect of pH on the separation. A pH range of 2.5 to 5.7 was explored. A $NaClO_4$ concentration of 0.050 *M* was used for all experiments. Plots of pH vs. k', α, and R_s for verapamil and norverapamil are shown in Fig. 4. These results show that pH has little effect on retention and α. Increased mobile phase pH resulted in a slight reduction in resolution. Maximum resolution was obtained at pH 3.0. Due to the buffer system being used, the pH of the mobile phase could not be adjusted to the pk of verapamil or norverapamil (*ca.* 8). If a pH closer to 8 could have been obtained it is possible that more drastic effects could have been realized.

The effect of buffer concentration for the chiral separation of verapamil and norverapamil was also investigated. Sodium perchlorate con-

TABLE III

RESULTS OF PREPARATIVE EXPERIMENTS FOR VERAPAMIL AND NORVERAPAMIL

HPLC conditions: Chiralcel OD (500 × 10 mm I.D.) containing approximately 25 g of packing; mobile phase, acetonitrile–0.05 *M* sodium perchlorate (35:65, pH 3.0 with perchloric acid); flow rate, 4.2 ml/min.

Compound	Loading (mg/g)	First eluting enantiomer		Second eluting enantiomer	
		Percent isolated[a]	mg per injection	Percent isolated[a]	mg per injection
Verapamil	1	83	10.4	0	–
	2	66	16.5	0	–
	4	26	13.0	0	–
Norverapamil	1	90	11.3	66	8.3
	2	83	20.8	38	9.5
	4	45	22.5	16	8.0

[a] Isolated yields determined by peak area integration of preparative chromatogram.

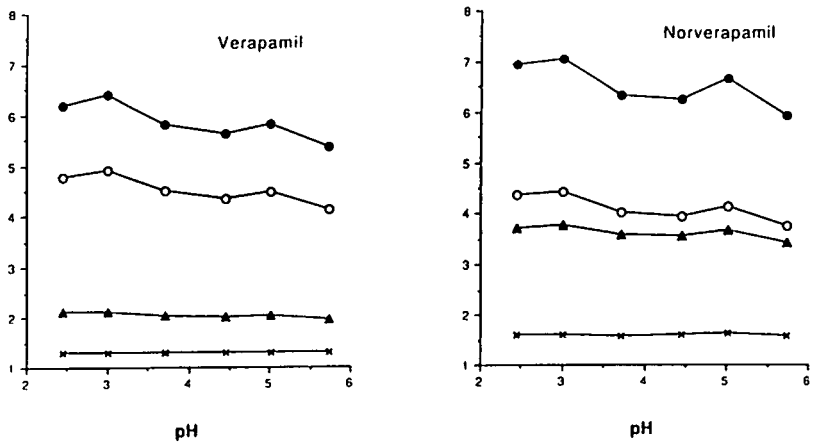

Fig. 4. Effect of pH on analytical HPLC separation of verapamil and norverapamil. See Fig. 3 for chromatographic conditions. ● = k' for second eluting enantiomer, ○ = k' for first eluting enantiomer, ▲ = resolution (R_s), × = alpha (α).

centrations between 0.01 *M* and 0.175 *M* were investigated. A pH of 3.0 was used for all experiments. The results of these studies are shown in Fig. 5. These data show that increasing sodium perchlorate concentration from 0.01 to 0.125 *M* results in an increase in retention for both verapamil and norverapamil. Retention is relatively unchanged above 0.125 *M*. Separation remained constant at all buffer concentrations studied. Increased buffer concentration resulted in an increase in resolution. Maximum resolution for both verapamil and norverapamil was obtained at 0.125 *M* sodium perchlorate. Resolution decreased slightly above 0.125 *M*.

The effect of temperature on the chiral separation of verapamil and norverapamil was also studied. Column temperatures between 10 and 55°C were investigated. The results of these experiments are summarized in Fig. 6. As expected, retention decreased with increasing temperature. Good linear correlations were observed between ln k' and $1/T$ for both verapamil and norverapamil, as shown in Fig. 7. Separation and resolution were maximized at subambient

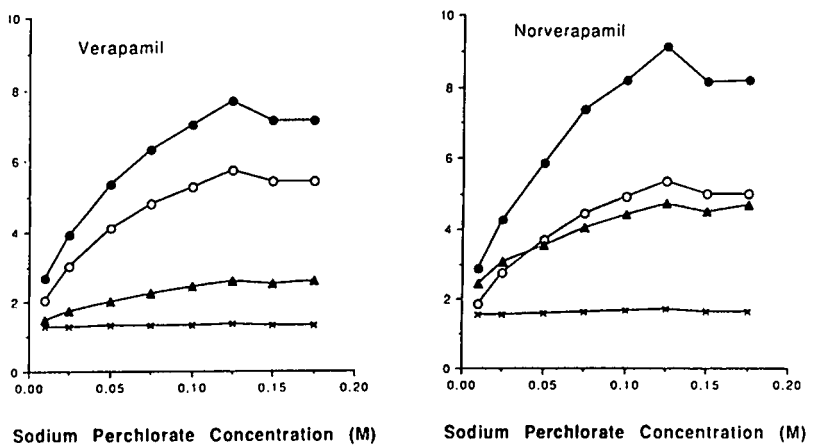

Fig. 5. Effect of buffer concentration on analytical HPLC separation of verapamil and norverapamil. See Fig. 3 for chromatographic conditions. Symbols as in Fig. 4.

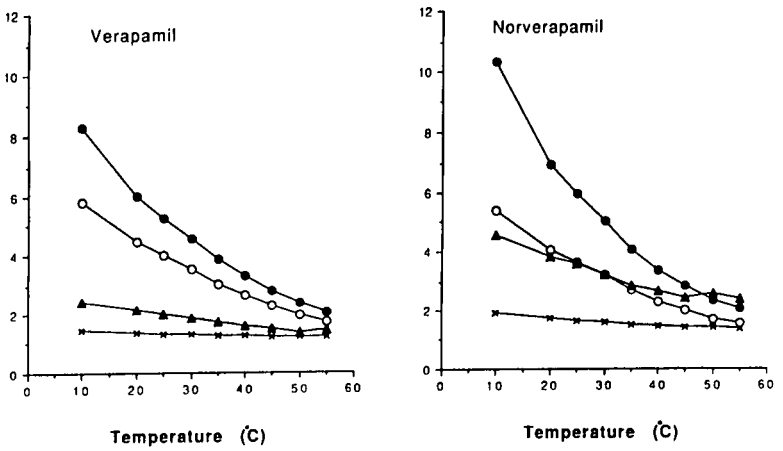

Fig. 6. Effect of temperature on analytical HPLC separation of verapamil and norverapamil. See Fig. 3 for chromatographic conditions. Symbols as in Fig. 4.

temperatures. This is probably due to an increase in the association times for the transient diastereomeric complexes formed between the chiral stationary phase and the solute.

CONCLUSION

Analytical and preparative HPLC can be used for the direct resolution of the enantiomers of verapamil and norverapamil. For the analytical resolution of verapamil and norverapamil using cellulose-based phases in the reversed-phase mode, pH has little effect on α, k' and resolution. Buffer concentration has little effect on α, while increased buffer concentration increases k' and resolution. Maximum analytical resolution of the enantiomers of verapamil and norverapamil was obtained at subambient temperatures, due to an increase in the association time between the chiral stationary phase and the solute. The resolution obtained at preparative loadings is directly related to the analytical separation.

The Chiralcel OD chiral stationary phase appears to be quite stable under the conditions used for this work. Mobile phase was continu-

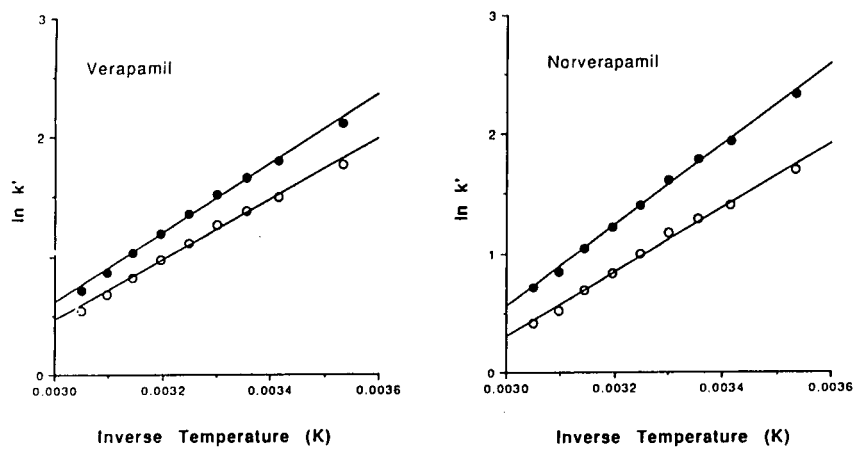

Fig. 7. Plot of ln k' *vs.* inverse temperature (K) for verapamil. Symbols as in Fig. 4.

ously flowing through the analytical column and injections made regularly over a six-month period before a reduction in resolution was observed.

ACKNOWLEDGEMENTS

The authors wish to thank Helga Bush, Terry Kosobud, John Ng, Cara Weyker, and Ed Yonan for their technical support. The compounds were provided by chemists in the Synthesis Development group and the Technical Operations group at Searle.

REFERENCES

1 L.J. Theodore and W.L. Nelson, *J. Org. Chem.*, 52 (1987) 1309.
2 G. Blaschke, *German Patent Application*, No. P 37 23 684.9 (1987).
3 Y. Chu and I.W. Wainer, *J. Chromatogr.*, 497 (1989) 191.
4 D.W. Armstrong, T.J. Ward, R.D. Armstrong and T.E. Beesley, *Science*, 232 (1986) 1132.
5 Y. Oda, N. Asakawa, T. Kajima, Y. Yoshida and T. Sato, *J. Chromatogr.*, 541 (1991) 411.
6 K. Ikeda, T. Hamasaki, H. Kohno, T. Ogawa, T. Matsumoto and J. Sakai, *Chem. Lett.*, (1989) 1089.

Journal of Chromatography, 648 (1993) 389–393
Elsevier Science Publishers B.V., Amsterdam

CHROM. 25 347

Prediction of gas chromatographic retention indices of some benzene derivatives

M. Jalali-Heravi* and Z. Garkani-Nejad

Chemistry Department, Shahid Bahonar University of Kerman, Kerman 76169 (Iran)

(First received February 22nd, 1993; revised manuscript received May 26th, 1993)

ABSTRACT

Gas chromatographic retention indices for some benzene derivatives on Apiezon MH were successfully modelled with the aid of a computer. Numerical descriptors were calculated and multiple linear regression analysis methods were used to generate model equations relating structural features to Kováts retention indices. These descriptors encode topological, geometric, electronic and calculated physical properties of the molecules. A model with $R = 0.998$ and $SE = 10.067$ was generated. Calculations of retention indices for a prediction set show that this model has a good predictive ability.

INTRODUCTION

The Kováts retention index in gas chromatography (GC) represents the retention behaviour of a compound relative to a standard set of hydrocarbons, utilizing a logarithmic scale. The retention index, I_A, for compound A is defined as

$$I_A = 100\,N + 100 \cdot \frac{\log t_R(A) - \log t_R(N)}{\log t_R(N+1) - \log t_R(N)} \quad (1)$$

where $t_R(A)$ is the adjusted retention time for compound A and $t_R(N+1)$ and $t_R(N)$ are the adjusted retention times for *n*-alkanes of carbon number $N+1$ and N that are larger and smaller, respectively, than the adjusted retention time for the unknown.

The identification of many compounds is often accomplished on the basis of GC peak comparisons with a standard sample of the suspected material. However, it is not always possible to obtain samples of pure standard materials for such comparisons. Therefore, the development of a theoretical model for estimating the retention index seems to be necessary. In this study, computer-assisted methods were employed to generate a statistical relationship between molecular-based structural parameters (descriptors) and the observed retention indices for some benzene derivatives. These techniques are based on the construction of linear mathematical models relating the observed retention indices to numerically encoded structural parameters called *descriptors*. These models have the general form

$$S = b_0 + b_1x_1 + b_2x_2 + \cdots + b_nx_n$$

where S is the predicted retention index for the molecule of interest, the X_i are numerical descriptors, the b_i are coefficients determined from a linear regression analysis of a set of observed retention indices and n denotes the number of descriptors in the model.

EXPERIMENTAL

The methodology used in this study consists of three fundamental stages: (a) selection of data set, (b) molecular descriptor generation and (c)

* Corresponding author.

0021-9673/93/$06.00

regression analysis. Computations of descriptors were performed by using some FORTRAN programs developed in our laboratory. The SPSS/PC package [1] was used for regression calculations.

Data set

The experimental data used in this study were reported by Khorasani [2]. The Kováts retention indices were determined on a stainless-steel column (2 m × 1.8 mm I.D.) packed with 10% (w/w) of hydrogenated Apeizon M (Apiezon MH) coated on acid-washed, dimethylchlorosilane-treated Chromosorb W (100–120 mesh) [2]. The retention indices for monosubstituted benzenes were normalized to 150°C by using least-squares plots of retention index against temperature. The other compounds were measured in the range 90°C (for fluorotoluene)–180°C (for bromochlorobenzene) [2]. Retention indices for 38 benzene derivatives studied ranged from 664.1 to 1287.7 index units (i.u.), with a mean retention index of 965.2 i.u. These compounds were divided randomly into a set used for constructing the equations (training set) and a set used for testing the validity of the generated model (prediction set) (Table I).

Descriptor generation

A total of 58 separate molecular structure descriptors were calculated for each compound in the data set. These descriptors can be classified into four major groups: topological, geometric, electronic and physico-chemical.

Topological descriptors include fragment, substructure and environment descriptors [3] and molecular connectivity indices [4]. Geometric descriptors include principal moments of inertia [5], shadow areas [6], Van der Waals volume [7], surface area [8], principal axes of the molecules and kappa index [9]. Electronic descriptors consist of dipole moments, molar refraction [10], electron density and partial charges of atoms with the most negative and positive charges and distance between atoms with the most positive and negative charges. Calculated physical property descriptors include molecular polarizability [11] and the logarithm of the partition coefficient in octanol–water (log P) [12].

Geometric and electronic descriptors depend on the three-dimensional coordinates of atoms. Therefore, in order to calculate these types of descriptors one needs to optimize the molecular structure of each molecule. In this work, MNDO [13], which is a semi-empirical molecular orbital method, was used for such an optimization.

TABLE I

DATA SET

No.	Compound	No.	Compound	No.	Compound
Training set		14	*p*-Fluoroanisole	28	*o*-Fluorotoluene
1	Benzene	15	*m*-Chloroanisole	29	*o*-Fluoroanisole
2	Fluorobenzene	16	*m*-Methylanisole	30	*o*-Xylene
3	Chlorobenzene	17	*m*-Xylene	31	*o*-Bromochlorobenzene
4	Bromobenzene	18	*m*-Chlorobromobenzene	32	*o*-Chlorofluorobenzene
5	Toluene	19	*m*-Bromotoluene		
6	Anisole	20	*m*-Fluorotoluene	*Prediction set*	
7	*p*-Chloroanisole	21	*m*-Chlorotoluene	1	*p*-Chlorofluorobenzene
8	*p*-Xylene	22	*m*-Chlorofluorobenzene	2	*p*-Methylanisole
9	*p*-Fluorotoluene	23	*m*-Dibromobenzene	3	*o*-Chlorotoluene
10	*p*-Bromotoluene	24	*m*-Dichlorobenzene	4	*o*-Bromotoluene
11	*p*-Bromofluorobenzene	25	*o*-Methylanisole	5	*m*-Fluoroanisole
12	*p*-Chlorobromobenzene	26	*o*-Chloroanisole	6	*m*-Bromofluorobenzene
13	*p*-Chlorotoluene	27	*o*-Bromofluorobenzene		

Regression analysis

Some of the 58 descriptors generated for each compound encoded similar information about the molecules of interest (they were highly correlated). It was therefore desirable to test each descriptor and eliminate those with high correlation coefficients. Correlations between two descriptors can be easily obtained from the correlation matrix. When a high correlation was detected ($R > 0.95$), one or more of the descriptors were removed from consideration. By using this criterion, thirteen of the original 58 descriptors were eliminated.

Linear models were formed by a stepwise addition of terms [14]. A deletion process was then employed where each variable in the model was held out in turn and a model was generated by using the remaining descriptors. A final set of selected equations were then tested for stability and validity through a variety of statistical methods. The choice of which equation to consider further was made by using four criteria: multiple correlation coefficient (R), standard deviation (SD), F statistic and the number of descriptors in the model. An ideal model is one that has high R and F values, low standard deviation, and least number of independent variables (descriptors).

RESULTS AND DISCUSSION

A number of good models for modelling GC retention indices of the benzene derivatives given in Table I were developed by using the descriptors available. The best equation found was

$$I = (137.114 \pm 3.359)XV_0 - (55.414 \pm 3.791)NOCH_3 + (2.321 \pm 0.344)VOL + (9.462 \pm 2.675)DIMO - 5.726 \pm 25.084$$

$$(n = 32,\ R = 0.998,\ F = 1835,\ SD = 10.067) \quad (2)$$

where I = retention index, XV_0 = zero-order valence term, $NOCH_3$ = number of methyl groups in the molecule, VOL = Van der Waals volume of the molecule and $DIMO$ = dipole moment of the molecule. The variables are listed in the order in which they were selected. The high values of R and the F statistic and low standard deviation indicate that this equation represents a very good model for calculating retention indices of benzene derivatives.

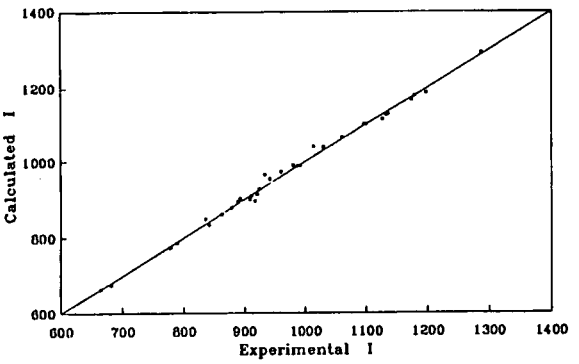

Fig. 1. Plot of calculated *versus* experimental retention indices.

The calculated and observed retention indices and structural descriptors employed in eqn. 2 are given in Table II for all the compounds studied. The plot of calculated *versus* observed retention indices is shown in Fig. 1 and reveals no deviation from linearity. Examination of the residuals (Fig. 2) indicates that they are normally distributed. The correlation matrix (Table III) for the four descriptors used in eqn. 2 shows no correlation between the parameters.

The variables in eqn. 2 encode different aspects of the molecular structures. The zero-order valence term (XV_0) is a topological descriptor

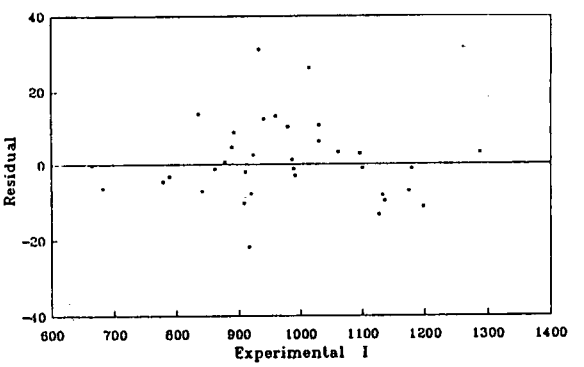

Fig. 2. Plot of residuals *versus* experimental retention indices.

TABLE II

EXPERIMENTAL AND CALCULATED RETENTION INDICES AND DESCRIPTORS EMPLOYED IN THE SELECTED MODEL

Compound[a]	Descriptor				Calculated retention index (i.u.)	Experimental retention index (i.u.)
	$NOCH_3$	XV_0	VOL	$DIMO$		
Training set						
1	0	3.464	88.618	0.000	674.9	681.3
2	0	3.163	93.558	1.995	664.0	664.1
3	0	4.591	102.304	1.837	878.6	877.9
4	0	5.371	105.972	1.392	989.8	979.6
5	1	4.387	105.096	0.068	784.9	788.2
6	0	4.795	113.870	1.072	926.2	923.6
7	0	5.921	127.585	2.242	1123.5	1131.7
8	2	5.309	121.642	0.001	893.7	889.2
9	1	4.086	110.077	1.960	773.1	777.7
10	1	6.294	122.492	1.384	1099.3	1096.3
11	0	5.070	110.923	0.667	953.2	940.9
12	0	6.497	119.634	0.463	1167.2	1174.4
13	1	5.513	118.808	1.826	987.8	989.2
14	0	4.494	118.855	2.353	908.6	910.6
15	0	5.921	127.506	1.096	1112.4	1126.0
16	1	5.718	130.453	1.534	1040.2	1029.6
17	2	5.309	124.332	0.061	900.5	892.0
18	0	6.497	119.596	1.585	1177.7	1179.0
19	1	6.294	122.387	1.378	1098.9	1100.0
20	1	4.086	110.058	1.998	773.5	778.0
21	1	5.513	118.779	1.827	987.7	990.9
22	0	4.290	107.228	1.873	849.1	835.4
23	0	7.278	123.271	1.315	1290.7	1287.7
24	0	5.717	115.941	1.744	1063.8	1060.5
25	1	5.718	130.495	1.459	1039.6	1013.5
26	0	5.922	127.615	2.482	1125.9	1135.6
27	0	5.070	110.900	2.743	972.8	959.6
28	1	4.086	110.085	1.952	773.1	777.4
29	0	4.494	118.910	2.674	911.8	919.7
30	2	5.309	121.534	0.073	894.2	916.2
31	0	6.497	119.609	2.490	1186.3	1197.6
32	0	4.290	107.171	3.123	860.8	862.0
Prediction set						
1	0	4.290	107.289	0.204	833.4	840.5
2	1	5.718	130.396	1.077	1035.7	1029.5
3	1	5.513	118.782	1.786	987.4	986.3
4	1	6.294	122.415	1.345	1098.7	1095.7
5	0	4.494	118.780	1.263	898.1	908.5
6	0	5.070	110.889	1.771	963.6	932.8

[a] The compounds are numbered as in Table I.

that encodes the size and degree of branching of the molecules. It contains corrections for the difference in the type of halogen in the molecules. The number of methyl groups in the molecule ($NOCH_3$) is also a topological descriptor. The Van der Waals volume (VOL) is a geometric descriptor. The presence of this descriptor in the model reveals the importance of

TABLE III

CORRELATION COEFFICIENTS BETWEEN THE DESCRIPTORS OF THE SELECTED MODEL

Descriptor	XV_0	$NOCH_3$	*VOL*	*DIMO*
XV_0	1.000			
$NOCH_3$	0.003	1.000		
VOL	0.761	−0.292	1.000	
DIMO	−0.076	−0.483	0.025	1.000

the size of the molecules in the retention mechanism. The dipole moment of the molecules (*DIMO*) is an electronic descriptor. This is in agreement with the idea that polarity can play an important role in the retention behaviour of molecules.

In order to illustrate the predictive ability of eqn. 2, the retention indices of six compounds outside the original data set were calculated by using this model. These compounds were not included in the procedure of model generation. The predicted and experimental retention indices for these compounds are compared in Table II. Except for *m*-bromofluorobenzene, the predicted values agree well with the observed retention indices. Dewar and Rzepa [15] have shown that the MNDO method is unable to calculate the heats of formation and molecular structures of fluorine-contaning molecules. Therefore, the discrepancies obtained for these types of compounds may be due to the *VOL* and *DIMO* descriptors, which depend on the optimized structures. In general, the predicted values agree well with the observed retention indices, confirming the validity of the model.

REFERENCES

1 *SPSS/PC, The Statistical Package for IBM PC*, Quiad Software, Ontario, 1986.
2 J.H. Khorasani, *Ph.D. Thesis*, University of Salford, Salford, 1989.
3 M.N. Hasan and P.C. Jurs, *Anal. Chem.*, 55 (1983) 263.
4 L.B. Kier and L.H. Hall, *Molecular Connectivity in Chemistry and Drug Research*, Academic Press, New York, 1976.
5 K.R. Symon, *Mechanics*, Addison-Wesley, Ontario, 1971, p. 402.
6 R.H. Rohrbaugh and P.C. Jurs, *Anal. Chim. Acta*, 199 (1987) 99.
7 T.R. Stouch and P.C. Jurs, *J. Chem. Inf. Comput. Sci.*, 26 (1986) 26.
8 R.S. Pearlman, *Quantum Chem. Program Exch. Bull.*, 1 (1981) 15.
9 L.B. Kier, *Quant. Struct. Act. Relat.*, 4 (1985) 109.
10 A.I. Vogel, *Elementary Practical Organic Chemistry, Part 2, Qualitative Organic Analysis*, Wiley, New York, 1966, p. 24.
11 K.J. Miller and J.A. Savchik, *J. Am. Chem. Soc.*, 101 (1979) 7206.
12 C. Hansch and A. Leo, *Substituent Constants for Correlation Analysis in Chemistry and Biology*, Wiley-Interscience, New York, 1979, p. 18.
13 M.J.S. Dewar and W. Thiel, *J. Am. Chem. Soc.*, 199 (1977) 4899.
14 N. Draper and H. Smith, *Applied Regression Analysis*, Wiley-Interscience, New York, 2nd ed., 1981, p. 307.
15 M.J.S. Dewar and H.S. Rzepa, *J. Am. Chem. Soc.*, 100 (1978) 58.

Journal of Chromatography, 648 (1993) 395–405
Elsevier Science Publishers B.V., Amsterdam

CHROM. 25 282

Practical aspects in the utilization of the Sadtler Standard Gas Chromatography Retention Index Library

Yiliang Sun*, Aijin Huang, Ruiyan Zhang and Lin He

Department of Chemistry, Peking University, 100871 Beijing (China)

(First received January 25th, 1993; revised manuscript received April 26th, 1993)

ABSTRACT

Sadtler standard gas chromatographic programmed-temperature retention indices were shown to be reproducible on either Hewlett-Packard standard fused-silica open-tubular (FSOT) columns or laboratory-made apolar columns by holding the programmed-temperature gas chromatographic characteristic parameter rt_0/β equal to 0.013 and 0.052°C, respectively, where r denotes oven heating rate, t_0 the gas hold-up time and β the phase ratio. Nitrogen could be used instead of hydrogen as the carrier gas, and other experimental parameters, such as column length and inner diameter, stationary phase film thickness and initial oven temperature could also be varied to a certain extent. The average linear velocity of the carrier gas, unclearly specified in the Sadtler Standard Gas Chromatography Retention Index Library, was experimentally determined. Special precautions should be taken to ensure that the column used has been well deactivated.

INTRODUCTION

Although coupled techniques of GC with mass, FT-IR and atomic emission spectrometry have made tremendous progress in the last decade or so, measurement of GC retention values, especially the retention index, is still widely used as a simple, effective, inexpensive and sensitive means of identification. As nearly 75% of GC analyses have been accomplished under programmed-temperature conditions, programmed-temperature retention indices (PTRI) are more frequently met in practice than isothermal values and are of particular importance for analysing complex mixtures. In contrast to isothermal retention indices, PTRI are susceptible to the variation of more experimental parameters and are difficult to reproduce between laboratories. To overcome this difficulty, several chromatographers (Giddings [1], Guiochon [2], Habgood and Harris [3] and Lee and Taylor [4]) proposed correlating PTRI with the isothermal retention index measured at some "equivalent temperature" and others (Grant and Hollis [5], Curvers and co-workers [6,7] and Guan *et al.* [8]) suggested obtaining PTRI by a calculation method after making isothermal runs at two selected temperatures. A more simple and straightforward way is to compile a PTRI database and numerous chromatographers (Jennings and Shibamoto [9], Sadtler Laboratories [10], Vassilaros *et al.* [11], Hayes and Pitzer [12], Saxton [13] and White *et al.* [14]) have been involved in such work. The Sadtler Standard Gas Chromatography Retention Index Library, published in 1984, is by far the largest. This is the only non-spectroscopic database which Sadtler Research Laboratories have ever provided. In comparison with similar PTRI databases compiled by others, the Sadtler Library paid much more attention to standardizing the instrumentation and the experimental parameters used for PTRI measurement. These include the model of gas chromatograph, column geometry (length L and inner diameter D), stationary phase film thick-

* Corresponding author.

0021-9673/93/$06.00

ness, d_f, carrier gas used and the temperature programme (initial oven temperature T_0 and oven heating rate r). In order to increase the repeatability and reproducibility of the measurement of PTRI, Sadtler Research Laboratories employed a highly sophisticated gas chromatograph and high-quality fused-silica capillary columns commercially available at that time. Weber [15] stressed that in order to reproduce the standard PTRI in the Sadtler Library by other chromatographers, all the experimental conditions should be strictly followed. In recent years, we have investigated how to reproduce PTRI under more flexible experimental conditions and found that rt_0/β is a characteristic parameter for reproducing PTRI in programmed-temperature GC, where r is the oven heating rate, t_0 the gas hold-up time and β the phase ratio [16]. As the average linear velocity of carrier gas was unclearly stated in the Sadtler Library, this characteristic parameter cannot be found from the Library, which makes the use of the PTRI standard data in it very difficult.

The objectives of this work were as follows: (1) to optimize the average linear velocity of carrier gas in order to reproduce the standard Sadtler PTRI; (2) to show that for reproducing standard PTRI on polar Carbowax 20M column a more rigorous test for column performance is needed; (3) to show that the initial oven temperature can be allowed to vary to a small extent without seriously affecting the reproducibility of PTRI; (4) to show that hydrogen is not the only carrier gas that can be used; (5) to show that a less sophisticated gas chromatograph can be applied for reproducing standard PTRI satisfactorily; and (6) to show the laboratory made columns of various geometries and film thickness can also be used, provided that the column used is well deactivated.

EXPERIMENTAL

Instrumentation

Two gas chromatographs were used: a Varian Model 3770, an instrument with constant pressure control, similar to the Hewlett-Packard Model 5880A used for Sadtler standard PTRI measurement, and a Shimadzu GC-9A, a constant flow-rate controlled gas chromatograph. Flame ionization detectors were used in both instances. The injector and detector temperatures were both held at 250°C. Shimadzu C-R1B and C-R2B data processors were used, respectively. Injections were performed manually. No autosampler was used. The calculation was completed on an IBM PC/XT microcomputer.

Columns

The standard columns used, all purchased from Hewlett-Packard, were as follows: (1) HP ultra-performance OV-1, cross-linked polydimethylsiloxane, 25 m × 0.32 mm I.D., $d_f = 52$ μm, $\beta = 150$; (2) HP ultra-performance SE-54, cross-linked 5% phenyl–polyphenylmethylsiloxane, 25 m × 0.32 mm I.D., $d_f = 0.52$ μm, $\beta = 150$; and (3) two HP high-performance Carbowax (CW) 20M, 25 m × 0.32 mm I.D., $d_f = 0.32$ μm, $\beta = 250$ (columns A and B). Both columns passed the test given by the manufacturer with a test mixture of ethyl undecanoate, nicotine, heptanoic acid and ethyl tridecanoate, giving four symmetrical peaks and excellent column efficiency at 145°C.

Laboratory-made fused-silica open tubular (FSOT) columns were also used. Fused-silica tubing with I.D. 0.22, 0.25 and 0.32 mm was purchased from Yongnian Optical Fibre Factory (Yongnian, Hebei Province, China). Columns of various lengths were coated statically [17] with SE-54 and OV-1 stationary phases purchased from Chrompack (Middelburg, Netherlands). The phase ratio of the column to be coated was estimated from the concentration of the stationary phase in the coating solution and determined experimentally by measuring the capacity factor of benzene on the column prepared and the standard column at an oven temperature of 60°C and then calculated using the equation

$$\beta_x = k_s\beta_s/k_x$$

where β_x and β_s are the phase ratios of the laboratory made and Hewlett-Packard standard columns, respectively, and k_x and k_s are the capacity factors of benzene measured on the two column. The phase ratios of the standard columns were reported to be 150 and those of

the laboratory-prepared columns varied from 60 to 205. The column efficiency was evaluated by determining the peak width at half-height of *n*-tridecane, the last peak in the chromatogram, in the seven-component Grob test mixture [18] at an oven temperature of 120°C and calculated by the well known equation. Most of the columns tested were carefully deactivated by the method of Woolley *et al.* [19]. Some were not deactivated in order to make a comparison with those subjected to deactivation. The columns after deactivation were further evaluated with the twelve-component Grob test mixture [20]. Deactivations were proved to be successful with the appearance of all twelve peaks symmetrical in the test chromatograms. The specification and performance of the columns used in this experiment are given in Table I.

Test compounds

Eleven compounds which are separable from each other and from admixed *n*-alkanes on the above columns were selected from the Sadtler Standard Gas Chromatography Retention Index Library. These compounds are listed in Tables II–VIII. Most test compounds were purchased from Fluka (Buchs, Switzerland). The test compounds were premixed with C_8–C_{23} *n*-alkanes and dissolved in redistilled *n*-hexane. The concentration of the solution and the injection splitting ratio were so chosen as to make the amount of each component entering the column inlet less than 10 ng.

Grob test mixture was purchased from Fluka. It consists of twelve components, *i.e.*, 2,3-butanediol, *n*-decane, octanol, *n*-undecane, nonanal, 2,6-dimethylphenol, 2,6-dimethylaniline, methyl decanoate, methyl undecanoate, methyl dodecanoate, dicyclohexylamine and 2-ethylhexanoic acid, dissolved in hexane and chloroform. Authentic samples of the individual components were also purchased for peak identification.

TABLE I

SPECIFICATION OF THE LABORATORY-MADE COLUMNS USED

Column[a]	*L* (m)	I.D. (mm)	β	*n*	State
O-1	25	0.32	126	2763	Deactivated
O-2	25	0.22	150	4187	Deactivated
O-3	25	0.32	105	2283	Deactivated
O-4	28	0.22	141	2609	Deactivated
O-5	14	0.22	131	1445	Deactivated
O-6	25	0.22	205	726	Deactivated
O-7[b]	13	0.25	130	4374	Deactivated
O-8	17	0.22	60	2056	Non-deactivated
S-1	23	0.25	145	3609	Deactivated
S-2	26	0.25	141	3521	Deactivated
S-3	24	0.32	135	2809	Deactivated
S-4	24	0.32	155	1690	Deactivated
S-5	23	0.25	138	—	Non-deactivated, cross-linked

[a] O and S denote OV-1 and SE-54 columns, respectively.
[b] The deactivation of column O-7 was unsuccessful.

PTRI calculation

The PTRI were calculated based on Van den Dool's definition [21]:

$$I_{pt} = 100z + 100\left(\frac{T_i - T_z}{T_{z+1} - T_z}\right)$$

where T_i, T_z and T_{z+1} are the retention temperatures of the test component and the *n*-alkanes eluting just before and just after it, respectively.

RESULTS AND DISCUSSION

Optimization of carrier gas velocity

For apolar columns. Carrier gas velocity is an important parameter affecting the reproducibility of the measurement of programmed-temperature retention indices. Golovnya and Uraletz [22] discussed the effect of carrier gas linear velocity on the measurement of the PTRI of *n*-alkanes and concluded that its effect should not be overlooked. Pell and Gearhart [23] observed that on using different carrier gas velocities in PTGC, elution order inversions might even occur. In the Introduction of the Sadtler Library [10], the compiler(s) wrote as follows: "Hydrogen carrier gas is used and the linear velocity is optimized for each column at 60°C on a routine basis". This statement is not very clear and difficult to follow. First, why is it necessary to optimize the gas velocity for a column having already been stan-

dardized? Moreover, what solute one should use for carrier gas velocity optimization?

According to the Golay equation [24], the dependence of the plate height of OTGC on the carrier gas velocity $\bar{u}$ may be expressed as follows:

$$h = B/\bar{u} + C\bar{u}$$

where
$B = 2D_g$ = the coefficient of molecular diffusion term;
$C = C_l + C_g$ = the coefficient of mass transfer terms

$$= \frac{r^2}{24D_g} \cdot \frac{1 + 6k + 11k}{(1+k)^2} + \frac{k^3}{6k^2(1+k)^2} \cdot \frac{r^2}{D_l}$$

$$= \frac{r^2 D_l \beta^2 (1 + 6k + 11k) + 4D_g k r^2}{24 D_l D_g (1+k)^2 \beta^2}$$

r = column radius;
k = capacity factor of the test solute;
D_g = diffusion coefficient of solute in gaseous phase;
D_l = diffusion coefficient of solute in stationary phase;
K = distribution constant of solute, $K = k\beta$;
β = phase ratio.

The optimum carrier gas velocity can thus be deduced:

$$\bar{u} = \left(\frac{B}{C}\right)^{1/2}$$

$$= \left[\frac{48 D_l D_g^2 (1+k)^2 \beta^2}{r^2 D_l \beta^2 (1 + 6k + 11k^2) + 4 D_g k r^2}\right]^{1/2}$$

Hence, for a given capillary column, D_g, D_l and k being solute dependent, $\bar{u}_{opt}$ becomes test solute dependent, different solutes giving different optimum average gas velocities.

The optimum average linear velocity for reproducing the Sadtler standard PTRI was found experimentally by measuring the PTRI of the test mixture following all the instructions given in the introduction of the Library with the exception of carrier gas velocity. Different carrier gas velocities were tried and the corresponding reproducibilities were compared. The best reproducibility was obtained at 43 cm/s (Table II). From this table it is obvious that the reproducibility of PTRI depended sensitively on the gas velocity applied. The dead time t_0 was

TABLE II

INFLUENCE OF CARRIER GAS VELOCITY ON REPRODUCING PTRI VALUES OF TEST COMPOUND ON THE HP SE-54 COLUMN

Varian 3770, $L = 25$ m, I.D. = 0.32 mm, $d_f = 0.52$ μm, $T_0 = 35$°C, $r = 8$°C/min, $n = 3$.

Compound	I_s [a]	$\bar{u}_1 = 43$ cm/s		$\bar{u}_2 = 35$ cm/s		$\bar{u}_3 = 28$ cm/s	
		I_{x1}	ΔI_1	I_{x2}	ΔI_2	I_{x3}	ΔI_3
o-Xylene	895.6	895.5	−0.1	896.7	1.1	898.1	2.5
n-Heptanol	970.7	969.6	−1.1	969.2	−1.5	969.1	−1.6
Limonene	1032.4	1032.5	0.1	1033.9	1.5	1035.4	3.0
Isophorone	1127.1	1126.4	−0.7	1128.2	1.1	1130.4	3.3
Camphor	1154.3	1153.5	−0.8	1156.0	1.7	1159.0	4.7
Cuminaldehyde	1250.2	1249.0	−1.2	1251.2	1.0	1253.6	3.4
Anethol	1292.7	1292.6	−0.1	1292.4	1.7	1296.1	3.4
Eugenol	1365.6	1365.3	−0.3	1367.0	1.4	1368.8	3.2
Diphenylether	1414.2	1413.8	−0.4	1417.1	2.9	1420.0	5.8
β-Ionone	1439.9	1438.1	−1.8	1440.4	0.5	1442.4	2.5
Benzyl benzoate	1785.0	1783.8	−1.2	1787.6	2.6	791.8	6.8
Mean absolute difference			0.70		1.70		3.66

[a] I_s is the PTRI in the Sadtler Standard GC RI Library at $r = 8$°C/min.

approximated by measuring the elution time of methane at the initial oven temperature of 35°C. The PTRI values in Table II are the mean values of three measurements. The reproducibility of PTRI can be conveniently expressed by the mean absolute difference (MAD), which is the mean of the absolute differences between measured and standard PTRI values. In this instance, MAD is 0.70 i.u. for the SE-54 column (Table III) and 0.50 i.u. for the OV-1 column (not shown). The maximum absolute difference is 1.8 i.u. for β-ionone. According to Sadtler, it is expected to have a reproducibility within 1 i.u. on non-polar columns. As the instrument we used was less sophisticated than the HP 5880A and no autosampler or calibration of oven temperature was applied, our results seemed to be satisfactory. The precision or repeatability of PTRI measurements can be expressed by the mean standard deviations of the measurements, MSD, being 0.15 and 0.24 i.u. for the SE-54 and OV-1 columns, respectively. For both SE-54 and OV-1 an average linear velocity of 43 cm/s is used, which is different from the value (35.0 cm/s at 60°C with benzene as test compound on the SE-54 column) calculated from the minimum of the H *vs.* $\bar{v}$ curve.

For polar columns. Here, the column inert-

TABLE III

INFLUENCE OF CARRIER GAS VELOCITY ON REPRODUCING SADTLER STANDARD PTRI ON HP CW 20M COLUMNS

Varian 3770, $L = 25$ m, I.D. $= 0.32$ mm, $d_f = 0.32$ μm, $\beta = 250$, $T_0 = 60$°C, $r = 8$°C/min, $n = 3$.

Column	Compound	I_s [a]	$\bar{u}_1 = 33$ cm/s		$\bar{u}_2 = 37$ cm/s		$\bar{u}_3 = 40$ cm/s		$\bar{u}_4 = 44$ cm/s	
			I_{x1}	ΔI_1	I_{x2}	ΔI_2	I_{x3}	ΔI_3	I_{x4}	ΔI_4
A	*o*-Xylene	1186.5	1189.0	2.5	1180.5	−6.0	1188.1	1.6	1200.0	13.5
	Limonene	1204.3	1206.0	1.7	1207.5	3.2	1204.8	0.5	1204.5	0.2
	n-Heptanol	1444.3	1460.6	16.3	1460.0	15.7	1462.7	18.4	1460.2	15.9
	Camphor	1507.5	1517.5	10.0	1514.1	6.6	1516.8	9.4	1511.7	4.2
	Isophorone	1576.8	1607.8	31.0	1595.8	19.0	1591.5	14.7	1600.0	23.2
	Cuminaldehyde	1767.4	1771.3	3.9	1767.2	−0.2	1772.1	4.7	1762.7	−4.7
	Anethol	1814.5	1810.5	−4.5	1807.4	−7.1	1811.3	−3.2	1802.5	−12.0
	β-Ionone	1835.6	1854.5	18.9	1850.4	14.8	1855.4	19.9	1846.1	10.5
	Diphenyl ether	2000.0	1984.8	−15.2	1980.8	−19.2	1984.0	−16.0	1975.8	−24.2
	Eugenol	2145.3	2167.8	22.5	2164.5	15.2	2167.6	22.3	2162.2	16.9
	MAD [b]			15.5		10.1		9.64		10.3

			$\bar{u}_1 = 37$ cm/s		$\bar{u}_2 = 40$ cm/s		$\bar{u}_3 = 43$ cm/s		$\bar{u}_4 = 46$ cm/s		$\bar{u}_5 = 4$ cm/s	
			I_{x1}	ΔI_1	I_{x2}	ΔI_2	I_{x3}	ΔI_3	I_{x4}	ΔI_4	I_{x5}	ΔI_5
B	*o*-Xylene	1186.5	1190.3	3.8	1189.3	2.8	1189.2	2.7	1188.9	2.4	1185.1	−1.3
	limonene	1204.3	1205.5	1.2	1204.9	0.6	1204.5	0.2	1204.5	0.2	1201.4	−2.9
	n-Heptanol	1444.3	1446.4	2.1	1446.6	2.3	1446.7	2.4	1446.6	2.3	1446.7	2.4
	Camphor	1507.5	1512.5	5.0	1510.7	3.2	1509.5	2.0	1508.0	0.5	1507.0	−0.5
	Isophorone	1576.8	1582.6	5.8	1581.6	4.8	1579.7	2.9	1578.5	1.7	1577.4	0.6
	Cuminaldehyde	1767.4	1771.8	4.4	1770.0	2.6	1768.6	1.2	1767.9	0.5	1766.7	−0.7
	Anethol	1814.5	1818.4	3.9	1817.7	3.2	1816.2	1.7	1815.6	1.1	1814.8	0.3
	β-Ionone	1835.6	1840.9	5.3	1840.1	4.5	1838.3	2.7	1837.4	1.8	1836.3	0.7
	Diphenyl ether	2000.0	2003.6	3.6	2000.0	0.0	2000.0	0.0	2000.0	0.0	2000.0	0.0
	Eugenol	2145.3	2147.6	2.3	2146.4	1.1	2145.6	0.3	2144.9	−0.4	2143.7	−1.6
	MAD [b]			3.46		2.28		1.55		0.97		1.00

[a] I_s is the Sadtler standard PTRI on the HP CV 20M column at $r = 8$°C/min.
[b] MAD = mean absolute difference between measured and standard values.

ness became an additional problem. We therefore had to make a reproducibility test by varying the average linear velocity to see whether an optimum average linear velocity for reproducing PTRI could be found. The failure or success of the flow-rate optimization test could provide valuable information on the status of the column.

From Table III (column A), evidently no matter how the average linear velocity varied, the mean absolute difference between the measured and the standard PTRI was always excessively large, usually exceeding 10 i.u., and the individual differences between measured and standard PTRI even exceeded 30 i.u. It was impossible to optimize the linear velocity on the column. When the second HP CW-20M column was tried, the situation was changed [Table III (column B)]. The mean absolute difference never exceeded 3.5 i.u. at any linear velocity tested, and the mean absolute difference showed a progressive decrease with increase in flow-rate from 37 to 46 cm/s. The mean absolute difference at the optimum linear velocity was nearly 1 i.u., with a maximum absolute difference of 2.9 i.u., in accordance with the demand of the Library.

On the first HP CW 20M column (A) a performance test was run with the Grob test mixture [20,25]. On the chromatogram from column A, 2,3-butanediol showed serious tailing with the 2-ethylhexanoic acid peak missing. On the other hand, the same test mixture eluted well with all twelve components giving nearly symmetrical peaks on column B. Evidently there is a close relationship between the inertness of a column and its capability for reproducing PTRI.

Although it is well known that the Grob test is a rigorous test for column evaluation, almost no column manufacturers use it as a routine method for quality control. So far as we know, only a limited number of commercial PEG 20M columns can pass the Grob test [20,26]. The first column that failed to pass the reproducibility test was used immediately after its arrival without being tested with the Grob test mixture. However, it did pass and can still pass the test recommended by the supplier [see column (3) under Experimental] [27]. Hence it is advisable for users who intend to use the polar column for

TABLE IV

INFLUENCE OF INITIAL OVER TEMPERATURE ON REPRODUCIBILITY OF PTRI ON THE HP SE-54 COLUMN

Varian 3770, $L = 25$ m, I.D. $= 0.32$ mm, $d_f = 0.52$ μm, $\bar{u} = 43$ cm/s, $r = 8$°C/min, $n = 3$.

Compound	I_s [a]	$T_0 = 35$°C		$T_0 = 40$°C		$T_0 = 45$°C		$T_0 = 50$°C	
		I_{x1}	ΔI_1	I_{x2}	ΔI_2	I_{x3}	ΔI_3	I_{x4}	ΔI_4
o-Xylene	895.6	895.5	−0.1	896.1	0.5	897.0	1.4	898.0	2.4
n-Heptanol	970.7	969.6	−1.1	969.2	−1.5	969.5	−1.2	968.1	−2.6
Limonene	1032.4	1032.5	0.1	1032.6	0.2	1032.8	0.4	1033.0	0.6
Isophorone	1127.1	1126.4	−0.7	1126.5	−0.6	1126.9	−0.2	1127.4	0.3
Camphor	1154.3	1153.5	−0.8	1153.8	−0.5	1153.8	−0.5	1154.3	0.0
Cuminaldehyde	1250.2	1249.0	−1.2	1249.1	−1.1	1249.3	−0.9	1249.5	−0.7
Anethol	1292.7	1292.6	−0.1	1292.7	0.0	1293.0	0.3	1293.2	0.5
Eugenol	1365.6	1365.3	−0.3	1365.4	−0.2	1365.5	−0.1	1365.2	−0.4
Diphenyl ether	1414.2	1413.8	−0.4	1413.7	−0.5	1413.9	−0.3	1414.0	−0.2
β-Ionone	1439.9	1438.1	−1.8	1437.8	−2.1	1438.3	−1.6	1437.8	−2.1
Benzyl benzoate	1785.0	1783.8	−1.2	1783.9	−1.1	1783.8	1.2	1783.7	−1.3
MAD			0.70		0.75		0.73		1.00

[a] See footnote to Table II.

reproducing PTRI to run the Grob test and check the quality of the column themselves. It is easy to understand that a column with significant adsorptive activity or excessive acidity or basicity will retain some of the test components with dual mechanisms [ref. 19], and the additional mechanism other than gas–liquid distribution will lead to adverse effects in reproducing PTRI.

Is it permissible to vary the initial oven temperature?

For some less sophisticated gas chromatographs and many laboratories without air conditioning during summer time, it is not convenient to hold the initial oven temperature at 35°C. It is of interest to know whether the initial oven temperature is permitted to increase to a certain extent. On the two apolar columns four different initial oven temperatures were chosen, from 35 to 50°C in 5°C increments. The average linear velocity of carrier gas was maintained at 43 cm/s, which was measured at 35°C without readjustment of the gas flow-rate after changing the initial oven temperature. From Table IV it can be seen that an increase in the initial oven temperature of 10–15°C did not appreciably affect the mean absolute difference between the measured and the standard values on the OV-1 column for the test compounds with PTRI higher than 1000 i.u. This phenomenon can be easily attributed to the initial focusing of the solute at the column inlet. Hence it can be deduced that for compounds with PTRI less than 800 the permissible elevation of the initial oven temperature will be decreased, whereas for compounds with higher PTRI the permissible elevation of the initial oven temperature may be increased. Similar results were obtained on the OV-1 column. The allowable elevation of the initial oven temperature depends on the particular solute tested. For the analysis of flavour and fragrance volatiles in our laboratory the initial oven temperature can usually be varied from 35 to 50°C on these apolar columns. For the polar CW 20M column the standardized initial oven temperature was chosen as 60°C. At this temperature the reproducibility of PTRI is more sensitive to the variation of the initial oven temperature. It is better to maintain the initial oven temperature at 60°C.

Is it allowed to use carrier gases other than hydrogen?

Hydrogen is undoubtedly the preferred carrier gas to use in open-tubular gas chromatography as it gives the fastest separation with sufficiently high efficiency. However, some chromatographers prefer to use helium whereas others prefer nitrogen. It is also of interest to know whether the Sadtler Standard GC PTRI can meet their needs. Based on previous work [16], the average linear velocity of nitrogen was lowered to 11.6 cm/s, a value near its optimum velocity with a simultaneous decrease in the oven heating rate from 8 to 2°C/min. The PTGC characteristic parameter rt_0/β became 0.048°C, which was close to the characteristic value of 0.052°C necessary for reproducing standard PTRI at $r = 8$°C/min. The experimental results on the SE-54 column with nitrogen as the carrier gas are given in Table V. The mean absolute difference between the measured and the standard values measured at $r = 8$°C/min were 0.90, 0.50 and 0.90 i.u. for the SE-54, OV-1 and CW 20M columns, respectively. The reproducibilities are as good as those obtained with hydrogen as the carrier gas. Moreover, helium can be used instead of nitrogen. The use of nitrogen as the carrier gas can certainly meet the routine requirements of some chromatographers but, as it leads to much longer times for retention index measurements than hydrogen, it is not recommended in practice.

Is it feasible to use a gas chromatograph with constant flow-rate control?

The column inlet of a gas chromatograph may be controlled with either constant pressure or constant flow-rate. Most gas chromatographs today belong to the former category, such as the Hewlett-Packard Model 5880A used for compiling the Sadtler Standard GC RI Library and the Varian Model 3770 used in our experiments. It is worth investigating whether an instrument of the latter type, such as a Shimadzu GC 9A, is suitable for our purposes. The influence of velocity on the reproducibility of PTRI is shown

TABLE V

REPRODUCIBILITY OF SADTLER STANDARD PTRI WITH NITROGEN AS CARRIER GAS ON THE HP SE-54 COLUMN

Varian 3770, $L = 25$ m, I.D. = 0.32 mm, $d_f = 0.52$ μm, $T_0 = 35$°C, $\bar{u} = 11.6$ cm/s, $R = 2$°C/min, $n = 3$.

Compound	I_s [a]	I_x			S.D.	I_x	Δ
		1	2	3			
o-Xylene	895.6	895.5	895.6	895.6	0.07	895.6	0.0
n-Heptanol	970.7	969.9	970.0	969.9	0.05	969.9	−0.8
Limonene	1032.4	1032.4	1032.2	1032.3	0.08	1032.3	−0.1
Isophorone	1127.1	1126.6	1126.6	1126.2	0.24	1126.5	−0.7
Camphor	1154.3	1153.3	1153.3	1153.0	0.19	1153.2	−1.1
Cuminaldehyde	1250.2	1248.7	1248.6	1248.5	0.10	1248.6	−1.6
Anethol	1292.7	1292.7	1292.6	1292.3	0.20	1292.5	−0.2
Eugenol	1365.6	1365.0	1365.0	1365.4	0.23	1365.1	−0.5
Diphenyl ether	1414.2	1413.3	1412.7	1413.4	0.42	1413.1	−1.1
β-Ionone	1439.9	1437.7	1437.3	1438.0	0.37	1437.7	−2.2
Benzyl benzoate	1785.0	1783.3	1783.2	1783.6	0.21	1783.4	−1.6
					MSD: 0.20		MAD: 0.90

[a] See footnote to Table II.

in Table VI and *ca.* 28 cm/s was found to be the best choice. The mean absolute difference reached 1.47 i.u. for the SE-54 column, which is considerably higher than that obtained on the Varian Model 3770. Hence it is recommended that an experiment be run on a constant-pressure controlled gas chromatograph if available.

Similar experiments to those described above

TABLE VI

INFLUENCE OF CARRIER GAS VELOCITY ON REPRODUCBILITY OF PTRI VALUES OF TEST COMPOUNDS ON A CONSTANT FLOW-RATE CONTROLLED GAS CHROMATOGRAPH

Shimadzu GC-9A, HP SE-54, $L = 25$ m, I.D. = 0.32 mm, $d_f = 0.52$ μm, $T_0 = 35$°C, $R = 8$°C/min, $n = 3$.

Compound	I_s [a]	$\bar{u}_1 = 28$ cm/s		$\bar{u}_2 = 30$ cm/s		$\bar{u}_3 = 33$ cm/s		$\bar{u}_4 = 36$ cm/s		$\bar{u}_5 = 43$ cm/s		$\bar{u}_6 = 51$ cm/s	
		I_{x1}	ΔI_1	I_{x2}	ΔI	I_{x3}	ΔI_3	I_{x4}	ΔI_4	I_{x5}	ΔI_5	I_{x6}	ΔI_6
o-Xylene	895.6	897.5	1.9	897.1	1.5	896.7	1.1	896.2	0.6	895.3	0.3	894.6	−1.0
n-Heptanol	970.7	969.4	1.3	969.6	−1.1	969.8	0.9	969.7	−1.0	970.0	−0.7	970.0	−0.7
Limonene	1032.4	1034.3	1.9	1033.8	1.4	1033.3	0.9	1032.8	0.4	1031.0	−0.6	1031.0	−1.4
Isophorone	1127.1	1129.0	1.9	1128.0	0.9	1127.4	0.3	1127.0	−0.1	1125.3	−1.8	1124.1	−3.0
Camphor	1154.3	1156.5	2.2	1155.3	1.0	1154.5	0.2	1153.7	−0.6	1151.4	−2.9	149.8	−4.5
Cuminaldehyde	1250.2	1251.2	1.0	1250.0	0.0	1249.3	−0.9	1248.9	−1.3	1246.8	−3.4	1245.4	−4.8
Anethol	1292.7	1294.1	1.4	1293.5	0.8	1292.8	0.1	1292.4	−0.3	1291.1	−1.6	1290.0	−2.7
Eugenol	1365.6	1366.4	0.8	1365.9	0.3	1365.1	−0.5	1364.8	−0.8	1363.4	−2.2	1362.2	−3.4
Diphenyl ether	1414.2	1415.5	0.8	1438.7	−1.2	1437.7	−2.2	1436.9	−3.0	1435.2	−4.7	1433.7	−6.2
Benzylbenzoate	1785.0	1783.3	−1.7	1782.0	3.0	1780.3	−4.7	1779.6	−5.4	1776.5	−8.5	773.7	−11.3
MAD			1.47		0.73		1.07		1.23		2.69		4.02

[a] See footnote to Table II.

were made to reproduce the Sadtler standard PTRI measured at $r = 2$°C/min, with equally satisfactory results.

It is possible to reproduce Sadtler standard PTRI on laboratory made columns?

Efficient deactivation of the column is of utmost importance for reproducing standard PTRI. Table VII shows that the first six OV-1 columns that passed the stringent Grob test were capable of reproducing the standard PTRI of the eleven test compounds with a mean absolute difference between the measured and the standard values lying between 0.68 and 1.41 i.u. with an average of 0.90 i.u. Similarly, on laboratory made SE-54 columns the average of the mean absolute differences on four columns (S-1–4) is 0.69 i.u. (Table VIII).

In contrast, the results with the non-deactivated columns (O-8 and S-5) and the poorly deactivated column (O-7), which had been washed excessively with solvent, leading to destruction of the deactivated layer, were all unsatisfactory. On column O-7 the influence of poor deactivation on retention index measurement was demonstrated by the exceptionally large difference for the two polar test solutes, *n*-heptanol and eugenol. As mentioned above, effective deactivation of a column was found to be of utmost importance for reproducing PTRI on a commercially available HP high-performance CW 20M column. The same is necessary for non-polar laboratory made OV-1 and SE-54 columns.

The influence of column efficiency on the capability of reproducing standard PTRI was demonstrated to be of only secondary importance. All the columns used in the experiment were prepared by a novice without previous experience in column technology. Among the six OV-1 columns prepared in the experiment, only column 2 was comparable in efficiency to the HP ultra-performance OV-1 column. Columns O-5 and O-6 gave very low efficiencies. Nevertheless, they could reproduce the standard Sadtler PTRI equally well. The reproducibilities of the Sadtler Standard PTRI on our laboratory made columns were slightly poorer than those stated in the Library.

The phase ratio β, film thickness d_f, column inner diameter and column length L need not to be standardized. Variations of L from 14 to 28 m,

TABLE VII

REPRODUCIBILITY OF SADTLER STANDARD PTRI ON LABORATORY-MADE OV-1 COLUMNS [DIFFERENCE BETWEEN MEASURED ($n = 3$) AND SADTLER STANDARD PTRI VALUES]

Compound	I_s	O-1	O-2	O-3	O-4	O-5	O-6	O-7	O-8
o-Xylene	876.7	0.35	−0.35	−0.51	0.07	1.22	0.98	1.38	−0.77
n-Heptanol	953.8	1.56	−0.67	−1.59	−0.81	1.32	−1.17	11.56	6.71
Limonene	1021.4	0.13	−0.42	−0.51	−0.24	−0.71	0.69	−0.24	−1.28
Isophorone	1090.1	−0.61	−0.49	−1.49	−0.11	0.78	0.52	3.24	−1.20
Camphor	1120.5	0.57	−1.21	−1.07	−0.34	0.46	1.03	−0.54	−2.24
Cuminaldehyde	1213.0	0.48	−0.58	−1.31	−0.69	1.70	0.43	3.22	−1.81
Anethol	1261.8	−0.48	−0.52	−1.33	−1.23	1.41	0.43	2.56	−1.86
Eugenol	1329.3	1.44	−0.71	−2.00	−1.60	1.16	0.28	12.54	0.60
Diphenyl ether	1376.3	1.13	−1.83	−2.83	−2.24	−0.58	−0.86	1.26	−3.82
β-Ionone	1408.8	0.59	−1.02	−1.81	−1.10	0.10	−0.53	1.37	−2.14
Benzyl benzoate	1728.4	0.18	−0.67	−1.54	−1.98	0.41	0.89	2.30	−3.54
MAD[a]		0.68	0.77	1.41	0.95	0.90	0.71	3.65	2.36
t_0 (min)[b]		0.95	0.94	0.69	0.95	0.82	1.24	0.83	0.40
rt_0/β (°C)		0.060	0.050	0.053	0.054	0.050	0.048	0.051	0.053

[a] MAD-mean absolute difference between the average of measured values and the Sadtler standard values at $r = 8$°C/min.
[b] u was chosen so as to make rt_0/β approximately equal to 0.052°C.

TABLE VIII

REPRODUCIBILITY OF SADTLER STANDARD PTRI ON LABORATORY-MADE SE-54 COLUMNS [DIFFERENCE BETWEEN MEASURED ($n = 3$) AND SADTLER STANDARD VALUES]

Compound	I_s	S-1	S-2	S-3	S-4	S-5
o-Xylene	895.6	0.15	0.05	0.19	−0.11	0.30
n-Heptanol	970.7	−0.43	−0.24	−0.40	−0.06	4.75
Limonene	1032.4	−0.31	−0.10	−0.31	−0.53	0.75
Isophorone	1127.1	0.59	1.30	1.04	0.16	8.67
Camphor	1154.3	0.50	0.25	0.07	−1.05	5.06
Cuminaldehyde	1250.2	−1.24	−0.38	−0.56	−1.60	1.85
Anethol	1292.7	0.05	0.37	0.37	−0.37	2.12
Eugenol	1365.6	−0.04	−0.02	−0.21	−0.59	3.24
Diphenyl ether	1414.2	−0.97	−0.37	−0.61	−1.84	1.85
β-Ionone	1439.9	−1.45	−1.57	−1.71	−2.12	3.19
Benzyl benzoate	1785.0	−1.45	−0.84	−1.22	−2.90	2.88
MAD[a]		0.65	0.50	0.61	1.01	3.06
t_0 (min)[b]		0.93	0.96	0.87	0.93	0.87
rt_0/β (°C)		0.051	0.054	0.052	0.048	0.050

[a] See footnotes to Table VII.

β from 105 to 205 and inner diameter from 0.22 to 0.32 mm did not significantly affect the reproducibility of the results. Therefore, the Sadtler Standard PTRI Library might be compatible with not only Hewlett-Packard ultra-performance and high-performance columns but also with many other well deactivated commercially available columns.

So far, we have not succeeded in preparing a polar Carbowax 20M fused-silica capillary column with high inertness, so we are still unable to reproduce the standard PTRI on laboratory-made polar columns.

ACKNOWLEDGEMENT

This work was kindly sponsored by the National Natural Science Foundation of China.

REFERENCES

1 J.C. Giddings, *Gas Chromatography*, Academic Press, New York, 1962, p. 57.
2 G. Guiochon, *Anal. Chem.*, 36 (1964) 661.
3 H.W. Habgood and W.E. Harris, *Anal. Chem.*, 36 (1964) 663.
4 J. Lee and D.R. Taylor, *Chromatographia*, 16 (1982) 286.
5 D. Grant and M. Hollis, *J. Chromatogr.*, 158 (1978) 3.
6 J. Curvers, J. Rijks and C. Cramers, *J. High Resolut. Chromatogr. Chromatogr. Commun.*, 8 (1985) 607.
7 J. Curvers, J. Rijks, C. Cramers, K. Knauss and P. Larson, *J. High Resolut. Chromatogr. Chromatogr. Commun.*, 8 (1985) 611.
8 Y. Guan, J. Kiraly and J. Rijks, *J. Chromatogr.*, 472 (1989) 129.
9 W. Jennings and T. Shibamoto, *Qualitative Analysis of Flavor and Fragrance Volatiles by Glass Capillary Gas Chromatography*, Academic Press, New York, 1980.
10 *The Sadtler Standard Gas Chromatography Retention Index Library*, Sadtler Research Laboratories, Philadelphia, 1984.
11 D.L. Vassilaros, R.C. Kong, D.W. Later and M.L. Lee, *J. Chromatogr.*, 252 (1982) 1.
12 P.C. Hayes, Jr., and E.W. Pitzer, *J. Chromatogr.*, 253 (1982) 179.
13 W.L. Saxton, *J. Chromatogr.*, 393 (1987) 175.
14 C.M. White, J. Hackett, R.R. Anderson, S. Kail and P.S. Spock, *J. High Resolut. Chromatogr.*, 15 (1992) 105.
15 L. Weber, *J. High Resolut. Chromatogr. Chromatogr. Commun.*, 9 (1986) 446.
16 H. Yin and Y. Sun, *Chromatographia*, 29 (1990) 39.
17 J. Bouche and M. Verzele, *J. Chromatogr.*, 6 (1968) 501.
18 K. Grob and G. Grob, *Chromatographia*, 4 (1971) 422.
19 C.L. Woolley, R.C. Kong, B.E. Richter and M.L. Lee, *J. High Resolut. Chromatogr. Chromatogr. Commun.*, 7 (1984) 329.
20 K. Grob, Jr., G. Grob and K. Grob, *J. Chromatogr.*, 156 (1978) 1.
21 H. Van den Dool and P.D. Kratz, *J. Chromatogr.*, 11 (1963) 463.
22 R.V. Golovnya and V.P. Uraletz, *J. Chromatogr.*, 36 (1968) 276.

23 R.J. Pell and H.L. Gearhart, *J. High Resolut. Chromatogr. Chromatogr. Commun.*, 10 (1987) 388.
24 M.L. Lee, F.J. Yang and K.D. Bartle, *Open Tubular Column Gas Chromatography*, Wiley, New York, 1984, p. 18.
25 K. Grob, G. Grob and K. Grob, Jr., *J. Chromatogr.*, 219 (1981) 13.
26 P.H. Silvis, J.W. Walsh and D.M. Shelow, *Int. Lab.*, March/April (1987) 34.
27 V.G. Berezkin and A.A. Korolev, *Chromatogaphia*, 21 (1986) 16.

Journal of Chromatography, 648 (1993) 407–414
Elsevier Science Publishers B.V., Amsterdam

CHROM. 25 333

Variables affecting the introduction of large sample volumes in capillary gas chromatography using a programmed-temperature vaporizer

F.J. Señoráns and J. Tabera

Instituto de Fermentaciones Industriales, CSIC, Juan de la Cierva 3, 28006 Madrid (Spain)

J. Villén

Escuela Politécnica de Albacete, Universidad de Castilla-La Mancha, Carretera de Peñas km 3.1, 02006 Albacete (Spain)

M. Herraiz* and G. Reglero

Instituto de Fermentaciones Industriales, CSIC, Juan de la Cierva 3, 28006 Madrid (Spain)

(First received March 17th, 1993; revised manuscript received May 24th, 1993)

ABSTRACT

The dependence of the programmed-temperature vaporizer (PTV) solvent split sampling technique on eight experimental variables affecting the introduction of large sample volumes in capillary GC was evaluated. The simplex method was used to improve the sensitivity of the analysis significantly by optimization of the operating conditions, namely sample volume, flow-rate during sampling, initial PTV temperature, length of the adsorbent bed, nature of the trapping material used in the glass liner, speed of sample introduction, elimination volume and solvent elimination temperature. With this method, reliable determinations of several volatile components at sub-ppb concentrations were obtained using a flame ionization detector, without the need for prior enrichment of the sample.

INTRODUCTION

Introduction of large volume samples in capillary GC is of special interest for the determination of trace compounds in strongly diluted or low-concentration samples. Also, injection of large amounts is usually required for on-line LC–GC coupling.

The determination of trace compounds by capillary GC has commonly been performed by using the so-called Grob-type splitless injection, which involves direct introduction into the chromatographic column of dilute solutions [1–3]. An evident disadvantage of this technique, however, is the high loading of the column with large amounts of solvents, as it may cause several problems mainly due to flooding sample liquid in the first portion of the capillary column, thus favouring phase stripping. The use of uncoated-column inlets with a reduced retention power (retention gaps) has proved suitable for reconcentrating the initial solute bands broadened in space. This reconcentration results from the accelerated movement of the solute materials through the uncoated inlet compared with the coated column [4]. Other approaches require the concentration of the sample prior to its intro-

* Corresponding author.

0021-9673/93/$06.00

duction into the injector [5–8], but all of them have several operational drawbacks and performance limitations.

Several years ago, an injection system allowing the introduction of up to 250 μl in a cold vaporizer was proposed for sampling large amounts of very dilute solutions [9,10]. Subsequently, a programmed-temperature vaporizer (PTV) was designed for a much wider field of application [11,12] and its usefulness for avoiding discrimination related to high-temperature sampling has been reported [13,15]. Moreover, the possibility of using the PTV injector as a pre-column enrichment device with a suitable adsorbent has also been emphasized [16–22].

The PTV vapour overflow technique is intended for introducing samples in large volumes of solvents by syringe injection. Evaporation and discharge of the solvent vapour occur by expansion, driven by the solvent vapour pressure. Subsequent heating of the vaporizing chamber brings about the transfer of the compounds into the column [23].

The use of a PTV operated in the solvent split (solvent elimination) mode [13,24], also allows the introduction of large-volumes of solvents with very high diluted samples by means of a syringe injection. With this mode of operation, the sample is transferred to the column after the solvent has been eliminated at low temperature, whereas the analyte solutes are retained in a suitable trapping material. A few seconds after the injection, the split valve is closed, the vaporizer heated and the sample vapour transferred to the column.

Concerning the operation of a PTV in the solvent elimination mode for the determination of trace compounds, its use is only recommended if high-boiling solutes are to be measured, as the most volatile compounds are partly lost by evaporation together with the solvent. Therefore, further optimization of the experimental operation, especially regarding the determination of highly volatile materials, is necessary [25,26].

On the other hand, it is well known that in the development, improvement or adaptation of analytical methods, those variables affecting the experimentation should be carefully adjusted in order to establish the set of conditions that give the best results. This is why efficient and straightforward optimization procedures are strongly required, especially if the variables interact with each other so that each variable cannot be optimized independently of the others. In this respect, the sequential simplex method, first presented by Spendley *et al.* [27], has proved to be a useful optimization procedure [28–33].

With regard to the use of the PTV solvent split sampling technique, previous studies on the optimization of experimental variables by using the so-called response surface methodology suggested the usefulness of increasing the number of variables considered [34].

In this work, the optimization of the direct determination of trace compounds by using a PTV operated in the solvent elimination mode was studied. Eight variables were considered and the modified simplex method was used [35].

EXPERIMENTAL

Instrumentation

A gas chromatograph (Perkin-Elmer Model 8320) equipped with a flame ionization detector and a PTV injector was used. Data collection was done by using 2600 Chromatography Software (Perkin-Elmer Nelson Systems).

Sampling was accomplished by means of a simple, inexpensive, laboratory-made device designed to allow the introduction of large sample volumes by using a syringe (SGE, 500 μl). This device allows one to control effectively the speed of sample introduction (ranging between 0.083 and 1.47 μl/s) in order to adjust the injection speed to the rate of solvent evaporation.

Sample mixtures

A synthetic test mixture consisting of ethyl pentanoate, 1-butanol, ethyl hexanoate, 1-pentanol, ethyl heptanoate, 1-hexanol, ethyl octanoate, 1-heptanol and 1-octanol was used. The compounds were dissolved in ethanol–water (1:1, v/v) and their concentrations were about 0.1 mg/l per compound. The composition, concentrations and solvent of the test mixture were selected for subsequent real analyses of alcoholic beverages and foods.

Gas chromatographic analysis

Helium at 36 p.s.i.g. (1 p.s.i. = 6894.76 Pa) was used as the carrier gas and the detector was operated at 250°C. Gas chromatographic separations were carried out on a SGE (Ringwood, Australia) fused-silica column (50 m × 0.22 mm I.D.) coated with cross-linked BP-21 (film thickness 0.25 μm). The column temperature was held at 35°C for 8 min, then programmed to 60°C at 2°C/min and to 180°C at 4°C/min.

The initial PTV temperature was varied, as mentioned below, according to the optimization procedure. The final PTV temperature (250°C) was established taking into account the thermal stability of the trapping materials used and the need to achieve thermodesorption of the trapped solutes. After reaching the final temperature in the injector, it was maintained for 5 min and then cooled.

A silylated quartz insert (90 mm × 1 mm I.D. × 2 mm O.D.) from the PTV injector was packed with different lengths of packing material and plugged at both ends with silanized glass-wool. The packed liners were conditioned for 120 min at 255°C under a purge gas (helium) flow. According to our previous experience, the use of both Tenax TA and Gas Chrom 220 as alternative sorbents is of interest for trace enrichment because of their complementary characteristics. In order to evaluate the influence of the functionality of the trapping material (*i.e.*, the affinity of the sorbent for different organic compounds) on the performance of the analysis, a mixture of the two adsorbents mentioned above was finally considered to be one of the eight variables to be optimized. In all instances, the trapping material had been previously washed with acetone and subsequently dried and conditioned under a stream of nitrogen which was maintained either for 30 min at 90°C, 30 min at 180°C, 60 min at 300°C and 120 min at 350°C (for Tenax TA) or for 30 min at 90°C, 30 min at 180°C and 120 min at 250°C (for Gas Chrom 220).

Operating conditions

Table I shows the eight variables which were optimized for large sample introduction in the PTV: sample volume (V_{IO}), flow-rate during sampling (F), initial temperature of the PTV (T_i), length of the adsorbent in the glass liner (L), percentage of Gas Chrom 220 in the mixture of adsorbents used as a trapping material (%), speed of sample introduction (v_i), volume of gas that is purged during the splitting period (elimination volume, V_{OE}) and solvent elimination temperature (T_e). Prior to the sample introduction, the column end was withdrawn from the injector body so that solvent elimination was effectively performed through the injector bottom.

TABLE I

BASE LEVEL, STEP SIZE AND EXPERIMENTAL VARIABLES CONSIDERED FOR THE SIMPLEX OPTIMIZATION OF THE PTV SOLVENT SPLIT SAMPLING OF LARGE VOLUMES

Experimental variable	Base level	Step size
Sample volume, V_{IO} (μl)	300	150
Flow-rate during sampling, F (ml/min)	600	300
Initial PTV temperature, T_i (°C)	40	15
Length of adsorbent, L (cm)	2	2
Gas Chrom 220 in the adsorbent (%)	0	45
Speed of sample introduction, v_i (μl/s)	0.2	0.07
Elimination volume, V_{OE} (ml)	3000	3000
Solvent elimination temperature, T_e (°C)	20	15

The simplex optimization was initiated according to the matrix of mathematical coordinates proposed by Spendley *et al.* [27]. The following equation was applied to calculate the physical values of the experimental variables:

$$X_{phys} = X_0 + X_{math}S_z \quad (1)$$

where X_0 is the starting physical value of the variable X (base level), X_{phys} its actual physical value, X_{math} the corresponding mathematical coordinate in the Spendley matrix and S_z (the so-called step size) the physical value corresponding to a mathematical unit of the variable X.

Table I also includes the base level corresponding to the studied variables and the step size that was considered for each experimental variable.

RESULTS AND DISCUSSION

As previously described by several workers, the sequential simplex technique of Spendley *et al.* [27] suffers from several limitations, mainly because it does not have provision for acceleration and the possibility of attaining a false optimum. In order to overcome these drawbacks, a modification was proposed (modified simplex method) that has the advantage of acceleration and adaptation to fit the particular response being considered, as it allows operations of expansion and contraction in the searching progress [33,35].

Table II gives the experimental runs performed for optimizing large sample volume introduction in a PTV operated in the solvent split mode by applying the modified simplex method. Vertex 1 is defined by the base level of each variable and corresponds to the starting point of the experimental study. In order to investigate the influence of a modification of the variables affecting the process in the performance of the method, the sensitivity achievable from each run was evaluated. In this regard, the sum of the ratios of the measured peak areas (in area units) for each compound to the elution order of the corresponding solute was considered. It should be kept in mind that an interesting feature of the method investigated is the possibility of minimizing losses of the most volatile solutes. This is why the selected response included the elution order observed for each solute. Data obtained for the evaluated response throughout the optimization procedure are also given in Table II.

As a simplex is a geometric figure defined by a number of points equal to one more than that of the number of dimensions of the space, the

TABLE II

EXPERIMENTAL RUNS AND RESULTS FOR THE SIMPLEX OPTIMIZATION OF THE PTV SOLVENT SPLIT INJECTION

Vertex No.	Simplex No.	Factor level (physical values)[a]								Response[b]
		V_{IO}	F	T_i	L	%	v_i	V_{OE}	T_e	
1	1	300	600	40	2.0	0.0	0.200	3000	20.0	3311
2	1	433	653	43	2.3	7.9	0.212	3530	22.6	3974
3	1	326	865	43	2.3	7.9	0.212	3530	22.6	3206
4	1	326	653	53	2.3	7.9	0.212	3530	22.6	3588
5	1	326	653	43	3.8	7.9	0.212	3530	22.6	6367
6	1	326	653	43	2.3	39.8	0.212	3530	22.6	7953
7	1	326	653	43	2.3	7.9	0.262	3530	22.6	2931
8	1	326	653	43	2.3	7.9	0.212	5651	22.6	3997
9	1	326	653	43	2.3	7.9	0.212	3530	33.2	2522
10	2	346	692	45	2.6	13.9	0.220	3928	11.4	5514
11	3	351	702	45	2.7	15.4	0.160	4027	19.0	5646
12	4	357	450	45	2.8	17.3	0.199	4151	18.3	5172
13	5	398	677	50	3.1	29.5	0.211	4970	20.5	6888
14	6	389	630	36	3.2	27.0	0.198	4799	17.3	9218
15[c]	7	421	619	27	3.6	36.5	0.191	5434	14.7	12 212
16[d]	8	453	608	18	4.0	46.0	0.184	6069	12.0	13 830
17[e]	9	485	597	9	4.5	55.5	0.177	6703	9.0	14 957
18	10	297	616	38	3.7	39.0	0.189	5593	14.0	9269
19	11	395	608	37	4.1	46.6	0.184	3457	11.8	10 493

[a] Units as in Table I.

[b] Sum of the ratios of the integration peak area (in area units) to the elution order of the corresponding solute (mean value of a minimum of two replicates).

[c] Obtained with expansion coefficient equal to 2.

[d] Obtained with expansion coefficient equal to 3.

[e] Obtained with expansion coefficient equal to 4.

initial simplex corresponding to the optimization of eight variables is formed by the first nine experimental runs (see Table II).

After having performed the initial simplex, the response values obtained were evaluated and the worst observation was rejected. Subsequently, a movement in the direction given by the rules of the simplex procedure was made. Experimentation was carried out until no further improvement of the response was observed. In all instances, a minimum of two replicates of each analysis were performed.

From Table II, the improvement observed in the sensitivity achievable with the analysis throughout the optimization is evident. As can be seen, experimental conditions defining vertex 17 (*i.e.*, sample volume 485 μl, flow-rate during sampling 597 ml/min, initial temperature of the PTV 9°C, length of the adsorbent in the glass liner 4.5 cm, percentage of Gas Chrom 220 in the mixture of adsorbents 55.5, speed of sample introduction 0.18 μl/s, elimination volume 6703 ml and solvent elimination temperature 9°C) should be considered as the most suitable for the analysis, as they render the highest response.

Figs. 1 and 2 show respectively the initial (base level) and final chromatograms resulting from optimizing the PTV solvent split introduction of large sample volumes into the vaporizer of a gas chromatograph. It is evident that the optimization procedure brings about a significant improvement of the sensitivity attainable with the analysis, as under the selected conditions (vertex 17 in Table II) the response obtained is nearly five times higher than that corresponding to the initial experimental conditions (vertex 1 in Table II). It should be emphasized that a blank run performed on the trapping material by using GC–MS showed that the peaks assigned as adsorbent peaks are mainly due both to styrene (Fig. 2) and different isomers of dimethylstyrene (Figs. 1 and 2). In this respect, it is evident that the degradation of the adsorbent avoided the reliable determination of ethyl octanoate (see Fig. 2).

It is worth noting that according to the rules of the simplex procedure, vertices 15, 16 and 17 resulted from accelerations with expansion coefficients of 2, 3 and 4, respectively. After having performed nineteen experimental runs, the search was halted as the response values decreased from vertex 17 onwards, and the improvement achieved by the optimization procedure was satisfactory.

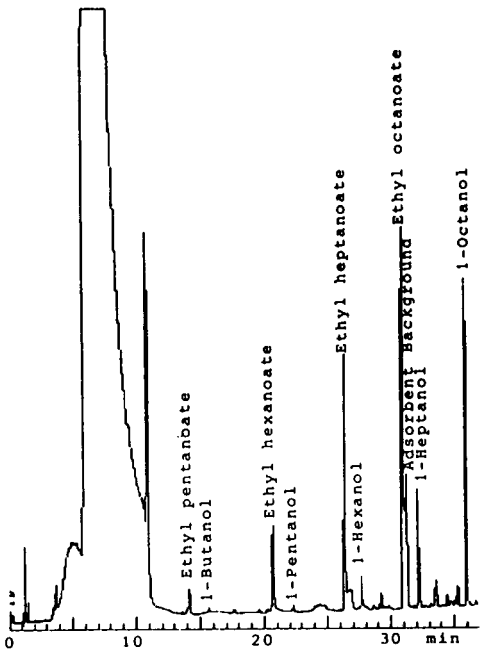

Fig. 1. Chromatogram resulting from the introduction of 300 μl of the test sample in a PTV operated in the solvent split mode under the initial experimental conditions of the optimization procedure (vertex 1 in Table II). The adsorbent background is due to different isomers of dimethylstyrene. See text for further details.

Table III gives the relative standard deviations obtained from the response values when a test mixture was analysed under the experimental conditions giving the highest response. As can be seen, values lower than 13% were generally obtained even though the analyses were performed with diffe-ent glass liners in the PTV body. It is clear, however, that the use of only one glass liner for different experimental runs gives more precise analyses.

Table III also includes the recoveries obtained for the investigated compounds. These values were calculated from normalized peak areas (n = 3) using as a reference the normalized peak areas resulting from the cold splitless injection (n = 6) of a 2-μl volume of the standard solution, so that the same amount of each component was intro-

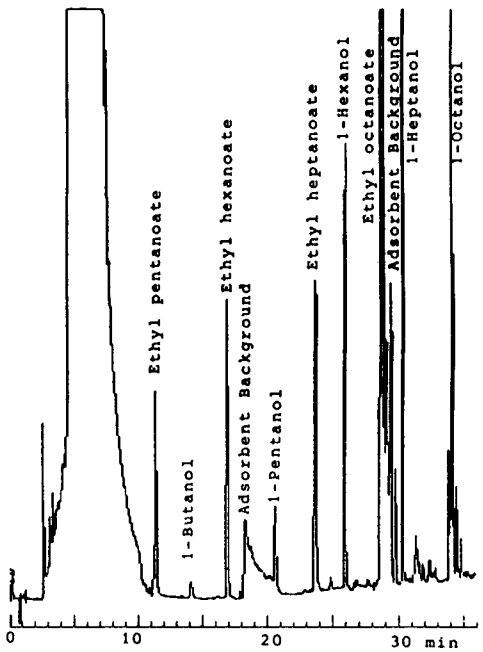

Fig. 2. Chromatogram following optimization of large volume sampling in the PTV solvent split mode of operation. Experimental conditions correspond to those of vertex 17 in Table II. The adsorbent background is mainly due to either (a) styrene or (b) different isomers of dimethylstyrene. See text for further details.

duced into the chromatographic column in both the cold splitless and the PTV solvent split modes of operation. Different procedures for the calculation of recoveries (including the consideration of both absolute peak areas and the ratio of the absolute peak area of each peak to that for 1-heptanol) provided similar results to those presented in Table III.

As expected, the highest recoveries were obtained for the less volatile compounds, but it is interesting that one of the most volatile components present in the sample (ethyl pentanoate) was more than 45% trapped. However, components with volatilities lower than or similar to that of ethyl pentanoate were largely lost. This was observed for the most volatile alcohols as the solvent mixture used for the standard dilution (ethanol–water) must promote the co-evaporation of the mentioned compounds during the solvent elimination period. Therefore, a reliable determination of 1-butanol is not possible using the proposed method, although the use of another solvent and subsequent optimization of the operating conditions would probably allow the determination of alcohols with higher recoveries and lower relative standard deviations.

Table IV gives the lowest concentrations that can be detected by using the described method, which involves (under the experimental conditions providing the best results) the injection of 485 μl, the speed of sample introduction being 0.18 μl/s. The mentioned detection limits are

TABLE III

RELATIVE STANDARD DEVIATIONS FOR THE RESPONSE VALUE (SUM OF THE RATIOS OF THE MEASURED PEAK AREAS FOR EACH COMPOUND TO THE ELUTION ORDER OF THE CORRESPONDING SOLUTE) FOR A TEST MIXTURE

Experimental conditions as given in Table II, vertex 17.

Compound	R.S.D. (%)[a]	R.S.D. (%)[b]	Recovery (%)
Ethyl pentanoate	3.5	3.4	45.3
1-Butanol	11.6	25.6	2.6
Ethyl hexanoate	2.0	6.1	77.6
1-Pentanol	9.9	13.1	15.8
Ethyl heptanoate	3.2	8.3	87.4
1-Hexanol	5.5	12.0	56.5
1-Heptanol	7.6	10.8	95.2
1-Octanol	3.3	8.1	95.1

[a] Data obtained from five analyses performed with one glass liner.
[b] Data obtained from five different glass liners. In all instances, a minimum of two replicates were carried out ($n = 10$).

TABLE IV

DETECTION LIMITS WITH THE PROCEDURE INVOLVING THE PTV SOLVENT SPLIT INTRODUCTION OF LARGE SAMPLE VOLUMES

Experimental conditions as given in Table II, vertex 17.

Compound	Detection limit[a] (ng/l)
Ethyl pentanoate	378
1-Butanol	6557
Ethyl hexanoate	232
1-Pentanol	1227
Ethyl heptanoate	197
1-Hexanol	181
1-Heptanol	111
1-Octanol	99

[a] Corresponding to a signal which is equal to twice the baseline noise. The noise is determined from the width of the baseline.

taken as the concentration of solute giving a signal twice the background noise. In this respect, the noise is determined from the width of the baseline. From the data in Table IV, it is evident that the optimization of the PTV sampling procedure may allow the determination of less than 200 ng/l of some compounds by injection of large volumes without requiring a previous extraction and/or concentration of the sample.

After having performed the optimization procedure, it was intended to evaluate the influence of each variable on the obtained response. First the relationships between the response measured and the experimental values of each factor (variable) were studied by simple linear regression. The best correlations were achieved for the following variables: percentage of Gas Chrom 220 in the adsorbent, linear correlation coefficient $r = 0.93$; length of adsorbent, $r = 0.88$; and initial PTV temperature, $r = -0.84$. Therefore, a high positive correlation was observed between the response and both the percentage of Gas Chrom 220 in the adsorbent and the length of adsorbent, whereas a high negative correlation was obtained for the initial PTV temperature. It is clear that the higher the percentage of Gas Chrom 220 in the adsorbent, the higher is the response obtained, as this material exhibits a high retention power which lowers the losses of volatile materials. Also, an increase in the length of the adsorbent promotes the possibility of soaking up larger amounts of liquid samples, thus preventing the liquid from running out of the packing in the insert. With regard to the influence of the initial PTV temperature, its negative correlation with the observed response is evident as the more volatile compounds will be more easily retained if the insert is maintained at low temperature.

ACKNOWLEDGEMENTS

This work was made possible by financial assistance from the Comisión Interministerial de Ciencia y Tecnología (Project ALI 91-0540). F.J.S. thanks the Ministerio de Educación y Ciencia for a grant. The authors are also indebted to J.H. Campos, S. Campos and J. Martin for their skillful assistance with the injection device.

REFERENCES

1 K. Grob and G. Grob, *J. Chromatogr. Sci.*, 7 (1969) 584.
2 K. Grob and G. Grob, *J. Chromatogr. Sci.*, 7 (1969) 587.
3 K. Grob and K. Grob, Jr., *J. Chromatogr.*, 94 (1974) 53.
4 K. Grob, *On-Column Injection in Capillary Gas Chromatography*, Hüthig, Heidelberg, 1987.
5 M. Novotny and R. Farlow, *J. Chromatogr.*, 103 (1975) 1.
6 P.M.J. van den Berg and Th.P.H. Cox, *Chromatographia*, 5 (1972) 301.
7 C.A. Cramers and E.A. Vermeer, *Chromatographia*, 8 (1975) 479.
8 J.W. de Leeuw, W.L. Maters, D. van den Memt and J.J. Boon, *Anal. Chem.*, 49 (1977) 1881.
9 W. Vogt, K. Jacob and H.W. Obwexer, *J. Chromatogr.*, 174 (1979) 437.
10 M. Vogt, K. Jacob, A.B. Ohnesorge and H.W. Obwexer, *J. Chromatogr.*, 186 (1979) 197.
11 G. Schomburg, in R.E. Kaiser (Editor), *Proceedings of the 4th International Symposium on Capillary Chromatography*, Hüthig, Heidelberg, 1981, p. 371.
12 F. Poy, S. Visani and F. Terrosi, *J. Chromatogr.*, 217 (1981) 81.
13 F. Poy, S. Visani and F. Terrosi, *J. High Resolut. Chromatogr. Chromatogr. Commun.*, 5 (1982) 355.
14 E. Loyola, M. Herraiz, G. Reglero and P. Martín-Alvarez, *J. Chromatogr.*, 398 (1987) 53.

15 G. Reglero, M. Herraiz, T. Herraiz and E. Loyola, *J. Chromatogr.*, 438 (1988) 243.
16 S. Nitz and E. Jülich, in P. Schreier (Editor), *Analysis of Volatiles, Proceedings of International Workshop, Würzburg, Germany, 1983*, Walter de Gruyter, Berlin, 1984, p. 151.
17 M. Herraiz, G. Reglero, E. Loyola and T. Herraiz, *J. High Resolut. Chromatogr. Chromatogr. Commun.*, 10 (1987) 598.
18 F. Poy and L. Cobelli, in P. Sandra (Editor), *Sample Introduction in Capillary Gas Chromatography*, Vol. 1, Hüthig, Heidelberg, 1985, p. 93.
19 S. Nitz, F. Drawert and E. Jülich, *Chromatographia*, 18 (1984) 313.
20 M. Herraiz, G. Reglero and T. Herraiz, *J. High Resolut. Chromatogr.*, 12 (1989) 442.
21 J. Staniewski and J.A. Rijks, in P. Sandra (Editor), *Proceedings of the 13th International Symposium on Capillary Chromatography*, Hüthig, Heidelberg, 1991, p. 1334.
22 J. Villén, T. Herraiz, G. Reglero and M. Herraiz, *J. High Resolut. Chromatogr.*, 12 (1989) 633.
23 K. Grob, *J. High Resolut. Chromatogr.*, 13 (1990) 540.
24 F. Poy, *Chromatographia*, 16 (1982) 345.
25 J. Staniewski and J.A. Rijks, *J. Chromatogr.*, 623 (1992) 105.
26 J. Staniewski, H.-G. Janssen, C.A. Cramers and J.A. Rijks, *J. Microcol. Sep.*, 4 (1992) 331.
27 W. Spendley, G.R. Hext and F.R. Himsworth, *Technometrics*, 4 (1962) 441.
28 J.C. Berridge, *Anal. Chim. Acta*, 191 (1986) 243.
29 R.J. Fisher, *Food Technol.*, 43 (1989) 90.
30 J. Tabera, G. Reglero, M. Herraiz and G.P. Blanch, *J. High Resolut. Chromatogr.*, 14 (1991) 392.
31 G.P. Blanch, J. Tabera, M. Herraiz and G. Reglero, *J. Chromatogr.*, 628 (1993) 261.
32 D.E. Long, *Anal. Chim. Acta*, 46 (1969) 193.
33 S.N. Deming and S.L. Morgan, *Anal. Chem.*, 45 (1973) 278 A.
34 J. Villén, F.J. Señoráns, M. Herraiz, G. Reglero and J. Tabera, *J. Chromatogr. Sci.*, 30 (1992) 261.
35 J.A. Nedler and R. Mead, *Comput. J.*, 7 (1965) 308.

Journal of Chromatography, 648 (1993) 415–421
Elsevier Science Publishers B.V., Amsterdam

CHROM. 25 298

Continuous gas chromatographic monitoring of low concentration sample streams using an on-line microtrap

Somenath Mitra* and Chen Yun

Department of Chemical Engineering Chemistry and Environmental Science, New Jersey Institute of Technology, Newark, NJ 07102 (USA)

(First received November 24th, 1992; revised manuscript received May 4th, 1993)

ABSTRACT

An on-line microtrap was made by packing a few centimeter long narrow bore capillary tubing with an adsorbent. The sample stream containing the analytes is introduced into the GC column through the microtrap. The analytes are trapped in the microtrap as they flow through it, and can be desorbed by heating the microtrap using a pulse of electric current. The heating is done very rapidly, so that the "desorption pulse" is sharp enough to be an injection for the GC separation. Thus, the microtrap serves as a sample pre-concentrator as well as an injector. Continuous monitoring is done by making these injections at fixed intervals of time (every few seconds to every few minutes) and for each injection a chromatogram is obtained. In this investigation, microtrap characteristics have been studied and particular attention has been given to its sample trapping characteristics.

INTRODUCTION

Continuous, on-line analysis of chemical processes and environmental emissions at trace levels is an interesting and challenging problem. Many analytical techniques such as Fourier transform infrared spectrophotometry (FT-IR) and mass spectrometry have been used in such applications. Recently some chemical microsensors have also been developed to carry out this type of analysis. Gas chromatography is particularly important as an on-line analysis technique because of its ability to separate and detect the different components of a mixture.

The important feature of any continuous, on-line GC instrumentation is the sample introduction device, which is required to make automatic, reproducible injections. In chemical industries, process gas chromatography is done using multi-port sample valves as injectors. Valves can automatically make injections from a sample stream intermittently into a GC column. However, sample valves have certain limitations. Being mechanical devices, they tend to wear during extended operations. Another problem with sample valves is that they withdraw a small fraction of the sample stream for injection into the GC. The sample size that is injected into the GC is between a few microliters to a couple of milliliters. Injecting a larger sample quantity causes excessive band broadening and degrades chromatographic resolution. A small injection volume results in a small sample quantity and this limits sensitivity. For example, a sub parts per million (v/v) gaseous sample stream can not be effectively analyzed using valves. In many applications, especially in environmental monitoring, low concentrations are encountered and sample valves are found to be inadequate.

Analysis of dilute gaseous streams containing organic analytes such as stack emissions and

* Corresponding author.

0021-9673/93/$06.00

ambient air is carried out by concentrating the analytes from a large sample volume (several milliliters to a few liters). The concentration is done either cryogenically (as in whole air samples such as Tedlar bags and Canisters) or using an adsorbent. These procedures usually require separate sampling and analysis steps. So the measurements can not be done on-line in a continuous fashion.

To do real-time GC monitoring of trace level analytes, not only is it necessary to have an automated injection device but also a sample preconcentrator. In this paper we report the use of an on-line microtrap for the dual purpose of sample concentration and injection.

On-line microtrap

An on-line microtrap is made by packing a small diameter tubing with an adsorbent. The sample containing the analyte is introduced into the analytical column through the microtrap. The analytes are trapped in the microtrap and can be thermally desorbed by electrical heating. When the heating is rapid enough, the "desorption pulse" serves as an injection for the GC column. The different components separate and are analyzed by the detector. The mode of operation for continuous monitoring is that electrical/thermal pulses or injections are made at fixed intervals of time and corresponding to each injection, a chromatogram is obtained. Due to its small size and thermal mass, it heats and cools rapidly, and frequent injections can be made as long as the GC separation is completed. Since the amount of sample trapped in the microtrap is proportional to the concentration of the stream flowing in, the microtrap response is proportional to sample concentration.

The principle of the microtrap is similar to that of thermal desorption modulators reported in previous papers [1–5]. In these applications, the temperature of a small segment of a capillary column was thermally modulated to generate a modulation signal from the sample being eluted by the mobile phase. The modulations have been done at the head of the GC column [1–4], as well as, in the middle of two columns used in multi-dimensional chromatography [5]. The microtrap is more like a small sorbent trap, which is put on-line with the sample stream, and is operated at a fixed intervals of time. In short, the microtrap traps the sample for a period of time and then releases it as a desorption pulse.

In a previous paper the effect of capacity factor in thermal desorption modulators was described [1]. Some of the same concepts can be used in the case of the microtrap. Both adsorption and desorption processes play important roles in the on-line trapping/desorption involved in the continuous monitoring. The microtrap does not necessarily trap a hundred percent of the analytes, as some tend to breakthrough. The sample desorption from the stationary phase generates a positive concentration profile, and the immediate sample readsorption generates a negative concentration profile. Thus, a microtrap peak contains a positive and a negative part and an example is shown in Fig. 1. The time interval AD in Fig. 1 is the time taken by the sample to migrate through the microtrap. This is denoted as

$$t_b = (k + 1)\, L/u \qquad (1)$$

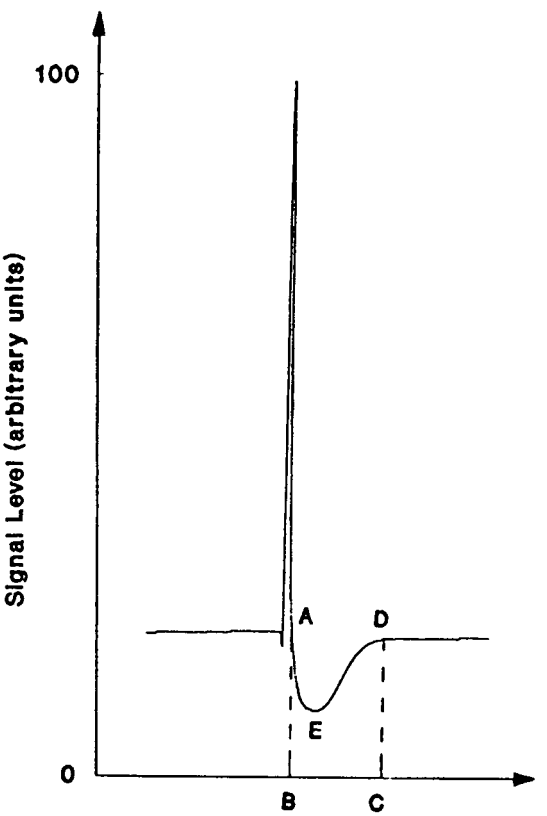

Fig. 1. Characteristic peak from a microtrap.

where L is the length of the microtrap, u is the flow-rate and k is the capacity factor of sample in the microtrap. As k increases, t_b increases, the negative peak becomes shallow and appears to merge with the baseline so that the chromatogram resembles a conventional chromatogram without a negative peak. The peak in Fig. 1 was obtained at a lower capacity factor so that the negative peak was exaggerated.

In this investigation, a microtrap has been developed for continuous, on-line analysis of somewhat volatile organic compounds. The microtrap characteristics have been studied and particular attention has been given to its sample trapping abilities.

EXPERIMENTAL

The experimental system is as shown in the Fig. 2. The sample stream was generated by entraining the analytes from a diffusion cell into a flow of nitrogen. The analyte concentrations was controlled by changing the capillary diameter and the height of the liquid level in the diffusion capillary [6]. The concentration of the stream was predicted using diffusion equations published by Savitsky and Siggia [6]. The concentration of the analytes was maintained between a few ppm to ppb level (on a volumetric basis). Although a variety of compounds have been used in the laboratory, data using benzene, toluene, xylene and hexane have been presented in this paper. The choice of these compounds was arbitrary.

A Hewlett-Packard GC (Model 5890) equipped with a flame ionization detector was used in this study. A megabore, DB-624 column (J&W Scientific, Folsom, CA, USA) with a 3-μm stationary phase was used for separation. The microtrap was made by packing a 23 gauge (0.33 mm I.D.) stainless-steel tubing (Hamilton, Reno, NV, USA) with Carbotrap C (Supelco, Supelco Park, PA, USA). The microtrap was heated by passing current directly through the walls of the metal tubing. Modulators were also made by packing 0.53 mm I.D. deactivated fused-silica tubing with Carbo Trap C. The fused-silica microtrap was externally coated with electrically conductive paint and could be heated by passing current through it. The current through the cool microtrap can be between 5 and 10 A, but as it heats up its resistance increases and the current is reduced. More details about the resistive heating process can be found elsewhere [3,4]. Power resistors were put in series with the microtrap to control the current through it. The injections were controlled by the personal computer (IBM compatible) using the digital output of the analog-to-digital converter (DAS8-PGA, Metrabyte, Elmwood Park, NJ, USA) and electronic switch (OAC5P, Opto 22, Huntington Beach, CA, USA). The microtrap was heated by turning on the current for a prespecified duration and at fixed intervals of time. The interval between injections were anywhere between 5 and 300 s. The duration for which the current was turned on was between 100 and 1000 ms. Since the microtrap heats up and cools down in 1 or 2 s, it is difficult to accurately measure the exact heating rate and the final temperature. A measurement using a thermocouple showed that temperature as high as 300°C can be obtained in fraction of a second.

The data acquisition was also done using the analog-to-digital converter and the personal computer. A computer program was written in Quick Basic for making injections as well as data acquisition.

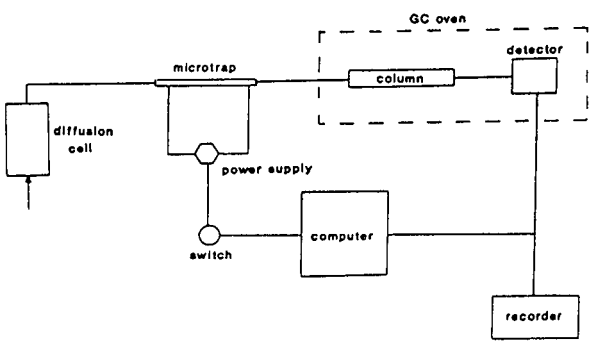

Fig. 2. Schematic diagram of the experimental system.

RESULTS AND DISCUSSION

On-line analysis

The operation of the continuous analysis system is demonstrated by continuously monitoring a stream containing benzene, toluene and

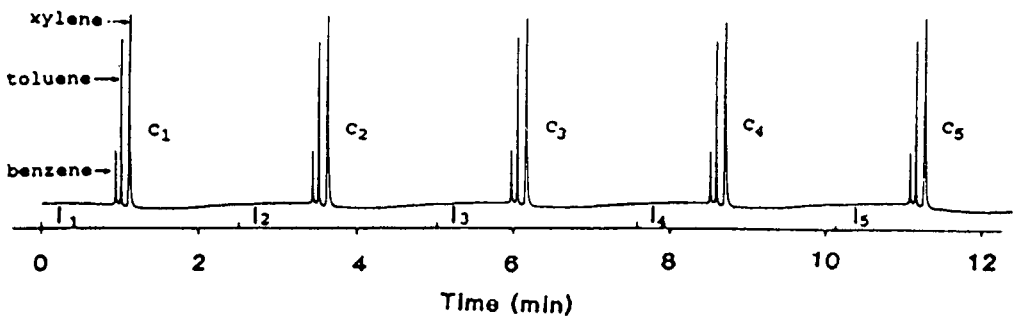

Fig. 3. Continuous monitoring of a stream containing ppb (v/v) levels of benzene, toluene and xylene using a 6.5 cm long fused-silica microtrap at 22°C. Corresponding to each injection I_1, I_2,I_3 . . . a chromatogram C_1,C_2,C_3 . . . was obtained. The microtrap current was turned on for 500 ms. The column flow-rate was 7.9 ml/min and temperature was 180°C.

xylene. The injection from a microtrap was similar to that from an injection port or an injection valve. A series of injections were made and corresponding to each injection a chromatogram containing the three peaks were obtained. A section of the recorder output is shown in Fig. 3. In Fig. 3, the capacity factor was such that negative peak disappeared. Some of the characteristics of the chromatograms are presented in Table I. An injection of the same compounds was also made using the split/splitless capillary injection port of the GC and comparative results at similar retention time are presented in Table I. Each quantity in Table I is based on five separate measurements.

Reproducibility of retention time as well as peak height was very good for the microtrap and was comparable to that of the injection port. The microtrap also produces sharp peaks and at the same retention time, the terminal band length (measured as the length of the solute zone emerging from the end of the column [7]; equivalent to four times the standard deviation) is somewhat smaller for the microtrap than for the injection port. This is to be expected, because there is practically no dead volume in the microtrap. In continuous GC monitoring, the goal is to make injections as frequently as possible. Since the microtrap has short heating/cooling cycle, the time needed for separation in the column becomes the limiting factor. As a result, the column conditions may be optimized for speed rather than efficiency.

The GC analysis in Fig. 3 was done isothermally. The heating/cooling of the column in a conventional GC oven is relatively slow and can not keep up with the injection frequency used in this study. Conceptually, temperature-programmed separation is feasible if the column temperature control system is designed for this application.

Trapping efficiency. The microtrap operation

TABLE I

COMPARISON OF MICROTRAP WITH INJECTION PORT

	Microtrap			Injection port		
	Benzene	Toluene	*p*-Xylene	Benzene	Toluene	*p*-Xylene
Retention time (s)	57.38	61.85	68.41	56.27	62.22	70.97
% R.S.D. of retention time	0.22	0.23	0.20	0.13	0.17	0.16
% R.S.D. of peak height	1.14	0.97	1.46	1.60	1.50	2.90
Band duration[a] (s)	0.76	0.78	1.12	0.80	1.00	1.20
Terminal band length[a] (mm)	385.09	365.74	475.62	411.30	467.02	490.38

[a] Measured at half height.

is somewhat different from conventional sorbent traps, which are normally much larger in size and are seldom used in a continuous operation. A microtrap has low capacity and may trap only a fraction of the sample flowing through it. However, it is desirable that the microtrap accumulate as much sample as possible before making an injection so that a large signal can be obtained at the detector. Moreover, the untrapped sample breaks through the microtrap and contributes to the detector background. Trapping efficiency of the microtrap is defined as the fraction of the incoming sample retained by the microtrap before a injection is made:

$$\text{Trapping efficiency } (T) = \frac{\text{sample retained}}{\text{sample entering microtrap}} \quad (2)$$

The retention mechanism in a microtrap is similar to that of a GC column. There is an equilibrium between the concentration of the sample in the stationary and the mobile phase. The injections are normally made at fixed intervals of time (referred to as injection interval). So trapping efficiency,

$$T = \frac{t_b M_s}{t_i M_t} \quad (3)$$

$$T = \frac{t_b M_s}{t_i (M_s + M_m)} \quad (4)$$

where, M_s is the amount of sample trapped per unit time in the stationary phase, M_t is the sample amount per unit time flowing into the microtrap, M_m is the amount of sample per unit time that remains in mobile phase and t_i is the injection interval. Thus the above equation reduces to:

$$T = (t_b/t_i)k/(k+1) \quad (5)$$

If the injections are made very frequently such that $t_i < t_b$ then the microtrap accumulates sample only for t_i and eqn. 5 becomes:

$$T = k/(k+1) \quad (6)$$

Thus in this case T depends only upon k and does not change with the injection interval t_i. If injection interval is large and $t_i > t_b$ then trapping efficiency is given by eqn. 5 and T is inversely proportional to t_i.

The trapping efficiency can be computed from the microtrap response such as in Fig. 1. The sample retained by the microtrap is proportional to the area under curve AED. The total sample flowing into the microtrap is equal to the area ABCD. The experimentally determined trapping efficiency as a function of injection interval (t_i) is presented in Fig. 4. When injection interval is less than t_b, as predicted by eqn. 6, the trapping efficiency is constant. When the interval is increased higher than t_b the trapping efficiency begins to decrease.

Factors effecting microtrap response

The value of t_b is an important microtrap characteristic and is given by eqn. 1. For a given analyte and microtrap packing, the temperature determines the capacity factor and in turn t_b. Variation of maximum trapping efficiency (corresponding to the flat portion of Fig. 4) and t_b with temperature is presented in Fig. 5. The trapping efficiency decreases with increase in microtrap temperature and its decrease closely parallels

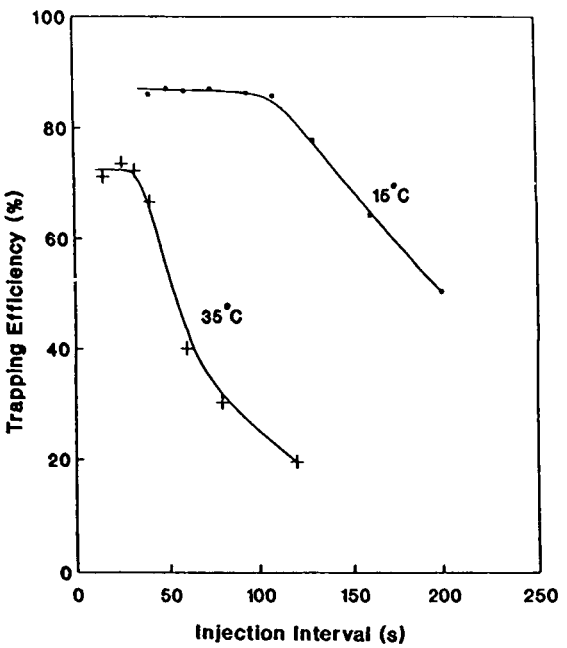

Fig. 4. Trapping efficiency as a function of injection interval. A 6 cm long fused-silica microtrap was used with hexane as the sample. The microtrap current was turned on for 500 ms.

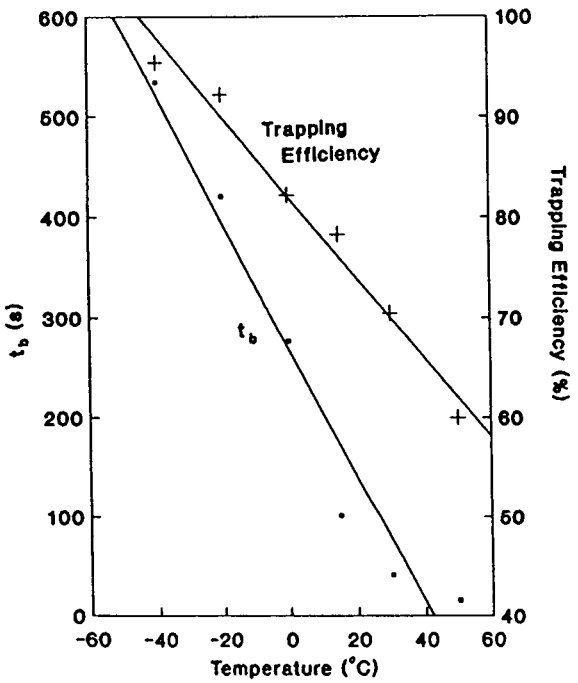

Fig. 5. Dependence of trapping efficiency and t_b of hexane on microtrap temperature. A 6 cm long fused-silica microtrap at a flow-rate of 8.1 ml/min was used. The microtrap current was turned on for 500 ms.

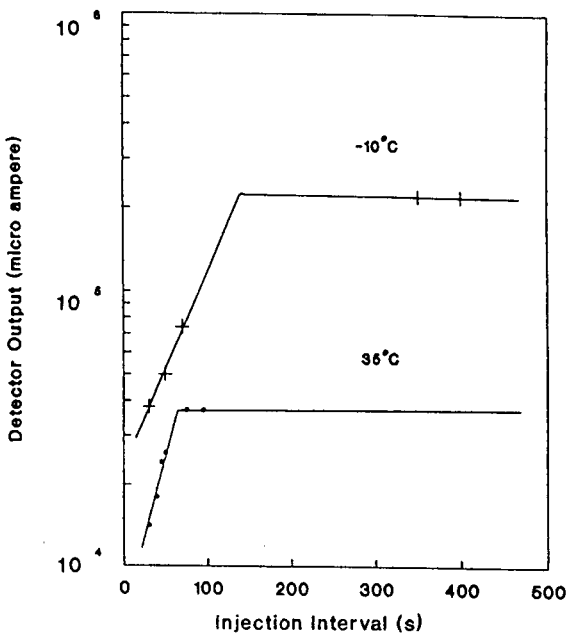

Fig. 6. Microtrap response as a function of injection interval at − 10°C and 35°C. Hexane was used as the analyte and a 5.5 cm long fused-silica microtrap at a flow-rate of 4.7 ml/min was used. The microtrap current was turned on for 500 ms.

that of t_b. This is to be expected because at a certain capacity factor, the trapping efficiency is directly proportional to t_b (eqn. 5). In fact, if T and t_b are plotted against one another, a linear relationship is obtained. The decrease in trapping efficiency and t_b with temperature may be approximated by linear relationships.

One of the factors that need to be taken into consideration during continuous operations is at what frequency the microtrap is to be operated. Making injections very often offers the advantages of obtaining information more often, but may have other disadvantages such as lower sensitivity and not enough time for chromatographic separation. It should be realized that the microtrap can not hold the sample very long. The sample trapping characteristics of a microtrap can be studied by operating the microtrap at different injection intervals. In Fig. 6 as we increase the injection interval, the sample accumulated by the microtrap increases and thus a larger peak is obtained. However, once the interval equals t_b, the sample begins to break through and the response cannot be increased further by increasing the injection interval. So the response profile involves a linear increase in microtrap response upto t_b followed by a constant response beyond t_b.

The microtrap temperature strongly effects the microtrap response. Due to higher trapping efficiency at a lower temperature, a larger desorption peak is generated from the microtrap, *i.e.*, sensitivity is increased. For example, at injection interval of 50 s (Fig. 6), the microtrap response at − 10°C is more than twice that at 35°C. The longer t_b at lower temperature also allows the microtrap to trap sample for a longer period of time. For a continuously flowing sample, this translates to larger sample accumulation in the microtrap and consequently higher sensitivity. Due to the dual effect of higher trapping efficiency and longer t_b, the maximum attainable response at − 10°C is nearly six times higher than that at 35°C. In short, the increase in sensitivity at lower microtrap temperature is observed

whether the injection interval is longer or shorter than t_b.

There may be certain limitations to lowering the temperature to very low values because some components may adsorb so strongly that they can not be desorbed from the microtrap. In practice one has to optimize the temperature for the analytes of interest. For example in Fig. 3, 22°C was appropriate for the sample studied and no sub-ambient cooling was necessary. However, sub-ambient cooling could be used to increase the sensitivity and to lower the detection limit. Moreover, since the microtrap response varies with temperature, it needs to be controlled carefully during extended periods of continuous operation. A change in temperature would require recalibration of the system as the sensitivity would change.

Linearity of the calibration curve is also an important consideration for on-line measurements. In this system, the linearity of the microtrap has to be taken into account. Conceptually, the retention characteristics of microtraps has been explained using theories of partition chromatography. The amount of sample trapped by the microtrap is theoretically proportional to concentration of sample flowing through it. The microtrap generated linear response in the ppm (v/v) to ppb (v/v) concentration range.

An important feature of the on-line microtrap is that the sample continuously flows through the system, *i.e*, sampling is done continuously and the microtrap produces a time-averaged response over the injection interval. So, if a large concentration spike was to occur between two injections, a microtrap would still be able to identify it. This is an advantage over monitoring devices that sample intermittently.

CONCLUSIONS

Due to the preconcentration effect, the on-line microtraps are able to continuously monitor low concentration sample streams. Their small size and thermal mass make them very fast and responsive devices, and the analysis can be done every few seconds as long as GC separation can be achieved within that time. The microtrap response is stable during long periods of operation and precision is comparable to other injection devices.

REFERENCES

1 S. Mitra and J.B. Phillips, *J. Chromatogr. Sci.*, 26 (1988) 620.
2. J.B. Phillips, D. Luu and J.B. Pawliszyn and G.C. Carle, *Anal. Chem.*, 57 (1985) 2779.
3 S. Mitra and J.B. Phillips, *Anal. Instrum. (N.Y.)*, 18 (1989) 127.
4 Z. Liu and J.B. Phillips, *J. Microcolumn Sep.*, 1 (1989) 250.
5 Z. Liu and J.B. Phillips, *J. Chromatogr. Sci.*, 29 (1991) 227.
6 A.C. Savitsky and S. Siggia, *Anal. Chem.*, 44 (1972) 1712.
7 W.L. Saxton, *J. High Resolut. Chromatogr. Chromatogr. Commun.*, 7 (1984) 118.

Journal of Chromatography, 648 (1993) 423–431
Elsevier Science Publishers B.V., Amsterdam

CHROM. 25 323

Analysis of chlorofluorocarbon replacement compounds by capillary gas chromatography

G.A. Sturrock*, P.G. Simmonds and G. Nickless

Biogeochemistry Centre, University of Bristol, Cantock's Close, Bristol BS8 1TS (UK)

D. Zwiep

Chrompack International B.V., P.O. Box 8033, 4330 EA Middelburg (Netherlands)

(First received March 9th, 1993; revised manuscript received May 12th, 1993)

ABSTRACT

Several thick film wall-coated open tubular and porous-layer open tubular (PLOT) type capillary columns have been investigated for the separation of wide boiling range (−57.8 to 61.2°C) of hydrofluorocarbons (HFCs) and halocarbons. The aim is to select the best column in terms of resolution, analysis time and conditions suitable for use in conjunction with an automated air analysis method for these compounds which are intended as replacements for the ozone-depleting chlorofluorocarbons. The problems associated with each column are reported with emphasis on the catalytic activity of two types of alumina PLOT columns towards certain HFCs and halocarbons. Due to their inherent basicity, the alumina PLOT columns induce dehydrochlorination reactions in spite of the additional deactivation of the alumina with KCl and Na_2SO_4.

INTRODUCTION

The use of many fully halogenated compounds is restricted by international agreement because chlorine has been linked to the destruction of stratospheric ozone [1]. Concern over the global environmental consequences of chlorofluorocarbons (CFCs) has lead to the development of alternative compounds [2]. Candidate replacements are composed of either carbon, hydrogen and fluorine (hydrofluorocarbons or HFCs) or carbon, hydrogen, chlorine and fluorine (hydrochlorofluorocarbons or HCFCs). For simplicity, both classes of compounds are referred to here as HFCs. The HFCs, unlike CFCs, are destroyed by reaction with atmospheric hydroxyl radicals due to the presence of the more labile carbon to hydrogen bond. This occurs principally in the troposphere —thus reducing the amount of chlorine radicals entering the stratosphere and the loss of ozone [3]. However, a portion of the emitted HFCs will eventually reach the stratosphere and with large estimated global release they will add substantially to the chlorine content of the stratosphere. More importantly, HFCs are highly effective absorbers of infrared radiation and their unrestrained use would contribute eventually to global warming [4]. Thus, it is vital to be able to identify and quantify individual HFCs and other halocarbons to assess their rates of accumulation. Any monitoring technique will require the separation of all HFCs with high resolution to allow correct identification and accurate quantitation.

Most early gas chromatographic analyses of volatile compounds in air have been performed on packed columns due to the ease of sample introduction and the advantageous phase ratio of this type of column. However, very volatile compounds (boiling point <150°C) can also be

* Corresponding author.

0021-9673/93/$06.00

analysed by capillary gas chromatography due to the development of both thick-film wall-coated open tubular (WCOT) and high-capacity porous-layer open tubular (PLOT) columns [5]. Specialized packed columns and combination packed columns, operated in series, have been described for the analysis of complex CFC and HFC mixtures [6,7]. In this paper, several types of capillary columns are evaluated in conjunction with a flame ionization detector for the analysis of volatile HFCs and halocarbons, both qualitative and quantitative observations are reported.

PLOT columns with aluminium oxide-coated fused-silica stationary phases have proved very suitable for GC separation of volatile organic compounds such as C_1–C_{10} hydrocarbons [8–10] and C_1–C_2 halocarbons [11]. However, without additional deactivation, the activity of the alumina surface causes peak tailing and the retention mechanism is very sensitive to the water content of the carrier gas. These adverse effects are reduced either by KCl or Na_2SO_4 deactivation of the alumina phase. Previous work has shown that the alumina/KCl PLOT column [12] and packed alumina columns [13] induce catalytic dehydrohalogenation of some halogenated compounds, due to the basicity of the alumina, which is enhanced by the presence of water or chlorine, thus forming a strong Brönsted acid. This catalytic activity, which is most efficient at the maximum operating temperature of the columns (200°C), may abstract HCl molecules from the HFCs —forming carbonium ions and subsequent reaction byproducts. The alumina/KCl column, already known for its destruction of HFC 22 [14], was also found in the experiment described below, to destroy CH_3Cl. Additional HFC's were also found to be destroyed on the alumina/Na_2SO_4 PLOT column, especially at elevated temperatures. The suspect HFCs were examined by comparison of their peak areas after separation on a WCOT CP Sil-5 CB (inert) column and on the alumina PLOT columns —to ascertain the suitability of these columns in the analysis of HFCs. Any decomposition of HFCs obviously restricts the use of these alumina PLOT columns despite the excellent baseline resolution of the HFC's from other ubiquitous halocarbons, CFCs and potentially interfering trace atmospheric gases.

To avoid any complications provided by the activity of the alumina towards volatile organic compounds [15], the utilization of porous polymers as packing materials [16] is now widespread in GC. Therefore, an assessment of the separation capabilities of three PoraPLOT columns (Q, S and U) was included in this study. PoraPLOT columns are conventional fused-silica PLOT capillary columns coated with styrene–divinylbenzene copolymers of different surface areas and polarities. The adsorbent is deposited onto the column as a thin layer of between 5–20 μm and achieves higher resolving power over the standard Porapak packed column [17]. These columns provide high selectivity for volatile compounds, short analysis times and good reproducibility. Their relative non-sensitivity to oxygen and water, and maximum operating temperature of 250°C are advantageous in temperature programming. Their principal disadvantages are their relatively long retention times for higher boiling compounds and bleed at elevated temperatures which complicates their use in GC–MS applications.

Three WCOT CP-Sil CB columns (CP-Sil 5 CB, 13 CB and 19 CB) were also studied to assess their separating ability for various HFC–halocarbon mixtures. These WCOT columns are again superior to packed columns due to greater inertness, longer life, shorter retention times, lower bleed, higher efficiencies and greater reproducibility. The stationary phase is a mixture of different chemically bonded siloxanes, allowing a variation in column polarity and selectivity. The simultaneous determination of polar and non-polar low-molecular-mass compounds has been demonstrated on these columns [18], but limited data is available on the behaviour of these columns relative to the resolution of HFCs. Earlier tests on the CP-Sil 5 CB column gave incomplete baseline resolution of the most volatile HFCs —even at a column temperature of 30°C. The two alternative CP-Sil 13 CB and 19 CB columns exhibit slightly greater polarity which it is hoped would enhance the resolution of the HFCs.

EXPERIMENTAL

Reagents and materials

Individual HFCs and CFCs investigated in the study are listed with their boiling points, structures and molecular mass in Table I. Individual HFC standards were prepared by dilution with nitrogen of pure standards supplied by ICI Chemicals (Runcorn, UK) in deactivated stainless steel canisters; 13B1 and CH_3Cl were purchased in lecture bottles (BDH, Poole, UK); 12B1 (BCF) from a fire extinguisher, CH_2Cl_2 and $CHCl_3$ as headspace from liquids (Aldrich, Gillingham, UK) and methane gas from the natural gas supply in the laboratory (% CH_4 in natural gas supply is 93% from independent experiment). Hydrogen, air and oxygen free nitrogen (BOC, Guildford, UK) were used for the flame ionization detector. The column carrier gas was purified helium (BOC).

Chromatographic conditions

The experiments were carried out on a CP 9000 gas chromatograph (Chrompack, Middelburg, Netherlands) with a flame ionization detector at 200°C and an injection temperature of 150°C. The columns, supplied by Chrompack, are shown in Table II. A helium carrier gas flow-rate of *ca.* 2 ml/min was used on the narrow-bore (0.32 mm I.D.) columns and *ca.* 5 ml/min on the wide-bore (0.53 mm I.D.) columns.

Individual HFCs and methane were injected at a series of different isothermal column temperatures. Syringe injections of 100 μl of halocarbons were made for narrow-bore columns using a 500-μl gas-tight Hamilton syringe. A sample loop of 50 μl and valve injection system was incorporated for the wide bore PoraPLOT S column. Columns were operated isothermally over a range of temperatures and with temperature programming. The isothermal retention data was used for the optimization of the various temperature-programmed gas chromatograph separations of the prepared HFC standard mixture, shown in Table III, on the PoraPLOT and Alumina PLOT columns. Temperature programming was not required on the WCOT columns.

Temperature programmes (TPs). TP 1: 40°C (3 min) 9°C/min; 85°C (3 min) 10°C/min; 140°C. A faster temperature gradient could be included at the end of the programme for the alumina PLOT columns to elute the less volatile CH_2Cl_2, HFC 123 and $CHCl_3$ in a more reasonable analysis time, so the following were used: TP 2: 30°C (3 min) to 180°C at 10°C/min, and TP 3: 40°C to 180°C at 10°C/min. However, the least volatile compounds are obscured by the greater column bleed on the alumina/Na_2SO_4 PLOT column at these higher temperatures.

Several olefins (ethene, propene, *n*-butene and pentene), CFCs (11, 12 and 113) and CH_3CCl_3 and CCl_4 (all ubiquitous in ambient air samples) were included in the temperature programmed analyses to see if they coeluted with any of the HFCs under study.

Analysis of a standard HFC mixture, containing HFCs as shown in Table III up to and including compound 12B1, on the WCOT columns at isothermal temperature was obtained for comparison of peak areas to assess the losses of the susceptible HFCs on the alumina PLOT columns. Examples of the separations of the HFCs obtained on all the columns are shown (Figs. 1–4).

TABLE I

COMPOUND DESCRIPTION

Trade name	Compound	Boiling point (°C)	Molecular mass
13B1	CF_3Br	−57.9	148.87
125	CF_2HCF_3	−48.8	120.02
143a	CF_3CH_3	−47.6	84.04
22	$CHClF_2$	−40.8	86.47
12	CF_2Cl_2	−29.8	120.00
134a	CH_2FCF_3	−25.9	102.03
40	CH_3Cl	−24.0	50.49
124	CF_3CFHCl	−11.8	136.48
142b	CH_3CF_2Cl	−9.8	100.50
12B1	$CBrClF_2$	−4.0	165.33
123	CF_3CHCl_2	20.0	152.93
11	$CFCl_3$	23.6	136.00
30	CH_2Cl_2	40.0	84.94
113	$CF_2ClCFCl_2$	47.7	186.00
20	$CHCl_3$	61.2	119.39

TABLE II

DESCRIPTION OF COLUMN TYPES

(A) Alumina PLOT columns			
Column type	PLOT-fused-silica		
Column length	50 m		
Stationary phase	Alumina (Al_2O_3)		
Deactivation by	(1) KCl;	(2) $NaSO_4$	
Film thickness (μm)	5.00	5.00	
I.D. (mm)	0.32	0.32	
O.D. (mm)	0.43	0.43	
(B) PoraPLOT columns			
Column type	PLOT fused-silica		
Column length	27.5 m × 2.5 m inclusive particle trap		
Stationary phase[a]	PoraPLOT Q	PoraPLOT S	PoraPLOT U
Surface area/m^2/g	582	460	366
Polarity	2.0	3.5	7.0
Film thickness (μm)	10	20	10
I.D. (mm)	0.32	0.53	0.32
O.D. (mm)	0.43	0.70	0.43
(C) WCOT columns			
Column type	WCOT fused-silica		
Column length	50 m		
Stationary phase	CP-Sil 5 CB	CP-Sil 13 CB	CP-Sil 19 CB
Chemical composition			
Dimethyl siloxane	100%	86%	85%
Phenyl siloxane		14%	7%
Cyanopropyl siloxane			7%
Vinyl siloxane			1%
Film thickness (μm)	5.00	2.50	2.50
I.D. (mm)	0.32	0.32	0.32
O.D. (mm)	0.43	0.43	0.43

[a] PoraPLOT Q = Styrene–divinylbenzene; PoraPLOT S = divinylbenzene–vinylpyridine; PoraPLOT U = divinylbenzene–ethyleneglycol–dimethylacrylate.

TABLE III

HFC STANDARD MIXTURE

Trade name	Volume (μl) in 100 ml	nmol/μl	μg/μl
13B1	400	0.179	26.583
125	100	0.045	5.358
143a	100	0.045	3.752
22	200	0.089	7.721
134a	100	0.045	4.555
40	100	0.045	2.254
124	100	0.045	6.093
142b	100	0.045	4.487
12B1	400	0.179	29.523
123	200	0.089	13.654
30	1000	0.446	37.920
20	1500	0.670	79.949

RESULTS AND DISCUSSION

The reproducibility of the retention times in both isothermal and temperature programmed analyses proved to be excellent for all the alumina/PLOT, PoraPLOT and WCOT columns studied. Data shown in Table IV.

Alumina/KCl PLOT and alumina/Na_2SO_4 PLOT capillary columns

Extensive hydrogen bonding was observed between the HFCs and the alumina PLOT columns which increases the retention of HFCs on these columns and alters their elution order from following the boiling point order exactly. The greatest increase in retention time is observed with HFC 125 and 124 and is probably due to the

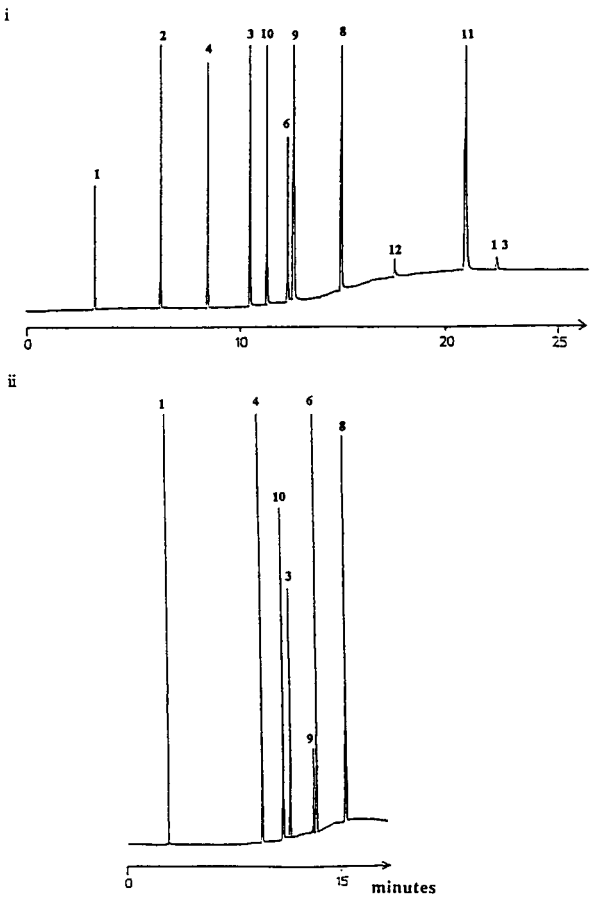

Fig. 1. Separation of HFC Standard mixture. Temperature programme: 40 to 180°C at 10°C/min. (i) Column: 50 m × 0.32 mm I.D. alumina/KCl PLOT; carrier gas: 100 kPa helium. (ii) Column: 50 m × 0.32 mm I.D. alumina/Na_2SO_4 PLOT; carrier gas: 120 kPa helium. Peak identification (also for all subsequent chromatograms): 1 = CH_4; 2 = 13B1; 3 = HFC 125; 4 = HFC 143a; 5 = HFC 22; 6 = HFC 134a; 7 = CH_3Cl; 8 = HFC 124; 9 = HFC 142b; 10 = 12B1; 11 = HFC 123; 12 = CH_2Cl_2; 13 = $CHCl_3$.

TABLE IV

REPRODUCIBILITY OF RETENTION TIMES FOR HFC 125 AND HFC 134

Compound	Column type	Conditions	Retention times (min) ($n = 6$)
125	Alumina/KCl	T.P. 2	14.35 ± 0.03%
	PoraPLOT Q	T.P. 1	6.35 ± 0.07%
	CP Sil 13 CB	40°C	4.74 ± 0.07%
134a	Alumina/KCl	T.P. 2	16.25 ± 0.04%
	PoraPLOT Q	T.P. 1	7.86 ± 0.09%
	CP Sil 13 CB	40°C	4.79 ± 0.08%

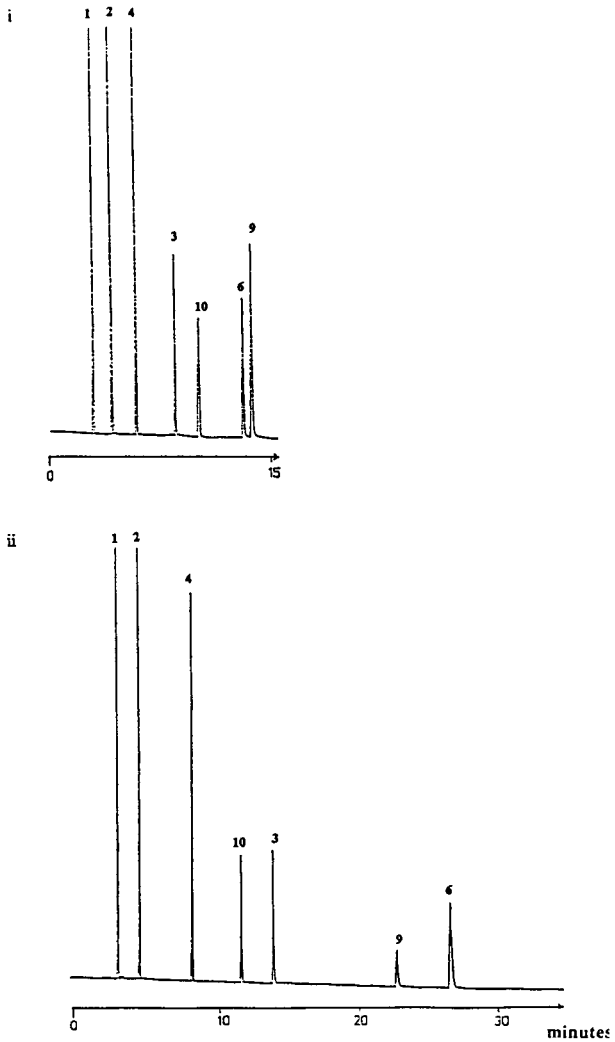

Fig. 2. Separation of HFC standard mixture up to and including compound 12B1 at 100°C, showing dehydrohalogenating effects on (i) alumina/KCl PLOT; carrier gas: 90 kPa helium; and (ii) alumina/Na_2SO_4 PLOT; carrier gas: 120 kPa helium.

presence of a lone polarisable hydrogen atom. Compounds 13B1 and 12B1, containing no hydrogen atoms, are the least retained compounds on both alumina columns with only HFC 143a eluting before 12B1 on the alumina/Na_2SO_4 PLOT at 100°C.

In addition to HFC 22 —already known to be dehydrohalogenated by the alumina/KCl PLOT column, CH_3Cl was progressively destroyed with increasing column temperatures. This resulted in the complete loss of response to CH_3Cl in all

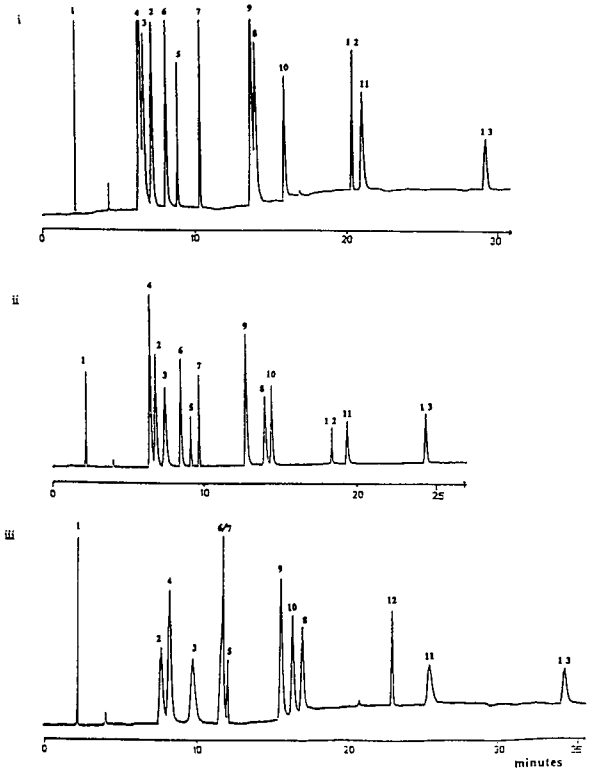

Fig. 3. Separation of HFC standard mixture on PoraPLOT columns. Temperature programme: 40°C (3 min) to 85°C at 9°C/min, 85°C (3 min) to 140°C at 10°C/min. (i) PoraPLOT Q; carrier gas: 65 kPa; (ii) PoraPLOT S; carrier gas: 25 kPa; and (iii) PoraPLOT U; carrier gas: 65 kPa.

temperature programmes. Similarly on the alumina/Na_2SO_4 PLOT column, both compounds HFC 22 and CH_3Cl are destroyed, and in addition HFC 142b is also partially dehydrohalogenated, especially at higher temperatures. The inherent basicity of the alumina stationary phase causes dehydrochlorination of certain HFCs probably leading to the formation of the corresponding unsaturated material. The extent of this breakdown varies according to the substituents on the carbon atoms, the more polar compounds having the highest tendency to undergo dehydrochlorination.

The stability factor K_s [15] is a measure for the inertness of a compound with respect to the reactivity of the alumina stationary phase and is expressed as:

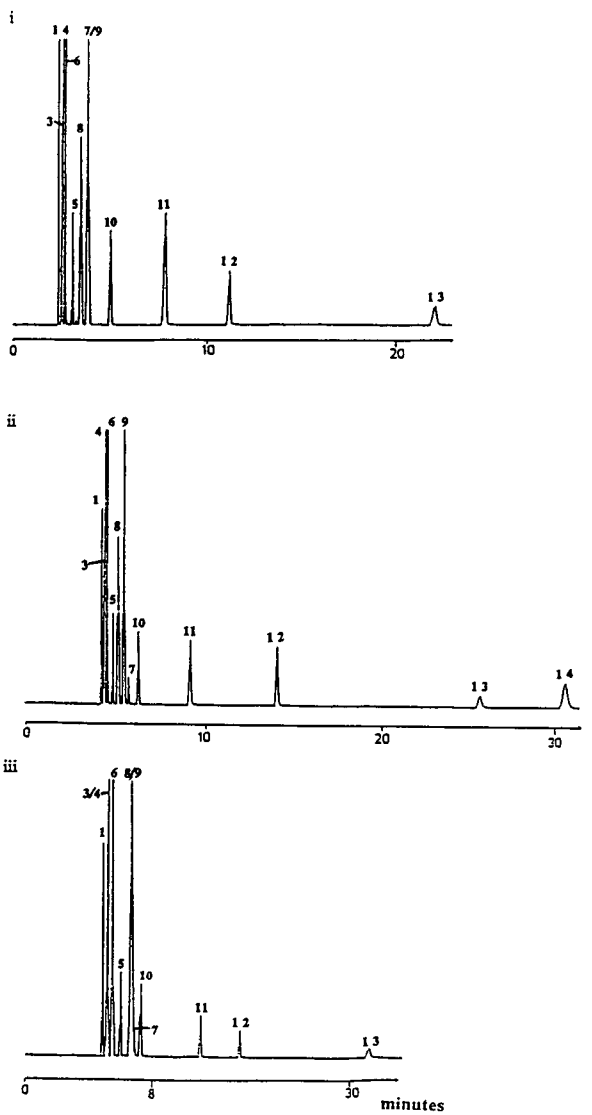

Fig. 4. Separation of HFC standard mixture on CP Sil CB columns at 40°C on (i) CP Sil 5 CB; carrier gas: 100 kPa; (ii) CP Sil 13 CB; carrier gas: 70 kPa; additional peak 14 = CH_3CCl_3; and (iii) CP Sil 19 CB; carrier gas: 70 kPa.

$$K_s = \frac{(A_j/A_s)_2}{(A_j/A_s)_1}$$

where A is the peak area of the respective HFC (j) and internal standard (s) for the CF Sil-5 CB column (1) and the alumina PLOT column (2). Irreversible adsorption or catalytic decomposition on the alumina PLOT column is indicated by $K_s = 0$ and no catalytic reactivity is indicated

by values close to unity. A comparison of the K_s values of several compounds are listed in Table V for the alumina/Na_2SO_4 PLOT column at various temperatures compared against the WCOT CP Sil-5 CB column, where no dehydrohalogenation occurs.

From Table V it is clear that the fluorine substituted HFCs (143a, 125 and 134a) all have K_s values close to unity and are therefore unaffected by the catalytic activity of the alumina phase. Similarly, the fully halogenated 12B1 is stable. Subsequent experiments have shown this is also true for all fully halogenated compounds. The compounds specifically affected are HFC 22, 142b, 123 [19] and CH_3Cl. Peaks corresponding to HFC 22 and CH_3Cl are absent on the alumina/Na_2SO_4 PLOT column and a significant decrease in the area of HFC 142b is also found as the temperature increases. Surprisingly HFC 124, which could potentially be dehydrochlorinated, appears to be stable [19].

Isothermal operation of the columns above 100°C is required for the elution of the higher boiling HFC 124 in a reasonable time and with good peak shape. The separation of all the compounds of interest is obtained on both alumina PLOT columns with high chromatographic resolution, and there is almost no coelution with other atmospheric CFCs. Isothermal operation below 100°C, although suitable for the most volatile compounds, causes severe peak broadening for compounds with boiling points greater than −10°C. However, despite the excellent peak resolution achieved, the dehydrohalogenating activity of these Alumina columns at elevated temperatures restricts their use to the fully halogenated and fluorine-substituted HFCs. It would, of course, still be possible to use multidimensional chromatography where the alumina PLOT column is used to resolve the stable HFCs, and a thick film WCOT column is used in the analysis of a wide boiling range of HFC and halocarbon mixtures, containing compounds specifically susceptible to dehydrochlorination.

TABLE V

STABILITY FACTORS (K_s) FOR CERTAIN HFCs ON THE ALUMINA/Na_2SO_4 PLOT COLUMN AT VARIOUS TEMPERATURES

HFC	Temperature (°C)					
	95	105	115	125	TP2	TP3
143a	0.95	1.01	0.93	0.94	0.98	1.03
12B1	1.07	1.22	1.08	1.14	1.14	0.93
125	0.93	1.02	0.93	0.94	0.99	1.07
142b	0.52	0.43	0.35	0.26	0.13	0.000025
134a	0.89	0.98	0.90	0.90	0.93	0.94
124	–	0.97	0.88	0.91	0.95	1.01
22	0.00	0.00	0.00	0.00	0.00	0.00
CH_3Cl	0.00	0.00	0.00	0.00	0.00	0.00

PoraPLOT columns

Both molecular mass and boiling point govern the separation of the HFCs and halocarbons on PoraPLOT columns, although the polarity of the sorbate and sorbent appear to be of some influence —this becoming more apparent on PoraPLOT S and U columns. The elution order and retention times can be explained by taking into account a compound boiling point along with its molecular size and possible surface interactions with the PoraPLOT stationary phase.

Surface area effect. The effect of interaction between the porous polymer surface and compound molecular size is especially prominent for compounds 13B1 and 12B1. These two compounds are essentially non polar and do not contain a polarisable hydrogen atom so any polarity effects can be ignored. Therefore, the retention of these compounds is governed by interaction of the large bromine group with the polymer surface. For PoraPLOT Q, which has the largest surface area, 13B1 is retained for longer than both the higher boiling, less volatile HFC 125 and 143a. For PoraPLOT S, 13B1 elutes between HFC 143a and 125; while on PoraPLOT U, 13B1 elutes first and the elution order follows increasing boiling points. Therefore, on PoraPLOT U, surface interaction with the large bromine atom does not appear to occur indicating a smaller surface area for this polymer type. This clearly demonstrates the reduction in polymer surface area of the PoraPLOT columns *i.e.* Q > S > U. 12B1 also contains a single

bromine atom and is less retained on the PoraPLOT U than on both the PoraPLOT Q and S columns, clearly shown by the reversal in elution order of HFC 124 and 12B1. Thus, the inclusion of a larger bromine atom in a compound will increase that compound's retention time relative to those of similar volatility due to a surface area interaction provided there is a similarity in compound size and stationary phase pore size.

Polarity effect. From all the results, it can be seen that the compounds containing a single polarisable hydrogen, HFCs 125, 22, 124 and 123, are retained longer on all the PoraPLOT columns than the compounds of similar volatility in the series studied. This indicates polarisation occurs between the lone hydrogen and porous polymer which increases the compound's retention. This explains the disruption of elution order in terms of compound boiling point.

It is possible to assign the polarity order of the three columns from the retention data, and calculation of column capacity factors k'. Taking compounds HFC 143a and 125:

PoraPLOT column	k'		Difference in k' values
	HFC 143a	HFC 125	
Q	1.88	2.00	0.12
S	1.83	2.23	0.40
U	2.62	3.28	0.66

The widest separation is achieved with the PoraPLOT U column —which is the highest polarity column available— so the greatest interaction is observed between the lone polarisable hydrogen present in HFC 125 and the stationary PoraPLOT U phase. The above data indicates the column polarity order of Q < S < U, as expected. However, stronger adsorption of the more polar HFCs, on the more polar PoraPLOT U column results in broader, less symmetrical peaks.

Overall, the PoraPLOT S column, a wide-bore column (25 m × 0.53 mm I.D.), gave the best chromatographic separation in the shortest time and with the least column bleed at the higher column temperatures. The capacity of a wide-bore column is higher than that of the narrow-bore columns, and they also have a higher net retention. This is especially important for PLOT columns, because the retention is directly related to the amount of adsorbent present in the column. The wide-bore PoraPLOT S column has a layer thickness of 20 μm which permits greater loadability [20]. However, CFC 12, a major contaminant of atmospheric air, was shown to co-elute with CH_3Cl at all temperatures, therefore CFC 12 could cause interference in any air samples analysed for this compound. The PoraPLOT Q column produced no co-elution for any of the relevant compounds, but the overall resolution for the compounds, especially the pairs HFCs 143a/125 and HFCs 142b/124, was poorer than on PoraPLOT S and greater column bleed was apparent at the higher column temperatures.

WCOT CP-Sil CB columns

The essentially non-polar CP-Sil 5 CB column elutes the compounds of interest in terms of their boiling point with the exception of HFC 22 which elutes after HFC 134a due to its methanogenic nature. However, even at the lowest possible column operating temperature (without the use of cryogenics), the earliest eluting HFCs, namely 125, 143a and 134a are not sufficiently separated to achieve baseline resolution. The more polar CP-Sil 13 CB column appears to give similar results, but with HFC 143a interacting more strongly with the stationary phase than HFC 125 giving separation of these two HFCs. Although the additional polarity of the CP-Sil 19 CB column enhances interaction of the phase with the single hydrogen of HFC 125, less interaction is observed between HFC 143a and the stationary phase resulting in co-elution. HFC 124 interacts more strongly with the stationary phase on the CP Sil 19 CB column than on the CP Sil 13 CB column, causing co-elution with HFC 142b. Thus, overall resolution is degraded on the CP Sil 19 CB column causing co-elution of HFCs 125/143a and HFCs 142b/124.

Unfortunately a direct comparison between the three columns is not possible due to the different film thickness of the stationary phases. Nevertheless, all the CP-Sil CB columns have

the advantage of low column operating temperatures, thus minimizing effects of column bleed, while still giving rapid analysis times and excellent peak shapes.

CONCLUSIONS

Complete chromatographic resolution of the HFCs and CFCs has proved difficult, due to their similar boiling points and physical properties. Consequently, no one chromatographic column was found to separate all of the compounds of interest. In general, the WCOT columns proved to be very successful for separation of all but the most volatile, earlier eluting HFCs. These columns had the advantage of low column operating temperatures. Conversely, the Pora-PLOT columns were effective for these more volatile HFCs, but not as suitable for the less volatile HFCs due to the higher operating temperatures required. The alumina PLOT columns were potentially the most attractive option since they exhibited excellent resolution of all compounds, although their use is complicated by catalytic activity towards certain HFCs and halocarbons. Passivation of the stationary phase is a possible solution, and work is continuing in our laboratory with an alumina PLOT column passivated with CH_3Cl, to determine whether dehydrohalogenating effects have been eliminated without the loss of the overall superior resolution of the HFCs.

REFERENCES

1 F. Sherwood Molina, *Environ. Sci. Technol.*, 25 (1991) 622–628.
2 G. Webb and J. Winfield, *Chem. Br.*, 28 (1992) 996–997.
3 D.A. Fisher, C.H. Hales, D.L. Filkin, M.K.W. Ko, N. Dak Sze, P.S. Connell, D.J. Wuebbles, I.S.A. Isaken and F. Stordal, *Nature*, 344 (1990) 508–512.
4 D.A. Fisher, C.H. Hales, W. Wang, M.K.W. Ko and N. Dak Sze, *Nature*, 344 (1990) 513–516.
5 J. de Zeeuw, R.C.M. de Nijs and L.T. Heinrich, *J. Chromatogr. Sci.*, 25 (1987) 71–83.
6 J.L. Glajch and W. Schindel, *LC · GC*, 4 (1986) 574–577.
7 D.G. Gehring, D.J. Barsotti and H.E. Gibbon, *J. Chromatogr. Sci.*, 30 (1992) 280–285.
8 R.C.M. de Nijs, *J. High Resolut. Chromatogr. Chromatogr. Commun.*, 4 (1981) 612–615.
9 L. Do and F. Raulin, *J. Chromatogr.*, 514 (1990) 65–69.
10 R.C.M. de Nijs and J. de Zeeuw, *J. Chromatogr.*, 279 (1983) 41–48.
11 F.R. Reinke and K. Bachmann, *J. Chromatogr.*, 323 (1985) 323–329.
12 L. Burgess and D.M. Kavanagh, *The Use of PLOT/Alumina columns in the Analysis of Hydrofluorocarbons*, Technical Note No. 12, IC 08596/12, ICI Chemicals & Polymers, September 1989.
13 W. Asche, *Chromatographia*, 11 (1978) 411–412.
14 Th. Noij, P. Fabian, R. Borchers, C. Cramers and J. Rijks, *Chromatographia*, 26 (1988) 149–156.
15 Th. Noij, J.A. Rijks and C.A. Cramers, *Chromatographia*, 26 (1988) 139–141.
16 J. de Zeeuw, R.C.M. de Nijs, J.C. Buyten and J.A. Peene, *J. High Resolut. Chromatogr. Chromatogr. Commun.*, 11 (1988) 162–167.
17 L. Do and F. Raulin, *J. Chromatogr.*, 481 (1989) 45–54.
18 L. Do and F. Raulin, *J. Chromatogr.*, 591 (1992) 297–301.
19 S. O'Doherty, *LINK-TAPM Report*, personal communication, 1992.
20 J. de Zeeuw, R.C.M. de Nijs, D. Zwiep and J.A. Peene, *Am. Lab.*, 23 No. 9 (1991) 44–51.

Journal of Chromatography, 648 (1993) 433–443
Elsevier Science Publishers B.V., Amsterdam

CHROM. 25 383

Analysis of thiocyanates and isothiocyanates by ammonia chemical ionization gas chromatography–mass spectrometry and gas chromatography–Fourier transform infrared spectroscopy☆

George P. Slater*

Plant Biotechnology Institute, National Research Council of Canada, 110 Gymnasium Place, Saskatoon, Saskatchewan S7N 1X2 (Canada)

John F. Manville

Forestry Canada, Pacific Forestry Centre, 506 West Burnside Road, Victoria, B.C. V8Z 1M5 (Canada)

(First received December 28th, 1992; revised manuscript received June 25th, 1993)

ABSTRACT

Under NH_3-chemical ionization (CI) conditions alkyl thiocyanates give mass spectra which show only the adduct ions $(M + NH_4)^+$ (base peak) and $(M + NH_4 \cdot NH_3)^+$. Allyl thiocyanate and aromatic thiocyanates show fragmentation similar to the corresponding isothiocyanates but still produce $(M + NH_4)^+$ as base peak and $(M + NH_4 \cdot NH_3)^+$ as a prominent ion. These properties allow the thiocyanates to be easily distinguished from isothiocyanates whose NH_3-CI mass spectra indicate considerable fragmentation but little, or no, adduct ion formation. The isothiocyanates are further characterized by relatively abundant M^+ and $(M + H)^+$ ions in spectra of the C_1–C_5 alkyl isomers and the ion at m/z 115 as base peak for the longer-chain alkyl isothiocyanates.

Thiocyanates and isothiocyanates can also be differentiated on the basis of their gas-phase Fourier transform (FT) IR spectra. The spectra of isothiocyanates are dominated by a very intense absorption band at *ca.* 2060 cm^{-1} (–NCS) similar to that seen in liquid film spectra. Thiocyanates, in contrast, show only weak absorption at *ca.* 2165 cm^{-1}. Due to their weak interaction with infrared, aromatic thiocyanates are difficult to detect by this technique. Allyl thiocyanate is a special case. Under normal GC–FT-IR conditions it quickly isomerizes to allyl isothiocyanate. Allyl thiocyanate was only detected in admixture with allyl isothiocyanate, with light-pipe temperatures below 100°C.

INTRODUCTION

Isothiocyanates are formed by enzymatic hydrolysis of glucosinolates with myrosinase [1] but occasionally thiocyanates are also produced. Allyl thiocyanate, for example, is the major product from autolysis of *Thlaspi arvense* [2,3], 4-methylthiobutyl thiocyanate is obtained from *Eruca sativa* [4] and benzyl thiocyanate from *Lepidium sativum* and *L. ruderale* [2].

Allyl thiocyanate represents a special situation as it isomerizes readily to the corresponding isothiocyanate [3,5] (reaction 1) and the reverse isomerization also occurs in the hot injector (> 150°C) of a gas chromatograph [3]. The latter isomerization has also been indicated for allyl isothiocyanate isolated from Japanese horseradish (*Wasabi japonica*) [6] and GC–electron impact (EI) MS of a commercial sample of allyl

* Corresponding author.
☆ NRCC No. 37239.

0021-9673/93/$06.00

isothiocyanate was also shown to contain two products having similar mass spectra [3,6]. Comparison with synthetic compounds [3] showed that the two products in commercial allyl isothiocyanate were in fact allyl thiocyanate and isothiocyanate.

$$CH_2{=}CH{-}CH_2{-}SCN \leftrightarrow SCN{-}CH_2{-}CH{=}CH_2 \quad (1)$$

The EI mass spectra of a number of isothiocyanates [7,8] and the similarity of the spectra of several thiocyanate–isothiocyanate pairs have been reported [9]. The main differences in the EI-MS of the short chain (C_1–C_5) alkyl isomers are the greater relative abundances of M^+ and the ion at *m/z* 72 (CH_2NCS) in spectra of the isothiocyanates. Jensen *et al.* [9] also reported that the mass spectra of alkyl thiocyanate and isothiocyanate isomers become less distinct with increasing chain length. As indicated in Fig. 1a and b, fragmentation of the allyl isomers under EI conditions does not allow unequivocal identification of thiocyanate and isothiocyanate and this is typical of other pairs of these isomeric compounds.

Because the EI mass spectra of allyl [3,6] and alkyl thiocyanates and isothiocyanates [9], do not permit unambiguous identification, it was decided to investigate other mass spectral techniques. Methane- and butane-chemical ionization (CI) MS of the allyl isomers gave identical spectra containing the $(M+1)^+$ ions as base peak together with the relevant adduct ions. However, using NH_3 as reagent gas, it was apparent that differences in the spectra of allyl thiocyanate and isothiocyanate (*cf.* Fig. 1c and d) would permit the identification of these two isomers. Subsequently, a number of alkyl/aryl thiocyanate–isothiocyanate pairs were examined by NH_3-CI-MS and the results are reported in this paper.

A complementary approach to differentiating between thiocyanates and isothiocyanates would be to utilize differences in the IR spectra of these compounds. The IR absorption bands of several thiocyanates and isothiocyanates have been listed by Bellamy [10] as occurring in the range 2174–2137 cm^{-1} and 2106–2045 cm^{-1}, respectively. Nakanishi and Solomon [11] indicated that alkyl thiocyanates have their –SCN bands in

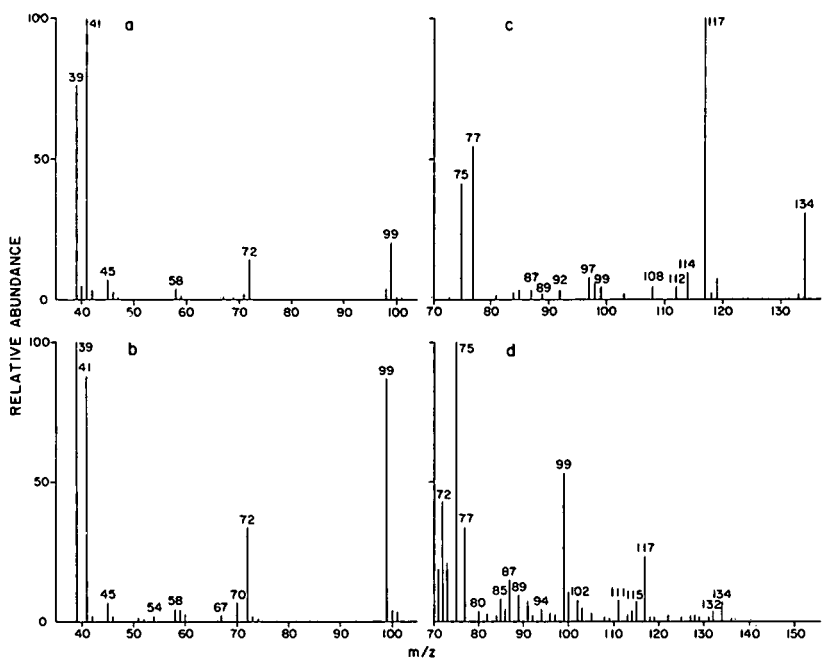

Fig. 1. EI mass spectra of (a) allyl thiocyanate; (b) allyl isothiocyanate; NH_3-CI mass spectra of (c) allyl thiocyanate; (d) allyl isothiocyanate.

the region of 2140 cm^{-1} with aryl thiocyanates showing this absorption at 2175–2160 cm^{-1}, while alkyl isothiocyanates have the–NCS absorption band at 2140–1990 cm^{-1} and aryl isothiocyanates at 2130–2040 cm^{-1}. Previously, Lieber *et al.* [12] reported that several thiocyanates and isothiocyanates could be differentiated on the basis of the vibration frequencies in the region of 2140 cm^{-1} and 2105–2060 cm^{-1}, respectively. The aforementioned citations refer exclusively to room temperature liquid film infrared spectra. Nevertheless, these properties suggest that thiocyanates and isothiocyanates may be distinguishable by GC–FT-IR. Accordingly, several isothiocyanates and thiocyanates were analyzed by GC–FT-IR–flame ionization detection (FID) and the unexpected results observed are included in this report.

EXPERIMENTAL

Chemicals were obtained from Aldrich (Milwaukee, WI, USA), Fairfield (Blythewood, SC, USA) or Dixon (Sherwood Park, Canada).

Allyl thiocyanate was prepared [3] by a modification of the procedure described by Emerson [13] and shown [3] to contain about 0.5% allyl isothiocyanate by GC–FID and GC–MS.

Allyl isothiocyanate free of thiocyanate was prepared [3] by treating allyl amine with 1,1′-thiocarbonyldiimidazole following the procedure of Staab and Walther [14].

The following thiocyanates were prepared by heating the corresponding bromides with NH_4SCN (1.1 equiv.) in ethanol on the steam bath for 4–8 h, adding ice–water and extracting with pentane: *n*-Pr, iso-Pr, *sec.*-Bu, iso-Bu, 3-butenyl, *n*-pentyl, *n*-heptyl, *n*-nonyl, *n*-decyl, 2-phenylethyl. *tert.*-Butyl thiocyanate was prepared by treating the bromide with NH_4SCN in ethanol at 0°C for 1 h followed by 2 h at room temperature. The pentane extract was concentrated by distillation at 45°C and the residual solvent removed by a stream of nitrogen at room temperature. Under these conditions approximately equal amounts of thiocyanate and isothiocyanate were obtained. Phenyl thiocyanate was synthesized from aniline by diazotisation followed by treatment with KSCN [15]. No attempt was made to optimize yields. GC–MS analyses confirmed the identities of the products and, in some cases, the presence of starting material.

3-Butenyl isothiocyanate was a gift from M. Chisholm (Plant Biotechnology Institute) and was prepared by treatment of the corresponding glucosinolate with myrosinase (EC 3.2.3.1).

Volatile products from homogenized stinkweed plants (*Thlaspi arvense*) were collected as described previously [16].

Instrumentation

GC analyses were performed on a Hewlett-Packard (Avondale, PA, USA) 5880 chromatograph fitted with a J & W Scientific DB-5 capillary column [60 m × 0.32 mm I.D., film thickness (d_f) 0.25 μm, Chromatographic Specialties, Brockville, Canada). The following conditions were used, unless stated otherwise: injector, 200°C; detector, 320°C; column, 20°C for 8 min, 4°C/min to 220°C, 10°C/min to 300°C; helium, 30 cm/s at 50°C. All samples were injected in the splitless mode with CH_2Cl_2 as solvent and toluene as internal reference.

A Finnigan 4000 GC–MS system (San Jose, CA, USA) was used for EI- and CI-MS and was operated under identical conditions as for GC analysis. The ammonia was adjusted to 0.40–0.45 Torr (1 Torr = 133.322 Pa) to maximize NH_4^+ and $(NH_4 \cdot NH_3)^+$. High-resolution MS data were obtained with a VG-250 SEQ mass spectrometer (VG Analytical, Altrincham, UK).

The IR spectra of allyl isothiocyanate (Aldrich) and allyl thiocyanate were obtained as liquid films (thickness unknown) on NaCl plates with a Bio-Rad (Mississauga, Canada) FTS 40 spectrometer. The allyl thiocyanate was kept on ice until ready for analysis.

A Hewlett-Packard 5890 gas chromatograph with an Ultra-2 (20 m × 0.22 mm I.D., d_f 0.25 μm, Hewlett-Packard), or Supelcowax-10 capillary column (20 m × 0.32 mm I.D., d_f 0.25 μm, Supelco Canada, Oakville, Canada) and a Nicolet FT-IR 20SXB spectrometer (Nicolet Instrument Canada, Mississauga, Canada) were used for gas-phase IR–FID determinations. The columns were connected directly to the light pipe via a heated transfer line. Unless stated other-

wise, the following conditions were used: column, 60°C for 1 min, 15°C/min to 275°C and hold 5 min; helium, 30 cm/s at 50°C; FID, 295°C. Samples in chloroform were introduced via a duck-bill cool-on-column injector. For most observations the light pipe was maintained at 180°C while the transfer line was held at 200°C. Effluent from the light pipe was transferred via a short megabore fused-silica capillary column to an FID system on the HP 5890 gas chromatograph.

RESULTS AND DISCUSSION

Gas chromatography

Under the chromatographic conditions used, baseline separation of all isothiocyanate–thiocyanate pairs is possible on a DB-5 column with the exception of *sec.*-BuNCS and *sec.*-BuSCN which essentially co-elute (t_R 23.13 and 23.21 min, respectively). In general, on the non-polar DB-5 or Ultra-2 columns, a thiocyanate elutes before the corresponding isothiocyanate with a quite regular difference in retention time. However, the *tert.*-butyl, and *sec.*-butyl isomers are exceptional in that the isothiocyanate elutes first.

Mass spectroscopy

In the ammonia CI-MS of the allyl isomers (Fig. 1c and d) the main distinguishing features are: (1) the base peak in the MS of the thiocyanate corresponds to $(M + NH_4)^+$ but the base peak of the isothiocyanate is at m/z 75; (2) the greater intensity of the ion at m/z 134, corresponding to $(M + NH_4 \cdot NH_3)^+$, in the spectrum of the thiocyanate; (3) the low intensity of M^+ in the spectrum of the thiocyanate; (4) the absence of the ion at m/z 72 in the spectrum of the thiocyanate.

The EI mass spectra of benzyl thiocyanate and benzyl isothiocyanate (not shown) are virtually identical. However, differences in the NH_3-CI-MS again permit distinction between the thiocyanate (Fig. 2a) and the isothiocyanate (Fig. 2b) since the MS of the latter is free of adduct ions (m/z 167, 184). For benzyl thiocyanate, the $(M + 18)^+$ ion is the base peak and is accompanied by the relatively abundant adduct ion at m/z (M + 35) but with no indica-

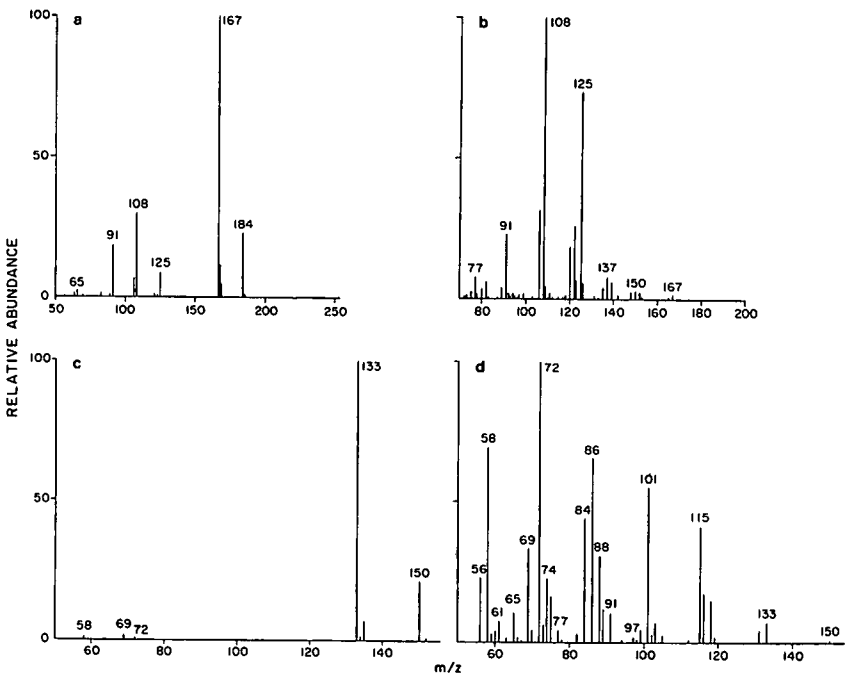

Fig. 2. NH_3-CI mass spectra of (a) benzyl thiocyanate; (b) benzyl isothiocyanate; (c) *sec.*-butyl thiocyanate; (d) *sec.*-butyl isothiocyanate.

tion of M^+ (Fig. 2a). In contrast to allyl isothiocyanate (Fig. 1d), the MS of benzyl isothiocyanate (Fig. 2b) shows only minor amounts of M^+ (m/z 149) and $(M+18)^+$ (m/z 167). For benzyl isothiocyanate, the base peak at m/z 108 is accompanied by a number of other prominent ions, some of which are also in the MS of the thiocyanate (Fig. 2a and b).

Analysis of additional pairs of isomers confirmed that the base peak for all thiocyanates examined occurs at m/z (M + 18) and is accompanied by a relatively abundant ion at m/z (M + 35) (*cf.* Figs. 1c and 2a and c). In contrast, these adduct ions have minimal abundances in the MS of the isothiocyanates with the exception of allyl isothiocyanate (Fig. 1d) and 2-phenylethyl isothiocyanate (Table I).

Table I contains selected data on representative isothiocyanates. Generally, the NH_3-CI-MS of alkyl (up to C_5) and aromatic isothiocyanates (except benzyl) contain a prominent molecular ion. For 3-butenyl, *tert.*-butyl, 2-methylbutyl, phenyl, *o*-, *m*-, *p*-methylphenyl and 1-naphthyl isothiocyanates, the M^+ is always the base peak but, for the other alkyl isothiocyanates up to C_5, the base peak may be M^+ or a smaller fragment (Table I, Figs. 1d and 2d). The longer-chain alkyl isothiocyanates all give the ion at m/z 115

TABLE I

RELATIVE ABUNDANCES OF IONS IN THE AMMONIA CHEMICAL IONIZATION MASS SPECTRA OF ISOTHIOCYANATES

Compound	Relative abundance (%)				
	M^+	$(M+1)^+$	$(M+18)^+$	$(M+35)^+$	Base peak (m/z)
MeNCS	100	17	6	–	M
EtNCS	100/46[a]	20	7	2	M/58
AllylNCS	55/21	10	25	5	75/58
iso-PrNCS	38/19	10	3	–	58/72
n-PrNCS	33/45	14	4	–	58/72
3-Butenyl-NCS	100	8	–	–	M
iso-BuNCS	33	26	5	–	78
n-BuNCS	100/89	12	2	–	M/86
sec.-BuNCS	41/18	17	7	–	72/86
tert.-BuNCS	100	–	58[b]	–	M
2-MeBuNCS	100	26	3	–	M
3-MeBuNCS	100/60	25	4	–	M/114
Pentyl-NCS	100/89	32	4	–	M/100
Hexyl-NCS	10	8	1	–	115
Heptyl-NCS	6	6	1	–	115
Octyl-NCS	5	10	1	–	115
Nonyl-NCS	13	11	–	–	115
Decyl-NCS	8	10	–	–	115
Phenyl-NCS	100	10	–	–	M
Benzyl-NCS	3	4	2	–	108
o-Tolyl-NCS	100	7	–	–	M
m-Tolyl-NCS	100	8	–	–	M
p-Tolyl-NCS	100	9	–	–	M
PhEtNCS[c]	20	10	45	–	108
1-Naphthyl-NCS	100	12	–	–	M

[a] Some of the isothiocyanates do not consistently give one particular ion as base peak. This is indicated by alternate values of relative abundance for M^+ and m/z values for the base peak.

[b] Relative abundance for ion at m/z (M + 17).

[c] PhEt = 2-Phenylethyl.

as the base peak (Table I). Kjaer *et al.* [7] reported that the ion at m/z 115 was prominent in the EI-MS of linear alkyl isothiocyanates with chain lengths greater than C_5. The spectra of the longer-chain (*i.e.* $>C_5$) isothiocyanates are also characterized by moderately abundant M^+ and $(M+1)^+$ ions (Table I). These features help distinguish the isothiocyanates from the isomeric thiocyanates.

The ease of distinction between alkyl thiocyanates and isothiocyanates by NH_3-CI-MS is typified by the spectra of the *sec.*-butyl isomers (Fig. 2c and d). Whereas the spectrum of the thiocyanate (Fig. 2c) contains only adduct ions, considerable fragmentation of the isothiocyanate is apparent (Fig. 2d). In this respect the NH_3-CI-MS of allyl thiocyanate (Fig. 1c) and benzyl thiocyanate (Fig. 2a) are anomalous as they indicate fragmentation similar to the corresponding isothiocyanates (Figs. 1d and 2b, respectively). This anomaly is also seen in the NH_3-CI-MS of phenyl thiocyanate and 2-phenylethyl thiocyanate (not shown) and may indicate that the presence of allyl or aromatic residues stabilizes these ions relative to their alkyl counterparts. Alternatively, this anomaly may be due to partial isomerization of the allyl and aromatic isomers in the ionization source. The tendency of allyl thiocyanate to isomerize to isothiocyanate is well known [3,5,14], and the reverse isomerization by brief exposure to temperatures greater than 150°C has also been demonstrated [3]. However, isomerization of aromatic thiocyanates is less well documented and no isomerization was detected in the present work using injector temperatures up to 200°C.

Isothiocyanates are known to react with ammonia to give thioureas (2) and some of the spectra do show minor ions at m/z $(M+NH_3)$ but this ion is prominent only in the spectrum of *tert.*-butyl isothiocyanate (Table I). However, the NH_3-CI mass spectra of the isomeric butyl thioureas (not shown) are identical and contain the ion at m/z $(M+1)$ {*i.e.* m/z $133 \equiv (M+NH_4)^+$ for the parent isothiocyanate} as the base peak and the adduct ion $(M+NH_4)^+$ at *ca.* 3% relative abundance. The NH_3-CI-MS of other alkyl thioureas, and benzyl thiourea, also give the $(M+H)^+$ ion as base peak and different fragments than the parent isothiocyanates (not shown). These observations suggest that little or no thiourea is formed during NH_3-CI-MS of isothiocyanates.

$$RCH_2\text{–}NCS + NH_3 \rightarrow RCH_2\text{–}NH\text{–}\underset{\displaystyle NH_2}{\overset{\displaystyle |}{C}}\text{=}S \qquad (2)$$

The fragmentation of the isothiocyanates under NH_3-CI conditions can be rationalized by postulating elimination of various neutral species from the adduct ions. For allyl isothiocyanate (Fig. 1d) the ions at m/z 77, 75 correspond to loss of cyclopropene and propylene, respectively, from the adduct $(M+NH_4)^+$. However, high-resolution MS showed the ion at m/z 72 has the same composition (CH_2NCS) as in the EI mass spectrum and is most likely derived from the relatively abundant molecular ion. Similarly, in the spectrum of *sec.*-butyl isothiocyanate (Fig. 2d) the molecular ion and the ion at m/z 72 are also abundant and other ions such as m/z 74, 91 appear to arise by loss of HNCS from the $(M+NH_4)^+$ and $(M+NH_4\cdot NH_3)^+$ adducts, respectively. Similar losses to give the base peak at m/z 108 and the ion at m/z 125 in the spectrum of benzyl isothiocyanate (Fig. 2b) were confirmed by high-resolution MS. The ion at m/z 108 is also the base peak in the spectrum of 2-phenylethyl isothiocyanate and is accompanied by the ion at m/z 125 (Table I). These ions are also prominent in the NH_3-CI mass spectrum of toluene which was used as a retention time reference. For toluene the ions at m/z 108, 125 obviously arise from adduct ions and can be represented by the elimination of H_2 from the $(M+NH_4)^+$ and $(M+NH_4\cdot NH_3)^+$ ions, respectively. The presence of the ions at m/z 108, 125 in the NH_3-CI-MS of these compounds suggests that these fragments are diagnostic for the benzyl group.

Infrared spectroscopy

A series of alkyl and aryl thiocyanates and isothiocyanates were examined by GC–FT-IR–FID (Table II). Fig. 3a shows the FID response and Fig. 3c the corresponding Gram–Schmidt reconstructed FT-IR chromatograms, respective-

TABLE II

THIOCYANATES AND ISOTHIOCYANATES EXAMINED BY GC–FT-IR

Peak No.	R	RNCS (ng)	RSCN (ng)	RSCN:RNCS
1	CH_3	68	2474	36
2	Et	60	2105	35
3	iso-Bu	62	2105	34
4	*n*-Bu	55	2000	36
5	*n*-C_5	50	363[a]	7
6	Ph	70	2500	36
7	*n*-C_7	53	1868	35
8	$PhCH_2$	56	2500	45
9	*n*-C_{10}	51	1974	39

[a] Sample contains 2138 ng/μl crude product comprising 17% thiocyanate which was not detected by GC–FT-IR (*cf.* Fig. 7, peak 5).

ly, for a mixture of isothiocyanates containing 50–70 ng of each compound (Table II). Fig. 3b and d show the corresponding responses for the isomeric thiocyanates at approximately 1900–2500 ng each. Comparison of Fig. 3b and d with Fig. 3a and c indicates that GC–FT-IR is appreciably more sensitive for the isothiocyanates than for the thiocyanates. Even when the thiocyanates are present in amounts 34–45 times greater than the corresponding isothiocyanates

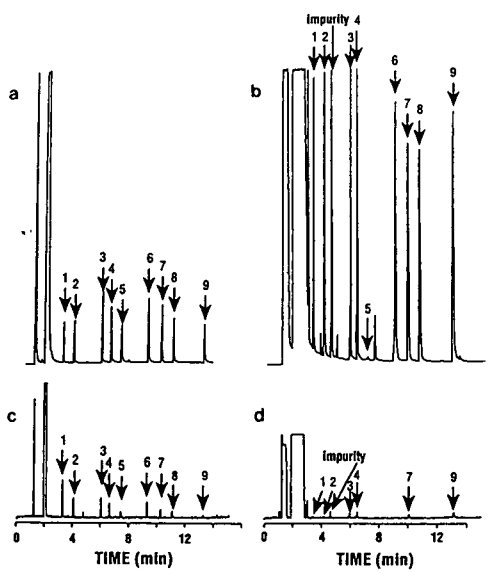

Fig. 3. GC–FID response of (a) isothiocyanates; (b) thiocyanates; and GC–FT-IR response of (c) isothiocyanates; (d) thiocyanates listed in Table II.

(Table II) their detection and subsequent identification by gas-phase FT-IR is not assured (Fig. 3d). Based on available information for liquid film spectra, these results were not expected.

In liquid film IR spectra, isothiocyanates display very strong, broad bands, or doublets, in the region 2200–2000 cm^{-1}, and thiocyanates are characterized by an intense, narrow band centred near 2160 cm^{-1} [11,17]. These features are exemplified by the liquid-film IR spectra of commercial allyl isothiocyanate (Fig. 4a), with the –NCS broad absorption band centred at *ca.* 2100 cm^{-1}, and allyl thiocyanate (Fig. 4b) with the –SCN absorption band at 2160 cm^{-1}. The liquid film spectrum of *n*-butyl thiocyanate [17] shows almost equal absorption intensities for the–SCN and alkyl groups. By comparing these liquid film spectra with the gas-phase spectra of *n*-butyl isothiocyanate (Fig. 4c), phenyl isothiocyanate (Fig. 4e) and the corresponding thiocyanates (Fig. 4d and f), it is obvious that the differences in detection sensitivity by GC–FT-IR is attributable to the relatively greater absorption intensity at *ca.* 2100 cm^{-1} of the–NCS chromophore in comparison to that of the much weaker–SCN chromophore. Examination of a number of alkyl and aryl isothiocyanates indicates that in the gas phase the–NCS chromophore is from 2–10 times more intense than the most intense C–H band. At the levels studied (50–90 ng), it is also possible to distinguish between alkyl and aromatic isothiocyanates by

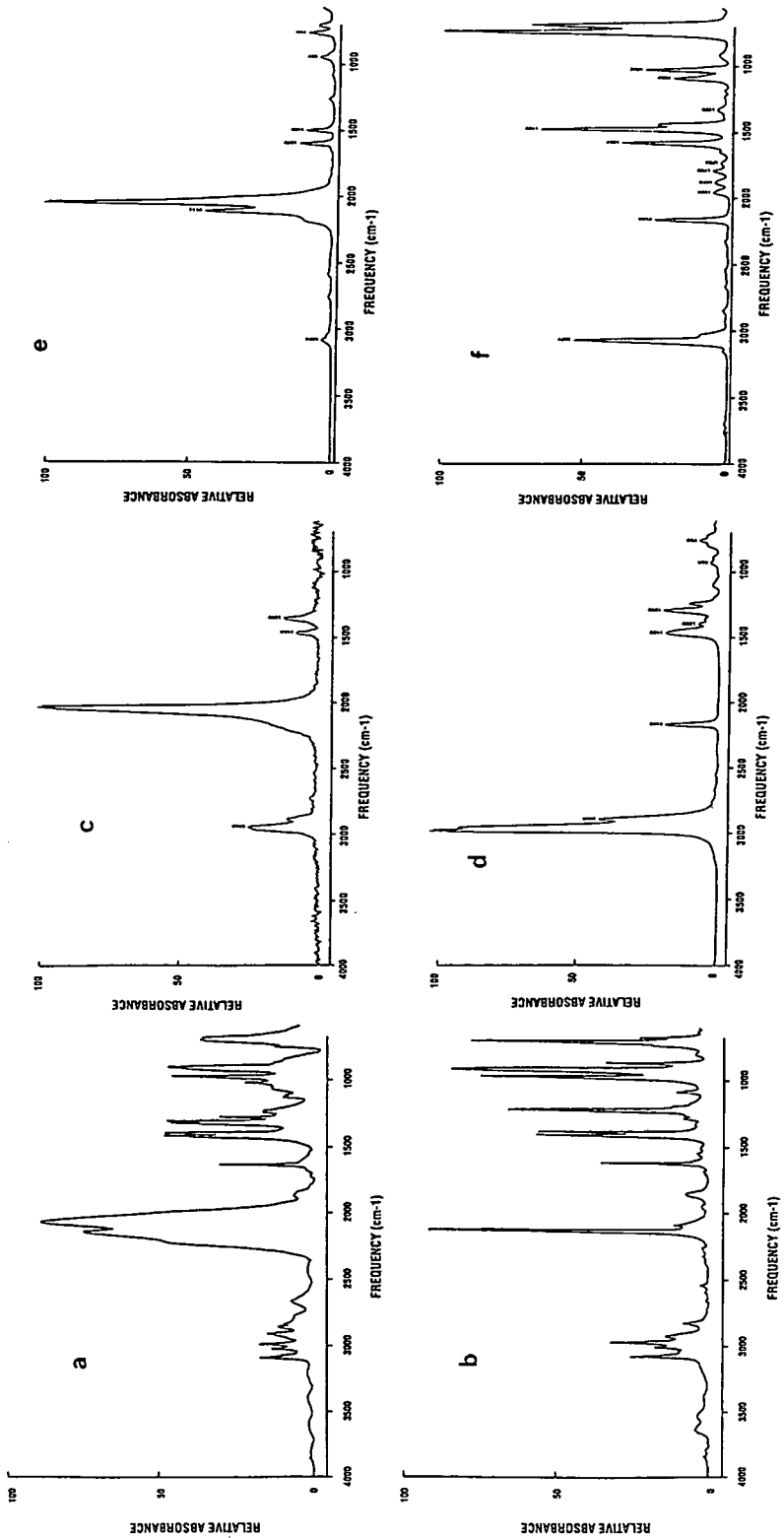

Fig. 4. FT-IR spectra (liquid film) of (a) allyl isothiocyanate (Aldrich); (b) allyl thiocyanate; GC–FT-IR spectra of (c) *n*-butyl isothiocyanate; (d) *n*-butyl thiocyanate; (e) phenyl isothiocyanate; (f) phenyl thiocyanate.

the bands in the region of 3000 cm^{-1} and 1600–1500 cm^{-1}, respectively (Fig. 4c and e).

In comparison to the isothiocyanates, gas-phase FT-IR detection of the thiocyanates is very poor relative to detection by FID (Fig. 3). The -SCN chromophore is only 0.1–0.3 times as intense as the most intense C–H band. Such findings were not expected based on available data (*cf.* Fig. 4b [10–12,17]).

The fact that aromatic compounds in general interact weakly with IR, coupled with the absence of an intense gas-phase thiocyanate absorption band, renders these molecules nearly transparent to the IR beam. Thus, neither the phenyl thiocyanate (Fig. 3b, peak 6) or benzyl thiocyanate (Fig. 3b, peak 8) in the amounts used (2500 ng, Table II), are detected by GC–FT-IR (Fig. 3d), even though they were present in concentrations greater than those of the detected alkyl thiocyanates (Table II). The GC–gas-phase IR spectra of *n*-butyl thiocyanate (Fig. 4d) and phenyl thiocyanate (Fig. 4f) are typical of the thiocyanates studied. However, allyl thiocyanate is a special case.

Analysis of allyl thiocyanate by GC–FT-IR is complicated by the tendency of this compound to isomerize, even at room temperature [3]. When an extract [16] of *Thlaspi arvense* (stinkweed, pennycress) is chromatographed with the light pipe at 100°C and transfer assembly at 125°C, two major peaks are observed (Fig. 5). The sharp peak (a) and the broad symmetrical peak (b) were previously identified [3] as allyl isothiocyanate and allyl thiocyanate, respectively. However, the gas-phase FT-IR spectra throughout the second peak are identical to the spectrum of allyl isothiocyanate (Fig. 6a) indicating complete racemization of the thiocyanate when the light pipe and transfer assembly are equal to, or greater than, the above temperatures.

When a partially racemized sample of allyl thiocyanate is chromatographed as above but with the light pipe at 70°C and transfer assembly at 80°C to reduce isomerization, the chromatogram in Fig. 6 (inset) is obtained. Allyl isothiocyanate exits the column first (7.67 min) followed by the thiocyanate peak beginning at about 8.10 min. Fig. 6b–f shows the variation of the IR spectra across the thiocyanate peak. The

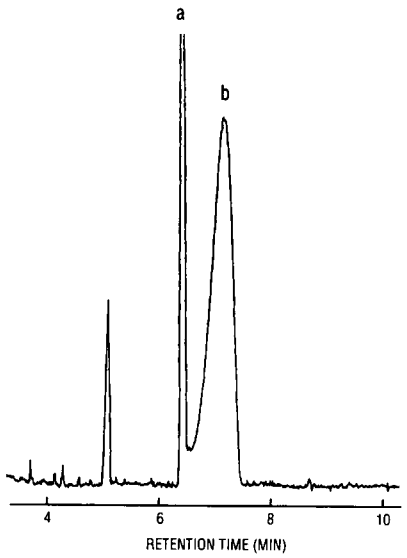

Fig. 5. GC–FT-IR chromatogram of *Thlaspi arvense* extract, cool-on-column (40°C) onto Supelcowax, light pipe at 100°C and transfer assembly at 125°C. See text.

spectrum at 9.04 min (Fig. 6b) indicates only allyl isothiocyanate (*cf.* Fig. 6a) whereas the spectrum taken at 11.80 min (Fig. 6f) suggests complete absence of this isomer. The ratio of the intensity of the band at *ca.* 2170 cm^{-1} to the most intense C–H band is similar to that found in GC–FT-IR spectra of aryl thiocyanates (*cf.* Fig. 4f). Thus, the spectrum in Fig. 6f appears to represent pure allyl thiocyanate (*cf.* Table III for IR data).The spectra in Fig. 6c–f are consistent with mixtures of this compound and progressively decreasing amounts of the isothiocyanate. Similar results are obtained with the light pipe at 60 or 80°C.

Searches of the gas-phase IR spectral libraries available from Nicolet/Aldrich, Hewlett-Packard/Aldrich and the US Environmental Protection Agency failed to correctly identify any of the thiocyanates examined in the present study. This is due to the scarcity of reliable data[a] for these compounds. Closest matches were for mercaptans, disulfides or halides.

[a] The Aldrich vapour library as supplied by Nicolet in 1985, contains only the spectra for *n*-octyl thiocyanate and benzyl thiocyanate. The latter appears to represent a mixture containing mostly benzyl isothiocyanate.

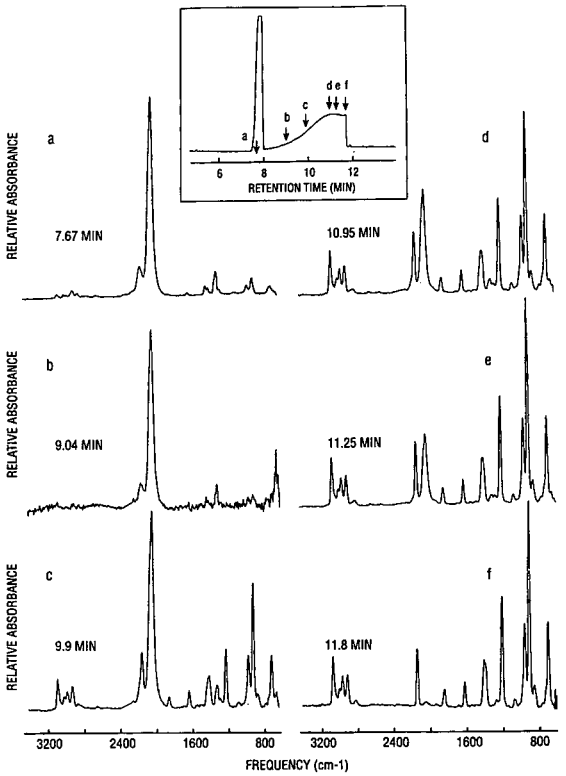

Fig. 6. GC–FT-IR chromatogram (insert) of partially racemized allyl thiocyanate, cool-on-column injection (40°C) onto Supelcowax, light pipe at 70°C, transfer line at 80°C. FT-IR spectra of (a) allyl isothiocyanate, (b–f) taken across the allyl thiocyanate peak.

The only essential difference between the GC–FT-IR system and that used for GC–MS analysis in the present, and previous work [3], is the light pipe. Since the previous work [3] showed that allyl thiocyanate injected at 75–100°C underwent mimimal isomerization, the present results indicate that isomerization during GC–FT-IR can occur in the light pipe, even at temperatures as low as 60°C, and may have been induced, in part, by the presence of the gold film and/or exposure to IR radiation.

CONCLUSIONS

Under normal GC–FT-IR conditions, allyl thiocyanate readily and completely isomerizes to the more stable allyl isothiocyanate. Allyl thiocyanate, in admixture with the isothiocyanate, can only be seen by GC–FT-IR if the light-pipe temperature is kept below 100°C. In general, isothiocyanates are readily detected and identified by GC–FT-IR. Thiocyanates are less easily detected and current gas-phase libraries do not give reliable identifications. Isothiocyanates give an intense–NCS band at *ca.* 2060 cm^{-1} which corresponds with their respective liquid film spectra. Conversely, the thiocyanates do not provide expected spectra by GC–FT-IR, only a weak band is observed at *ca.* 2160 cm^{-1}.

TABLE III

VAPOR-PHASE INFRARED SPECTRAL DATA FOR ALLYL THIOCYANATE WITH LIGHT PIPE AT 60°C

Peak No.	Wavelength (cm^{-1})	Intensity	Bandwidth (cm^{-1})
1	723.5	44	43
2	875.5	12	24
3	932.9	104	35
4	983.4	43	42
5	1234.9	57	38
6	1420.4	24	46
7	1434.6	25	22
8	1645.8	15	31
9	1869.6	11	49
10	2169.8	31	38
11	2846.4	6	46
12	2940.4	18	41
13	2996.9	18	26
14	3030.5	11	35
15	3101.7	27	31

The NH_3-CI mass spectra of alkyl thiocyanates contain only the base peak at m/z $(M + NH_4)^+$ and the comparatively abundant adduct ion $(M + NH_4 \cdot NH_3)^+$. This permits ready distinction of these compounds from the corresponding isothiocyanates whose NH_3-CI mass spectra are more complex and generally include M^+ and $(M + H)^+$ but essentially no adduct ions. The NH_3-CI mass spectra of linear alkyl isothiocyanates containing more than five carbons are further characterized by the presence of the ion at m/z 115 as the base peak. Although the allyl and aromatic thiocyanates fragment similarly to the corresponding isothiocyanates under NH_3-CI conditions, these isomers can also be distinguished easily by the presence of the ion

$(M + NH_4)^+$ as base peak and an abundant $(M + NH_4 \cdot NH_3)^+$ ion in the spectra of the thiocyanates.

Although GC–FT-IR does permit distinction between thiocyanates and isothiocyanates, the method, especially for thiocyanates, is not as sensitive as NH_3-CI-MS. In addition, the relative simplicity of the NH_3-CI spectra of thiocyanates allows ready distinction from the more complex fragmentation of the corresponding isothiocyanates.

ACKNOWLEDGEMENTS

The authors would like to thank L.L. Hoffman for technical assistance, D. Olson and L. Hogge (Plant Biotechnology Institute) for mass spectral analysis, and T. Fraser and J.R. Nault (Pacific Forest Centre), for FT-IR determinations. We also acknowledge the help of D. Hasman and R. Leibrand, Hewlett-Packard, in confirming our FT-IR findings and for providing some of the spectra used in Fig. 4 in this paper.

REFERENCES

1 H.L. Tookey, C.H. VanEtten and M.E. Daxenbichler, in I.E. Liener (Editor), *Toxic Constituents of Plant Foodstuffs*, Academic Press, New York, 1980, p. 103.
2 R. Gmelin and A.I. Virtanen, *Acta Chem. Scand.*, 13 (1959) 1474.
3 G.P. Slater, *Chromatographia*, 34 (1992) 461.
4 A. Kjaer and R. Gmelin, *Acta Chem. Scand.*, 9 (1955) 542.
5 A. Fava, in N. Kharasch and C.Y. Meyers (Editors), *The Chemistry of Organic Sulfur Compounds*, Vol. 2, Pergamon, London, 1961, Ch. 3.
6 A. Shinohara, A. Sato, H. Ishi and N. Onda, *Chromatographia*, 32 (1991) 357.
7 A. Kjaer, M. Ohashi, J.M. Wilson and C. Djerassi, *Acta Chem. Scand*, 17 (1963) 2143.
8 G.F. Spencer and M.E. Daxenbichler, *J. Sci. Food Agric.*, 31 (1980) 359.
9 K.A. Jensen, A. Holm and C. Wentrup, *Acta Chem. Scand.*, 20 (1966) 2107.
10 L.J. Bellamy, in *Advances in Infrared Group Frequencies*, Methuen, London, 1968, pp. 58–59.
11 K. Nakanishi and P.H. Solomon, in *Infrared Absorption Spectroscopy*, Holden-Day, Oakland, CA, 2nd ed., 1977, p. 23.
12 E. Lieber, C.N.R. Rao and J. Ramachandran, *Spectrochim. Acta*, 13 (1959) 296.
13 D.W. Emerson, *J. Chem. Educ.*, 48 (1971) 81.
14 H.A. Staab and G. Walther, *Ann.*, 657 (1962) 104; *Chem. Abstr.*, 58 (1963) 1379.
15 L. Gatterman and W. Hausknecht, *Ber.*, 23 (1890) 738.
16 K.A. Pivnick, B.J. Jarvis, G.P. Slater, C. Gillott and E.W. Underhill, *Environ. Entomol.*, 19 (1990) 704.
17 C.J. Pouchert, in *The Aldrich Library of Infrared Spectra*, Edition III, Aldrich, Milwaukee, MI, 3rd ed., 1981.

Journal of Chromatography, 648 (1993) 445–449
Elsevier Science Publishers B.V., Amsterdam

CHROM. 25 391

Construction of a robust stainless-steel clad fused-silica restrictor for use in supercritical fluid extraction

Mark D. Burford, Steven B. Hawthorne* and David J. Miller

Energy and Environmental Research Center, University of North Dakota, Box 9018, Grand Forks, ND 58202 (USA)

Joe Macomber

ISCO Inc., P.O. Box 5347, Lincoln, NE 68505 (USA)

(Received May 24th, 1993)

ABSTRACT

Fused-silica restrictors used for off-line supercritical fluid extraction (SFE) frequently break when extractions are performed with polar supercritical fluids [*e.g.*, $CHClF_2$ (Freon 22) or CO_2 containing polar modifiers (*e.g.*, methanol)]. Securing the fused-silica restrictor inside a 1/16 in. (1.6 mm) O.D. stainless-steel tube with an epoxy resin eliminated the restrictor breakage and allowed restrictors to be connected to the extraction cell with conventional stainless-steel fittings. The stainless-steel clad fused-silica restrictor was simple and inexpensive to construct, physically robust, and proved ideal for SFE applications since no artifacts from the clad restrictor were detected in the collection solvent.

INTRODUCTION

The linear flow or capillary restrictor constructed of fused-silica tubing is the most common type of restrictor used in analytical-scale supercritical fluid extraction (SFE), because the restrictors are inexpensive, disposable, available with several inner diameters to achieve desired flow-rates, and can be used with a variety of collection systems. However, these restrictors often break when they are used with polar fluids such as $CHClF_2$ (Freon 22) [1] and when polar modifiers such as methanol [2] are added to CO_2. Fused-silica restrictors clad in an external tube may reduce the breakage that occurs with polar fluids [3–5]. The aim of this study was to construct an inexpensive, simple, robust, and disposable restrictor which could be used with a number of polar SFE fluids without breakage. This was achieved by using an epoxy resin to secure the fused-silica capillary restrictor inside a stainless-steel tube.

EXPERIMENTAL

Construction of stainless-steel clad restrictor

Stainless-steel clad restrictors were made from either 32 μm I.D. × 145 μm O.D. fused-silica tubing (Polymicro Technologies, Phoenix, AZ, USA) inserted into 1/16 in. (1.6 mm) O.D. × 0.02 in. (0.51 mm) I.D. stainless-steel tubing, or 29 μm I.D. × 370 μm O.D. fused-silica tubing inserted into 1/16 in. (1.6 mm) O.D. × 0.03 in. (0.76 mm) I.D. stainless steel tubing. A 5-ml disposable plastic syringe with a male Luer lock outlet (Becton Dickinson & Co, Rutherford, NJ, USA), the fused-silica restrictor, and the stain-

* Corresponding author.

0021-9673/93/$06.00

less-steel tube were connected to a 1/16 in. (1.6 mm) stainless-steel tee-piece so that the fused-silica restrictor extended through the stainless-steel tube and the tee-piece (Fig. 1). The fused-silica restrictor was then secured inside the stainless-steel tube by injecting an epoxy resin "Epo-tek 353ND" (Epoxy Technology, Billerica, MA, USA) from the syringe into the metal tubing to fill the void space between the stainless-steel tube and the fused-silica restrictor. The epoxy-filled tube containing the restrictor was then disconnected from the tee-piece and placed in a 80°C oven for 2 h to cure the epoxy resin. Finally, the excess fused-silica protruding from the stainless-steel tubing was removed using a scoring tool (Supelco, Bellefonte, PA, USA), or the metal tubing was cut with an SSI tube cutter (SSI, State College, PA, USA) so that the fused-silica restrictor was flush with the tube. Note, when using the SSI cutter, cylinder pressure CO_2 (*ca.* 90 atm) was flowed through the restrictor to avoid blocking the restrictor tip with pieces of metal.

Evaluation of stainless-steel clad restrictors

The ability of the stainless-steel clad fused-silica restrictor to avoid restrictor breakage during SFE was evaluated using pure supercritical fluid chromatography (SFC)-grade CO_2, $CHClF_2$ (Freon 22), premixed CO_2–methanol (90:10, v/v), or CO_2–toluene (90:10, v/v) (Scott Gases, Plumsteadville, PA, USA). Each fluid was pumped by an ISCO Model 260D syringe pump

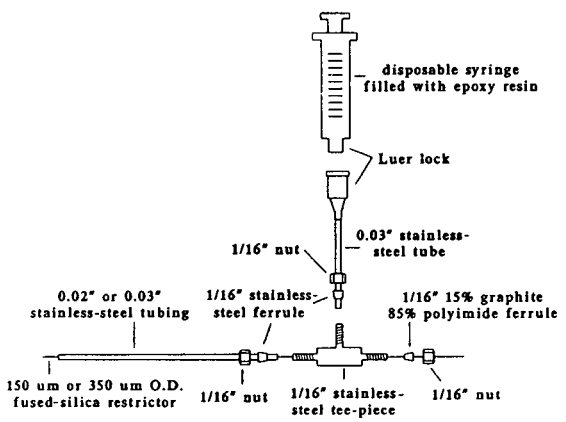

Fig. 1. Equipment used to construct stainless-steel clad fused-silica restrictors. " = inch.

(ISCO, Lincoln, NE, USA) which was connected to an empty 0.5-ml extraction cell (30 mm long × 4.6 mm I.D.) with 1/16 in. (1.6 mm) O.D. stainless-steel tubing and "Slip-free" fingertight connectors (Keystone Scientific, Bellefonte, PA, USA). A 1-m long coil of 1/16 in. (1.6 mm) tubing (placed before the extraction cell to pre-warm the fluid to the extraction temperature) and the extraction cell were placed inside a tube heater to maintain the extraction temperature. The flow-rate of the supercritical fluid through the extraction cell was controlled by a 10-cm long fused-silica restrictor or 10-cm long stainless-steel clad fused-silica restrictor connected to a "Slip-free" fingertight connector via a tubing union (1/16 in. × 1/16 in). The outlet of the restrictor was inserted into a 7.4-ml vial containing 5 ml pesticide-grade methylene chloride [for GC–flame ionization detection (FID) analysis] or 5 ml Fisher "Optima Grade" acetone [for GC–electron-capture detection (ECD) analysis] to simulate normal SFE procedures. Collection solvent volume was maintained by small additions of solvent during SFE.

The 1-m long tubing and the empty 0.5-ml extraction cell were pre-heated in a tube heater for 15 min before SFE at 400 atm (1 atm = $1.01 \cdot 10^5$ Pa) was begun with pure CO_2 (60°C or 150°C), CO_2–toluene (90:10) (80°C), CO_2–methanol (90:10) (60°C), or $CHClF_2$ (100°C). The supercritical fluid was pumped through the extraction system until either the restrictor broke or until the complete 240 ml volume of pressurized fluid in the syringe pump had been used (*ca.* 4 h).

To determine whether the epoxy resin used in the construction of the stainless-steel clad restrictors could contribute artifacts to the SFE extracts, 500 mg cured epoxy resin (0.5–0.2 mm pieces) was placed on a bed of 80-mesh silanized glass beads inside a 0.5-ml extraction cell and extracted for 20 min with 400 atm CO_2–methanol (90:10) at 60°C or 400 atm $CHClF_2$ at 100°C at a flow-rate of *ca.* 0.8 ml/min of compressed fluid (measured at the pump).

RESULTS AND DISCUSSION

Using the syringe device shown in Fig. 1, several of the clad restrictors can be made in one

hour. If wide bore (0.03 in. I.D.) stainless-steel tubing is used in the construction, up to 50 cm of the clad restrictor could be produced at one time and then cut into the desired lengths. For the smaller 0.02 in. I.D. stainless-steel tube only *ca.* 15 cm lengths of clad restrictor can be made because of the added pressure needed to inject the epoxy.

As shown in Table I, the conventional fused-silica restrictors did not break when pure CO_2 (60°C and 150°C) or CO_2–toluene (90:10) were used as the extraction fluids. However, when the polar fluids CO_2–methanol (90:10) or $CHClF_2$ were used with the conventional fused-silica restrictors, the restrictors soon became brittle and broke into two or more pieces. Restrictor breakage with $CHClF_2$ proved to be the worst for the supercritical fluids so far encountered [1]. Longer extraction times were possible using a thick walled (*i.e.*, 370 μm O.D.) instead of a thin walled (*i.e.*, 145 μm O.D.) fused-silica restrictor with the polar fluids, however within *ca.* 30 min even the thick walled restrictors had broken. Similar breakage problems have been encountered with several different batches of fused-silica tubing.

Examination of the broken fused-silica restrictor tip under the light microscope (×80 magnification) revealed an uneven break with fine cracks and grooves along the broken surface. Conversely, a freshly cut restrictor using a scoring tool had a "clean" break and the cut surface had a smooth, uniform appearance. The presence of cracks and grooves in the restrictor may be related to the increased instability of glass and fused-silica in the presence of polar solvents like methanol [6]. Furthermore, the location of the break in the fused-silica restrictor was random, and the ability of the restrictor to withstand polar supercritical fluids varied. When breakages occur above the collection solvent, not only is the extract lost, but the analyst experiences a significant risk of exposure when toxic compounds are being extracted. Fortunately, by securing the fused-silica restrictor inside a stainless-steel tube, restrictor breakage due to polar fluids was eliminated for the maximum time tested (*e.g.*, *ca.* 4 h, Table I).

As shown in Figs. 2 and 3, the epoxy resin used to secure the fused-silica restrictor in the stainless-steel tube did not add significant contaminants to the extracts since none of the SFE [*e.g.*, 400 atm CO_2–methanol (90:10) at 60°C and 400 atm $CHClF_2$ at 100°C] extractable components from the 0.5-g cured epoxy resin sample (Fig. 2iii, iv and Fig. 3iii, iv) were detected in the collection solvent from the blank extractions using the clad restrictors (Fig. 2i, ii and Fig. 3i, ii). However, trace amounts (ppb concentration) of several other components were found in the collection solvent from the clad restrictor evaluation, though the majority of

TABLE I

BREAKING TIMES FOR FUSED-SILICA RESTRICTORS AND STAINLESS-STEEL CLAD FUSED-SILICA RESTRICTORS WITH DIFFERENT SUPERCRITICAL FLUIDS

Supercritical fluid	Time[a]			
	29 μm I.D. × 370 μm O.D. restrictor	32 μm I.D. × 145 μm O.D. restrictor	29 μm I.D. × 370 μm O.D. stainless-steel clad restrictor	32 μm I.D. × 145 μm O.D. stainless-steel clad restrictor
400 atm 60°C or 150°C CO_2	>4 h	>4 h	>4 h	>4 h
400 atm 80°C CO_2–toluene (90:10)	>4 h	>4 h	>4 h	>4 h
400 atm 60°C CO_2–methanol (90:10)	Broke (28 ± 5 min)	Broke (5 ± 2 min)	>4 h	>4 h
400 atm 100°C $CHClF_2$	Broke (23 ± 3 min)	Broke (7 ± 5 min)	>4 h	>4 h

[a] >4 h is the time taken to pump the contents of a 260-ml syringe pump through the restrictor and the time in parentheses is the time elapsed before the restrictor physically broke. All the evaluations were carried out in triplicate.

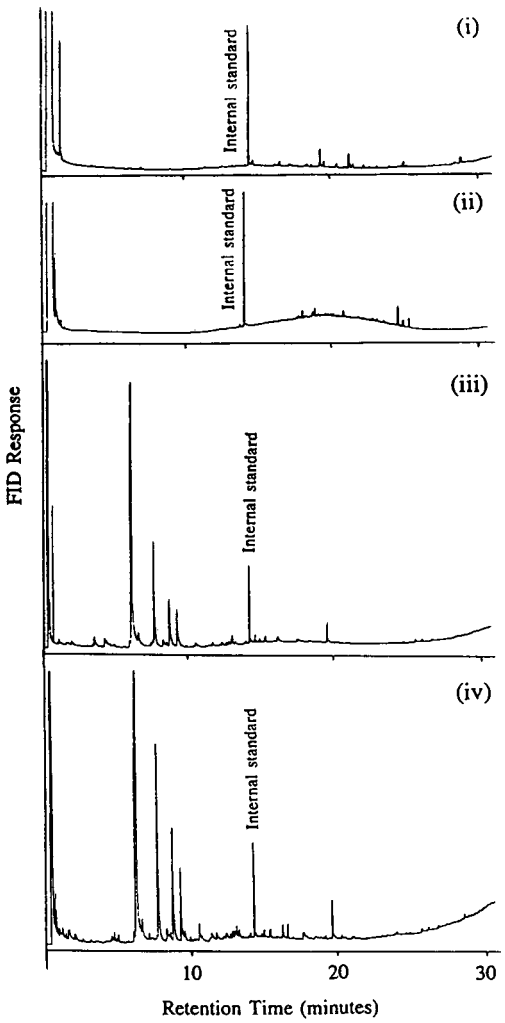

Fig. 2. Gas chromatography with flame ionization detection (GC–FID) analysis of the collection solvent used to collect the extracts from: (i) CO_2–methanol (90:10) using a stainless-steel clad fused-silica restrictor; (ii) $CHClF_2$ (Freon 22) using a stainless-steel clad fused-silica restrictor; (iii) a 0.5-g sample of cured epoxy resin extracted with CO_2–methanol (90:10); (iv) a 0.5-g sample of cured epoxy resin extracted with $CHClF_2$. Analysis was performed on a 25 m × 0.32 mm I.D. (0.17 μm film thickness) HP-5 fused-silica capillary column with an oven temperature program of 40°C followed by a temperature ramp at 8°C/min to 300°C. Phenanthrene was the internal standard (54 μg was added to the 5 ml collection solvent used for the epoxy resin extract and 3 μg was added to the 5 ml collection solvent used for the restrictor evaluation). The detection limit for the internal standard was *ca.* 75 pg in the splitless mode (3:1 signal-to-noise ratio).

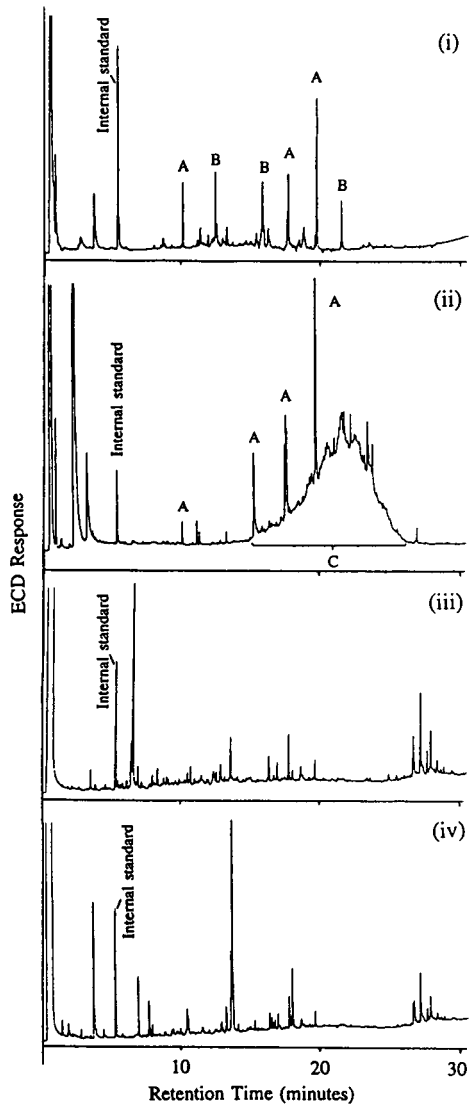

Fig. 3. Gas chromatography with electron capture detection (GC–ECD) analysis of the collection solvent used to collect the extracts from: (i) CO_2–methanol (90:10) using a stainless-steel clad fused-silica restrictor; (ii) $CHClF_2$ (Freon 22) using a stainless-steel clad fused-silica restrictor; (iii) a 0.5-g sample of cured epoxy resin extracted with CO_2–methanol (90:10); (iv) a 0.5-g sample of cured epoxy resin extracted with $CHClF_2$. Peaks marked A were contaminants from the acetone collection solvent, B from the methanol-modified CO_2, and C from the $CHClF_2$ extraction fluid. GC column and temperature program conditions were the same as Fig. 2. 1,2,4-Trichlorobenzene was the internal standard (2.0 μg added to the 5 ml collection solvent used for the epoxy resin extract and 0.2 μg added to the 5 ml collection solvent used for the restrictor evaluation). The detection limit for the internal standard was *ca.* 2 pg in the splitless mode (3:1 signal-to-noise ratio).

these were artifacts found to be from the collection solvent (acetone), the modifier (methanol), or the $CHClF_2$ extraction fluid (Fig. 3i, ii). Furthermore, since the trace contaminants were also present in the collection solvent when using a conventional unclad fused-silica restrictor, it is clear that the epoxy resin used to construct the stainless-steel clad restrictors did not contribute detectable contaminants to the SFE extracts. (Note, Clark and Jones [7] also successfully used the epoxy resin "Epo-tek 353 ND" to secure a fused-silica restrictor to a capillary column in a SFC system, and no contaminants from the epoxy resin were detected in the chromatograms.)

CONCLUSIONS

The breakage of fused-silica restrictors which occurs with polar supercritical fluids was prevented by securing the restrictor inside a stainless-steel tube with an epoxy resin. The stainless-steel clad fused-silica restrictors are simple, inexpensive, several restrictors can be made in an hour, and the epoxy resin does not contribute significant contaminants to the SFE extracts. The clad restrictor is also easy to connect to the extraction apparatus since a standard 1/16 in. stainless-steel ferrule can be used.

ACKNOWLEDGEMENTS

The financial support of the US Environmental Protection Agency (EMSL-LV), and the joint support of the American Petroleum Institute and the US Department of Energy are gratefully acknowledged, as are instrument loans from ISCO.

REFERENCES

1 S.B. Hawthorne, D.J. Miller, M.D. Burford, J.J. Langenfeld, S. Eckert-Tilotta and P.K. Louie, *J. Chromatogr.*, 15 (1993) 1.
2 H. Engelhardt and P. Haas, *J. Chromatogr. Sci.*, 31 (1993) 13.
3 W.H. Griest, R.S. Ramsey, C.H. Ho and W.M. Caldwell, *J. Chromatogr.*, 600 (1992) 273.
4 N.L. Porter, A.F. Rynaski, E.R. Campbell, M. Saunders, B.E. Richter, J.T. Swanson, R.B. Nielsen and B.J. Murphy, *J. Chromatogr. Sci.*, 30 (1992) 367.
5 S.M. Pyle and M.M. Setty, *Talanta*, 38 (1991) 1125.
6 B.C. Bunker, D.M. Haaland, T.A. Michalske and W.L. Smith, *Surf. Sci.*, 222 (1986) 95.
7 J. Clark and B.A. Jones, *J. High Resolut. Chromatogr.*, 15 (1992) 341.

Journal of Chromatography, 648 (1993) 451–457
Elsevier Science Publishers B.V., Amsterdam

CHROM. 25 327

Supercritical fluid chromatographic separation of fatty acid methyl esters on aminopropyl-bonded silica stationary phase

Keiji Sakaki

National Institute of Materials and Chemical Research, Tsukuba, Ibaraki 305 (Japan)

(First received December 11th, 1992; revised manuscript received May 18th, 1993)

ABSTRACT

Aminopropyl-bonded silica packings with various bonding densities were prepared, and the separation behaviour of fatty acid methyl esters on the prepared packings was investigated by supercritical fluid chromatography. The chromatographic behaviour of the esters could be described by two kinds of selectivity: selectivity according to the chain-length and selectivity according to the degree of unsaturation. The selectivity according to chain length increased with the aminopropyl bonding density of the packing. On the other hand, the selectivity according to degree of unsaturation decreased as the aminopropyl bonding density increased. These selectivities were useful for the characterization of commercially available amino-bonded packings.

INTRODUCTION

Amino-bonded silica has often been used for the separation of saccharides by high-performance liquid chromatography (HPLC) [1–3]. This packing material has also been used in supercritical fluid chromatography (SFC) [4,5] and found to be useful in the separation of fatty acid esters [6]. However, there are few kinds of amino-bonded packings commercially available compared with octadecyl-bonded packings, and chromatographic behaviour on an amino-bonded stationary phase has not yet been fully investigated by SFC.

In this study, aminopropyl-bonded silicas with various bonding densities were prepared, and the supercritical fluid chromatographic behaviour of fatty acid methyl esters on the prepared packings was investigated.

EXPERIMENTAL

Preparation of the packing

Aminopropyl-bonded silica was prepared as previously reported by Jones *et al.* [7]. Two types of silica, Wakosil II-5sil-100 (10 nm pore size, 5 μm, Wako, Tokyo, Japan) and Finesil 100-5 (10 nm pore size, 5 μm, Jasco, Tokyo, Japan), were used to prepare the aminopropyl-bonded packings. Silica was dried *in vacuo* at 393 K over 4 h prior to its reaction with silane. A 3-g amount of silica gel was placed in a 200-ml round-bottomed flask and refluxed in 50 ml of dry hexane (stored over molecular sieves 3A 1/16 inch) with 3-aminopropyltriethoxysilane (Aldrich, Milwaukee, WI, USA) for 30 min. After the reaction, the slurry was filtered through glass microfibre and washed with hexane, acetone and methanol. The prepared packings were then

0021-9673/93/$06.00

dried *in vacuo* at 373 K over 24 h. The carbon and nitrogen contents of the packings were determined by elemental analysis.

Preparation of the column

The packing equipment used consisted of a slurry reservoir of 20 ml and a stainless-steel column of 150 × 4.6 mm I.D. A 1.5-g amount of packing was suspended in 20 ml of water and the slurry was placed in the reservoir. The slurry was forced into the column and compressed to a compact bed by pumping methanol at 35 MPa. The solvent in the prepared column was replaced with acetone, then replaced with hexane, and finally the columns were completely purged by passing supercritical CO_2.

Supercritical fluid chromatography

The chromatographic system used has been described previously [8]. Not only the prepared packed columns but also three commercially available columns, Cosmosil NH_2 (10 μm, 150 × 4.6 mm I.D., Nacalai tesque, Kyoto, Japan), Wakosil NH_2 (5 μm, 150 × 4.6 mm I.D., Wako) and Super NH_2 (10 μm, 150 × 4.6 mm I.D., Jasco), were tested. Myristic acid ($C_{14:0}$), palmitic acid ($C_{16:0}$), stearic acid ($C_{18:0}$), oleic acid ($C_{18:1}$), linoleic acid ($C_{18:2}$) and α-linolenic acid ($C_{18:3}$) methyl esters were used as test samples. Fatty acid methyl esters derived from fish oil were also separated on each column. The eluent was monitored with a UV detector at 200 nm.

Liquid chromatography

In order to characterize the prepared packings, the retention behaviour of glucose and fructose on each packing was investigated in liquid chromatograpy. An acetonitrile–water mixture (4:1) was used as mobile phase. The saccharides were detected with a refractive index detector.

RESULTS AND DISCUSSION

The carbon and nitrogen contents of the packings prepared at various silane concentrations are listed in Table I. Wakosil II originally contained carbon, which was probably derived from the surfactant added in the process of synthesizing silica gel. Thus, the carbon content in Table I shows the sum of carbon contents derived from the added surfactant and the bonding aminopropyl groups. In this report, the aminopropyl bonding density of each packing was calculated on the basis of its nitrogen content. A plot of aminopropyl bonding density *vs.* silane:silica ratio is shown in Fig. 1. The bonding density increased with silane:silica ratio, and above 20% (w/w) it gradually levelled off. Jones *et al.* [7] determined the support loading of the prepared packings by measuring the weight loss after combustion, and in their study the support

TABLE I

CARBON AND NITROGEN CONTENTS AND BONDING DENSITIES OF PREPARED PACKINGS

Carbon and nitrogen contents were determined by elemental analysis, and bonding density was calculated on the basis of nitrogen content.

Packing	Silane:silica ratio (%, w/w)	C (%, w/w)	N (%, w/w)	Bonding density (mmol/g)
Wakosil II	–	1.38	–	–
WN1	5.3	2.82	0.16	0.11
WN2	10.1	3.79	0.58	0.41
WN3	20.6	5.48	1.13	0.81
WN4	26.4	5.97	1.18	0.84
WN5	33.0	5.03	1.13	0.81
WN6	41.1	6.19	1.34	0.96
WN7	52.7	5.34	1.27	0.91
Finesil	–	0.08	–	–
FN1	33.0	3.78	1.08	0.77

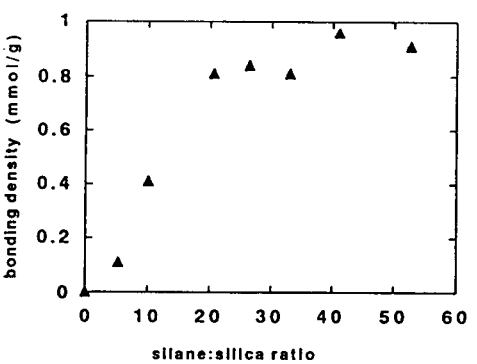

Fig. 1. Dependence of aminopropyl bonding density on silane:silica ratio (in %, w/w).

loading increased with silane:silica ratio without levelling off. They also investigated the liquid chromatographic behaviour of saccharides on the prepared packings in order to evaluate the state of bonding on the silica surface, and concluded that the polymerization of the silane monomers was predominant above a support loading of 8.5% (w/w), whereas the capacity factor was constant for a particular sugar. In this study, the retentions of glucose and fructose on the prepared packings were measured by LC, and the result is shown in Fig. 2. The capacity factors of both saccharides increased with bonding density with no plateau. Figs. 1 and 2 show that in this study silane monomers at a silane:silica ratio higher than 20% (w/w) did not take part in the reaction on the silica surface, and only very little polymerization of the silane monomers occurred on the silica surface even at high silane concentration. This is because the reaction mixtures contained little water, which causes the polymerization of silane monomers.

The highest bonding density achieved in this experiment was about 1 mmol per g of packing, and this is equivalent to 2.9 μmol/m^2 considering the surface area of Wakosil II (350 m^2/g according to the catalogue). The average value of the surface hydroxyl concentration of silica is about 8 μmol/m^2 [9,10], and one molecule of a trifunctional silane reacts with one or two hydroxyl groups on the silica surface [11]. This information shows that some hydroxyl groups remained on the surface of each prepared packing, even on the packing of maximum bonding density.

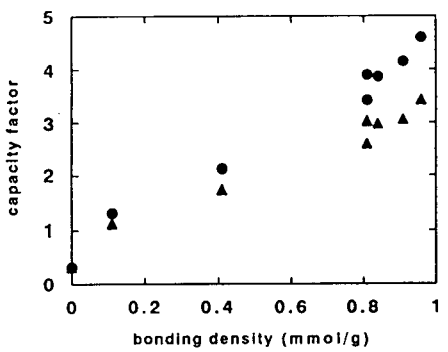

Fig. 2. Dependence of capacity factors of (●) glucose and (▲) fructose on aminopropyl bonding density in liquid chromatography. Mobile phase: acetonitrile–water (4:1). Temperature: 303 K.

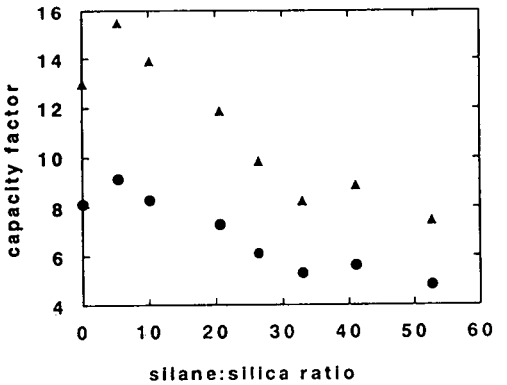

Fig. 3. Dependence of capacity factors of (●) palmitic acid and (▲) linoleic acid methyl esters on silane:silica ratio (in %, w/w). Base silica, Wakosil II; mobile phase, CO_2; temperature 313 K; outlet pressure, 15 MPa.

The capacity factors in SFC of palmitic acid and linoleic acid methyl esters are plotted as a function of silane concentration in Fig. 3. The solute retentions were measured at 313 K and 15 MPa. Except for the results on silica alone, the capacity factors of both esters decreased with an increase in the silane:silica ratio up to about 30% (w/w). Above this value, the capacity factor (k') of each ester remained constant. The same retention data are plotted as a function of the bonding density of the packings in Fig. 4. Although the capacity factor decreased with the bonding density, it varied widely at high bonding density. The variation in the k' value observed at high bonding density can be regarded as reflect-

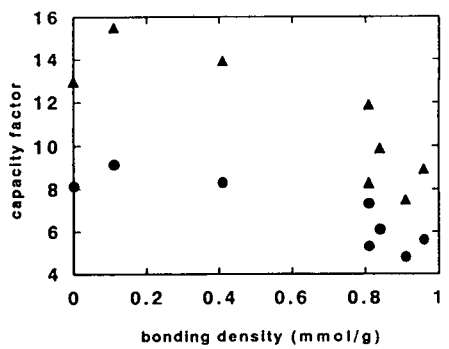

Fig. 4. Dependence of capacity factors of (●) palmitic acid and (▲) linoleic acid methyl esters on aminopropyl bonding density. See Fig. 3 for conditions.

ing a difference in the state of the bonding phase, for example a difference in the average number of hydroxyl groups reacting with one molecule of trifunctional silane (between one and two [11]), or the occurrence of uncontrollable polymerization caused by a slight amount of water in the reaction mixture. In the case of the separation of saccharides by LC, the k' value did not vary greatly at high bonding density, as shown in Fig. 2. The difference in the retention properties between SFC and LC may be because chromatographic behaviour in SFC is more sensitive to the properties of the stationary phase than in LC [5,12–16].

In our previous studies [16,17], the retention behaviour of fatty acid methyl esters on octadecylsilyl (ODS)-bonded silicas was investigated by SFC. In the case of the separation of esters by SFC, a well-end-capped ODS silica gave a smaller capacity factor than bare silica at the same pressure and temperature. For example, the k' value of methyl palmitate on ODS silica was less than 1 at 313 K and 15 MPa [16,17], and it was much smaller than the value on bare silica ($k' = 8$ on Wakosil II in Fig. 3). This suggests that the polarity of the packing contributes to the intensity of solute retention. The aminopropyl group is less polar than the hydroxyl group on a silica surface, so an increase in aminopropyl bonding density leads to a decrease in the polarity of packings and thus to a decrease in capacity factors.

On an ODS column, fatty acid esters were separated from one another depending upon the difference in chain length and the degree of unsaturation [16,17]. On an ODS packing, esters with long hydrocarbon chains and low degrees of unsaturation were retained strongly. It is reasonable to expect that the capacity factors of esters are also correlated with their chain length and degree of unsaturation on aminopropyl-bonded silicas. Fig. 5 shows the plots of capacity factor *vs.* carbon number of fatty acids on prepared packings, and Fig. 6 shows the plots of capacity factor and the number of double bonds of fatty acids. The capacity factors of myristic acid, palmitic acid and stearic acid methyl esters are shown in Fig. 5, and the capacity factors of stearic acid, oleic acid, linoleic acid and linolenic

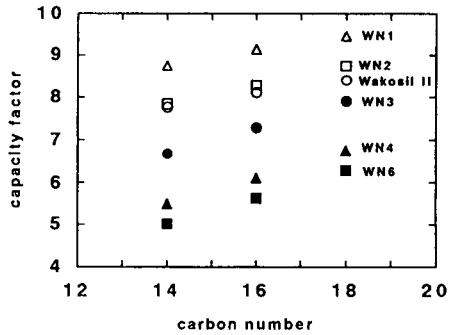

Fig. 5. Plots of capacity factors of saturated fatty acid methyl esters on each prepared packing *vs.* carbon number of fatty acids. Myristic acid, palmitic acid and stearic acid methyl esters were used as samples. See Fig. 3 for conditions.

acid methyl esters are shown in Fig. 6. Esters with more double bonds were strongly retained, the opposite to what was observed on ODS silicas.

As Figs. 5 and 6 show, the retention of fatty acid methyl esters depends on their chain length and degree of unsaturation. Thus the selectivity of esters can be divided into two types: selectivity according to the difference in carbon number and selectivity according to the difference in the number of double bonds. In this study, the former and the latter are indicated by α_{CN} and α_{DB}, respectively, and defined as follows:

$$\alpha_{CN} = k'(C_{16:0})/k'(C_{14:0})$$

$$\alpha_{DB} = k'(C_{18:1})/k'(C_{18:0})$$

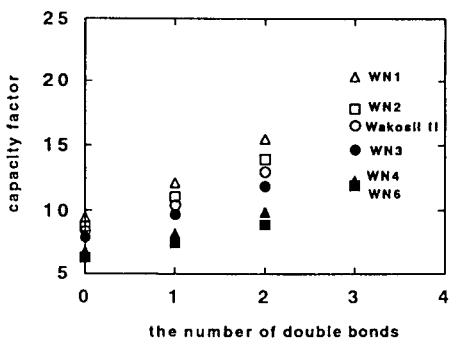

Fig. 6. Plots of capacity factors of fatty acid methyl esters on each prepared packing *vs.* the number of double bonds of fatty acids. Stearic acid ($C_{18:0}$), oleic acid ($C_{18:1}$), linoleic acid ($C_{18:2}$) and α-linolenic acid ($C_{18:3}$) methyl esters were used as samples. See Fig. 3 for conditions.

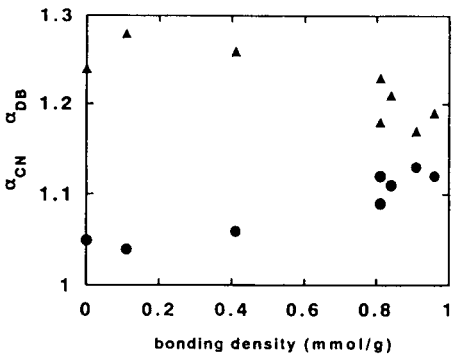

Fig. 7. Dependence of (●) α_{CN} and (▲) α_{DB} on aminopropyl bonding density. See Fig. 3 for conditions.

Fig. 7 shows the relation between the two selectivities and bonding density. With the exception of the value on bare silica α_{DB} decreased as bonding density increased. On the other hand, α_{CN} increased with bonding density. As described above, the ester with more double bonds was retained strongly on aminopropyl-bonded silicas ($\alpha_{DB} > 1$); on the other hand, it was retained weakly on ODS silicas ($\alpha_{DB} < 1$). This suggests that α_{DB} should be closely related to the polarity of packings. The decrease in α_{DB} can be attributed to the decrease in packing polarity with the increase in bonding density. The increase in α_{CN} with bonding density can be attributed to the increase in the number of hydrocarbon chains on the silica surface. This view is supported by the high α_{CN} value observed on an ODS packing that has longer hydrocarbon chains on its surface. For example, the value of α_{CN} on a commercial ODS column was about 1.4 at 313 K and 15 MPa [16,17], although the value of α_{CN} on each aminopropyl-bonded silica was below 1.13. It is also well known that in reversed-phase LC chromatographic selectivity depends strongly on the bonding density or carbon content of the packings.

The prepared aminopropyl-bonded silica columns and three commercial amino-bonded silica columns were used for the separation of methyl esters derived from fish oil. The supercritical fluid chromatograms of the esters derived from fish oil are shown in Fig. 8. The esters were separated at 313 K, and the separation pressures were 20 MPa for Wakosil II and WN2, 15 MPa for WN4, WN6, FN1 and Super NH_2, 12 MPa for Wakosil NH_2, and 10 MPa for Cosmosil NH_2. On bare silica packing (Wakosil II), the esters were separated according to their degree of unsaturation. On the aminopropyl-bonded silica packings of high bonding density, the esters were better separated from one another because of the increase in the selectivity according to chain length.

Some differences in the separation behaviour of the esters were observed with the commercial amino-bonded silica columns. The observed differences could arise from differences in the properties of the base silica used as well as the aminopropyl bonding density. For the characterization of the aminopropyl-bonded silica packings, the effects of chain length and degree of unsaturation of esters on the chromatographic retention and selectivity were investigated. Figs. 9 and 10 show the plots of k' ($C_{18:1}$) *vs.* k' ($C_{16:0}$) and α_{DB} *vs.* α_{CN}, respectively. A plot of k' ($C_{18:1}$) *vs.* k' ($C_{16:0}$) gives a straight line regardless of the type of base silica used. Fig. 10 indicates that aminopropyl-bonded packings with higher α_{CN} values generally exhibit lower α_{DB} values. The plots for the packings with the same base silica, WN1 to WN7, made one curve, and the points of the commercial packings deviated from the curve. The difference in chromatographic behaviour observed among commercial amino-bonded packings in Fig. 8 is based on the difference in α_{CN} and α_{DB}. Fig. 10 is useful for the evaluation of amino-bonded packings.

CONCLUSIONS

Aminopropyl-bonded silicas with varying bonding densities were prepared, and the supercritical fluid chromatographic behaviour of the fatty acid methyl esters on the prepared packings was investigated. As the aminopropyl bonding density increased, the selectivity according to the chain length of esters increased. On the other hand, the selectivity according to the degree of unsaturation of esters decreased with the increase in the aminopropyl bonding density. As to the separation of fatty acid esters, the aminopropyl-bonded silicas, including commercially

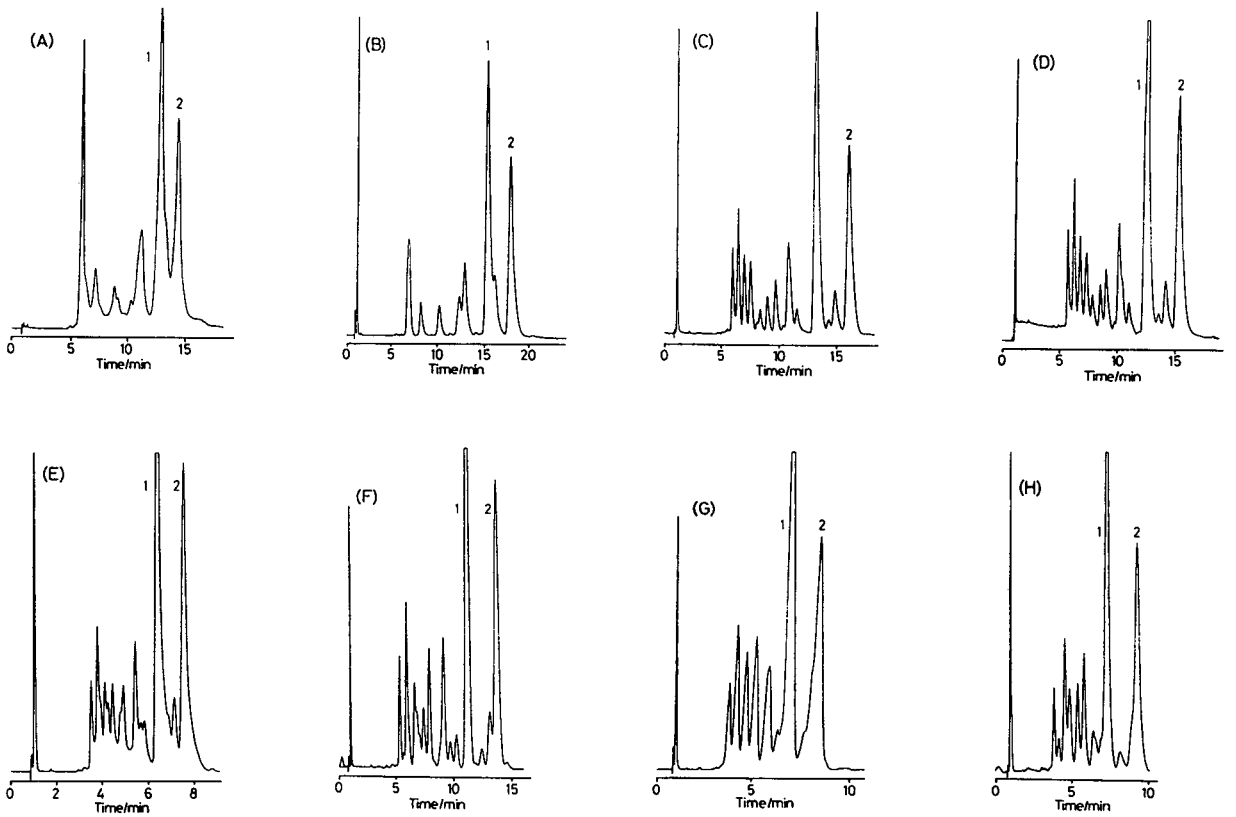

Fig. 8. Separation of methyl esters derived from fish oil. Temperature 313 K, flow-rate 1.4 l/min. (A) Column Wakosil II, outlet pressure 20 MPa; (B) column WN2, outlet pressure 20 MPa; (C) column WN4, outlet pressure 15 MPa; (D) column WN6, outlet pressure 15 MPa; (E) column FN1, outlet pressure 15 MPa; (F) column Super NH_2, outlet pressure 15 MPa; (G) column Wakosil NH_2, outlet pressure 12 MPa; (H) column Cosmosil NH_2, outlet pressure 10 MPa. 1 = eicosapentaenoic acid ($C_{20:5}$) methyl ester; 2 = docosahexaenoic acid ($C_{22:6}$) methyl ester.

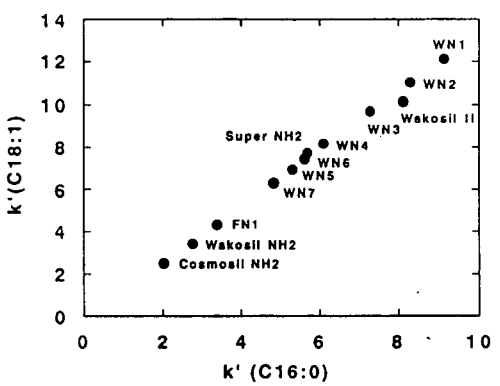

Fig. 9. Correlation between k' ($C_{18:1}$) and k' ($C_{16:0}$) on various packings. See Fig. 3 for conditions.

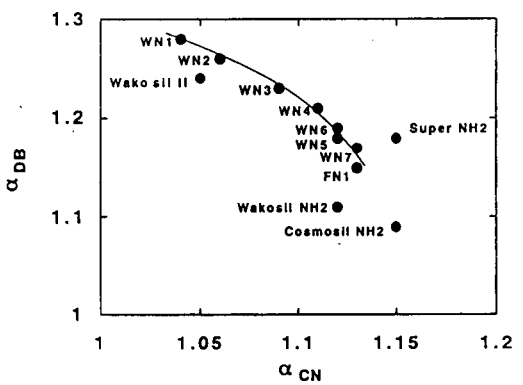

Fig. 10. Correlation between α_{DB} and α_{CN} on various packings. See Fig. 3 for conditions.

available amino-bonded silicas, were well characterized by two kinds of selectivities, α_{CN} and α_{DB}.

REFERENCES

1 R. Schwarzenbach, *J. Chromatogr.*, 117 (1976) 206.
2 S.R. Abbott, *J. Chromatogr. Sci.*, 18 (1980) 540.
3 L.W. Doner and L.M. Biller, *J. Chromatogr.*, 287 (1984) 391.
4 M. Ashraf-Khorassani and L.T. Taylor, *J. Chromatogr. Sci.*, 26 (1988) 331.
5 L.T. Taylor and H-C.K. Chang, *J. Chromatogr. Sci.*, 28 (1990) 357.
6 K. Sakaki, in S. Furusaki, I. Endo and R. Matsuno (Editors), *Biochemical Engineering for 2001, Proc. Asia–Pacific Biochemical Engineering Conference 1992*, Springer, Tokyo, 1992, p. 563.
7 A.D. Jones, I.W. Burns, S.G. Sellings and J.A. Cox, *J. Chromatogr.*, 144 (1977) 169.
8 K. Sakaki and H. Hirata, *J. Chromatogr.*, 585 (1991) 117.
9 K.K. Unger, *Porous Silica*, Elsevier, Amsterdam, (1979).
10 P.K. Iler, *J. Chromatogr.*, 209 (1981) 341.
11 K.K. Unger, *J. Chromatogr.*, 125 (1976) 115.
12 H. Engelhardt, A. Gross, R. Mertens and M. Petersen, *J. Chromatogr.*, 477 (1989) 169.
13 E. Lesellier, A. Tchapla, M.-R. Pechard, C.R. Lee and A.M. Krstulović, *J. Chromatogr.*, 557 (1991) 59.
14 A. Nomura, J. Yamada and K. Tsunoda, *J. Chromatogr.*, 448 (1988) 87.
15 A. Nomura, J. Yamada, K. Tsunoda, K. Fukushima and K. Nobuhara, *Anal. Sci.*, 5 (1989) 335.
16 A. Nomura, J. Yamada, K. Tsunoda, K. Sakaki and T. Yokochi, *Anal. Chem.*, 61 (1989) 2076.
17 K. Sakaki, T. Sako, T. Yokochi, T. Sugeta, N. Nakazawa, M. Sato, O. Suzuki and T. Hakuta, *J. Jpn. Oil Chem. Soc.*, 36 (1987) 943.

Journal of Chromatography, 648 (1993) 459–468
Elsevier Science Publishers B.V., Amsterdam

CHROM. 25 382

Characterization of metallothionein isoforms

Comparison of capillary zone electrophoresis with reversed-phase high-performance liquid chromatography

Mark P. Richards*

Nonruminant Animal Nutrition Laboratory, LPSI, Agricultural Research Service, US Department of Agriculture, Building 200, Room 201, BARC-East, Beltsville, MD 20705-2350 (USA)

John H. Beattie

Division of Biochemical Sciences, Rowett Research Institute, Bucksburn, Aberdeen AB2 9SB, Scotland (UK)

(First received March 30th, 1993; revised manuscript received June 7th, 1993)

ABSTRACT

The purpose of this study was to compare and contrast the separation of metallothionein (MT) isoforms by reversed-phase high-performance liquid chromatography (RP-HPLC) with capillary zone electrophoresis (CZE). RP-HPLC was performed on a Vydac C_8 column eluted with a linear acetonitrile gradient. CZE was performed in a 57 cm × 75 μm I.D. fused-silica tube at an operating voltage of 30 kV. Phosphate buffer (10 m*M*) at pH 2.5, 7.0 and 11.0 was used for both separations. CZE at pH 2.5 resolved three distinct peaks of rabbit liver MT which were incompletely resolved at pH 7.0 or 11.0. RP-HPLC at pH 2.5 gave two peaks and the resolution was not as good as with CZE at the same pH. At pH 7.0 and 11.0, RP-HPLC of rabbit liver MT gave a single predominant peak of unresolved MT-1 and MT-2. Purified rabbit liver MT-1 and MT-2 were used to verify the identity of these peaks. In contrast, MT from horse kidney demonstrated three predominant peaks which were best resolved by CZE at pH 11.0, whereas RP-HPLC resolved only two peaks at pH 11.0 and 7.0. At pH 2.5, RP-HPLC of horse kidney MT gave three peaks, though two of the peaks were incompletely separated. We conclude that pH has a considerable impact on the resolution of MT isoforms by CZE and RP-HPLC and that it is possible to exploit changes in pH to optimize the separation of isoforms for a particular species of MT. When samples of human and sheep liver MT-1, both of which exhibit microheterogeneity, were subjected to CZE, a single predominant peak was observed at each pH value. RP-HPLC of human liver MT-1 at pH 2.5 yielded two peaks that were incompletely resolved. Purified chick liver MT and rat liver MT-1 and MT-2 gave a single predominant peak at all pH values on CZE. In contrast, pig liver MT-1 and MT-2 each exhibited multiple peaks when subjected to CZE, the number of which depended on the pH used to separate the MT. In conclusion, CZE, with its orthogonal selectivity, and RP-HPLC make an excellent combination for the separation and characterization of MT isoforms. Because CZE is rapid (run times typically < 10 min) and requires little sample (< 100 nl), MT samples can readily be analyzed by CZE in conjunction with RP-HPLC or other techniques in order to maximize the information obtained about the individual isoforms.

INTRODUCTION

Because of continuing interest in the unique metal-binding properties of the metallothionein (MT) protein, its putative role in heavy-metal metabolism and numerous investigations into the mechanisms involved in MT gene expression, there is a need for analytical techniques that are capable of rapid separation and sensitive detection of MT isoforms. Although immunological-

* Corresponding author.

0021-9673/93/$06.00

based assays such as radioimmunoassay and enzyme-linked immunosorbent assay have been developed to detect extremely low levels of MTs in tissues and physiological fluids [1–3], in general, they lack sufficient molecular specificity to detect the complete range of isoforms that may be present. In order to study the functional significance of individual MT isoforms, analytical techniques that offer a high degree of resolution are required. Reversed-phase high-performance liquid chromatography (RP-HPLC), which separates compounds based on their hydrophobic character, represents one of the most powerful techniques currently available for the isolation, characterization and quantification of MT isoforms [4]. While the resolution of MT isoforms achieved by RP-HPLC is quite good, this technique can involve relatively lengthy analysis times and requires the use of expensive columns and organic solvents. Although it is possible to separate six isoforms from human liver MT in a single chromatographic step using RP-HPLC at neutral pH [5], this is not always possible for MTs isolated from other eukaryotic species which may require prior purification before they are subjected to RP-HPLC. Recently, capillary zone electrophoresis (CZE) which separates compounds based on their charge-to-mass ratio has shown promise as a rapid, effective and quantitative method for the separation of MT isoforms [6,7]. The objectives of this work were to compare and contrast the separation of MT isoforms achieved by RP-HPLC *vs.* that achieved by CZE using a common phosphate buffer system at acidic, neutral and alkaline pH.

EXPERIMENTAL[a]

Instruments

CZE was performed on a P/ACE System 2100 (Beckman Instruments, Palo Alto, CA, USA). A 57.0 cm (50 cm to detector) × 75 μm I.D. fused-silica capillary column was used. RP-HPLC was performed on a Waters (Waters/Millipore, Milford, MA, USA) chromatography system consisting of dual pumps, an autoinjector, a variable-wavelength UV–Vis monitor and a Vydac C_8 pH-stable reversed-phase column (250 × 4.6 mm). Data were collected and processed from both instruments using System Gold software (Beckman Instruments).

Materials

Standard Cd,Zn-MTs were purchased from a commercial source (rabbit liver and horse kidney, Sigma, St. Louis, MO, USA) or were prepared by sequential gel permeation and ion-exchange column chromatography [8]. Chick liver Zn-MT was further purified by RP-HPLC according to the method of Richards and Steele [9] prior to CZE. Rat and human liver MT isoforms were provided by Dr. Chiharu Tohyama (National Institute of Environmental Studies, Tsukuba, Japan). All buffers and chemicals were reagent grade.

Methods

CZE was performed under the following conditions: Prior to each run, the capillary was flushed for 1.0 min with 0.1 *M* NaOH followed by water and 10 m*M* phosphate buffer, pH 2.5, 7.0 or 11.0. Samples of MT were dissolved in deionized water at a final concentration of 1.0 mg/ml and were loaded into the capillary by pressure injection. After a sample was loaded, the run was initiated by applying 30 kV across the capillary. All CZE was conducted at 25°C. RP-HPLC was conducted under the following conditions: samples of MT were dissolved in deionized water at a final concentration of 1.0 mg/ml and loaded onto the column by an autoinjector. Buffer A was 10 m*M* phosphate adjusted to pH 2.5, 7.0 or 11.0. Buffer B consisted of 60% acetonitrile in buffer A. MT Isoforms were eluted at a flow-rate of 1.0 ml/min using a two-part linear gradient consisting of 0% B by 5 min, 0-25% B by 10 min and 25–50% B by 55 min at ambient temperature. Detection of MT isoforms was accomplished by monitoring absorbance at 200 nm (CZE) or 214 nm (RP-HPLC).

[a] Mention of a trade name, proprietary product or specific equipment does not constitute a guarantee or warranty by the U.S. Department of Agriculture and does not imply its approval to the exclusion of other suitable products.

RESULTS

Rabbit liver Cd,Zn-MT subjected to CZE at pH 2.5 yielded three resolved peaks, whereas only two peaks were resolved at pH 7.0 or 11.0 (Fig. 1). To verify the identity of the three peaks obtained from the CZE separation conducted at pH 2.5, samples of purified MT-1 and MT-2 from rabbit liver were subjected to CZE individually or as an equal mixture of each (Fig. 2). Under these conditions, the MT-1 isoform yielded two predominant peaks whereas the MT-2 isoform produced a single predominant peak, thus accounting for the three major peaks detected in Fig. 1. Similarly, horse kidney Cd,Zn-MT subjected to CZE at pH 11.0 yielded three resolved peaks, while at pH 2.5 and 7.0 only two were resolved (Fig. 3).

Overall, RP-HPLC gave the best resolution of Cd,Zn-MT isoforms at pH 2.5, but at this pH only two peaks were resolved for rabbit liver and two to three were incompletely resolved for horse kidney (Figs. 4 and 5). At pH 7.0 or 11.0, rabbit liver MT isoforms coeluted from RP-HPLC, whereas the horse kidney MT-1 and MT-2 isoforms were incompletely resolved.

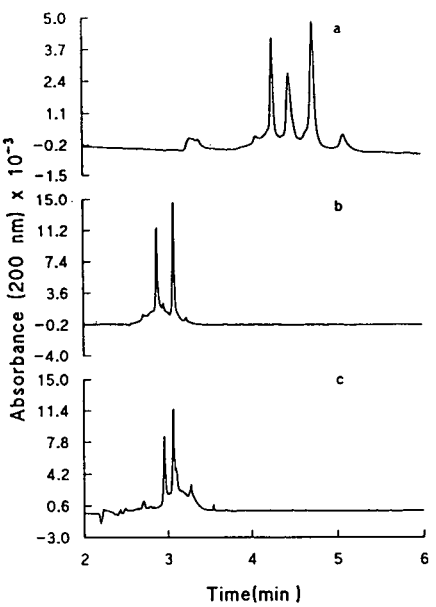

Fig. 1. Capillary zone electropherograms of rabbit liver Cd,Zn-MT conducted at different pH values. MT was dissolved at a concentration of 1.0 mg/ml in deionized water and loaded into the capillary by pressure injection for 1 s. A 57 cm (50 cm to detector) × 75 μm fused-silica, uncoated capillary was used. The running buffer was 10 m*M* sodium phosphate adjusted to pH 2.5, 7.0 or 11.0 and the running voltage was 30 kV. (a) pH 2.5, (b) pH 7.0, (c) pH 11.0.

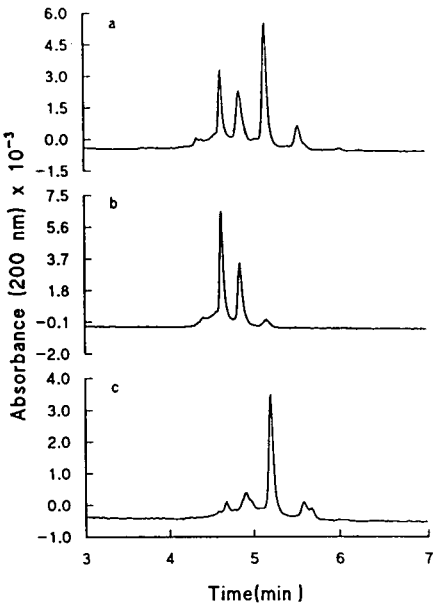

Fig. 2. Capillary zone electropherograms of rabbit liver Cd,Zn-MT isoforms: (a) MT, (b) MT-1, (c) MT-2. Samples of MT isoforms were dissolved at a concentration of 1.0 mg/ml in deionized water and equal volumes of MT-1 and MT-2 solutions were mixed to produce the MT sample. CZE was conducted as described in the caption to Fig. 1 with a running buffer of 10 m*M* sodium phosphate at pH 2.5.

Human liver MT-1, which is known to be heterogeneous, migrated as a single predominant peak on CZE at each of the three pH values tested (Fig. 6), whereas two predominant peaks were incompletely resolved by RP-HPLC at pH 2.5 (Fig. 7). Sheep liver Zn-MT-1, also characterized by microheterogeneity, migrated as a single peak when subjected to CZE (Fig. 8). The order of migration during CZE for the major MT isoforms (MT-1 and MT-2) from sheep liver reversed as the pH was increased from 2.5 to either 7.0 or 11.0 indicating differences in acidic and basic amino acid composition between these two classes of MT.

Rat liver Cd,Zn-MT-1 and Cd,Zn-MT-2 (Fig. 9) and chicken liver Zn-MT (Fig. 10) migrated as single peaks on CZE at each of the pH values tested. As observed with sheep liver Zn-MT, the

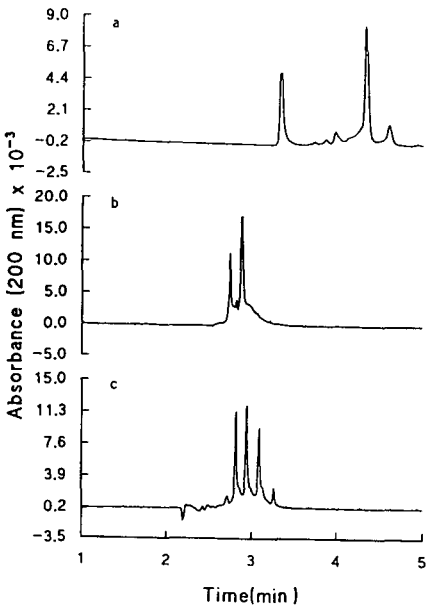

Fig. 3. Capillary zone electropherograms of horse kidney Cd,Zn-MT conducted at different pH values. MT was dissolved at a concentration of 1.0 mg/ml in deionized water and CZE was conducted as described in the caption to Fig. 1. (a) pH 2.5, (b) pH 7.0, (c) pH 11.0.

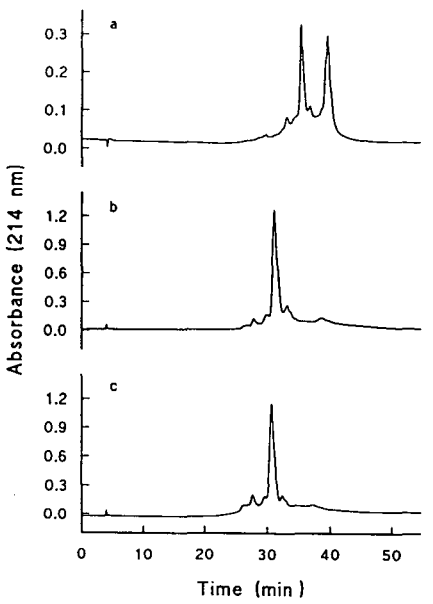

Fig. 4. Rabbit liver Cd,Zn-MT subjected to RP-HPLC at different pH values. MT was dissolved at a concentration of 1.0 mg/ml in deionized water. A 50-μl volume of the MT sample was injected onto a Vydac C_8 pH-stable column (250 × 4.6 mm) and eluted at a flow-rate of 1.0 ml/min with a two-step linear gradient of acetonitrile (CH_3CN) in 10 m*M* sodium phosphate buffer at (a) pH 2.5, (b) pH 7.0 or (c) pH 11.0 (0–30% CH_3CN over 55 min).

order of migration for rat liver MT-1 *vs.* MT-2 was reversed when the pH of the buffer was increased from 2.5 to 7.0 or 11.0. In contrast, pig liver Zn-MT-1 (Fig. 11) and Zn-MT-2 (Fig. 12) exhibited multiple peaks on CZE. The number of peaks depended on the pH.

DISCUSSION

MTs isolated from rabbit liver and horse kidney can be separated into three major peaks using CZE. Further analysis of the two major isoform classes from rabbit liver indicated that two of the major peaks originated from the MT-1 isoform group and the third was determined to be MT-2. Our results clearly demonstrate the power of the alternative separation selectivity associated with CZE. Verification of these species as true MT isoforms must await amino acid sequence analysis of the individually collected peaks. However, our findings are consistent with the work of Klauser *et al.* [10] which demonstrated by RP-HPLC that MT from rabbit liver is comprised of at least four distinct species, while horse kidney MT is comprised of at least three, each differing in their amino acid composition. In addition, we were able to qualitatively assess the stability of our MT standard solutions prepared in deionized water using CZE. Even after several months of storage at 4°C, there was no evidence of additional peaks nor was there any apparent change in MT isoform peak shape or integrated peak area indicative of MT breakdown [7]. These findings also argue against the possibility that the peaks detected in our study were artifacts arising from MT degradation or modification produced prior to or during CZE. The fact that rabbit liver and horse kidney MTs contain both Cd and Zn could lead to the possibility of MTs differing in their metal content (*i.e.*, metalloforms). Metalloforms could conceivably have different properties related to differences in structure. However, we have found that the type of metal bound to MT does not appear to affect isoform migration time for CZE (unpublished results). Therefore, we do not

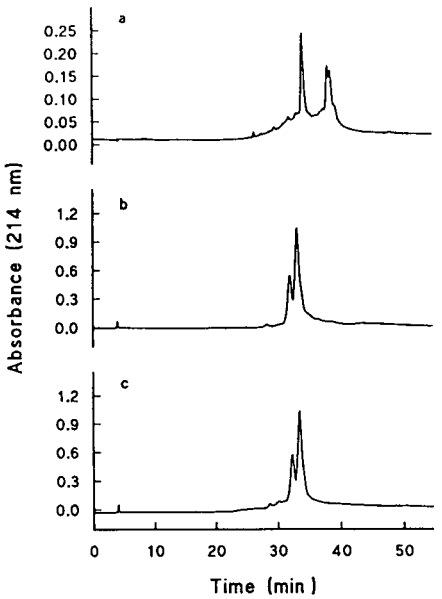

Fig. 5. Horse kidney Cd,Zn-MT subjected to RP-HPLC at different pH values. MT was dissolved at a concentration of 1.0 mg/ml in deionized water and RP-HPLC was conducted as described in the caption to Fig. 4.

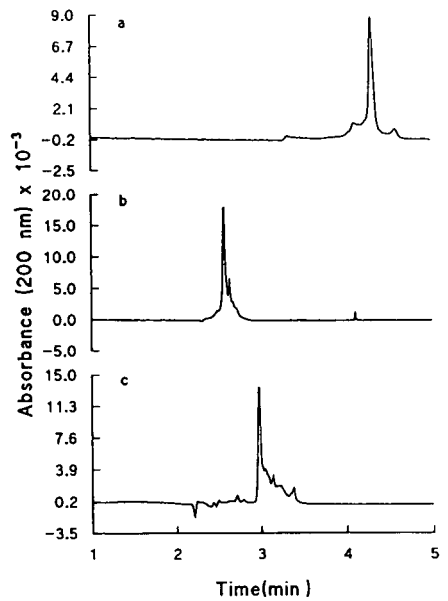

Fig. 6. Capillary zone electropherograms of human liver MT-1 conducted at different pH values. MT-1 was dissolved at a concentration of 1.0 mg/ml in deionized water and CZE was conducted as described in the caption to Fig. 1. (a) pH 2.5, (b) pH 7.0, (c) pH 11.0.

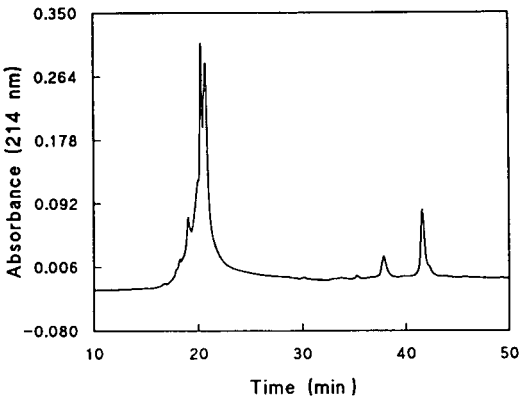

Fig. 7. Human liver MT-1 subjected to RP-HPLC at pH 2.5. MT was dissolved at a concentration of 1.0 mg/ml in deionized water and RP-HPLC was conducted as described in the caption to Fig. 4 with an elution buffer of 10 m*M* sodium phosphate at pH 2.5.

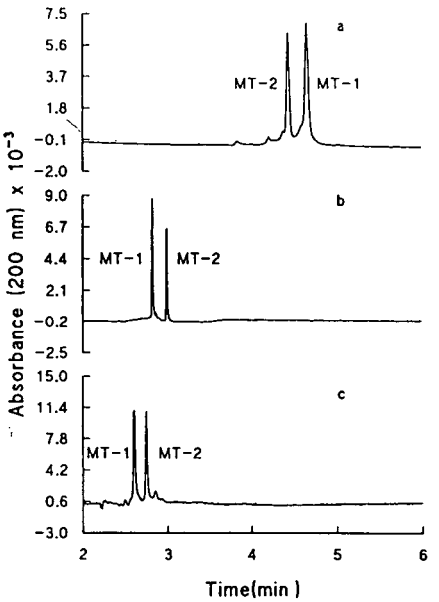

Fig. 8. Capillary zone electropherograms of sheep liver Zn-MT isoforms (MT-1 and MT-2) conducted at different pH values. Samples of MT isoforms were dissolved at a concentration of 1.0 mg/ml in deionized water and equal volumes of MT-1 and MT-2 solutions were mixed to produce the MT sample subjected to CZE. CZE was conducted as described in the caption to Fig. 1. (a) pH 2.5, (b) pH 7.0, (c) pH 11.0.

think that the issue of MT metalloforms represents a complicating factor for interpreting the nature of the individual peaks generated by CZE.

The apparent pH dependency for rabbit liver

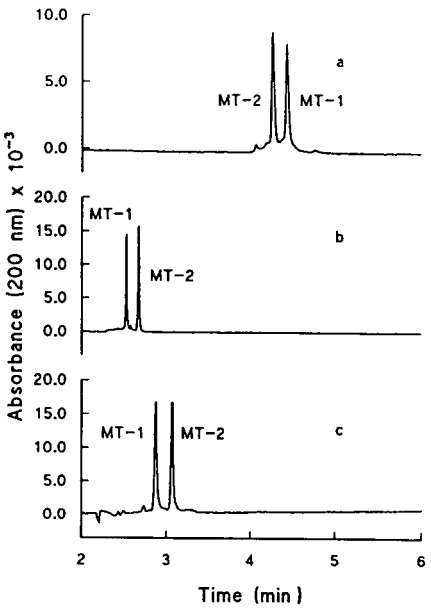

Fig. 9. Capillary zone electropherograms of rat liver Cd,Zn-MT isoforms conducted at different pH values. Samples of MT isoforms were dissolved at a concentration of 1.0 mg/ml in deionized water and equal volumes of MT-1 and MT-2 solutions were mixed to produce the MT sample subjected to CZE. CZE was conducted as described in the caption to Fig. 1. (a) pH 2.5, (b) pH 7.0, (c) pH 11.0.

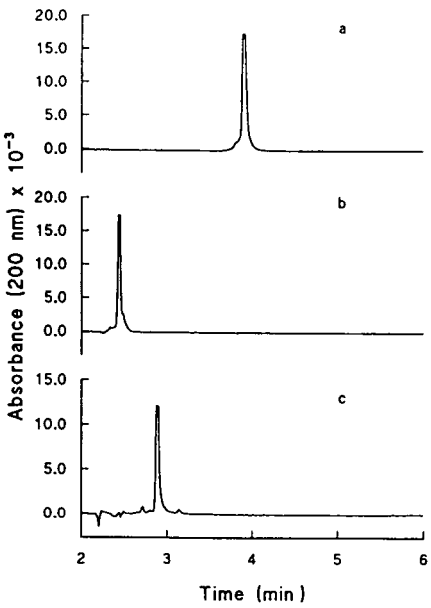

Fig. 10. Capillary zone electropherograms of chicken liver Zn-MT conducted at different pH values. MT was dissolved at a concentration of 1.0 mg/ml in deionized water and CZE was conducted as described in the caption to Fig. 1. (a) pH 2.5, (b) pH 7.0, (c) pH 11.0.

and horse kidney MT isoform separation by CZE is indicative of significant differences in their acidic and basic amino acid contents [11]. Even small changes in pH can produce dramatic shifts in peaks migrating on CZE, especially at or near the p*I* of the protein because of the contributions of both the basic and acidic amino acids to the net charge on the protein molecule. The metal–thiolate bonds characteristic of MT also contribute negative charge to the molecule at neutral pH and above. This coupled with the contributions of the acidic and basic amino acids results in the overall net negative charge on the MT molecule above the p*I* (3.9–4.6) of the protein [11]. Since the amino acid substitutions characteristic of MT isoforms do not change the mass of the polypeptide appreciably, the net charge on the molecule undoubtedly determines its behavior on CZE. This most likely explains the separation of three putative MT isoforms from horse kidney at pH 11.0. Moreover, CZE should prove to be an effective means of separat-

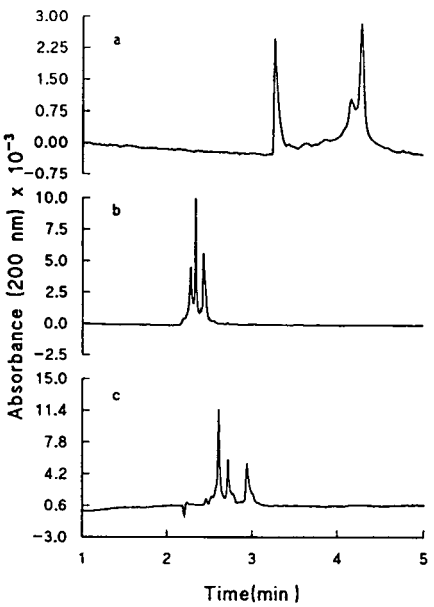

Fig. 11. Capillary zone electropherograms of pig liver Zn-MT-1 conducted at different pH values. MT-1 was dissolved at a concentration of 1.0 mg/ml in deionized water and CZE was conducted as described in the caption to Fig. 1. (a) pH 2.5, (b) pH 7.0, (c) pH 11.0.

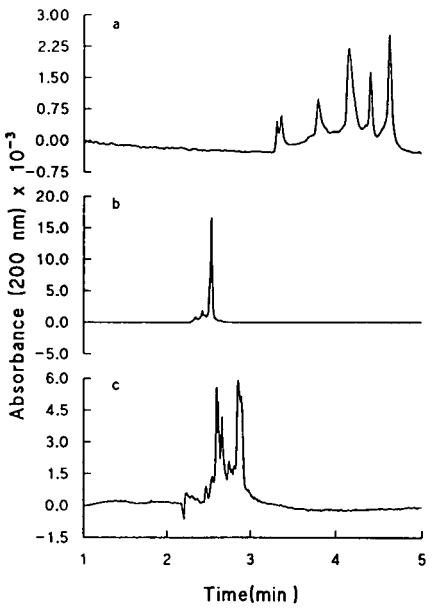

Fig. 12. Capillary zone electropherograms of pig liver Zn-MT-2 conducted at different pH values. MT-2 was dissolved at a concentration of 1.0 mg/ml in deionized water and CZE was conducted as described in the caption to Fig. 1. (a) pH 2.5, (b) pH 7.0, (c) pH 11.0.

ing a newly discovered isoform class of MT (MT-3) which is expressed only in brain tissue and is characterized by the insertion of three additional glutamic acid residues near the carboxyl terminal portion of the molecule (human MT-3) making it unusually acidic [12,13].

In contrast, at low pH (2.5), where rabbit liver MT showed the best resolution of isoforms, the zinc normally associated with the protein would have dissociated leaving either the metal-free protein (thionein) or a partially metalated species containing cadmium which dissociates from thionein at pH 2.0. The existence of partially metalated MT isoforms (*i.e.*, Cd_4-MT-2a) in a sample of rabbit liver MT-2 has recently been demonstrated by electrospray mass spectrometry [14]. Since metal-binding imparts a distinct tertiary structure to thionein [11], it is likely that at low pH different amino acid residues are exposed to the solvent as a result of metal loss and subsequent unfolding of the polypeptide chain. However, if thionein is first prepared in vitro by exposing MT (rabbit liver Cd,Zn-MT-2) to 0.1 *M* HCl, a broad peak is observed when this material is subjected to CZE at pH 2.5 (unpublished results). It would thus appear that differences may exist between subjecting native MT *vs.* thionein to CZE at low pH. This could perhaps reflect differences in structure or stability of the two molecules related to their resultant metal content. It is assumed that metals remain associated with the thionein polypeptide at neutral pH or above. This is apparently true for RP-HPLC conducted at neutral pH [4]; however, it is not currently known what if any loss of metal occurs during CZE at neutral or basic pH. At pH 2.5, even if there is complete dissociation of metal from MT, the quantity present in the buffer and its subsequent dilution would probably result in amounts insufficient to affect the electrophoretic properties of the resulting thionein polypeptide. However, metals such as zinc have been added at m*M* concentrations directly to the running buffer to improve the separation of peptides subjected to CZE under acidic conditions by differentially decreasing their electrophoretic mobilities [15–17]. This approach seems to be particularly effective for small peptides containing histidine [15]. What effects the addition of metals such as zinc to the running buffer might have on the resolution of MT isoforms by CZE at acidic pH remains to be explored. This study demonstrates the utility of altering pH as a means to improve the separation of MT isoforms by CZE.

From a quantitative standpoint, conducting the analysis of MT isoforms by CZE at acidic pH may offer some advantages over a similar analysis at neutral or alkaline pH. By lowering the pH of the running buffer sufficiently to dissociate all of the metals from the isoforms, the absorbance monitored at 200 nm would reflect the peptide portion of the molecule exclusively. Although both RP-HPLC and CZE conducted at neutral or alkaline pH have been successfully applied to the quantification of MT isoforms [4,6,7], the validity of quantitative estimates relies on the fact that no metal is lost from the protein during the isolation procedure. Under these conditions absorbance originating from the metal–thiolate charge transfer contributes significantly to the overall UV absorbance which is the basis for

quantification of the protein. Trifluoroacetic acid (TFA) has previously been reported to be preferable to phosphate–perchlorate for the RP-HPLC separation of MT isoforms because of its volatile nature [10]. More recently, TFA has been employed in the quantitation of individual MT isoforms by RP-HPLC [18]. These authors reported that because of the low pH of the TFA buffer (*ca.* 1.8–1.9), zinc and cadmium would completely dissociate from the thionein protein and thus result in a more accurate estimate of actual protein quantity. Thus, the conduct of CZE or RP-HPLC separations of MT isoforms under acidic conditions may yield better estimates of actual protein quantity [18]. However, the resultant reduction in UV absorbance due to the loss of the metal–thiolate charge transfer under these conditions may also reduce the sensitivity of the technique by raising the limits of detection. Since TFA is not commonly used for CZE separations, we chose to use phosphate buffer in this study in order to compare RP-HPLC and CZE on a common basis. However, it is feasible (though perhaps not optimal) to conduct CZE separations of MT isoforms using TFA (unpublished results) so that comparisons of RP-HPLC and CZE using this buffer are possible. Moreover, it is also possible to analyze peaks collected from RP-HPLC in TFA buffer directly using CZE (unpublished results).

Sheep liver MT-1 has been shown to be encoded by a family of three expressed genes [19]. It could be that the amino acid substitutions characteristic of the sheep MT-1 isoforms are such that they do not change the molecule sufficiently, either in its net charge or its hydrophobic character, to obtain complete separation of the individual isoform species under the conditions employed in this study for CZE and RP-HPLC. Less is known about pig liver MTs, since there has been no in-depth analysis of the genes encoding porcine MT. However, from previous studies of the purified isoMTs from porcine liver, there is some indication of heterogeneity beyond the major MT isoform classes [20,21]. It is also possible that incomplete resolution of the MT-1 and MT-2 isoforms during the prior purification by anion-exchange chromatography resulted in some cross-contamination of the two samples and this occurrence could account for a portion of the observed heterogeneity. The existence of heterogeneity in both the MT-1 and MT-2 isoforms from pig liver detected by CZE in this study is consistent with earlier findings using RP-HPLC [9]. However, as we noted earlier, the ultimate verification of the peaks detected by CZE as distinct MT isoforms depends on subsequent amino acid sequence analysis of the individually collected peaks.

RP-HPLC alone, both as applied in this study and in others [4,10,22] is only capable of resolving the two major MT isoform classes (*i.e.*, MT-1 and MT-2) from rabbit liver and horse kidney. However, if the major MT isoform classes are fractionated by anion-exchange chromatography prior to RP-HPLC, then it is possible to detect additional isoform species for horse kidney and rabbit liver MTs [10]. Without this prior purification step, the different isoform species can co-elute on RP-HPLC and thus would not be detected separately. This was clear from our current study which demonstrated coelution or significant overlap of MT-1 and MT-2 isoform peaks from rabbit liver and horse kidney when subjected to RP-HPLC at pH 7.0 or 11.0. In contrast, human liver MT subjected directly to RP-HPLC under neutral conditions has been successfully fractionated into its component isoforms (six altogether) in a single step [5]. It has been reported that human liver MT-1 consists of five subisoform species whereas MT-2 consists of a singular species. In our study, RP-HPLC of pre-purified rabbit liver MT isoforms (MT-1 and MT-2) at pH 2.5 did detect the presence of two major peaks for MT-1 and a singular peak for MT-2 (data not shown), thus confirming our findings with CZE. Our results with human liver MT-1 subjected to RP-HPLC at pH 2.5 indicated some degree of heterogeneity but the two peaks detected were incompletely resolved. Unfortunately, there was insufficient material to fully characterize the separation of human MT-1 on RP-HPLC at pH 7.0 or 11.0. However, CZE of human liver MT-1 at all three pH values studied failed to discriminate significant heterogeneity, yielding instead a single predominant peak. The reasons for these two findings could be due to the nature of the human MT-1 sample used in

the present study since it has been reported that the relative proportions of the five subisoforms for MT-1 can vary significantly from sample to sample [5]. It is also possible that CZE and RP-HPLC as conducted in this study were not optimized and, therefore, lacked the ability to completely resolve the individual human liver MT-1 subisoform species.

Rat liver MT-1 and MT-2 and chicken MT each of which has been found previously to be comprised of a single species on RP-HPLC [10], migrated as a single peak on CZE. Moreover, by changing the pH of the running buffer it was possible to reverse the migration order of MT-1 and MT-2 on CZE which presumably reflects the differences in the net charge of these two classes of molecules. With all of the changes made in buffer pH, at no time were additional peaks indicative of heterogeneity detected for these MT samples. Taken together, the findings of the present study suggest that MTs from different eukaryotic species behave differently when subjected to RP-HPLC and CZE and that both of these modes of separation require optimization for a particular type of MT in order to achieve the best possible separation of the individual isoforms.

In addition to optimizing the conditions under which RP-HPLC or CZE analyses are conducted, some consideration needs to be given to sample preparation. This is particularly true when attempting to analyze for MT isoforms in complex matrices such as liver cytosol. Although this study made use of purified MT samples, both RP-HPLC [4,10] and CZE [6,7] have also been applied to the analysis of MT isoforms in more complex sample matrices such as heat-treated and solvent-fractionated liver cytosols and cell extracts. In fact, it may be possible to combine both of these techniques by performing solid-phase extraction on a reversed-phase support followed by CZE on the fraction eluted to contain MT.

Because it is becoming apparent that no single separation technique possesses the resolving power necessary to completely separate all of the MT isoforms, a multi-dimensional approach applied to the separation of MT isoforms may represent the best approach. Since CZE and RP-HPLC represent orthogonal separation techniques, a combination of both would give additional capability as opposed to the application of either technique alone. Such a multi-dimensional approach has been successfully applied to the analysis of vasoactive intestinal peptide from rat brain extracts [23] and the separation of tryptic peptides from two species of cytochrome *c* [24]. Moreover, we have shown that CZE can be successfully applied as a second dimension to gel permeation column chromatography for the separation of MT isoforms from a sheep liver cytosol [6]. We have also been able to directly analyze fractions from RP-HPLC using CZE (unpublished results). In this study, the feasibility of a common buffer system for both CZE and RP-HPLC has been demonstrated. Therefore, a combined approach involving initial sample preparation followed by RP-HPLC and CZE may well offer the most complete separation of MT isoforms to date. Clearly, more work is required to assess the potential of such an approach.

In conclusion, CZE is a new analytical technique for the characterization of MT isoforms which offers rapid analysis times, small sample requirements and alternative separation selectivity as compared to RP-HPLC. CZE affords an excellent means of separating MT isoforms that differ in their net charge. By varying the pH of the buffer used in CZE, it is possible to affect the selectivity of the separation. Since CZE separates proteins according to mass and charge and RP-HPLC separations reflect differences in hydrophobicity, the two techniques are complimentary to each other and, therefore, form a powerful combination for the isolation and characterization of MT isoforms.

REFERENCES

1 R.K. Mehra and I. Bremner, *Biochem. J.*, 213 (1983) 459.
2 J.S. Garvey, R.J. Vander Mallie and C.C. Chang, *Methods Enzymol.*, 84 (1982) 121.
3 A. Grider, K.J. Kao, P.A. Klein and R.J. Cousins, *J. Lab. Clin. Med.*, 113 (1989) 221.
4 M.P. Richards, *Methods Enzymol.*, 205 (1991) 217.
5 P.E. Hunziker and J.H.R. Kägi, *Biochem. J.*, 231 (1985) 375.

6 J.H. Beattie, M.P. Richards and R. Self, *J. Chromatogr.*, 632 (1993) 127.
7 M.P. Richards, J.H. Beattie and R. Self, *J. Liq. Chromatogr.*, 16 (1993) 2113.
8 M. Vasak, *Methods Enzymol.*, 205 (1991) 41.
9 M.P. Richards and N.C. Steele, *J. Chromatogr.*, 402 (1987) 243.
10 S. Klauser, J.H.R. Kägi and K.J. Wilson, *Biochem. J.*, 209 (1983) 71.
11 J.H.R. Kägi and Y. Kojima (Editors), *Metallothionein II*, Birkhäuser Verlag, Basel, 1987, p. 25.
12 Y. Uchida, K. Takio, K. Titani, Y. Ihara and M. Tomonaga, *Neuron*, 7 (1991) 337.
13 R.D. Palmiter, S.D. Findley, T.E. Whitmore and D.M. Durnam, *Proc. Natl. Acad. Sci. U.S.A.*, 89 (1992) 6333.
14 X. Yu, M. Wojciechowski and C. Fenselau, *Anal. Chem.*, 65 (1993) 1355.
15 R.A. Mosher, *Electrophoresis*, 11 (1990) 765.
16 H. Kajiwara, *J. Chromatogr.*, 559 (1991) 345.
17 H.J. Issaq, G.M. Janini, I.Z. Atamna, G.M. Muschik and J. Lukszo, *J. Liq. Chromatogr.*, 15 (1992) 1129.
18 M. Wan, J.H.R.H. Kägi and P.E. Hunziker, *Protein Expression Purif.*, 4 (1993) 38.
19 M.G. Peterson, F. Hannan and J.F.B. Mercer, *Eur. J. Biochem.*, 174 (1988) 417.
20 I. Bremner and B.W. Young, *Biochem. J.*, 155 (1976) 631.
21 M. Webb, S.R. Plastow and L. Magos, *Life Sci.*, 24 (1979) 1901.
22 H. van Beek and A.J. Baars, *J. Chromatogr.*, 442 (1988) 345.
23 J. Soucheleau and L. Denoroy, *J. Chromatogr.*, 608 (1992) 181.
24 P.M. Young, N.E. Astephen and T.E. Wheat, *LC·GC*, 10 (1992) 26.

Journal of Chromatography, 648 (1993) 469–473
Elsevier Science Publishers B.V., Amsterdam

CHROM. 25 400

Double-chain surfactant as a new and useful micelle-forming reagent for micellar electrokinetic chromatography

Minoru Tanaka*, Takeshi Ishida, Takashi Araki, Araki Masuyama, Yohji Nakatsuji and Mitsuo Okahara

Department of Applied Chemistry, Faculty of Engineering, Osaka University, Yamada-oka, Suita, Osaka 565 (Japan)

Shigeru Terabe

Department of Material Science, Faculty of Science, Himeji Institute of Technology, Kamigori, Hyogo 678-12 (Japan)

(Received April 8th, 1993)

ABSTRACT

Disodium 5,12-bis(dodecyloxymethyl)-4,7,10,13-tetraoxa-1,16-hexadecanedisulphonate, a surfactant with two ionic groups and two lipophilic chains, was first utilized in micellar electrokinetic chromatography (MEKC). A good linear relationship was obtained between the capacity factors of several model analytes tested and the concentrations of the surfactant. Compared with widely used sodium dodecyl sulphate, this new surfactant exhibited remarkably different selectivity for several substituted naphthalene and benzene derivatives and gave a wider migration time window. MEKC could be performed at surfactant concentrations at most one order of magnitude lower, because of the low critical micelle concentration.

INTRODUCTION

Micellar electrokinetic chromatography (MEKC) [1] was developed for the separation of electrically neutral analytes by electrophoresis with an ionic micellar solution as a separation solution, and has become a method of great importance. The separation principle of MEKC is based on the differential partition of the analyte between the micelle and water. Therefore, selectivity in MEKC is considered to be essentially dependent on the choice of surfactant. Since most analytes interact with micelles at their surfaces, the ionic group is generally more important in terms of selectivity. For instance, for the polar analytes, sodium dodecyl sulphate (SDS) and sodium tetradecyl sulphate exhibit very similar selectivity, but SDS and sodium N-lauroyl-N-methyltaurate yield considerably different selectivity [2]. Corticosteroids cannot be successfully separated with SDS but are completely resolved with sodium cholate [3]. Addition of a second surfactant to form a mixed micelle also affects the selectivity. Mixed micelles are successfully employed in separations of enantiomers [4–6]. The addition of a non-ionic surfactant to an ionic one causes a narrower migration time window because of the lower electrophoretic mobility of the mixed micelle.

Until now, surfactants with one hydrophilic group and one lipophilic chain, especially SDS, have been used widely in MEKC. Recently, synthetic amphipathic compounds with several

* Corresponding author.

0021-9673/93/$06.00

lipophilic chains have attracted much attention as biomimetic functional materials [7]. In our previous papers [8,9], we have shown that amphipathic compounds containing two sulphate or sulphonate groups and two long alkyl chains, which are derived from glycol diglycidyl ethers, have good water solubility and excellent surface-active properties in water. These new types of surfactants have not yet been utilized as micelle-forming reagents in MEKC. Consequently, their use in MEKC is of great interest and is expected to bring about dramatic selectivity changes.

In this paper, preliminary results on the separation behaviour of several model analytes by MEKC using disodium 5,12-bis(dodecyloxymethyl)-4,7,10,13-tetraoxa-1,16-hexadecanedisulphonate (DBTD) as a double-chain surfactant are compared with the results with SDS.

EXPERIMENTAL

Apparatus

An Applied Biosystems Model 270A capillary electrophoresis system (CA, USA) was used with a 72 cm (50 cm from inlet to detector) × 50 μm I.D. fused-silica capillary. On-column UV detection was at 210 nm. The temperature and applied voltage were held constant at 35°C and 15 kV, respectively. Sample solutions ($1.0 \cdot 10^{-2}$% in 10% methanol) were injected by the vacuum technique (12.7 cmHg pressure difference for 0.5 s). For data processing, a Hitachi D-2500 Chromato-Integrator (Hitachi, Japan) was used. All experiments were performed in duplicate to ensure reproducibility.

Reagents

DBTD, whose structure is shown in Fig. 1, was synthesized as reported previously [8]. All other reagents were of analytical-reagent grade and used as received.

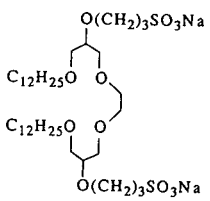

Fig. 1. Structure of a double-chain surfactant, DBTD.

Separation solutions were prepared by dissolving DBTD in a buffer solution of 0.1 *M* sodium dihydrogenphosphate–0.05 *M* sodium borate at pH 7.0. Methanol was used as a marker of the electroosmotic flow and Sudan III as a micelle tracer.

RESULTS AND DISCUSSION

From several double-chain synthetic surfactants bearing two ionic groups, DBTD was chosen in this work because of its low critical micelle concentration (CMC) (0.014 m*M*), low Krafft point (below 0°C) and high purity. On the other hand, SDS has a much higher CMC of 8.1 m*M* and a higher Krafft point of 16°C. It is suggested that MECK may be performed with DBTD at lower concentrations. This will result in low viscosities of separation solutions and in low currents, which is quite favourable for MEKC.

Separation with DBTD

Several benzene and naphthalene derivatives were used as model analytes, and their migration times were measured in the DBTD concentration range of 0–10 m*M* in 0.1 *M* phosphate–0.05 *M* borate buffer at pH 7.0.

Six naphthalene derivatives were baseline separated at DBTD concentrations above 7.5 m*M*. A typical chromatogram is shown in Fig. 2. At DBTD concentrations above 1.0 m*M*, 1- and 2-naphthol could be readily baseline separated. 1,3-Dihydroxybenzene, phenol, nitrobenzene and *p*-nitroaniline were also resolved at DBTD concentrations above 5.0 m*M*.

The capacity factor of a neutral analyte in MEKC can be calculated by the following equation [1].

$$k' = \frac{t_R - t_0}{t_0(1 - t_R/t_{mc})} \quad (1)$$

where t_R, t_0 and t_{mc} are the migration times of the analyte, the solute that does not interact with the micelle (methanol peak) and the micelle (Sudan III peak), respectively. When micellar

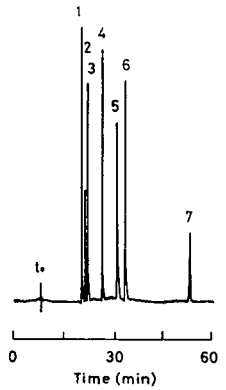

Fig. 2. Separation of naphthalene derivatives with $1.0 \cdot 10^{-2}$ *M* DBTD. Peaks: 1 = 1-naphthalenemethanol; 2 = 1,6-dihydroxynaphthalene; 3 = 1-naphthylamine; 4 = 1-naphthaleneethanol; 5 = 2-naphthol; 6 = 1-naphthol; 7 = Sudan III.

concentrations are low, k' is approximately related to the surfactant concentration by eqn. 2 [10].

$$k' = Kv(C_{sf} - \mathrm{CMC}) \quad (2)$$

where K is the distribution coefficient of the analyte, and v and C_{sf} are the partial specific volume of the micelle and the surfactant concentration, respectively.

The plots of calculated k' *vs.* concentration of DBTD are shown in Figs. 3 and 4 for the naphthalene and benzene derivatives, respectively. Table I gives the results of the regression analyses. For each analyte, a good linear relationship (correlation coefficient range 0.993–

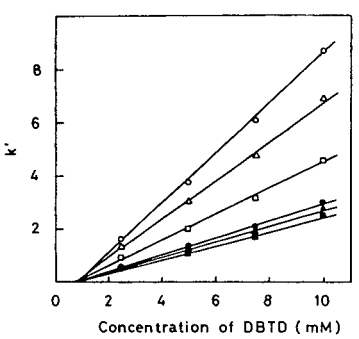

Fig. 3. Dependence of capacity factor (k') of the naphthalene derivatives on concentration of DBTD (C_{sf}). Analytes: ■ = 1-naphthalenemethanol; ▲ = 1,6-dihydroxynaphthalene; ● = 1-naphthylamine; □ = 1-naphthaleneethanol; △ = 2-naphthol; ○ = 1-naphthol.

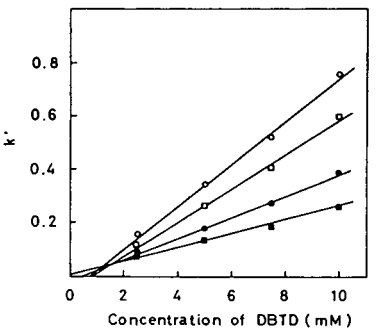

Fig. 4. Dependence of capacity factor (k') of the benzene derivatives on concentration of DBTD (C_{sf}). Analytes: ■ = 1,3-dihydroxybenzene; ● = phenol; □ = nitrobenzene; ○ = *p*-nitroaniline.

0.998) was obtained, which suggests that the distribution coefficients remain constant at least at the DBTD concentrations measured. Similar linear plots were also obtained for SDS.

From eqn. 2, the intercepts of plots in Figs. 3 and 4 extrapolated to $k' = 0$ can be interpreted to be the CMC of the surfactant under the conditions used. The averaged CMC value estimated is 0.76 m*M*, except for 1,3-dihydroxybenzene and phenol exhibiting considerably low k' values. This CMC value is too high in comparison with the measured value of 0.014 m*M* in water. The reason for this discrepancy is not clear at present.

Comparison of selectivity

It is quite interesting and of great value to compare the migration behaviour in DBTD and SDS solutions. As mentioned above, the six naphthalene derivatives were baseline separated at 7.5 m*M* DBTD. Similar separation of the five analytes except for 2-naphthol was attained at an SDS concentration of 50 m*M*. The capacity factors of the analytes at these concentrations are listed in Table II, together with those of the other analytes used here. In MEKC with DBTD, the analytes were eluted in the order given in the first column in the table (from 1,3-dihydroxybenzene to 1-naphthol). Apparently, this elution order is different from that in MEKC with SDS, especially for the naphthalene derivatives. The elution order in the DBTD solution is 1-naphthalenemethanol < 1,6-dihydroxynaphthalene < 1-naphthylamine < 1-naphthaleneethanol < 2-

TABLE I

CORRELATION BETWEEN CONCENTRATION OF DBTD (C_{sf}) AND CAPACITY FACTOR (k')

y = Capacity factor of the analyte; x = concentration of DBTD (2.5–10.0 mM).

Analyte	Regression equation	Correlation coefficient
1,3-Dihydroxybenzene	$y = 0.0248x + 0.0095$	0.993
Phenol	$y = 0.0396x - 0.0171$	0.995
Nitrobenzene	$y = 0.0629x - 0.0475$	0.993
p-Nitroaniline	$y = 0.0793x - 0.0520$	0.995
1-Naphthalenemethanol	$y = 0.260x - 0.176$	0.995
1,6-Dihydroxynaphthalene	$y = 0.296x - 0.207$	0.995
1-Naphthylamine	$y = 0.323x - 0.259$	0.996
1-Naphthaleneethanol	$y = 0.496x - 0.417$	0.994
2-Naphthol	$y = 0.738x - 0.575$	0.995
1-Naphthol	$y = 0.940x - 0.825$	0.998

naphthol < 1-naphthol and 1,6-dihydroxynaphthalene < 1-naphthylamine < 1-naphthalenemethanol < 1-naphthol < 2-naphthol < 1-naphthaleneethanol in the SDS solution. 1-Naphthaleneethanol eluted last and the elution order of 1- and 2-naphthol was reversed in the SDS system. In the SDS system, the isomers could not be baseline separated, though this was readily done in the DBTD system, as described above.

A wide migration time window between t_0 and t_{mc} is favourable for high resolution, although a long analysis time may be required. The t_{mc}/t_0 value is directly related to the width of the migration time window. The larger the value of t_{mc}/t_0, the wider the migration time window. The t_{mc}/t_0 value is about 5.0 for 50 mM SDS and about 6.3 for 7.5 mM DBTD. The value decreases from 5.0 for 50 mM SDS to 4.3 for 7.5 mM SDS.

Thus DBTD shows remarkably different selectivity and a wider migration time window compared with SDS. In general, introduction of new surfactants exhibiting essentially different selectivity and wider migration time windows is desirable for enhancing MEKC performance. Several surface-active properties of DBTD were measured, but its micellar size and shape have not yet been characterized. Therefore, further work is needed to discuss and convincingly explain the above-mentioned selectivity change of DBTD in detail. Attempts to do this are now in progress.

TABLE II

CAPACITY FACTORS OF THE ANALYTES IN 7.5 mM DBTD AND 50 mM SDS

Analyte	Capacity factor	
	DBTD	SDS
1,3-Dihydroxybenzene	0.182	0.220
Phenol	0.261	0.524
Nitrobenzene	0.392	1.36
p-Nitroaniline	0.507	1.08
1-Naphthalenemethanol	1.66	6.70
1,6-Dihydroxynaphthalene	1.89	2.08
1-Naphthylamine	2.04	5.32
1-Naphthaleneethanol	3.07	13.34
2-Naphthol	4.66	7.18
1-Naphthol	6.06	6.99

REFERENCES

1 S. Terabe, K. Otsuka, K. Ichikawa, A. Tsuchiya and T. Ando, *Anal. Chem.*, 56 (1984) 111.
2 H. Nishi, T. Fukuyama, M. Matsuo and S. Terabe, *J. Pharm. Sci.*, 79 (1990) 519.
3 H. Nishi, T. Fukuyama, M. Matsuo and S. Terabe, *J. Chromatogr.*, 513 (1990) 279.
4 A. Dobashi, T. Ono, S. Hara and J. Yamaguchi, *Anal. Chem.*, 61 (1989) 1986.
5 K. Otsuka and S. Terabe, *J. Chromatogr.*, 515 (1990) 221.

6 K. Otsuka, J. Kawahara, K. Tatekawa and S. Terabe, *J. Chromatogr.*, 559 (1991) 209.
7 H. Ringsdorf, B. Schlarb and J. Venzer, *Angew. Chem., Int. Ed. Engl.*, 27 (1988) 113.
8 Y.-P. Zhu, A. Masuyama, T. Nagata and M. Okahara, *J. Jpn. Oil. Chem. Soc. (Yukagaku)*, 40 (1991) 473.
9 Y.-P. Zhu, A. Masuyama and M. Okahara, *J. Am. Oil. Chem. Soc.*, 67 (1990) 459.
10 S. Terabe, K. Otsuka and T. Ando, *Anal. Chem.*, 57 (1985) 834.

Journal of Chromatography, 648 (1993) 475–480
Elsevier Science Publishers B.V., Amsterdam

CHROM. 25 386

Chiral separations using dextran and bovine serum albumin as run buffer additives in affinity capillary electrophoresis

Peng Sun, Nian Wu, Geoffrey Barker and Richard A. Hartwick*

Department of Chemistry, State University of New York at Binghamton, Binghamton, NY 13902 (USA)

(First received March 23th, 1993; revised manuscript received June 10th, 1993)

ABSTRACT

A method utilizing dextran as a run buffer additive in addition to bovine serum albumin (BSA) for chiral separation by means of affinity capillary electrophoresis (ACE) has been developed. By adding different amounts of dextran to the run buffer, the net velocity of BSA can be adjusted to a desired rate. Enantiomers of some drugs [ibuprofen (IB) and leucovorin (LV)] and amino acids (dansyl-DL-leucine and dansyl-DL-norvaline) were separated on a capillary with 20 cm effective length by this method. The effect of dextran concentration on the retention of BSA and resolution of sample enantiomers was studied. Enantiomers of mandelic acid (MA), which have very weak affinity for BSA, were also resolved. Qualitative information pertaining to the binding interaction of the samples with BSA can be obtained by this method.

INTRODUCTION

Many pharmaceutical drugs have asymmetric centers with most of them being used clinically in the racemic form. However, drug enantiomers can have quantitative or even qualitatively different physiological actions. With the improved understanding of the biological action of pharmaceutical drugs with respect to their stereochemistry, investigations concerning the pharmacology and toxicology of individual drug enantiomers have become more and more important. The pharmaceutical industry has, therefore, a tremendous interest in techniques for enantioseparations to investigate the optical purity of drugs. Some proteins, *e.g.* bovine serum albumin (BSA) [1–3], α-acid glycoprotein (α-AGP) [4,5], and ovomucoid [6,7], have been successfully used in high-performance liquid chromatography (HPLC) as stationary phases. However, protein immobilized columns in HPLC often show poor efficiency [8].

Capillary electrophoresis (CE), which has developed considerably during the past ten years, represents an attractive alternative method to HPLC in chiral separation due to its high efficiency and selectivity [9]. Electrokinetic chromatography (EKC), an extension of CE which was introduced by Terabe *et al.* [10], is also very useful in chiral separations. Early work applying the principle of ligand-exchange electrophoresis to CE was done by Zare *et al.* [11]. Cyclodextrin and their derivatives [12,13] as well as chiral crown ethers [14] have been widely used to form inclusion complexes with enantiomers in CE. Chiral resolution has been demonstrated in micellar EKC which employs an ionic micelle as a run buffer modifier [15–17]. Recently, a new method for the determination of the (6*R*) and (6*S*) stereoisomers of leucovorin (LV) using EKC in the affinity mode has been developed in our laboratory [18]. In this method, BSA was used as a run buffer additive to incorporate

* Corresponding author.

0021-9673/93/$06.00

enantiomeric selectivity into the system. Excellent separation of LV isomers was obtained by this method. A major drawback of this method occurs when the net mobility of the sample is similar to that of the run buffer additive, resulting in a loss of enantiomeric resolution unless very long capillaries are employed.

Recently, the dynamic polymer sieving matrices which are called polymer networks, such as low concentration linear polyacrylamide and dextran solution have become a popular technique for DNA and protein separation [19–22]. Karger *et al.* [23] recently used a UV-transparent polymer network of dextran to substitute polyacrylamide with successful molecular mass sieving of SDS–protein complexes. One of the major advantages of using dextran is that the UV-absorbance of dextran is much lower than that of polyacrylamide [23].

In this paper, dextran was employed as a run buffer additive in addition to BSA for chiral separation by means of CE. The addition of different amounts of dextran to the run buffer, allows the net velocity of BSA to be controlled to a desired rate. Enantiomers of some drugs and amino acids, which are difficult to separate using BSA solely as the only buffer additive in CE, can be separated by this method. The effect of dextran concentration on the retention of BSA and the resolution of sample enantiomers is also discussed.

EXPERIMENTAL

Apparatus

The experiments were performed on a laboratory-constructed instrument using a CZE 1000 PN 30 high-power supply (Spellman, Plainview, NY, USA) and a high-power supply local control (Chamonix Industries, Binghamtom, NY, USA). The detector was a Spectra Physics Model 100 and was connected to a Spectra Physics 4400 integrator (Spectra Physics, Reno, NV, USA). Fused-silica capillary (75 μm I.D. × 360 μm O.D., Polymicro Technologies, Phoenix, AZ, USA) was coated with linear polyacrylamide by the method reported by Hjerten [24]. The effective length of capillaries was 20 or 60 cm. The high voltage applied was 300 V/cm. Cooling was achieved by fan.

Procedure

Stock solutions of 5% dextran were made by dissolving dextran in run buffer (10 m*M* phosphate at pH 7.12). Lower concentration solutions were obtained by dilution. Buffer containing BSA (1 mg/ml) was made by dissolving BSA in buffer.

Samples were electrically injected (5 kV × 4 s) from the negative side, and detected at 210 or 230 nm.

Chemicals

Calcium leucovorin (LV) was obtained from Lederle Laboratories, American Cyanamid (Pear River, NY, USA). Ibuprofen (IB), mandelic acid (MA), dansyl-DL-leucine, dansyl-DL-norvaline, BSA and dextran (M_r 2 000 000) were purchased from Sigma (St. Louis, MO, USA). Acrylamide, N,N,N′,N′-tetramethylethylenediamine (TEMED) and ammonium persulfate (APS) were obtained from Bio-Rad Labs. (Richmond, CA, USA). 3-Methacryloxypropyltrimethoxysiline was obtained from Hüls America (Bristol, PA, USA) and all other chemicals from Fisher (Fair Lawn, NJ, USA).

RESULTS AND DISCUSSION

Effect of dextran concentration on the retention of BSA and samples

The experiments describing the effect of dextran concentration on the retention of BSA, the various drug samples, and amino acids were performed under the electrophoretic conditions stated in the Experimental section. Fig. 1 shows the results. It can be seen that before the dextran is added to the run buffer, BSA is detected at 6.31 min. After 5% dextran is added, the retention time increases to 10.83 min, whereas the changes in retention time of the drug and amino acid samples are much smaller than that of BSA. The molecular mass of BSA (*ca.* 65 000) is much higher than that of the samples. The polymer network, which is the dextran solution in this experiment, has a much larger effect on the mobility of the large species (BSA in this case) when compared to the samples. Therefore migration of BSA decreases considerably upon the addition of dextran to the buffer, while the retention time of the low molecular mass sam-

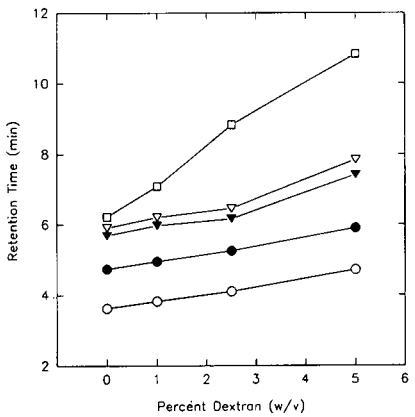

Fig. 1. Effect of dextran concentration on retention of BSA and samples. Conditions: linear polyacrylamide coated capillary with a 20 cm effective length; electric field strength, 300 V/cm; 10 m*M* phosphate buffer at pH 7.12; detection wavelength at 230 nm. ○ = leucovorin; ● = ibuprofen; ▼ = dansyl-DL-norvaline; ▽ = dansyl-DL-leucine; □ = BSA.

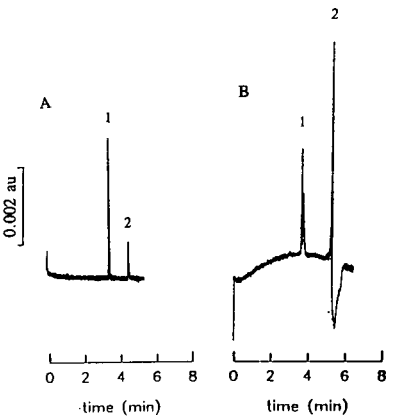

Fig. 2. Electropherograms of (1) LV and (2) IB mixture. CE conditions are the same as those of Fig. 1. (A) pH 7.12, 10 m*M* phosphate buffer; (B) pH 7.12, 10 m*M* phosphate buffer with BSA (1 mg/ml).

ples does not change much when compared to BSA..

By using the method developed in our laboratory recently [18], excellent chiral separation for LV was obtained by adding BSA to buffer. To obtain chiral resolution in a reasonable amount of time by this method, the difference between the velocities of BSA and the sample must be relatively large. For example, the velocity of dansyl-DL-leucine and dansyl-DL-norvaline are very close to that of BSA in the absence of dextran (Fig. 1), and chiral separation can not be achieved by this method even though these samples appear to have a strong affinity for BSA. By adding different percentages of dextran to the run buffer with BSA, one can slow down the velocity of BSA to the desired rate. In this way, the difference between the velocity of sample and BSA can be increased and chiral separation becomes feasible.

Chiral separation of drug and amino acid sample by using dextran and BSA as buffer additives

Fig. 2 shows the electropherograms for LV and IB. It can be seen that with the absence of BSA in the run buffer, both LV and IB elute as one peak. By using a run buffer modified with BSA (1 mg/ml), enantiomers of LV are separated to some degree while chiral separation of IB can not be obtained on a capillary with a relatively short effective length (20 cm). Interestingly the retention times of the isomers of LV do not change considerably when BSA is added to the run buffer. The retention time of IB experiences a change similar in magnitude to that of BSA, and the UV absorbance increases considerably for IB. This indicates that IB has a greater affinity for BSA than LV. After BSA has been added to the run buffer, an undefined negative peak appears following the peak of sample which has a strong affinity for BSA. The reason for this is not understood.

From Fig. 3 one can see that by adding dextran to the run buffer with BSA, optical enantiomers of both LV and IB can be resolved in 9 min on a capillary with an effective length of 20 cm. As the dextran concentration increases, the resolution of LV enantiomers increases and better chiral separation for IB is obtained. Again, it should be noted that the retention of IB changes considerably when the dextran polymer network is used because the velocity of BSA decreases largely when dextran is added to the run buffer and IB exhibits a strong interaction with BSA.

This new method can also be applied to the chiral separation of amino acids. Fig. 4 shows the chiral separation of dansyl-DL-leucine. With the addition of BSA alone to the run buffer, enantiomers of leucine cannot be resolved in the absence of dextran. A baseline separation of

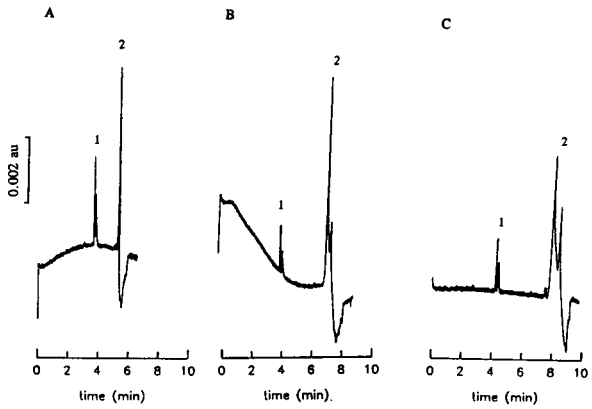

Fig. 3. Effect of dextran on chiral separation of (1) LV and (2) IB. Conditions are the same as those of Fig. 2B except different amount dextran was added to the buffer. (A) 0% Dextran, 1 mg BSA/ml; (B) 2.5% dextran, 1 mg BSA/ml; (C) 5% dextran, 1 mg BSA/ml.

leucine enantiomers is obtained when 5% dextran is added to the run buffer with BSA (1 mg/ml). In addition, it can be seen that dansyl-leucine has a strong affinity for BSA. Chiral separation of dansyl-DL-norvaline is also obtained by this method.

Fig. 5 illustrates the effect of dextran concentration of the run buffer on the retention of enantiomers for the different samples. In the absence of dextran in the run buffer, enantiomers of IB, leucine, and norvaline can not be separated using BSA (1 mg/ml in the run buffer). As the dextran concentration changes from 0 to 5% and the BSA concentration is kept constant, the difference between the retention of enantiomers for the samples increases. For LV the retention does not change much as the dextran concentration increases, since LV does not show a strong interaction with BSA. On the other hand, the retention times of IB, leucine, and norvaline evidently increase with the increase of dextran concentration because of their greater affinity for BSA. Therefore by using this method one can compare the binding ability of different drug samples qualitatively.

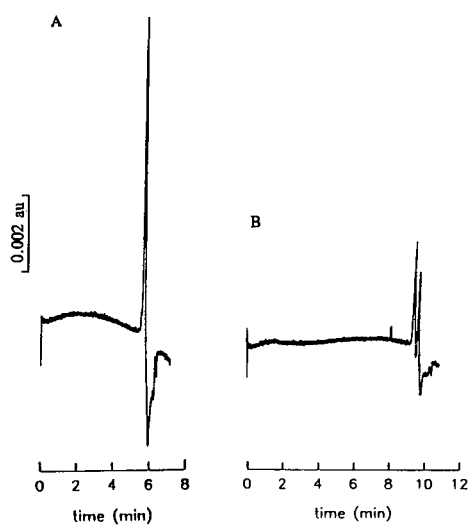

Fig. 4. Effect of dextran on the chiral separation of dansyl-DL-leucine. Conditions are the same as those of Fig. 2B except dextran was added to the buffer. (A) 0% Dextran, 1 mg BSA/ml; (B) 5% dextran, 1 mg BSA/ml.

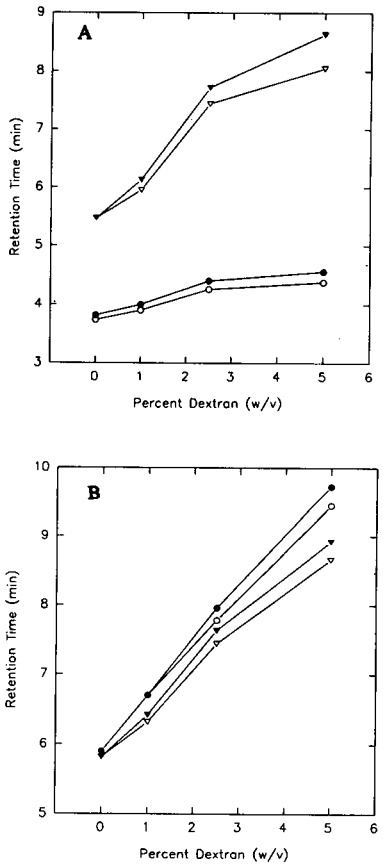

Fig. 5. Effect of dextran concentration on retention of enantiomers of drug and amino acid samples. (A) ○ and ●: enantiomers of LV; ▽ and ▼: enantiomers of IB. (B) ○ and ●: enantiomers of dansyl-DL-norvaline; ▽ and ▼: enantiomers of dansyl-DL-leucine.

Chiral separation of mandelic acid

When the sample, *e.g.* MA, has weak interaction with BSA, it is difficult to obtain chiral separation if only BSA is used as a run buffer additive, even in the case of using a capillary with a relatively long effective length of 60 cm (Fig. 6B). From Fig. 6 it can be seen that after BSA is added to a phosphate run buffer (1 mg BSA/ml), the retention of MA does not change considerably. This indicates that MA has a weak affinity for BSA at pH 7.12. After 5% dextran is added, the velocity of BSA decreases, the MA enantiomers interact with BSA more efficiently, and chiral separation of the MA isomers is achieved in 18 min.

Fig. 7 shows electropherograms of a LV and MA mixture. The mobilities of LV and MA are relatively close to each other in the free buffer system (Fig. 7A). If BSA is the only run buffer additive, the peaks of MA and LV overlap. Even though the enantiomers of LV can be separated

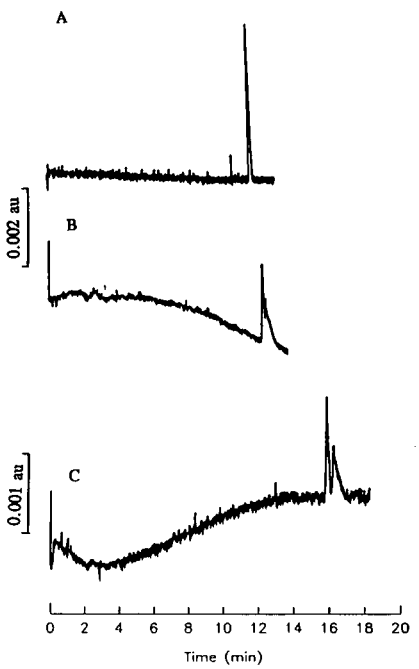

Fig. 6. Electropherograms of mandelic acid (MA). Conditions: linear polyacrylamide coated capillary with a 60 cm effective length; electric field strength, 300 V/cm; detection wavelength at 210 nm. (A) pH 7.12, 10 m*M* phosphate buffer; (B) pH 7.12, 10 m*M* phosphate buffer with BSA (1 mg/ml); (C) pH 7.12, 10 m*M* phosphate buffer with BSA (1 mg/ml) and 5% dextran.

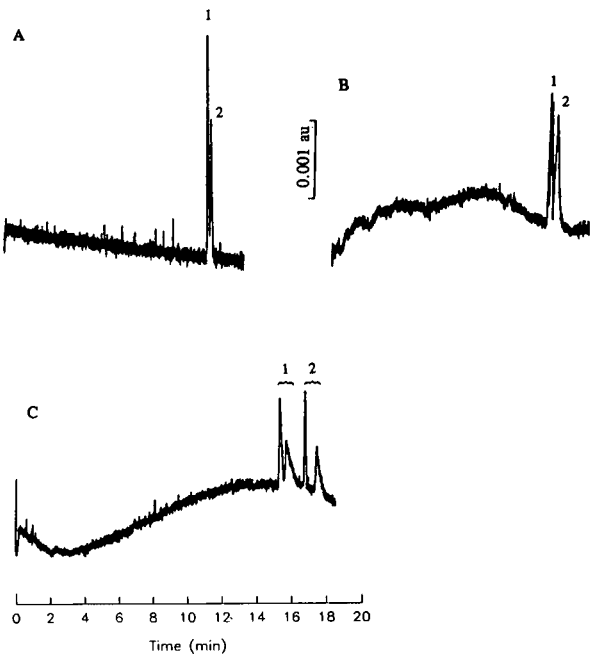

Fig. 7. Electropherograms of (1) MA and (2) LV mixture. Conditions are the same as those of Fig. 6. (A) pH 7.12, 10 m*M* phosphate buffer; (B) pH 7.12, 10 m*M* phosphate buffer with BSA (1 mg/ml); (C) pH 7.12, 10 m*M* phosphate buffer with BSA (1 mg/ml) and 5% dextran.

under these conditions, they elute with the MA sample. However, chiral separation of both MA and LV is obtained when 5% dextran is added to the run buffer with BSA. Since LV exhibits a stronger affinity for BSA than MA, the retention time of the LV enantiomers increases relative to that of the MA enantiomers when the velocity of BSA is lowered. The second peak in some of the enantiomeric pairs, such as in Fig. 7C, shows tailing. The second peak corresponds to the enantiomer with the stronger binding ability. The reason for this tailing is not well understood, but is currently under investigation in this lab.

CONCLUSION

The results show that a dextran polymer network is very useful for controlling the velocity of BSA for chiral separations. The enantiomers of samples which have mobilities similar to that of BSA or have very weak affinity for BSA are difficult to be separated by the method that

involves using only BSA as a run buffer additive. But the samples can be enantiomerically separated when dextran and BSA are used together as run buffer additives. The effect of dextran concentration on the velocity of BSA is much larger than the effect on the velocity of samples that have much lower molecular masses. The resolution of drug and amino acid enantiomers increases with the increase of dextran concentration in the run buffer when used in conjunction with BSA.

In this method the velocity of BSA can be controlled at the desired rate by adjusting the dextran concentration. The combination of this method with the method using BSA as a run buffer additive [18] and the protein immobilized method [25] recently developed in this lab should allow the technique using a biological species with high chiral selectivity (*e.g.* BSA) for chiral separation more general for CE.

ACKNOWLEDGEMENTS

This work was supported by Thermo Separation Products (Fremont, CA) and the Center for Biotechnology, SUNY-Stonybrook.

REFERENCES

1 S. Allenmark and B. Bromgren, *J. Chromatogr.*, 264 (1983) 63.
2 K.E. Choi and R.L. Schilsky, *Anal. Biochem.*, 169 (1988) 398.
3 L. Silan, P. Jaduad, L.R. Whitfield and I.W. Wainer, *J. Chromatogr.*, 532 (1990) 227.
4 J. Hermansson, *J. Chromatogr.*, 269 (1983) 71.
5 J. Hermansson and M. Eriksson, *J. Liq. Chromatogr.*, 9 (1986) 621.
6 T. Miwa, M. Ichikawa, M. Tsuno, T. Hattori, T. Miyakawa, M. Kayano and Y. Miyake, *Chem. Pharm. Bull.*, 35 (1987) 682.
7 K.M. Kirkland, K.L. Neilson and D.A. McCombs, *J. Chromatogr.*, 545 (1991) 43.
8 P. Erlandsson, L. Hansson and R. Isaksson, *J. Chromatogr.*, 370 (1986) 475.
9 R. Kuhn and S.H. Kuhn, *Chromatographia*, 34 (1992) 505.
10 S. Terabe, K. Otsuka, K. Ichikawa, A. Tsuchiya and T. Ando, *Anal. Chem.*, 56 (1984) 111.
11 E. Gassmann, J.E. Kwo and R.N. Zare, *Science*, 230 (1985) 813.
12 S. Fanali, *J. Chromatogr.*, 545 (1991) 437.
13 A. Guttman, A. Paulus, S. Cohen, N. Grinberg and B.L. Karger, *J. Chromatogr.*, 448 (1988) 41.
14 R. Kuhn, F. Stocklin and F. Erni, *Chromatographia*, 33 (1992) 32.
15 S. Terabe, M. Shibata and Y. Miyashita, *J. Chromatogr.*, 480 (1989) 403.
16 A. Dobashi, T. Ono, S. Hara and J. Yamagushi, *Anal. Chem.*, 61 (1989) 1986.
17 K. Otsuka, J. Kowahara, K. Tatekawa and S. Terabe, *J. Chromatogr.*, 559 (1991) 209.
18 G.E. Barker, P. Russo and R.A. Hartwick, *Anal. Chem.*, 64 (1992) 3024.
19 D.N. Heiger, A.S. Cohen and B.C. Karger, *J. Chromatogr.*, 516 91990) 33.
20 S. Hjertén, L. Valtcheva, K. Elenbring and P.J. Eaker, *J. Liq. Chromatogr.*, 12 (1989) 2471.
21 M. Zhu, D.L. Hanson, S. Bird and F. Garrison, *J. Chromatogr.*, 480 (1989) 311.
22 H.E. Schwartz, K.J. Ulfelder, F.J. Sunzeri, M.P. Busch and R.G. Brownlee, *J. Chromatogr.*, 559 (1991) 267.
23 K. Ganzler, K.S. Greve, A.S. Cohen, B.L. Karger, A. Guttman and N.C. Cooke, *Anal. Chem.*, 64 (1992) 2665.
24 S. Hjertén, *J. Chromatogr.*, 347 (1985) 191.
25 P. Sun, G. Barker, R.A. Hartwick, N. Grinberg and R. Kaliszan, *J. Chromatogr.*, 652 (1993) 247.

Journal of Chromatography, 648 (1993) 481–484
Elsevier Science Publishers B.V., Amsterdam

CHROM. 25 354

Short Communication

Post-column immobilized tyrosinase reactor for determination of L-3,4-dihydroxyphenylalanine and L-tyrosine by high-performance liquid chromatography with fluorescence detection

Nobutoshi Kiba*, Masatoshi Itoi and Motohisa Furusawa

Department of Applied Chemistry and Biotechnology, Faculty of Engineering, Yamanashi University, Kofu 400 (Japan)

(First received March 30th, 1993; revised manuscript received June 1st, 1993)

ABSTRACT

Immobilized tyrosinase was used as a reactor in a liquid chromatographic system for the selective detection of L-3,4-dihydroxyphenylalanine (L-DOPA) and L-tyrosine. Tyrosinase was immobilized on controlled-pore glass beads. The compounds were separated on an ODS column with 0.1 *M* phosphate buffer (pH 7.2) as mobile phase. The fluorescent dihydroxyindol formed was detected at 490 nm (excitation at 360 nm). For L-DOPA the linear working range was 0.005–15 μM, with a detection limit of 1 n*M* (6 pg in a 30-μl injection); for L-tyrosine the range was 0.01–30 μM, with a detection limit of 5 n*M* (27 pg in a 30-μl injection). The reactor was stable for at least 2400 injections. Its usefulness for simultaneous determination of L-DOPA and L-tyrosine in serum is described.

INTRODUCTION

L-3,4-Dihydroxyphenylalanine (L-DOPA) is synthesized by the hydration of L-tyrosine with tyrosine hydroxylase in peripheral and central catecholaminergic neutrons and chromaffin cells of the adrenal medulla [1–3]. Usually, high-performance liquid chromatography (HPLC) with electrochemical detection (ED) is used successfully for simultaneous determination of catechols and phenols [4,5]. Several papers have discussed the use of immobilized enzyme in post-column reactors for the selective determination of L-tyrosine and several amino acids [6–8], but there is no paper on the determination of catechols.

Tyrosinase (EC 1.14.18.1) catalyses the oxidation of catechols and phenols to *o*-quinones [9]. Immobilized tyrosinase was used in a flow-injection system for the determination of L-tyrosine in serum with fluorescence detection [10]. This paper describes the use of immobilized tyrosinase as a post-column reactor in a liquid chromatographic system for the simultaneous determination of L-DOPA and L-tyrosine. The compounds eluted from the separation column are oxidized to dopaquinone in a reactor. The quinone formed is rearranged to fluorescent 2,3-

* Corresponding author.

0021-9673/93/$06.00

dihydro-5,6-dihydroxyindole-2-carboxylic acid (indol) in a strongly alkaline solution. The indol is monitored by fluorescence detection.

EXPERIMENTAL

Reagents

Tyrosinase (2400 U mg^{-1}, from mushrooms), L-DOPA and L-tyrosine were obtained from Sigma (St. Louis, MO, USA). Aminopropyl–controlled-pore glass (CPG) (mean pore diameter 59 nm, amine concentration 76 μmol g^{-1}, particle size 55 ± 20 μm) was supplied by CPG (NJ, USA). TSKgel ODS-80T_M (5 μm) was obtained from Tosoh (Tokyo, Japan). All other reagents were of analytical-reagent grade. The preparation of the immobilized enzyme was similar to that described previously [9]. The immobilized enzyme was packed into a stainless-steel column (2 cm × 4 mm I.D.).

HPLC

Chromatography was carried out with a Model L-6000 pump (Hitachi, Tokyo), a Model 7125 injector valve (Rheodyne, CA, USA) with a 30-μl loop, a separation column (15 cm × 4 mm I.D.) and an immobilized tyrosinase reactor. A Model KHU-W-52 pump (Kyowa Seimitsu, Tokyo, Japan) was linked, via a T-piece junction, into the system after the reactor. Peaks were detected using a Model FP-210 spectrofluorimeter (Jasco, Tokyo, Japan), at excitatory and emission wavelengths of 360 nm and 490 nm, respectively, and peaks were integrated using a Chromatocorder II (System Instrument, Tokyo, Japan). The immobilized tyrosinase reactor was installed between the separation column and the T-piece junction. The separation of L-DOPA and L-tyrosine was achieved using a mobile phase of 0.1 *M* phosphate buffer (pH 7.2). The flow-rate was 0.6 ml min^{-1}. The reactor eluate was made basic by mixing with 3 *M* sodium hydroxide, which was pumped at 0.6 ml min^{-1} into the system via the T-piece junction using the KHU-W-52 pump. The mixing coil tubing was 2 m × 0.5 mm I.D. PTFE.

Procedure

Serum (500 μl) was deproteinated by adding 0.60 *M* perchloric acid (500 μl) and mixing on ice for 10 min. The mixture was filtered and the filtrate (50 μl) was neutralized with 0.15 *M* dipotassium hydrogenphosphate (50 μl). The neutralized solution was cooled at 4°C for 10 min and the supernatant (40 μl) was diluted with 0.1 *M* phosphate buffer (pH 7.2) to 100 μl. By this treatment, samples are diluted 10-fold. Aliquots of 30 μl were injected for HPLC determination.

RESULTS AND DISCUSSION

Reactor performance

To evaluate the properties of immobilized tyrosinase, the system was used in flow-injection mode by omitting the analytical column. The flow-rate of phosphate buffer was 0.6 ml min^{-1}. The influence of pH on the enzymatic reaction was studied over the pH range 6.5–7.8 by injecting 0.1 μM L-DOPA (30 μl). The optimum pH for the enzymatic reaction was from 7.2 to 7.4, as shown in Fig. 1. The buffer of pH 7.2 was selected for further work. The reactor was placed in a water bath and the temperature was varied between 20 and 40°C. The reactor exhibited the highest activity at 30°C, although the activity was not strongly influenced by the temperature (Fig. 1). The reactor was used by repeated injections of L-DOPA solution (5 μM) at a sample speed of 5 h^{-1}. The activity decreased gradually and remained at 80% of the initial value after 2400 injections. The responses to L-DOPA, L-tyrosine and other related compounds were as follows: L-DOPA (100), L-tyrosine (85), D-tyrosine (26), epinephrine (23), D,L-synephrine (4), L-tyrosyl-L-alanine (9), L-

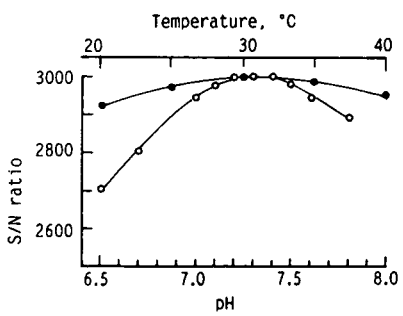

Fig. 1. Effects of (○) pH and (●) temperature on the signal-to-noise (*S/N*) ratio for L-DOPA. The *S/N* ratio was obtained by dividing the peak height (mm) by the baseline noise (mm).

tyrosyl-L-leucine (13), L-tyrosyl-L-glycine (15), L-tyrosyl-L-glutamic acid (9) and L-tyrosyl-L-glycyl-L-glycine (6).

Indol formation reaction

The eluate from the reactor was mixed with various concentrations of sodium hydroxide solution. The concentration was varied from 2 to 4 *M*. The maximum response was obtained at 3 *M* sodium hydroxide. The effect of flow-rate was studied by changing the flow-rate of 3 *M* sodium hydroxide from 0.3 to 1.0 ml min^{-1}. Maximum response was obtained from 0.6 to 0.8 ml min^{-1}. With increasing flow-rate of sodium hydroxide the baseline stability became poor because of the incomplete mixing. A flow-rate of 0.6 ml min^{-1} was chosen.

Chromatogram

A representative chromatogram illustrating resolution of standard mixtures of L-DOPA and L-tyrosine is shown in Fig. 2. The ratio of peak heights for L-DOPA and L-tyrosine was 100:67. The peak height was plotted against the concentration of the compounds. The concentration ranges of linear response were from 0.005 to 15 μM for L-DOPA and from 0.01 to 30 μM for L-tyrosine. The detection limits (signal-to-noise ratio 3) for L-DOPA and L-tyrosine were 1 n*M* (6 pg) and 5 n*M* (27 pg in a 30-μl injection), respectively. Repeated determination ($n = 7$) of standard mixtures at a concentration of 0.1 μM gave relative standard deviation (R.S.D.) of 1.8% for L-DOPA and 2.1% for L-tyrosine.

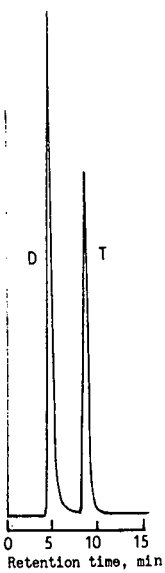

Fig. 2. Chromatogram of a standard mixture of L-DOPA and L-tyrosine. The 30-μl injection consisted of aqueous mixture containing 100 n*M* each. D = L-DOPA; T = L-tyrosine; mobile phase, 0.1 *M* phosphate buffer (pH 7.2) (0.6 ml min^{-1}); separation column, TSKgel ODS-80T_M (5 μm) (15 cm × 4 mm I.D.); reactor, immobilized tyrosinase (2 cm × 4 mm I.D.); basifier, 3 *M* sodium hydroxide (0.6 ml min^{-1}); detection, fluorimetry ($\lambda_{ex.}$ 360 nm, $\lambda_{em.}$ 490 nm).

Application

This system was used to determine the amounts of L-DOPA and L-tyrosine in serum. A sample of human serum containing known L-DOPA and L-tyrosine concentrations was supplemented with L-DOPA and L-tyrosine to give final concentrations of 0.1–6 μM L-DOPA and 65–255 μM L-tyrosine. The recoveries were 98–103% for L-DOPA and 99–101% for L-tyrosine. The detection limit (signal-to-noise = 3) for L-DOPA for serum samples was 10 n*M*. This method was used for the determination of L-DOPA and L-tyrosine in the serum obtained from a Parkinsonian patient treated with Sinemet. L-DOPA and L-tyrosine in the serum were 4.5 μM [R.S.D. ($n = 5$) 2.4%] for L-DOPA and 67.6 μM (2.6%) for L-tyrosine. The detection limits (signal-to-noise ratio = 3) for L-DOPA and L-tyrosine for serum samples were 10 n*M* and 50 n*M*, respectively.

CONCLUSIONS

We have shown that an immobilized tyrosinase reactor is useful for the simultaneous detection of L-DOPA and L-tyrosine using reversed-phase HPLC and fluorimetric detection. The reactor in a post-column system is stable enough to permit the measurement of more than 2400 samples for 20 days. Although this method can be easily used routinely for the determination of L-DOPA and L-tyrosine in the serum of Parkinsonian patients on DOPA therapy, endogenous L-DOPA (*ca.* 15 n*M* [11]) in the serum of non-treated and/or normal subject cannot be determined by this method. The HPLC–ED methods are sensitive but require rather complicated sample clean-up procedures and maintenance for electrodes [12,13]. This method proved to be simple and

selective for the simultaneous determination of therapeutic L-DOPA and L-tyrosine in serum.

REFERENCES

1 S. Udenfriend and J.B. Wyngaarden, *Biochim. Biophys. Acta*, 20 (1956) 48.
2 T. Nagatsu, M. Levitt and S. Udenfriend, *J. Biol. Chem.*, 239 (1964) 2910.
3 T. Nagatsu, M. Levitt and S. Udenfriend, *Anal. Biochem.*, 9 (1964) 122.
4 K. Zech, in A. Henschen, K.-P. Hupe, F. Lottspeich and W. Voelter (Editors), *High-Performance Liquid Chromatography in Biochemistry*, VCH, Weinheim, 1985, pp. 340–342.
5 F. Boomsma, F.A.J. van de Hoorn, A.J. Man in 't Veld and M.A.D.H. Schalekamp, *Clin. Chim. Acta*, 178 (1988) 59.
6 N. Kiba and M. Kaneko, *J. Chromatogr.*, 303 (1984) 396.
7 H. Jansen, U.A.Th. Brinkman and R.W. Frei, *J. Chromatogr.*, 440 (1988) 217.
8 D.W. Taylor and T.A. Nieman, *J. Chromatogr.*, 368 (1986) 95.
9 J. McGuire, *Biochem. Biophys. Res. Comm.*, 40 (1970) 1084.
10 N. Kiba, M. Ogi and M. Furusawa, *Anal. Chim. Acta*, 224 (1989) 133.
11 M. Lee, H. Nohta, K. Ohtsubo, B. Yoo and Y. Ohkura, *Chem. Pharm. Bull.*, 35 (1987) 235.
12 S. Ito, T. Kato, K. Maruta, K. Fujita and T. Kurahashi, *J. Chromatogr.*, 311 (1984) 154.
13 D.S. Goldstein, R. Stull, R. Zimlichman, P.D. Levinson, H. Smith and H.R. Keiser, *Clin. Chem.*, 30 (1984) 815.

Journal of Chromatography, 648 (1993) 485–490
Elsevier Science Publishers B.V., Amsterdam

CHROM. 25 446

Short Communication

Analysis of United Kingdom purchased spices for aflatoxins using an immunoaffinity column clean-up procedure followed by high-performance liquid chromatographic analysis and post-column derivatisation with pyridinium bromide perbromide

R. Colin Garner*, Matthew M. Whattam, Patrick J.L. Taylor and Martin W. Stow

Biocode Limited, University Road, Heslington, York, YO1 5DE (UK)

(First received January 12th, 1993; revised manuscript received July 19th, 1993)

ABSTRACT

An immunoaffinity column method has been developed to analyse aflatoxins with greater than 70% recoveries from a variety of spices purchased from local stores. Samples of chilli powder, ground ginger, black pepper, cayenne pepper, paprika and cumin were initially screened semi-quantitatively; this provides a rapid means of analysing a large number of spice samples. Those samples that had aflatoxin levels greater than 1 ppb (w/w) total aflatoxins were re-analysed quantitatively by high-performance liquid chromatography (HPLC) using a newly developed post-column derivatisation procedure with pyridinium bromide perbromide (PBPB). Some samples of spices, in particular chilli powder, were found to contain aflatoxins at 20 ppb (w/w) or higher.

INTRODUCTION

The aflatoxins are a group of mycotoxins produced by the food spoilage fungi *Aspergillus*, particularly *flavus* and *parasiticus*. There are four naturally occurring aflatoxins, *viz.* aflatoxin B_1, B_2, G_1 and G_2, and all have varying degrees of biological activity [1]. Aflatoxin B_1 is the most potent and has been shown to be a toxin, mutagen and animal carcinogen. The aflatoxins as a group on the basis of epidemiological evidence have been classified as human liver carcinogens by the World Health Organisation [2]. Most countries in the Western world have introduced regulations controlling the level of aflatoxins in human and animal food although contamination levels are much lower than in the Third World [3]. In the Third World as a result, particularly where hepatitis B infection is endemic, liver cancer is very common [4]. A wide variety of food matrices have been shown to be contaminated by the aflatoxins and it is therefore essential to have available simple and quantitative methods for aflatoxin analysis.

Traditionally aflatoxin analysis has been performed using solvent extraction, usually with chloroform, followed by sample clean-up by

* Corresponding author.

0021-9673/93/$06.00

silica gel chromatography, prior to either TLC or HPLC analysis. More recently immunological methods have been introduced which permit more rapid and reliable aflatoxin analyses to be conducted [5–8]. The immunoaffinity approach offers a simple means of specifically concentrating aflatoxin from blended food sample solvent extracts using columns containing an anti-aflatoxin antibody [9]. The technique enables a wide variety of food matrices to be analysed using a one-step extraction protocol without the need to use halogenated hydrocarbon solvents for extraction.

In this study we have used a commercially available immunoaffinity (aflatoxin EASI-EXTRACT) column to screen a large number of spices purchased from local stores using firstly a semi-quantitative procedure in which the immunoaffinity purified extract is assayed using silica–Florisil mini-columns [10] and fluorescence. The semi-quantitative procedure is very rapid and allows a large number of samples to be processed efficiently. Any samples containing aflatoxin levels higher than 1 ppb were re-analysed by HPLC. A new method of post-column derivatisation of the aflatoxins was developed using a solution of pyridinium bromide perbromide (PBPB). This mild brominating agent enhances the fluorescent signal produced by aflatoxin B_1 and G_1 and hence increases the sensitivity of the analytical method.

The following spices have been examined: chilli powder, ground ginger, black pepper, cayenne pepper, paprika and cumin.

EXPERIMENTAL

Materials

Total aflatoxin EASI-EXTRACT columns and analytical silica–Florisil columns were from Biocode Ltd (York, UK). The manufacturer's specifications for EASI-EXTRACT columns are that they will recover $>80\%$ total aflatoxins when 3.5 ng of each aflatoxin B_1, B_2, G_1 and G_2 is applied in 175 ml of diluted peanut butter extract (equivalent to 1 ppb contamination level), and that they have a total capacity of >5 μg when 10 μg aflatoxin B_1 is applied in 50 ml of 5% (v/v) methanol in phosphate buffered saline pH 7.4 (PBS). Analytical reagent grade acetonitrile, methanol and chloroform were purchased from FSA (Loughborough, UK). All water used was purified by reverse osmosis followed by ion exchange/activated carbon column clean-up. Aflatoxins B_1, B_2, G_1 and G_2 and PBPB were purchased from Sigma (Poole, UK). PBS was prepared using PBS tablets from Biocode Ltd. All other reagents were laboratory reagent grade.

Sample preparation

Powdered spice (10 g), purchased from local supermarkets and health food shops, was vigorously blended for two min using an Ultra Turrax homogeniser (Sartorius, Epsom, UK) with 40 ml methanol–water (80:20, v/v). The resulting suspension was centrifuged at 1600 *g* (av) for 15 min at room temperature and the supernatant collected. This was diluted to 10% (v/v) methanol with PBS and re-centrifuged at 1600 *g* (av) for a further 15 min. The supernatant was applied to immunoaffinity columns.

Immunoaffinity purification

Semi-quantitative analysis for initial screening of spice samples. The diluted spice extracts (112 ml) prepared as above were applied either manually via a syringe or using a peristaltic pump (Watson-Marlow, Falmouth, UK) to the aflatoxin immunoaffinity columns as per the manufacturer's instructions, *i.e.* at a flow rate of 5 ml/min. After sample application, the columns were washed with 20 ml purified water and any bound aflatoxins eluted slowly with 1.5 ml neat methanol. To this methanol eluate, 6 ml PBS was added followed by 3 ml chloroform. The whole mixture was vigorously shaken for one min, the chloroform layer removed and applied to an analytical column. These glass columns consist of a number of powders including alumina (to remove non-specific fluorescent material), silica and Florisil. Any aflatoxin is concentrated at the silica–Florisil interface and can be visualised under UV light. Once the chloroform extract had been allowed to drip through the analytical

column it was washed with 3 ml chloroform–acetone (9:1). The analytical column was then examined under long wave ultraviolet light (6 W at 360 nm) in a dark box. The intensity of the fluorescence at the silica–Florisil interface was compared with analytical columns to which known amounts of aflatoxin B_1 (0, 4, 10, 20 ng) had been applied in order to provide a measure of the level of aflatoxin contamination.

Quantitative analysis by HPLC. For spice samples that contained greater than 1 ppb total aflatoxin as determined by the above procedure, a quantitative analysis was performed using an automated HPLC system (Anachem, Luton, UK). The spice extracts were immunopurified as above and any bound aflatoxins slowly eluted with 1.5 ml methanol using an automated robotic sample preparation system (ASPEC, Anachem). The eluate was subsequently diluted by the system with 2 ml of purified water before 500 μl was injected onto the HPLC system. This automated system has been described previously for the analysis of mycotoxins by Sharman and Gilbert [11].

High-performance liquid chromatography and post-column derivatisation

For the analysis of aflatoxins, a reverse-phase Spherisorb ODS2 HPLC column (5 μm particle size, 25 cm × 4.6 mm I.D.) was used with an isocratic mobile phase of 40% (v/v) acetonitrile:methanol (5:4) in HPLC grade water at a flow rate of 0.75 ml/min. The post-column derivatisation reagent PBPB (at 0.05 mg/ml in HPLC grade water) was mixed at a flow rate of 0.3 ml/min with the eluate from the HPLC column at a T piece junction. The reagent was allowed to react for 30 cm length of tubing (0.25 mm I.D.) before monitoring for the presence of aflatoxins with an Applied Biosystems (Anachem) Model 980 fluorescence detector (excitation 362 nm, emission 418 nm).

When iodine was used as the post-column derivatisation reagent, a saturated solution in water was mixed with the eluate from the HPLC column at 0.6 ml/min. The reaction occurred over a 5-m length of coil heated to 50°C before entering the fluorescence detector.

RESULTS AND DISCUSSION

A semi-quantitative screening of a wide range of chilli powder, ground ginger, black pepper, cayenne pepper, cumin and paprika samples was conducted to detect aflatoxin contamination of >1 ppb. The amount of the diluted extract applied to the column determines the detection limit. In this case, 112 ml of extract was applied, which is equivalent to 3.5 g of spice. As 4 ng of aflatoxin is required on the analytical column in order to see a fluorescent band, samples contaminated at a level of greater than 1 ppb gave a positive result on the analytical column. The results indicated that more than 50% of samples were contaminated at levels higher than 1 ppb. No positive samples were detected when either cumin or paprika were analysed. The black pepper samples gave large amounts of yellow-green fluorescence over areas of the analytical column and this interfered with the semi-quantitative analysis of aflatoxin. Those spices that were positive gave clear, sharp blue fluorescent bands at the silica–Florisil interface, indicative of the presence of aflatoxins.

The extraction efficiency of the 80% (v/v) methanol–water method was assessed by spiking spice samples (which had previously been shown to be non-contaminated using the semi-quantitative analysis procedure) at the 4 ppb level each with aflatoxins B_1, B_2, G_1, and G_2. These samples were then processed as described in the methods section and the eluates analysed by HPLC. Each spice sample was analysed using duplicate EASI-EXTRACT columns and the eluate from each column was injected in duplicate onto the HPLC. The percentage recoveries obtained are shown in Table I. The unspiked spice samples were also analysed at the same time and any natural aflatoxin contamination present taken into consideration during the recovery calculation.

The accuracy and reproducibility of the automated ASPEC–HPLC system was investigated by analysing multiple samples of naturally contaminated spice extracts through the EASI-EXTRACT columns. Five extracts of each spice were analysed and every eluate was injected in duplicate onto the HPLC system. The results

TABLE I

PERCENTAGE RECOVERIES OF AFLATOXINS FROM SPICE SAMPLES SPIKED AT 4 ppb LEVEL WITH EACH OF THE AFLATOXINS B_1, B_2, G_1 AND G_2

Spice	% Recovery			
	AFG_2	AFG_1	AFB_2	AFB_1
Black pepper	97	89	92	74
Chilli powder	78	69	78	73
Ginger powder	92.5	70	102.5	112.5

expressed as means and R.S.D.s are shown in Table II. The R.S.D.s of the cayenne pepper and chilli powder samples contaminated with aflatox-

TABLE II

THE REPRODUCIBILITY/ACCURACY OF THE AUTOMATED ASPEC/HPLC SYSTEM FOR THE ANALYSIS OF AFLATOXIN CONTAMINATION IN CHILLI POWDER AND CAYENNE PEPPER

R.S.D. values are shown in brackets.

Sample	Mean contamination level (ppb)	
	AFB_2	AFB_1
Chilli powder	0.9 (2.2%)	19.8 (4.7%)
Cayenne pepper	0	4.0 (4.6%)

in B_1 around the 4 ppb and 20 ppb levels were 4.6 and 4.7%, respectively.

With the described extraction procedure in conjunction with the HPLC system the limit of quantification of the method is 0.14 ppb of aflatoxin. The limit of detection will be less, around 0.06 ppb.

The spice samples which were found to contain >1 ppb aflatoxin following an initial screening by semi-quantitative analysis were re-analysed using a HPLC based quantitative method. The results are detailed in Fig. 1. Typical HPLC chromatograms of a highly contaminated chilli powder sample and a contaminated ginger sample are shown in Fig. 2. The ground ginger samples typically show contamination by all four aflatoxins while the chilli powder contains predominantly aflatoxin B_1 and B_2.

The highest levels of total aflatoxin contamination were found in chilli powder and ground ginger samples.

A direct comparison between the use of iodine and PBPB as post-column derivatisation reagents was conducted. The results detailed in Table III are those obtained when the system for each reagent was optimised for sensitivity (as described in the method section). The results show that the fluorescence of all the aflatoxins is increased especially that of AFB_1. The day-to-day reproducibility of the system was found to be good.

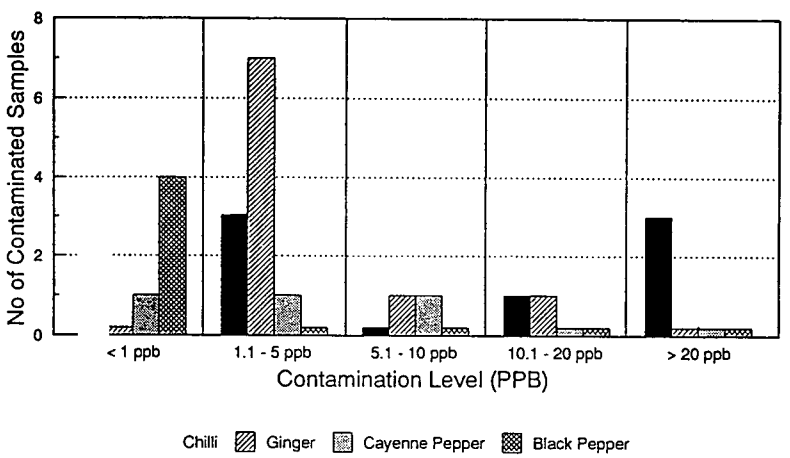

Fig. 1. Total aflatoxin levels in spices analysed by HPLC following initial semi-quantitative screening.

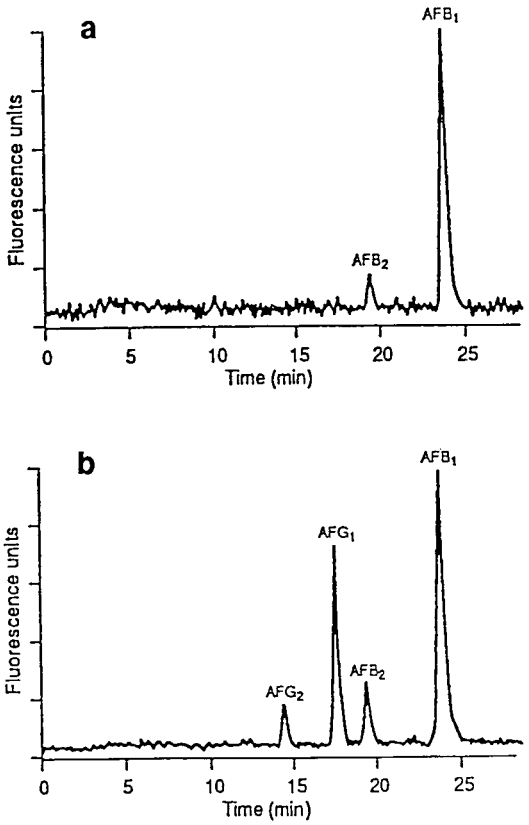

Fig. 2. HPLC chromatograms illustrating the analysis of aflatoxin peaks for aflatoxin B_1 normalised to full scale deflection in each chromatogram - (a) naturally contaminated chilli powder sample, (b) naturally contaminated ginger powder sample.

CONCLUSIONS

In the United Kingdom, regulations exist controlling the level of aflatoxin contamination in some human and animal food. Nevertheless the regulations, particularly for human food, apply to only certain food matrices (nuts, nut products, dried figs and dried fig products). In the study reported here we have developed simple quantitative methods for aflatoxin analysis and have applied this to a variety of spices. We chose these to study, since spices are difficult to analyse using conventional analytical methods and there were literature reports that aflatoxin contamination of spices does occur [12].

We have analysed a variety of powdered spices purchased in local supermarkets and health food stores. More than 50% of the spice samples were found to be contaminated at levels of greater than 1 ppb. Of these 17 out of 32 samples purchased from supermarkets and 3 out of 4 samples purchased from health food shops, were contaminated at these levels.

Immunoaffinity column methods for sample clean-up provide specific and sensitive procedures for food analysis. The chromatograms obtained from immunoaffinity purified extracts are relatively free from contaminating chemicals thus increasing the assay sensitivity. Spices are particularly difficult to analyse for aflatoxins, because of the highly coloured contaminating materials that are co-extracted with the aflatoxins. Immunoaffinity methods provide a quick, one-step solution to sample clean-up which should speed up aflatoxin analysis.

The post-column derivatisation method reported here is an improvement over existing procedures particularly the use of iodine [13]. PBPB provides a stable solution which needs no long reaction times or elevated temperatures to enhance aflatoxin fluorescence. Aflatoxin peaks are as a result narrower and in addition, peak

TABLE III

A COMPARISON OF AFLATOXIN PEAK AREAS AFTER POST-COLUMN DERIVATISATION WITH EITHER IODINE–WATER OR PBPB–WATER

Reagent system	Mean peak area				R.S.D.			
	AFG_2	AFG_1	AFB_2	AFB_1	AFG_2	AFG_1	AFB_2	AFB_1
Iodine–water	76073	43801	57033	32411	2.1	2.0	2.8	3.5
PBPB–water	112510	47683	86511	82063	2.0	3.8	2.8	4.5

height is increased over that produced by iodine–water again enhancing sensitivity. The system also has the advantage of not requiring expensive equipment such as the method of post-column derivatisation using electrochemically generated bromine [14].

Of the spices analysed, chilli powder and ground ginger were the most likely to be contaminated; some samples contained over 20 ppb total aflatoxins. Chilli powder is used in a wide variety of foods including ethnic dishes and snack foods. Ginger root powder is used as a flavouring agent in drinks, biscuits, cakes as well as ethnic foods. In the UK, the number of foods containing spices is increasing, particularly in the snack food business. Hence exposure to aflatoxins from these sources will also be increasing, putting some additional health risk to the consumer. It is important that all food with the potential for aflatoxin contamination is analysed and that regulations cover all sources of human exposure.

ACKNOWLEDGEMENTS

We would like to thank Tim Wilkinson and Elaine Bisson for their help and encouragement.

REFERENCES

1 W.F. Busby and G.N. Wogan, in C.E. Searle (Editor), *Chemical Carcinogens (ACS Monograph 182)*, 2nd ed., American Chemical Society, Washington, 1984, p. 945.
2 *IARC Monographs on the Evaluation of Carcinogenic Risks to Humans*, Supplement 7, IARC, Lyon, 1987, p. 83.
3 H.P. van Egmond, *Food Add. Contam.*, 6 (1989) 139.
4 G.N. Wogan, *Cancer Res. Suppl.*, 52 (1992) 2114s.
5 O. El-Nakib, J.J. Pestka and F.S. Chu, *J. Assoc. Off. Anal. Chem.*, 64 (1981) 1077.
6 M.W. Trucksess, K. Young, K. Donahue, D.K. Morris and E. Lewis, *J. Assoc. Off. Anal. Chem.*, 73 (1990) 425.
7 A. Farjam, N.C. Van De Merbel, A.A. Nieman, H. Lingeman and U.A.Th. Brinkman, *J. Chromatogr.*, 589 (1992) 141.
8 A. Farjam, N.C. Van de Merbel, H. Lingeman, R.W. Frei and U.A.Th. Brinkman, *Int. J. Environ. Anal. Chem.*, 45 (1991) 73.
9 M. Carvajal, F. Mulholland and R.C. Garner, *J. Chromatogr.*, 511 (1990) 379.
10 C.E. Holaday, *J. Am. Oil Chem. Soc.*, 58 (1981) 931A.
11 M. Sharman and J. Gilbert, *J. Chromatogr.*, 543 (1991) 220.
12 P.M. Scott and B.P.C. Kennedy, *J. Assoc. Off. Anal. Chem.*, 56 (1973) 1452.
13 L.G.M.Th. Tuinstra and W. Haasnoot, *J. Chromatogr.*, 282 (1983) 457.
14 Th.C.H. Van Neer, W.A. Traag and L.G.M.Th. Tuinstra, *J. Chromatogr*, 367 (1986) 231.

Journal of Chromatography, 648 (1993) 491–496
Elsevier Science Publishers B.V., Amsterdam

CHROM. 25 392

Short Communication

Analysis of C_{60} and C_{70} fullerenes by high-performance liquid chromatography

Yongqing Wu, Yiliang Sun*, Zhennan Gu, Qinwei Wang, Xihuang Zhou, Yan Xiong and Zhaoxia Jin

Department of Chemistry, Peking University, Beijing 100871 (China)

(First received May 10th, 1993; revised manuscript received June 29th, 1993)

ABSTRACT

Some common solvents were roughly classified into four classes according to their decreasing solubility for fullerenes. Good solvents should be used in designing a practical liquid chromatographic separation method. Several stationary phases were tested to separate C_{60} and C_{70} fullerenes. They included ODS-, C_6H_5-, NH_2- and CN-silica, silica gel and three synthesized ones containing mono-/di- nitrobenzamidopropyl functionalities. All the stationary phases studied, with the exception of silica gel, had some retention and separation capability for C_{60} and C_{70} fullerenes. The three nitrobenzamidopropyl group-containing packings showed more pronounced retention and were capable of being used with good solvent added in the mobile phase. 3,5-Dinitrobenzamidopropyl chemically bonded phase, the most retentive packing, was used as stationary phase in HPLC for the analysis of C_{60} and C_{70} fullerenes. It was shown that with toluene–light petroleum as mobile phase this method was rapid and accurate.

INTRODUCTION

Fullerenes, which were first proposed by Kroto *et al.* [1] in 1985 and produced in bulk by Kraetschmer *et al.* [2] in 1990, have stirred a flurry of research in physics, chemistry and materials sciences. These all-carbon molecules are arranged as polyhedra with hexagonal and pentagonal faces [1,3]. They are formed in an electric arc with graphite as electrodes. C_{60} and C_{70} fullerenes, being the most abundant species isolated from a crude soot product, have been characterized in detail, *e.g.*, by NMR, Fourier transform IR, MS and UV–VIS spectra [4–6]. To isolate C_{60}, C_{70} and other higher fullerenes is a challenging task because of their poor solubility in most organic solvents [4]. Many authors have attempted to do so. Most of them used LC with silica gel [4], alumina [4,6] and chemically bonded phases, *e.g.*, ODS [7–10], 2,4-dinitroanilinopropyl (DNAP) [5], Pirkle type [11] and multi-legged phenyl [12] and others [13], as stationary phases and *n*-hexane, toluene, *p*-xylene, dichloromethane, methanol, acetonitrile, etc., or mixture of these, as mobile phases. MS was and still is frequently used to identify and quantify the mixture of fullerenes. Field desorption (FD), laser desorption (LD) and fast atom bombardment (FAB) are the most effective ionization sources in MS, while electron impact (EI) and desorption chemical ionization (DCI)

* Corresponding author.

0021-9673/93/$06.00

are not appropriate [14]. MS is very sensitive, however it has the drawback that it is not a routine method and requires an experienced operator. The low volatility of fullerenes may in some cases cause discrimination of the sample and pollution of the ionization source. HPLC is an easy, effective and accurate routine method. In this paper, an HPLC method for separating fullerenes was devised with 3,5-dinitrobenzamidopropyl (DNBAP) chemically bonded phase as packing and toluene–light petroleum as mobile phase. Based on the mechanism of electron donor–acceptor interaction, fullerenes can undergo more pronounced interaction with this bonded phase, which permits a good solvent, *e.g.* toluene, to be added to the mobile phase to increase the sample load as well as the sensitivity of the method.

EXPERIMENTAL

Apparatus

A Vista 56 liquid chromatograph (Varian) with a UV-100 LC detector, a Valco six-port injector with 10-μl sample loop and a VISTA 401 recorder was used.

Detection was performed either at a wavelength of 254 nm using *n*-hexane or light petroleum as mobile phases or at 330 nm with toluene added in the mobile phase.

All separations were carried out at ambient temperature.

Columns

Packings of ODS-, NH_2-, C_6H_5- and CN-silica were purchased from Tianjin Second Reagent Factory, China. Silica gel was purchased from Qingdao Oceanic Chemical Factory, China.

3-Nitrobenzamidopropyl (mNBAP), 4-nitrobenzamidopropyl (pNBAP) and DNBAP silica gel chemically bonded phases were synthesized according to Felix and Bertrand [15] with some modification. The NH_2-silica gel was produced by reacting silica gel (10 μm) with γ-aminopropyltrimethoxysilane (Chemical Factory attached to Wuhan University, China). Then NH_2-silica gel was modified to mNBAP, pNBAP or DNBAP with 3-nitrobenzoyl, 4-nitrobenzoyl or 3,5-dinitrobenzoyl chloride, respectively. All the packings were packed into 15 × 0.4 cm I.D. stainless-steel columns using a conventional high-pressure slurry packing procedure.

Materials and reagents

Raw fullerene materials (consisting of about 85% C_{60} and 15% C_{70}) were extracted from soot with toluene as previously described [1,16]. All reagents were of analytical grade and were used as obtained.

RESULTS AND DISCUSSION

The solubility of fullerenes in various solvents

One of the basic requirements of a suitable mobile phase in a liquid chromatographic system is good solubility for the solutes to be separated. Thus, a knowledge of the solubility of fullerenes in various solvents is of great importance to optimizing chromatographic systems, including both the mobile phase and the stationary phase. A few papers on this subject have been published [4]. A spot plate test was carried out. For a good solvent the colour turned to wine red or brown red, depending on the extent of solubility of fullerenes in the solvent tested; for a fair solvent the colour turned to pinkish; for a poor solvent the solution became slightly pinkish; and finally for a bad solvent the test solvent remained colourless. Thus, solvents can be divided into four categories according to their decreasing solubilities as follows:

(1) Good solvents: benzene, toluene, ethylbenzene, *o*-xylene, *m*-xylene, *p*-xylene, 1,3,5-trimethylbenzene, 1,2,4,5-tetramethylbenzene, tetralin, carbon disulphide.

(2) Fair solvents: *n*-hexane, light petroleum (b.p. 60–90°C), *n*-octane, chloroform, dichloromethene, dichloroethane, carbon tetrachloride.

(3) Poor solvents: decane, cyclohexane, diethyl ether, ethyl acetate, tetrahydrofuran.

(4) Bad solvents: *n*-pentane, methanol, ethanol, 2-propanol, acetone, acetonitrile, water, dimethyl sulphoxide.

Recently a study which quantitated the solubility of buckminsterfullerene in several organic solvents was reported [17].

It can be concluded form our simple experiment that:

(1) It is advisable to use a good solvent, such as benzene or toluene, as the mobile phase or as one of the components of a mixed-solvent mobile phase to increase sample load, which may in turn increase the sensitivity of the analytical method or the throughput of the preparative method.

(2) Reversed-phase liquid chromatography is not ideal for fullerene separation, though it is the most commonly used mode in HPLC. This is because of the poor solubility of fullerenes in water, methanol, acetonitrile and tetrafuran, etc., which are widely used in reversed-phase liquid chromatography.

(3) Normal-phase liquid chromatography is preferred for the analytical or preparative separation of fullerenes.

Retention behaviour of C_{60} and C_{70} fullerenes on some commercially available packings

Packings commercially available are easily accessible and of high quality, and are thus preferable when a new separation method is to be developed. ODS-, CN-, NH_2-, C_6H_5-silica and silica gel were tried first. *n*-Hexane was used as the mobile phase since it has distinct solubility for fullerenes and is one of the least polar solvents. The results (see Table I and Fig. 1) demonstrated that, of the five packings tested, both ODS- and CN-silica gave baseline separation of C_{60} and C_{70}, NH_2- and C_6H_5-silica gave partial separation, while silica gel was incapable of achieving separation because of its insignificant retention of C_{60} and C_{70}. The selectivity factors (α) between C_{70} and C_{60} on these packings seemed to be sufficiently large (see Table I and Fig. 2), which is easily understandable because of the relatively large difference in the molecular masses of the fullerenes to be separated. Ajie *et al.* [4] claimed that silica gel did produce a definite separation of fullerenes. This difference in observation can be attributed to the probable difference in the activity of silica gel

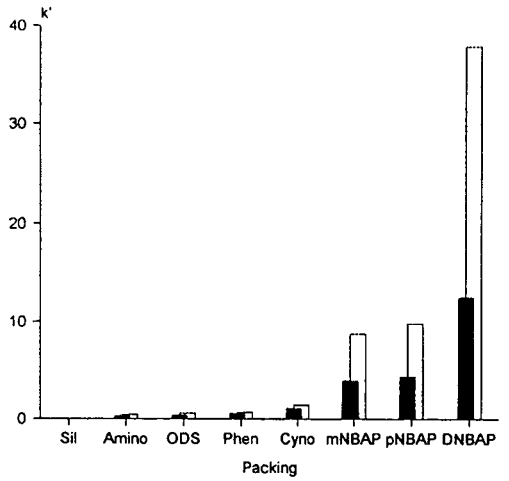

Fig. 1. Capacity factors for (■) C_{60} and (□) C_{70} on different packings. Sil = silica gel; ODS = octadecylsilyl; Phen = phenyl; Cyno = CN.

TABLE I

CAPACITY FACTORS, k', AND SELECTIVITY FACTORS, α, FOR C_{60} AND C_{70} ON DIFFERENT PACKINGS

$k' = (t_R - t_0)/t_0$, $\alpha = k'_{C_{70}}/k'_{C_{60}}$. The retention time of toluene was used as t_0.

No.	Packing	Eluent	$k'_{C_{60}}$	$k'_{C_{70}}$	α
1	Silica gel	*n*-Hexane	0	0	–
2	NH_2-Silica	*n*-Hexane	0.32	0.44	1.37
3	ODS-Silica	*n*-Hexane	0.36	0.60	1.67
4	C_6H_5-Silica	*n*-Hexane	0.55	0.66	1.20
5	CN-Silica	*n*-Hexane	1.04	1.42	1.36
6	mNBAP	*n*-Hexane	3.87	8.72	2.25
7	pNBAP	*n*-Hexane	4.31	9.80	2.27
8	DNBAP	*n*-Hexane	12.5	37.8	3.02
9	DNBAP	*n*-Hexane–toluene (90:10, v/v)	4.78	10.8	2.26

packings used in the two laboratories. A common drawback of these commercially available packings is their low retention for C_{60} and C_{70}, compared with the three packings containing a nitrobenzamidopropyl group, shown below. Thus, these packings have low tolerance towards the addition of good solvent to *n*-hexane.

Retention behaviour of fullerenes on synthetic packings

Cox *et al.* [5] used DNAP and Jinno *et al.* [8] devised and synthesized multi-legged phenyl chemically bonded stationary phases for separating C_{60} and C_{70}. Welch and Pirkle [13] evaluated the retention behaviour of C_{60} and C_{70} using ten HPLC stationary phases, including some specifically designed for recognition of the fullerenes, and they claimed that a novel tripodal π-acidic stationary phase designed for simultaneous multipoint interaction with buckminsterfullerene provided the greatest retention and the greatest separation for the C_{60}/C_{70} mixture.

At the beginning of this study 2 years ago, it was postulated that fullerene molecules might possess certain aromaticity and they might show electron-donor properties. As nitrobenzamidopropyl functionalites can show pronounced interaction with some aromatic hydrocarbons [18,19] it is worth trying this type of packing. Only one simple step was needed for the synthesis of mNBAR, pNBAP and DNBAR packings from NH_2-silica packing, and high overall yields could be obtained even by novices. These packings gave k' values ranging from 3.87 to 12.5 for C_{60} and from 8.72 to 37.8 for C_{70} (Table I and Fig. 1). The separation factors, α, between C_{70} and C_{60} became larger than 2 on mNBAP and pNBAP, and reached 3.02 on DNBAP. Evidently, mNBAP, pNBAP and DNBAP are more suitable for the separation of C_{60} and C_{70} than the commercially available packings. In addition, DNBAP interacts with fullerenes more than mNBAP and pNBAP. In fact, the best-performing stationary phase DNBAP proposed is similar in structure to the stationary phase VI in ref. 13, although they differ by one methylene group, *i.e.* Welch *et al.* [13] introduced a dinitrobenzamidobutyl (DNBAB) group. Moreover, our synthetic route seems to be much simpler.

In this study, a fraction of good solvent was intentionally introduced into the mobile phase to increase the sample load and improve the separation. By so doing, the mobile phase became more soluble for fullerenes. The detection wavelength, however, had to be changed to 330 nm and the detection limit of fullerenes became somewhat higher than when only *n*-hexane was used as mobile phase with the detection wavelength at 254 nm. Nevertheless, the overall sensitivity of the analytical method can still increase as a result of the increasing sample load.

HPLC analysis of C_{60} and C_{70}

Selection of mobile phase. For LC separation of C_{60} and C_{70}, the solubility of fullerenes is the most important factor to be considered. With DNAP as the stationary phase, Cox *et al.* [5] used an *n*-hexane to 50% dichloromethane–*n*-hexane gradient as the mobile phase, while Nondek and Kuzilek [20] improved the solubility of fullerenes by using a more soluble mobile phase, an *n*-hexane–benzene binary mixture. With ODS-silica as the stationary phase, Diederich *et al.* [7] used toluene–acetonitrile, while Yan *et al.* [9] used methanol–benzene, methanol–toluene and methanol–*m*-xylene. Cui *et al.* [10] examined methanol–diethyl ether as the mobile phase with four different polysiloxane stationary phases, including ODS- or phenyl-substituted stationary phases.

In this paper, a good solvent, toluene, together with light petroleum was used as the mobile phase. In our experiment, the light petroleum consisted mainly of *n*-hexane with a small fraction of *n*-heptane (*ca.* 10%) and had the same elution capacity for fullerenes as pure *n*-hexane. However, light petroleum is much cheapter than *n*-hexane. This mobile phase was found to have good solubility for C_{60} and C_{70} fullerenes.

To optimize the LC system, mobile phases of different ratios of toluene–light petroleum were tested. Fig. 3 displays the relationship of the fullerenes' capacity factors (k') *vs.* ratio of toluene–light petroleum. The k' values decreased as the content of toluene in the mobile phase increased. Separation of C_{60} and C_{70} can thus be carried out under up to 30% toluene

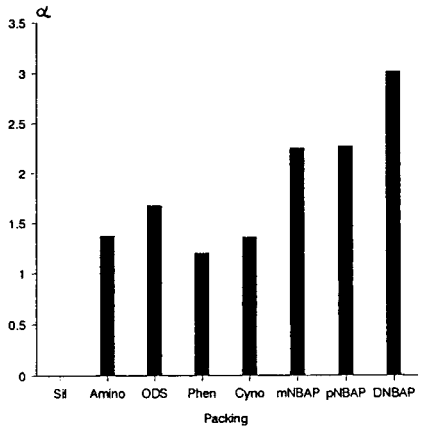

Fig. 2. Selectivity factors for C_{70} to C_{60} on different packings.

content on a newly packed column with an efficiency of 20 000 plates per metre. When the column efficiency deteriorated the column could still be used for a long time by reducing the toluene content in the mobile phase. Fig. 4 is the chromatogram of the analysis of C_{60} and C_{70} using DNBAP stationary phase.

Calibration of C_{60} and C_{70} fullerenes. Quantitative analysis of C_{60} and C_{70} fullerenes is very useful in optimizing the experimental parameters for producing carbon arc soot, selection of proper extraction solvents and determining the purity of separated fullerenes. Using the HPLC system established [DNBAP as stationary phase and toluene–light petroleum (20:80, v/v) as mobile phase], pure C_{60}(>99.9%) and C_{70}(>99.5%) were obtained in our laboratory, and their solutions at various concentrations were prepared and injected. The regression equations of the calibration curves of C_{60} and C_{70} are, respectively:

$$C_{60}: \log A = 6.576 + 0.9521 \log C, \; r = 0.99998$$

$$C_{70}: \log A = 6.188 + 0.9621 \log C, \; r = 0.99977$$

where A presents peak area (μV s) and C is sample concentration (mg/ml) injected. It can be seen that the absorption coefficient of C_{60} is larger than that of C_{70} at a wavelength of 330 nm. Thus, the real percentage of C_{60} and C_{70} in the mixture should be calculated by multiplying their areas by correction factors. The HPLC

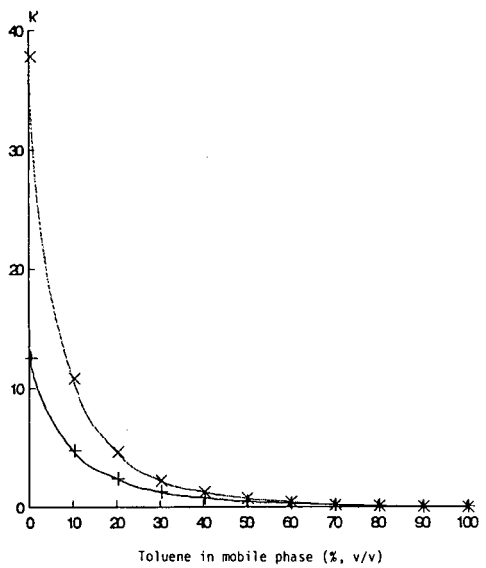

Fig. 3. Relationship between capacity factor (k') *vs.* toluene in mobile phase. The experimental conditions are the same as in Fig. 4, except for the mobile phase. + = C_{60}; × = C_{70}.

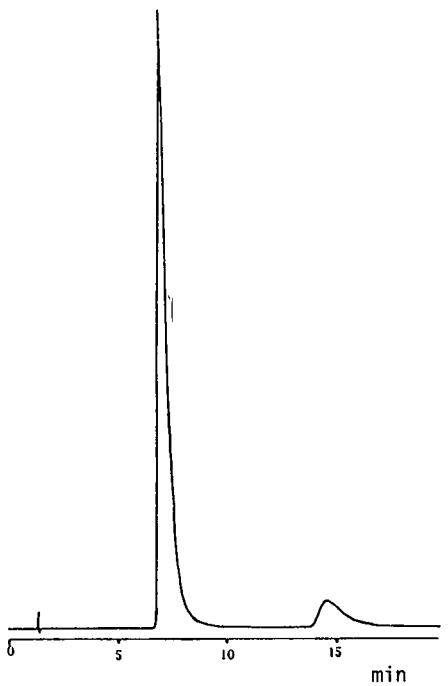

Fig. 4. Chromatogram of the separation of C_{60} (t_R = 7.16 min) and C_{70} (t_R = 14.63 min). Column: DNBAP–silica column (150 × 4 mm I.D.). Mobile phase: toluene–light petroleum (10:90, v/v), 1.0 ml/min. Detection wavelength: 330 nm.

method proposed for analysing C_{60} and C_{70} is more convenient than MS, and the column has already been used for thousands of injections for routine analysis for about 18 months.

As the production of C_{60} is becoming easier as the result of several innovative studies [21–25], the proposed chromatographic system is less useful for the preparation of C_{60} and is at present restricted to analytical use. The chromatographic system has, however, been modified with the use of *o*-xylene instead of toluene in the mobile phase to increase fullerene solubility and scaled up to prepare satisfactorily pure C_{70} (purity *ca.* 99.5%) and C_{84} (purity *ca.* 99.5%) fullerenes. Reports of these studies are now in preparation.

CONCLUSIONS

This paper compared eight packings and demonstrated an HPLC system for the analysis of C_{60} and C_{70} fullerenes with DNBAP chemically bonded phase as the stationary phase and toluene–light petroleum as the mobile phase.

ACKNOWLEDGMENTS

This work is jointly supported by the State Commission of Education, the National Natural Science Foundation and the State Commission of Science and Technology of China.

REFERENCES

1 H.W. Kroto, J.R. Heath, S.C. O'Brien, R.F. Curl and R.E. Smalley, *Nature (London)*, 318 (1985) 162.
2 W. Kraetschmer, K. Fostiropoulos and D.R. Huffman, *Chem. Phys. Lett.*, 170 (1990) 167.
3 P. Fowler, *Nature*, 350 (1991) 20.
4 H. Ajie, M.M. Alvarez, S.J. Anz, R.D. Beck, F. Diederich, K. Fostiropoulos, D.R. Huffman, W. Kraetschmer, Y. Rubin, K.E. Schriver, D. Sensharma and R.L. Whetten, *J. Phys. Chem.*, 94 (1990) 8630.
5 D.M. Cox, S. Behal, M. Disko, S.M. Gorun, M. Greaney, C.S. Hsu, E.B. Kollin, J. Millar, J. Robbins, W. Robbins, R.D. Sherwood and P. Tindall, *J. Am. Chem. Soc.*, 113 (1991) 2940.
6 R. Taylor, J.P. Hare, A.K. Abdul-Sada and H. W. Kroto, *J. Chem. Soc., Chem. Commun.*, 20 (1990) 1423.
7 F. Diederich, R.L. Whetten, C. Thilgen, R. Ettl, I. Chao, M.M. Alvarez, *Science*, 254 (1991) 1768.
8 K. Jinno, T. Uemura, H. Nagashima and K. Itoh, *J. High Resolut. Chromatogr.*, 15 (1992) 627.
9 F. Yan, Y.T. Liu and J.S. Ma, *Chinese Chem. Lett.*, 3(11) (1992) 903.
10 Y. Cui, S.T. Lee, S.V. Olesik, W. Flory and M. Mearini, *J. Chromatogr.*, 625 (1992) 131.
11 J.M. Hawkins, T.A. Lewis, S.D. Loren, A. Meyer, J.R. Heath, Y. Shibato and R.J. Saykally, *J. Org. Chem.*, 55 (1990) 6250.
12 K. Jinno, K. Yamamoto, T. Ueda, H. Nagashima, K. Itoh, J.C. Fetzer and W.R. Biggs, *J. Chromatogr.*, 594 (1992) 105.
13 C.J. Welch and W.H. Pirkle, *J. Chromatogr.*, 609 (1992) 89.
14 F. Diederich, R. Ettl, Y. Rubin, R.L. Whetten, R. Beck, M. Alvarez, S. Anz, D. Sensharma, F. Wudl, K.C. Khemani and A. Koch, *Science*, 252 (1991) 548.
15 G. Felix and C. Bertrand, *J. High Resolut. Chromatogr. Chromatogr. Commun.*, 7 (1984) 160.
16 Z. Gu, J. Qian, X. Zhou, Y. Wu, X. Zhu, S. Feng and Z. Gan, *J. Phys. Chem.*, 95(24) (1991) 9615.
17 N. Sivaraman, R. Dhamodaran, I. Kaliappan, T.G. Srinivasan, P.R. Vasudeva Rao and C.K. Mathews, *J. Org. Chem.*, 57 (1992) 6077.
18 W. Holstein and H. Hemetsberger, *Chromatographia*, 15(3) (1982) 186.
19 W. Holstein and H. Hemetsberger, *Chromatographia*, 15(4) (1982) 251.
20 L. Nondek and V. Kuzilek, *Chromatographia*, 33(7/8) (1992) 344.
21 M.S. Meier and J.P. Selegue, *J. Org. Chem.* 57 (1992) 1924.
22 A. Guegel and K. Muellen, *J. Chromatogr.*, 628 (1993) 23.
23 D.L. Stalling, K.C. Kuo, C.Y. Guo and S. Saim, *J. Liq. Chromatogr.*, 16(3) (1993) 699.
24 W.A. Scrivens, P.V. Bedworth and J.M. Tour, *J. Am. Chem. Soc.*, 114 (1992) 7917.
25 N. Coustel, P. Bernier, R. Azner, A. Zahab, J.-M. Lambert and P. Lyard, *J. Chem. Soc., Chem. Commun.* (1992) 1402.

Journal of Chromatography, 648 (1993) 497–500
Elsevier Science Publishers B.V., Amsterdam

CHROM. 25 420

Short Communication

Direct determination of enantiomeric excess of carbocyclic esters by chiral capillary gas chromatography

Kevin D. Belfield*, Todd S. Hofmeister and Jeongbeob Seo

Department of Chemistry, University of Detroit Mercy, P.O. Box 19900, Detroit, MI 48219-0900 (USA)

(First received March 19th, 1993; revised manuscript received June 2nd, 1993)

ABSTRACT

Enantiomer separations of monocyclic and bicyclic esters (methyl and ethyl esters) were carried out directly by capillary gas chromatography (GC) using a chiral γ-cyclodextrin fused-silica capillary GC column. The direct determination of enantioselectivity of an asymmetric alkylation reaction was achieved. Larger enantiomer separations were found for the bicyclic esters ($\alpha = 1.038–1.079$) compared to the monocyclic esters ($\alpha = 1.013–1.022$). Molecular dimensions, derived from MM2 energy-minimized structures of a monocyclic ester and a bicyclic ester, correlate well with thermodynamic data and are consistent with more than one mechanism of enantio-differentiation.

INTRODUCTION

During the course of studies directed towards the enantioselective synthesis of bicyclic dienes, enantiomeric purity measurements of our reaction products were necessary. Chromatographic methods potentially offer both high precision and excellent reproducibility for enantiomeric purity determination, most commonly by derivatization to diastereomers and subsequent analysis on achiral chromatography columns or by the use of chiral chromatography columns [1–10]. O-Alkylated cyclodextrins have found use as chiral stationary phases in capillary gas chromatography (GC) for the enantiomeric separation of a wide variety of compounds [7–10] and offer the possibility of reversing the order of enantiomer elution [11]. Herein, we report the first chromatographic enantiomeric separation and direct enantiomeric excess (ee) determination of diketoesters **1**(***S***) and **1**(***R***) (Figs. 1 and 2),

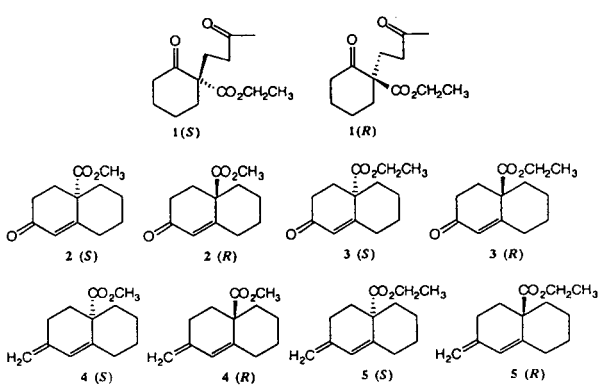

Fig. 1. Structures.

* Corresponding author.

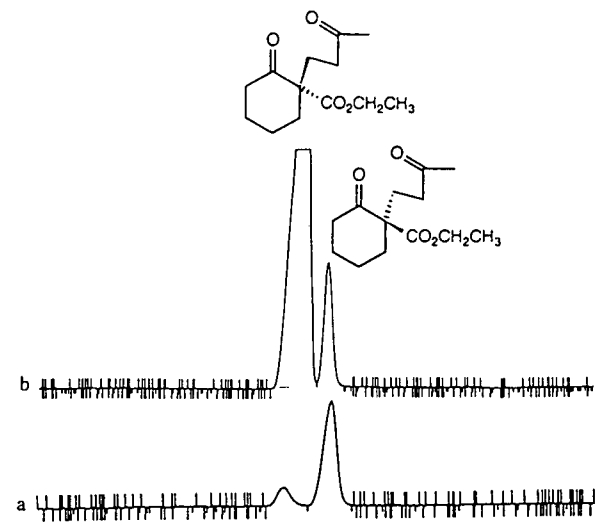

Fig. 2. Enantiomer separation of diketoesters **1**(*S*) and **1**(*R*) on the FS-Lipodex E chiral phase capillary column (140°C); (a) predominantly (*R*)-enantiomer and (b) predominantly (*S*)-enantiomer.

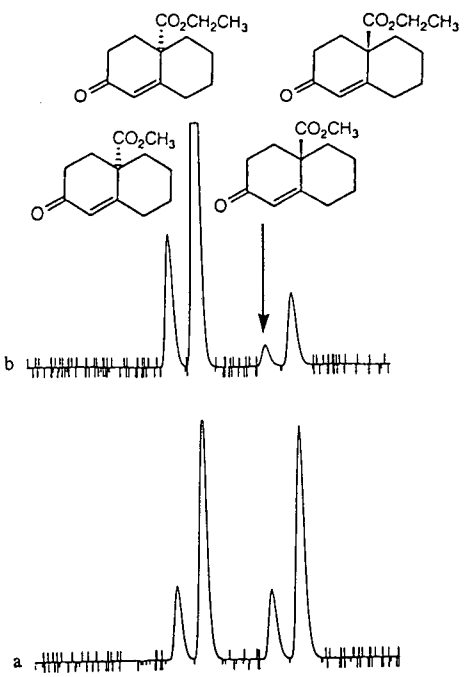

Fig. 3. Enantiomer separation of methylester enones **2**(*S*) and **2**(*R*) and ethylester enones **3**(*S*) and **3**(*R*) on the FS-Lipodex E chiral phase capillary column (150°C); (a) racemic mixture and (b) optically active mixture.

carbocyclic ester enones **2**(*S*), **2**(*R*), **3**(*S*) and **3**(*R*) (Fig. 3) and carbocyclic ester dienes **4**(*S*), **4**(*R*), **5**(*S*) and **5**(*R*) (Fig. 4)[a]. A brief discussion of enantio-differentiation of these compounds based on molecular size and thermodynamic parameters is presented.

EXPERIMENTAL

Racemic and optically active versions of compounds **1–5** were prepared from ethyl-2-cyclohexanone carboxylate, the details of which will be reported in a forthcoming publication. Chiral GC analyses were done with a Macherey–Nagel 50 m × 0.25 mm I.D. FS-Lipodex E fused-silica capillary column, a Hewlett-Packard 5890 instrument with flame ionization detector, and a Hewlett-Packard 3392A reporting integrator (helium column flow 51.7 ml/min, detector temperature 300°C, injector temperature 160°C, oven temperature 110–150°C).

RESULTS AND DISCUSSION

Quantitative separations of the carbocyclic esters were achieved on an octakis-(2,6-di-O-pentyl-3-O-butyl)-γ-cyclodextrin fused-silica capillary GC column (FS-Lipodex E) between 110 and 150°C (Table I, Figs. 2–4). Enantiomeric excesses of 72 and 71% ee were obtained for mixtures comprised predominantly of the (*S*)- and (*R*)-enantiomer, respectively. These values are similar to those reported previously for compounds **1** and **3**, in which an indirect method was utilized (polarimetry correlated with ^{13}C NMR) [12]. The chromatographic method employed here provides more precise results since, in all cases, complete resolution of enantiomers was achieved.

As evidenced in Table I, larger separation factors were obtained for the relatively compact bicyclic compounds **2–5** (Figs. 3 and 4), than the spatially more demanding monocyclic diketoester **1** (Fig. 2). The separation factor, α, is equal to the ratio of the retention times of the longer

[a] The asymmetric syntheses of these compounds will be reported by us elsewhere.

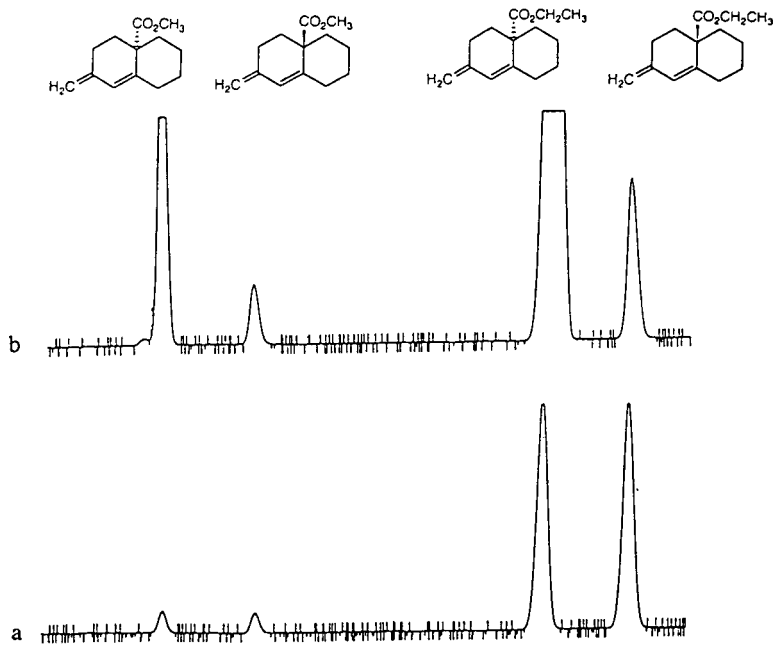

Fig. 4. Enantiomer separation of methylester dienes **4**(*S*) and **4**(*R*) and ethylester dienes **5**(*S*) and **5**(*R*) on the FS-Lipodex E chiral phase capillary column (110°C); (a) racemic mixture and (b) optically active mixture.

retained enantiomer (t_2) to the lesser retained enantiomer (t_1), *i.e.*, $\alpha = t_2/t_1$. From the separation factor, the difference in free energy of association of an enantiomeric pair with the chiral stationary phase was estimated (Table II) [3]:

$$-\Delta(\Delta G^0) = RT \ln \alpha$$

After obtaining chromatographic data at several temperatures, the following equation was used to afford a plot of $R \ln \alpha$ *versus* $1/T$ [7]:

$$R \ln \alpha = -\Delta(\Delta H^0)/T + \Delta(\Delta S^0)$$

From this plot, values of $\Delta(\Delta H^0)$ and $\Delta(\Delta S^0)$ were derived for the same enantiomeric pair (Table II). Straight-line plots were obtained in all cases, indicating that $\Delta(\Delta H^0)$ was constant

TABLE I

GAS CHROMATOGRAPHIC DATA FOR ENANTIOMERIC SEPARATION ON OCTAKIS-(2,6-DI-O-PENTYL-3-O-BUTYL)-γ-CYCLODEXTRIN FUSED-SILICA COLUMN (FS-LIPODEX E)

Compound[a]	T (°C)	α	Optical purity (% ee)
1(*S*)	140	1.013	72
1(*R*)	140	1.022	71
2(*S*)	150	1.079	72
3(*S*)	150	1.075	72
3(*R*)	150	1.074	71
4(*S*)	110	1.058	72
5(*S*)	110	1.038	72

[a] For optically active samples, tentative assignment of the absolute configuration of the predominant enantiomer is indicated.

TABLE II

THERMODYNAMIC PARAMETERS DETERMINED BY CHIRAL CAPILLARY GC ON AN FS-LIPODEX E COLUMN

Compound	$-\Delta(\Delta G^0)$ (J/mol)	$-\Delta(\Delta H^0)$ (J/mol)	$-\Delta(\Delta S^0)$ (J/mol · K)
1	60 ± 21, 140°C	682	1.5
2	258 ± 7, 150°C	2731	5.8
3	248 ± 7, 150°C	3907	8.6

over the experimental temperature range. All three thermodynamic parameters, $\Delta(\Delta G^0)$, $\Delta(\Delta H^0)$ and $\Delta(\Delta S^0)$, were substantially larger for the more compact bicyclic esters relative to the monocyclic ester. The larger values of $\Delta(\Delta G^0)$ and $\Delta(\Delta H^0)$ are indicative of stronger enantioselective interactions for compounds **2** and **3**, likely due, in part, to diffusion into the cyclodextrin cavity, as discussed below. A larger decrease in entropy is expected for cyclodextrin inclusion complex formation, possibly due to a decrease in degrees of freedom of the included molecule [7]. Larger negative values of $\Delta(\Delta S^0)$ were indeed obtained for bicyclic compounds **2** and **3** relative to monocyclic **1**.

A preliminary assessment of the size and shape selectivities exhibited here can be made by comparison of the molecular dimensions of compounds **1** and **3**, derived from the energy minimized structures calculated by the MM2 molecular mechanics program available in Chem 3D Plus (Cambridge Scientific Computing, Cambridge, MA, USA) with the reported cavity dimensions of underivatized γ-cyclodextrin (9.5 Å I.D. and 7.8 Å depth) [13][a]. The longest dimension of **3** was found to be 6.909 Å, small enough to fit into the cyclodextrin cavity. However, the 10.355 Å distance from the termini of the 2,2-substituents of **1** is large enough to be inhibited from diffusing fully into the cyclodextrin cavity.

The size/shape selectivity, based on molecular dimensions, parallels the thermodynamic parameters. These preliminary results support the possibility of more than one enantioselective retention mechanism, in accord with previously reported results [7]. The more compact molecules (**2**–**5**) may form a classic inclusion complex, while the more sterically demanding monocyclic enantiomers (**1**) may have limited interactions within the cavity but interact via weaker, external associations with the cyclodextrin.

Analysis of products from asymmetric alkylation reactions on an O-alkylated γ-cyclodextrin capillary GC column provides for fast, accurate, and reproducible determination of the enantioselectivity of the reaction. Thus, a level of accuracy hitherto unrealized for the enantiomeric purity evaluation of the aforementioned cyclic esters was realized. Further studies, directed towards optimizing asymmetric reactions, are expected to be expedited by employing this extremely versatile chiral chromatographic method.

ACKNOWLEDGEMENTS

We wish to acknowledge Professor John E. Baldwin (Syracuse University) for the use of GC equipment and the University of Detroit Mercy for support of this work.

REFERENCES

1 F.M. Pasutto, *J. Clin. Pharm.*, 32 (1992) 917.
2 A.M. Dyas, *J. Pharm. Biomed. Anal.*, 10 (1992) 383.
3 W.A. Konig, *The Practice of Enantiomer Separation by Capillary Gas Chromatography*, Hüthig, Heidelberg, 1987.
4 C.L. Young, H. Frank, C.R. Stewart and I.W. Wainer, *Chirality*, 1 (1989) 235.
5 B. Wong and M. Castellanos, *J. Chromatogr.*, 495 (1989) 21.
6 D.A. Both and M. Jemal, *J. Chromatogr.*, 558 (1991) 257.
7 A. Berthod, W. Li and D.W. Armstrong, *Anal. Chem.*, 64 (1992) 873; and references cited therein.
8 D.W. Armstrong, W.Y. Li and C.D. Chang, *Anal. Chem.*, 62 (1990) 914.
9 V. Schurig, H.-P. Nowotny and D. Schmalzing, *Angew. Chem., Int. Ed. Eng.*, 28 (1989) 736.
10 P. Fischer, R.Aichholz, U. Bolz, M. Juza and S. Krimmer, *Angew. Chem., Int. Ed. Eng.*, 29 (1990) 427.
11 D.W. Armstrong, W.Y. Li and J. Pitha, *Anal. Chem.*, 62 (1990) 214.
12 H. Brunner, J. Kraus and H.-J. Lautenschlager, *Monatsh. Chem.*, 119 (1988) 1161.
13 J. Szejtli, B. Zsadon and T. Cserhati, in W.L. Hinze and D.W. Armstrong (Editors), *Ordered Media in Chemical Separations*, American Chemical Society, Washington, DC, 1987, Ch. 11.

[a] It should be noted that the dimensions of the underivatized γ-cyclodextrin are used as an estimation only, due to lack of empirical data for the alkylated γ-cyclodextrin used in this study.

Journal of Chromatography, 648 (1993) 501–506
Elsevier Science Publishers B.V., Amsterdam

CHROM. 25 437

Short Communication

Gas chromatographic screening for neostigmine and physostigmine using temperature-programmed retention indices

Mariitta Kokko

Department of Chemistry, P.O.Box 6, Vuorikatu 20, SF-00014 University of Helsinki, Helsinki (Finland)

(First received October 20th, 1992; revised manuscript received May 13th, 1993)

ABSTRACT

Temperature-programmed gas chromatographic retention indices, relative to *n*-alkane (C standard) and *n*-alkylbis(trifluoromethyl)phosphine sulphide (M standard) homologous series, were determined for two low-volatile, highly toxic carbamates, neostigmine and physostigmine on SE-54 fused-silica capillary columns. The influence of temperature programme and sample concentration on the absolute values of the indices were evaluated. Reproducibility of the indices was good in both linear and multistep temperature programmes, but the reproducibility and peak shapes were better in the multistep temperature programme. When the compounds were present in high concentration, C standards and a flame ionization detector were used successfully, but multidetector M standards, which also can be seen with the selective alkali thermoionization detector, were superior when concentrations were low. Similarly M standards which can be seen also with other selective detectors (electron-capture, flame photometric and photoionization) could be a suitable index standard series for screening of different types of compounds containing heteroatoms.

INTRODUCTION

A retention index system based on homologous *n*-alkanes has been widely adopted in analytical toxicology, where the rapid identification of unknown substances is of key importance. When a great many samples must be analysed, retention index monitoring in GC analysis improves efficiency by reducing the number of samples needing to be reanalysed by another independent technique (MS or Fourier transform IR). Retention index monitoring also allows use of the retention index data determined in another laboratory.

The first compilations of the GC retention indices of toxicologically relevant compounds were based on measurements done by the packed columns with dimethylpolysiloxane stationary phases as SE-30 or OV-1 and *n*-alkanes as index standards [1,2]. The programmed and isothermal indices of hundreds of drugs have been used in combination with the differences between the retention indices measured on two different columns, OV-1 and OV-17 and found to allow reliable identifications [3,4]. Different column types like SE-30 equivalent narrow-bore thin-film capillary columns, wide-bore thick-film capillary columns and packed columns have been used and high correlation between the isothermal retention indices of physostigmine and of other compounds of toxicological interest have been found [5]. A major disadvantage of *n*-

0021-9673/93/$06.00

alkanes in screening for drugs is that they cannot be seen by selective detectors [6]. 1-Nitroalkanes have been proposed as alternative retention index standards for drug analysis in isothermal runs since these compounds can be detected with electron-capture (ECD), alkali thermoionization (ATD) and flame ionization (FID) detection in GC and they can also be used in HPLC [7]. Structurally, however, they are very different from most drugs. Selected mixtures of drugs are to be used as reference standards for optimum results. Their retention indices based on *n*-alkanes as reference substances have to be determined beforehand. This procedure is regarded as a standard practice in systematic toxicological analysis. Extensive evaluations in different laboratories have shown that for packed and capillary columns dimethylpolysiloxane is the preferred phase for screening in analytical toxicology. Only for special purposes, *e.g.* the differentiation of substances within a certain group, can other phases be useful, such as OV-17 or OV-225 [2,8].

In this work the usefulness of *n*-alkylbis(trifluoromethyl)phosphine sulphides (multidetector M standards), and for comparison *n*-alkanes (C standards), was investigated for the GC retention index monitoring of neostigmine and physostigmine. These low-volatile highly toxic carbamates were chosen as test compounds because they are cholinesterase inhibitors and potential chemical warfare agents. Except at extreme exposure and concentration the symptoms of carbamate poisoning are not as severe as those associated with organophosphorus compounds and so it was possible to investigate safely the effect of concentration of the test compounds on the retention indices.

The usefulness of multidetector M series as index standards was investigated when the concentration of neostigmine and physostigmine was changed from 5 ng/μl to 2 μg/μl and also when multistep temperature programmes were used. The retention indices were determined by two-channel GC with two similar columns connected to the same injector and to two similar or two different detectors.

Most drugs have heteroatoms which can be detected with the same selective detectors like M standards. A particular advantage of the M standards is that they can be used at trace level: they are detectable at levels of 0.4–0.6 pmol with FID, 2–7 fmol with ATD and 3–5 fmol with ECD [9].

EXPERIMENTAL

Instrumentation and chromatographic conditions

The gas chromatograph was a Micromat HRGC 412 microcomputer-controlled instrument (HNU-Nordion) with two-channel integration and printing software. Two fused-silica capillary columns 15 m × 0.32 mm, 0.25 μm cross-linked SE-54 film (dimethylpolysiloxane, 5% phenyl with 1% vinyl groups), were used, with FID and ATD. Standard chromatographic conditions were as follows: injector and detector temperature (FID or ATD) 250°C, carrier gas (He) flow-rate 2 ml/min, splitting ratio 1:10, septum purge 10 ml/min, starting point of the temperature programme 40°C (or 100°C), temperature-programming rate 10°C/min (or multistep), and end temperature of the programme 300°C.

Chemicals

Alkylbis(trifluoromethyl)phosphine sulphides, $(CF_3)_2P(S)(CH_2)_nCH_3$, $n = 5 \ldots 19$ (M standards), were diluted in ethyl acetate, *n*-alkanes (C standards) in hexane. The M series is commercially available from HNU-Nordion. Neostigmine iodide (**Ia**) and physostigmine (**II**) (Fig. 1) were diluted in acetone.

Calculations and computer programmes

Retention indices (I) were calculated according to Van den Dool and Kratz [10] with the formula, in both linear and multistep temperature programming, $I_{C\ (\text{or}\ M)} = 100C_n + 100(C_{n+i} - C_n)(t_{R(x)} - t_{R(n)}) \ / \ (t_{R(n+i)} - t_{R(n)})$, where C_n and C_{n+i} are carbon numbers of the C standards (or carbon numbers of the alkyl chain of M standards) eluted on either side of the unknown compound, $t_{R(x)}$ is the retention time of the unknown and $t_{R(n)}$ and $t_{R(n+i)}$ are the retention times of C_n (or M_n) and C_{n+i} alkanes (or M_{n+i}), respectively.

SC-Workstation software (Sunicom, Helsinki,

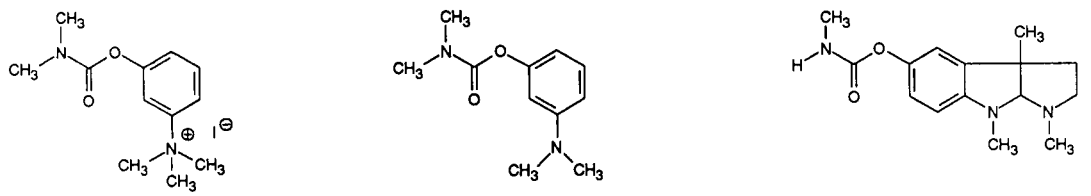

Ia Ib II

Fig. 1. Structural formulas of neostigmine iodide (**Ia**), 3-(N,N-dimethylaminophenyl) dimethylcarbamate (**Ib**) and physostigmine (**II**).

Finland) was used for creating the method, generating the compound library, data acquisition and integration, identification and quantification of compounds. SC-software is based upon MS-Windows (Microsoft) and it can be used also with systems which have their own data acquisition and basic chromatogram manipulation software.

To set up a retention index-based identification method you need to introduce standard compounds to every sample. Index standards may also be normal sample components, provided that these components can be found in all samples. Normally a small amount of index standard mixture is added to the sample, preferably just before injection. Many of the autosamplers can do this.

The first and most critical step of the identification process is finding the retention index standard peaks among all other peaks. This is accomplished automatically by the programme through sophisticated pattern recognition algorithm. After that index values are calculated for each peak. During the final step the programme compares the calculated retention index values with the compound-specific retention index values stored in the library and if the calculated value is within the selected identification limit, the compound is tentatively identified.

Normally the internal standard method was used for quantification. It requires quantitative calibration which means calculation of response factors. Each compound quantified must have a reference compound (internal standard). Both the standards and the compounds have been calibrated, so that they have response factors. Mean or linear response factors can be calculated for tens of data files.

It is possible to produce quality control reports directly from the chromatographic data both in textual and in graphic format. Also statistical reports on quantification parameters can be obtained easily.

RESULTS AND DISCUSSION

Physostigmine is not thermally stable and it slowly decomposes on standing in air, particularly at pH < 5 [11]. Neostigmine iodide loses methyliodide on heating and elutes as 3-(N,N-dimethylaminophenyl)dimethylcarbamate (**Ib**) in GC, as shown by an analysis of the mass spectra. Fig. 2 shows a typical gas chromatogram for a sample containing neostigmine and physostigmine together with the M standards.

Study was made of the influence of the starting point (40 and 100°C) of the linear temperature programme on the retention indices of neostigmine and physostigmine. The results were compared with indices obtained in multistep temperature programmes (Table I). The differences in retention indices when the initial temperature was 40 and 100°C were less than 1.0 index unit (i.u.), but the peak shape of physostigmine was better when the temperature programme was started at 100°C. The absolute values of the indices were higher when the multistep programmes were used; the reproducibility was as good as with the linear temperature programme; peak shapes were improved for more accurate integration, and the time required for analysis was shorter.

The influence of the concentration of the carbamates on the retention indices has been investigated. Studies by Rijks [12] on hydrocarbons have shown that when the peak is

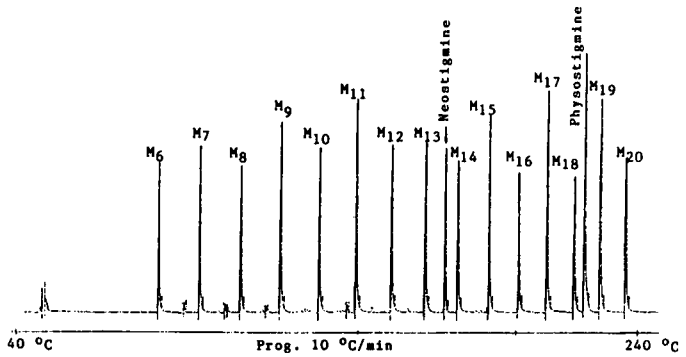

Fig. 2. Chromatogram of neostigmine and physostigmine together with M standards. Column, fused silica, cross-linked SE-54, 15 m × 0.32 mm, film thickness 0.25 μm; detection, ATD.

symmetrical, even a ten-fold increase in the sample concentration has no significant effect on the isothermal retention indices. The quantity of the different compounds in his samples was between 10 ng and 100 pg. Yin *et al.* [13] found that, when the quantity of a compound was large, there was a large effect on nearby peaks and a slight variation in the isothermal retention indices. However, the thicker the film the smaller the differences in the retention indices.

For a number of drugs a strong dependence of retention indices on concentration has been found. For example, the retention indices differed by 5 to 130 i.u. when the amount was increased from 1 ng to 4 μg [14]. The final amount was probably too large, causing overloading of columns. The film thickness, the retention time, and the similarity in polarity between the solute and the stationary phase have been shown to determine the maximum amount of compound that can be present in the sample. In a temperature-programmed run, the amount is lower for compounds with large retention indices than for compounds with small retention indices. Wang and Sun [15] recommend a sample size of 10 ng per compound for measurement of retention index values to an accuracy of ± 1 i.u. on common capillary columns (film thickness, 0.1–0.5 μm, I.D. 0.20–0.32 mm), although in some cases the amount of compound in a sample for retention index measurements can be as much as 100 ng.

Usually sample preparation sets limits on the concentration levels achievable. The practical limits of concentration should be known, therefore, before retention index monitoring is ap-

TABLE I

EFFECT OF THE TEMPERATURE PROGRAMME ON THE RETENTION INDICES OF NEOSTIGMINE AND PHYSOSTIGMINE

Temperature programmes: (I) from 40 to 300°C at 10°C/min; (II) from 100 to 300°C at 10°C/min; (III) from 40 to 200°C at 20°C/min, then from 200 to 300°C at 10°C/min; (IV) from 40 to 200°C at 20°C/min, then from 200 to 300°C at 5°C/min.

		I		II		III		IV	
		I, 5 runs	S.D.	I, 5 runs	S.D.	I, 5 runs	S.D.	I, 5 runs	S.D.
Neostigmine	I_C	1805.9	0.4	1806.3	0.4	1812.7	0.2	1812.2	0.2
	I_M	1360.9	0.1	1361.4	0.2	1368.8	0.2	1367.5	0.2
Physostigmine	I_C	2279.2	1.1	2278.3	0.8	2286.1	0.4	2278.7	0.6
	I_M	1839.9	0.4	1838.9	0.5	1849.5	1.4	1838.5	0.6

TABLE II

EFFECT OF THE CONCEENTRATION OF THE LOW-VOLATILE CARBAMATES ON THE RETENTION INDICES

Standard chromatographic conditions (see Experimental section).

Concentration	Neostigmine		Physostigmine	
	I_M	I_C	I_M	I_C
5 ng/μl	1360.7		1853.3	
25 ng/μl	1360.5		1845.0	
50 ng/μl	1360.6, 1360.0	1803.9	1840.1, 1840.4	2275.3
250 ng/μl		1804.1		2276.9
500 ng/μl		1805.0		2281.5
1 μg/μl		1806.8		2281.6
2 μg/μl	1367.9		1847.4	

plied. In this investigation the concentration of neostigmine and physostigmine was varied from 5 ng/μl to 2 μg/μl and the injection volume was 1 μl. ATD was used at lower concentrations of 5 ng/μl–50 ng/μl and FID at concentrations 50 ng/μl–2 μg/μl. Table II shows the results.

At concentrations of neostigmine between 5 and 250 ng/μl, the difference in the retention indices was less than 0.8 i.u. At higher concentrations the value began to increase: at 1 μg/μl the retention index was about 3 i.u. higher than at 5 ng/μl, and at 2 μg/μl about 7 i.u. higher indicating overloading of the column.

For physostigmine the situation was more complex. At concentration levels 50–250 ng/μl the retention indices were within 1.6 i.u. of each other. But when the concentration was lower or higher the retention indices increased. The structure of the compound and the nature of the stationary phase evidently were the dominant factors in determining this behaviour. Both at low and at high concentration physostigmine shows a slightly tailing peak on SE-54.

CONCLUSIONS

The results indicate the usefulness of the retention index method in GC screening for neostigmine and physostigmine. The reproducibility of the indices was good in each of the temperature programmes (0.2–1.4 i.u.), though the absolute values differed between programmes. Fast and reliable identifications are thus possible when the temperature programme used in the analytical run is the same as that used to record the library data. At concentration level 5–500 ng/μl the retention index window ± 2 i.u. is suitable for neostigmine but for physostigmine a larger window ± 6 i.u. may be necessary. With a different temperature programme, a larger index window has to be used also for neostigmine. Mixtures of selected drugs as retention index standards surely resemble more closely drugs to be analysed and this procedure is regarded as a standard practice in systematic toxicological analysis. But selected drugs cannot be added into the mixture in cases when some of them is among compounds to be analyzed quantitatively. M standards may then be one possibility to resolve the problem. Relative to the C standards, M standards allowed retention indices to be determined for much lower concentrations of neostigmine and physostigmine. Since many drugs possess heteroatoms, the M standards, used with selective detectors, may be useful for toxicological analysis, where concentration levels often are very low. Positive identifications by GC retention index monitoring must, of course, always be confirmed by another independent technique such as MS or Fourier transform IR.

REFERENCES

1 A.C. Moffat, *J. Chromatogr.*, 113 (1975) 69.
2 R.E. Ardrey, B.S. Finkle, J.P. Franke, A.C. Moffat, M.R. Möller, R.K. Müller and R.A. de Zeeuw, *Gas Chromatographic Retention Indices of Toxicologically Relevant Substances on SE-30 or OV-1*, VCH, Weinheim, 2nd ed., 1985.
3 E. Marozzi, V. Gambaro, F. Lodi and A. Pariali, *Farmaco, Ed. Prat.*, 31 (1976) 180; *C.A.*, 85 (1976) 14793c.
4 E. Marozzi, F. Gambaro, F. Lodi and A. Pariali, *Farmaco, Ed. Prat.*, 32 (1977) 330; *C.A.*, 87 (1977) 128220k.
5 M. Japp, R. Gill and M.D. Osselton, *J. Forensic Sci.*, 2 (1987) 1574.
6 M.E. Sharp, *Can. Soc. Forens. Sci. J.*, 19 (1986) 83.
7 R. Aderjan and M. Bogusz, *J. Chromatogr.*, 454 (1988) 345.
8 R.A. de Zeeuw, J.P. Franke, H.H. Maurer and K. Pfleger, *Gas Chromatographic Retention Indices of Toxicologically Relevant Substances on Packed or Capillary Columns with Dimethylsilicone Stationary Phases*, VCH, Weinheim, 3rd ed., 1992.

9 A. Manninen, M.-L. Kuitunen and L. Julin, *J. Chromatogr.*, 349 (1987) 465.
10 H. van den Dool and P.D. Kratz, *J. Chromatogr.*, 11 (1963) 463.
11 M. Kneczke, *J. Chromatogr.*, 198 (1980) 529.
12 J.A. Rijks, *Ph.D. Thesis*, Technical University, Eindhoven, 1973, p. 39.
13 H.F. Yin, Y. Zhu and Y.L. Sun, *Chromatographia*, 28 (1989) 502.
14 M. Bogusz, J. Wijsbeek, J.P. Franke and R.A. de Zeeuw, *J. High Resolut. Chromatogr. Chromatogr. Commun.*, 6 (1983) 40.
15 T. Wang and Y. Sun, *J. High Resolut. Chromatogr. Chromatogr. Commun.*, 10 (1987) 603.

Author Index

BIOAFFINITY CHROMATOGRAPHY

By **J. Turková,** Czechoslovak Academy of Sciences, Institute of Organic Chemistry and Biochemistry, Prague, Czech Republic

Journal of Chromatography Library Volume 55

Bioaffinity chromatography is now the preferred choice for the purification, determination or removal of many biologically active substances. The book includes information on biologically active substances with their affinants, solid supports and methods of coupling, summarized in tables covering classical, high-performance liquid and large-scale bioaffinity chromatography.

Optimization of the preparation and the use of highly active and stable biospecific adsorbents is discussed in several chapters. Following a chapter dealing with the choice of affinity ligands, affinity-sorbent bonding is described in detail. Other chapters give information on solid supports, the most common coupling procedures and a general discussion of sorption and elution. Several applications of bioaffinity chromatography are described, e.g. quantitative evaluation of biospecific complexes and many applications in medicine and in the biotechnology industry.

Contents:

© 1993 819 pages Hardbound
Price: Dfl. 495.00 / US $ 282.75
ISBN 0-444-89030-0

ELSEVIER
SCIENCE PUBLISHERS

ORDER INFORMATION

For USA and Canada
ELSEVIER SCIENCE PUBLISHERS
Judy Weislogel, P.O. Box 945
Madison Square Station
New York, NY 10160-0757
Fax: (212) 633 3880

In all other countries
ELSEVIER SCIENCE PUBLISHERS
P.O. Box 330
1000 AH Amsterdam
The Netherlands
Fax: (+31-20) 5862 845

US$ prices are valid only for the USA & Canada and are subject to exchange rate fluctuations; in all other countries the Dutch guilder price (Dfl.) is definitive. Customers in the European Community should add the appropriate VAT rate applicable in their country to the price(s). Books are sent postfree if prepaid.

TrAC - Trends in Analytical Chemistry: Reference Edition

Volume 11: 1992

TrAC Compendium Series Volume 11

The Reference Edition of Trends in Analytical Chemistry (TrAC) is a compilation of the archival material reprinted from the regular issues of the journal. TrAC provides a topical digest of current developments and new ideas in the analytical sciences. It does so in the form of broadly-based, easy-to-read scientific reviews, backed up by news and other features of interest to the international analytical chemistry community. For subscribers to the library edition of TrAC, the reference editions form an integral part of the annual subscription, but for others these indispensable sources of information can be purchased individually. They provide informative and stimulating reading for all those who use analytical methods.

This latest volume contains all the archival material published in 1992. It covers a wide range of analytical techniques and applications of interest to academic and research workers in chemistry, biochemistry, clinical chemistry, pharmaceutical chemistry and toxicology.

A selection of the Contents.

Capillary Electrophoresis in Chemical/Pharmaceutical Quality Control *(A. Pluym, W. Van Ael, M. De Smet)*. Image Analysis in Chemistry. I. Properties of Images, Greylevel Operations, the Multivariate Image. II. Multivariate Image Analysis *(P. Geladi et al.)*. Silica Based, Solid Phase Reagents for Derivatizations in Chromatography *(F.-X. Zhou, J.M. Thorne, I.S. Krull)*. Mapping Post-Translational Modifications of Viral Proteins by Mass Spectrometry *(J.J. Gormann)*. Fluorescence Detection in Capillary Electrophoresis *(L.N. Amankwa, M. Albin, W.G. Kuhr)*. Biomolecular Tracing through Accelerator Mass Spectrometry *(J.S. Vogel, K.W. Turteltaub)*. Solid-Phase Reactors in Flow Injection Analysis *(M.D. Luque de Castro)*. Capillary Electrophoresis: A Powerful Tool for Biomedical Analysis and Research? *(D. Perrett, J. Ross)*. Bioanalytical Sample Preparation using Microdialysis and Ultrafiltration Capillaries *(M.C. Linhares, P.T. Kissinger)*. Models of Time-Series Analysis - a Helpful Tool for Evaluation of Noisy Data in Distribution Analysis *(K. Doerffel)*. Bio-Analytical Applications of Fourier Transform Infrared Spectroscopy *(M. Jackson, H.H. Mantsch)*. X-ray Absorption Spectroscopy in Chemistry. I. Extended X-ray Absorption Fine Structure. II. X-ray Absorption near Edge Structure *(P. Behrens)*. Mechanism of the Peroxyoxalate Chemiluminescence Reaction *(P.J.M. Kwakman, G.J. de Jong, U.A.Th. Brinkman)*. Plasma Spectrometric Detection for Supercritical Fluid Chromatography *(J.M. Carey, J.A. Caruso)*. Electrochemistry of Biopolymers *(J.A. Cox, A. Pryzjazny)*. High-Field NMR Spectroscopy as an Analytical Tool for Quantitative Determinations: Pitfalls, Limitations and Possible Solutions *(Cs. Szántay, Jr.)*. Abrasive Stripping Voltammetry - an Electrochemical Solid State Spectroscopy of Wide Applicability *(F. Scholz, B. Lange)*. Polymer Coatings as Stationary Phases in High-Performance Liquid Chromatography *(M. Hanson, K.K. Unger)*. Lasers in Mass Spectrometry *(J. Gorbally)*. Author Index. Subject Index.

1993 viii + 402 pages
Price: US $ 354.25 / Dfl. 620.00
ISBN 0-444-89926-X

ELSEVIER
SCIENCE PUBLISHERS

ORDER INFORMATION

For USA and Canada
ELSEVIER SCIENCE PUBLISHERS
Judy Weislogel
P.O. Box 945
Madison Square Station,
New York, NY 10160-0757
Tel: (212) 989 5800
Fax: (212) 633 3880

In all other countries
ELSEVIER SCIENCE PUBLISHERS
P.O. Box 211
1000 AE Amsterdam
The Netherlands
Tel: (+31-20) 5803 753
Fax: (+31-20) 5803 705

US$ prices are valid only for the USA & Canada and are subject to exchange rate fluctuations; in all other countries the Dutch guilder price (Dfl.) is definitive. Customers in the European Community should add the appropriate VAT rate applicable in their country to the price(s). Books are sent postfree if prepaid.

PUBLICATION SCHEDULE FOR THE 1993 SUBSCRIPTION

Journal of Chromatography and *Journal of Chromatography, Biomedical Applications*

MONTH	1992	J–A	M	J	J	A	S	O	N	D
Journal of Chromatography	Vols. 623–627	Vols. 628–636	637/1 637/2 638/1 638/2	639/1 639/2 640/1 + 2	641/1 641/2 642/1 + 2 643/1 + 2 644/1	644/2 645/1 645/2 646/1	646/2 647/1 647/2	648/1 648/2		
Cumulative Indexes, Vols. 601–650[a]										
Bibliography Section		649/1		649/2			650/1			650/2
Biomedical Applications		Vols. 612, 613 and 614/1	614/2 615/1	615/2 616/1	616/2 617/1	617/2 618/1 + 2	619/1 619/2	620/1 620/2	621/1 621/2	622/1 622/2

[a] To appear in 1994.

INFORMATION FOR AUTHORS

(Detailed *Instructions to Authors* were published in Vol. 609, pp. 437–443. A free reprint can be obtained by application to the publisher, Elsevier Science Publishers B.V., P.O. Box 330, 1000 AH Amsterdam, Netherlands.)

Types of Contributions. The following types of papers are published in the *Journal of Chromatography* and the section on *Biomedical Applications:* Regular research papers (Full-length papers), Review articles, Short Communications and Discussions. Short Communications are usually descriptions of short investigations, or they can report minor technical improvements of previously published procedures; they reflect the same quality of research as Full-length papers, but should preferably not exceed five printed pages. Discussions (one or two pages) should explain, amplify, correct or otherwise comment substantively upon an article recently published in the journal. For Review articles, see inside front cover under Submission of Papers.

Submission. Every paper must be accompanied by a letter from the senior author, stating that he/she is submitting the paper for publication in the *Journal of Chromatography.*

Manuscripts. Manuscripts should be typed in **double spacing** on consecutively numbered pages of uniform size. The manuscript should be preceded by a sheet of manuscript paper carrying the title of the paper and the name and full postal address of the person to whom the proofs are to be sent. As a rule, papers should be divided into sections, headed by a caption (*e.g.*, Abstract, Introduction, Experimental, Results, Discussion, etc.) All illustrations, photographs, tables, etc., should be on separate sheets.

Abstract. All articles should have an abstract of 50–100 words which clearly and briefly indicates what is new, different and significant. No references should be given.

Introduction. Every paper must have a concise introduction mentioning what has been done before on the topic described, and stating clearly what is new in the paper now submitted.

Illustrations. The figures should be submitted in a form suitable for reproduction, drawn in Indian ink on drawing or tracing paper. Each illustration should have a legend, all the *legends* being typed (with double spacing) together on a *separate sheet.* If structures are given in the text, the original drawings should be supplied. Coloured illustrations are reproduced at the author's expense, the cost being determined by the number of pages and by the number of colours needed. The written permission of the author and publisher must be obtained for the use of any figure already published. Its source must be indicated in the legend.

References. References should be numbered in the order in which they are cited in the text, and listed in numerical sequence on a separate sheet at the end of the article. Please check a recent issue for the layout of the reference list. Abbreviations for the titles of journals should follow the system used by *Chemical Abstracts.* Articles not yet published should be given as "in press" (journal should be specified), "submitted for publication" (journal should be specified), "in preparation" or "personal communication".

Dispatch. Before sending the manuscript to the Editor please check that the envelope contains four copies of the paper complete with references, legends and figures. One of the sets of figures must be the originals suitable for direct reproduction. Please also ensure that permission to publish has been obtained from your institute.

Proofs. One set of proofs will be sent to the author to be carefully checked for printer's errors. Corrections must be restricted to instances in which the proof is at variance with the manuscript. "Extra corrections" will be inserted at the author's expense.

Reprints. Fifty reprints will be supplied free of charge. Additional reprints can be ordered by the authors. An order form containing price quotations will be sent to the authors together with the proofs of their article.

Organofluorine Compounds in Medicinal Chemistry and Biomedical Applications

Edited by **R. Filler, Y. Kobayashi** and **L.M. Yagupolskii**

Studies in Organic Chemistry Volume 48

An examination of the important role of fluorine in medicinal chemistry reveals that, in most cases, an organic compound needs be only lightly substituted with fluorine. Indeed, a single fluorine atom or a trifluoromethyl group, located in a key position of a bioactive molecule, can exert a profound pharmacological effect. Recently, developments in previously well-studied fields have been augmented by exciting reports in newer areas. The topics chosen by the authors are likely to be of broad interest and represent the work of established international leaders in their areas of research.

Keeping in mind the question *"what does fluorine provide that is so special?"*, the reader will find information on anticancer and antiviral agents and be brought up to date on volatile anesthetics and central nervous system agents, areas in which fluorine has played a pivotal role for almost forty years. Antibiotics receive special attention, with coverage of β-lactams and fluoroquinolone antibacterials. Newer applications of biologically-active fluorine compounds are reviewed, including cardiovascular drugs, fluoroamino acids and peptides, and the prostaglandins and leukotrienes of the arachidonic acid cascade. Biomedical applications, such as ^{18}F in positron emission tomography (PET) and fluorinated surfactants are exceptionally well covered. In the opening chapter, an overview of the field is given, including brief reports on areas not otherwise covered in the book, e.g. recent advances in antidiabetic and hypolipidemic agents.

Contents:

©1993 394 pages Hardbound
Price: Dfl. 395.00 (US $ 225.75)
ISBN 0-444-89768-2

ELSEVIER
SCIENCE PUBLISHERS

ORDER INFORMATION

For USA and Canada
ELSEVIER SCIENCE PUBLISHERS
Judy Weislogel, P.O. Box 945
Madison Square Station
New York, NY 10160-0757
Fax: (212) 633 3880

In all other countries
ELSEVIER SCIENCE PUBLISHERS
P.O. Box 330
1000 AH Amsterdam
The Netherlands
Fax: (+31-20) 5862 845

US$ prices are valid only for the USA & Canada and are subject to exchange rate fluctuations; in all other countries the Dutch guilder price (Dfl.) is definitive. Customers in the European Community should add the appropriate VAT rate applicable in their country to the price(s). Books are sent postfree if prepaid.